Spatial Dynamics in Lakes:

Modelling Spatial Distributions of Phytoplankton and their Causative Processes

Richard Hedger

Doctor of Philosophy

University of Edinburgh

1999

Abstract

Water quality characteristics of a lake are determined not just by their mean but also by their *spatial distribution*. Spatial distributions are dependent upon *spatial dynamics*. That is, the system response so that it exists in dynamic equilibrium with the forces affecting it. Spatial dynamics within lakes have implications for lake management, such as the determination of where and when cyanobacterial blooms will accumulate. This thesis explored the spatial dynamics of phytoplankton within lakes through the modelling of their spatial distributions and their causative processes. Spatial dynamics were investigated using by a two-stage procedure. Initially, spatial distributions of phytoplankton within lakes in North West Scotland, the English Lake District, and the Dutch Loosdrecht and Northern Vecht area were investigated using remotely sensed images. Spatial distributions evident in the images of these lakes were explained in terms of causative processes: nutrient gradients leading to differential growth, and wind-forced and inflow-forced hydrometry leading to spatial displacement. Then, using the relationships established in the exploratory analysis as pointers for further investigation, the spatial dynamics of phytoplankton were investigated through the use of Computational Fluid Dynamics (CFD) process modelling. For this, an existing CFD was modified so that it could simulate both a hydrometry that was appropriate to that occurring in natural lakes, and biological processes including the vertical movements and growth rates of diatoms, cyanobacteria and dinoflagellates. CFD modelling was used to provide information on spatial dynamics through two approaches. Firstly, real events occurring within selected lakes were simulated to enable the spatial dynamics in a fully complex environment to be determined. Secondly, hypothetical events occurring within hypothetical basins were simulated. This enabled the simulation of the effects of a far wider range of causative processes on phytoplankton spatial dynamics under carefully controlled conditions. It was found that the spatial dynamics of phytoplankton were dependent upon the lake morphometric, atmospheric, fluvial network and hydrometric properties. This dependence existed because of two types of interaction. Firstly, there was the interaction between the morphometric properties of the phytoplankton (such as cell mass and volume) and the hydrometry (which in turn was dependent upon morphometric, atmospheric and fluvial network properties). Secondly, there was the interaction between the growth properties of the phytoplankton and the nutrient field. It was concluded that the spatial dynamics of phytoplankton operated at a wide range of scales in all three spatial dimensions simultaneously, and existed in a non-steady state equilibrium with lake boundary conditions. Because the spatial dynamics of phytoplankton depended upon the interaction between a large number of phytoplanktonic and environmental properties, including numerous feedback mechanisms, they were greatly sensitive to the precise boundary conditions (both past and present). The implication of this in the analysis and management of lake systems it that it is necessary for procedures to be specific to the lake conditions under consideration.

I declare that this thesis is my own work, and that when the work of others has been used it has been acknowledged.

Richard Hedger

12 June 1999

Acknowledgements

This thesis was funded by a NERC CASE Studentship (GT4/95/85/F) involving the Department of Geography at Edinburgh University, the Department of Geography at Southampton University, and the Institute of Freshwater Ecology (Windermere). I would like to express my gratitude to all involved in this thesis.

More specifically, I would to thank supervisors Dr T.J. Malthus, Dr P.M. Atkinson and Dr D.G. George for their continued advice and encouragement throughout this thesis. I would also like to thank Dr N.R.B. Olsen of the Norwegian University of Science and Technology for his assistance in the adaptation of the Computational Fluid Dynamics package *SSIIM1.5* for use in this thesis and his advice on the hydrodynamic modelling component. Without the support of these people, this thesis would not have been possible.

I would also like to thank the many other people who have contributed to the provision of data and advice. These include Tony Bailey-Watts and Alec Lyle of the Institute of Freshwater Ecology (Edinburgh) and Dianne Hewitt of the Institute of Freshwater Ecology (Windermere). Additionally, Dick Jater of the Scottish Environmental Protection Agency, and Jos Mormon, Herman Gons and Maarten Ouboter of the Dutch Limnological Institute. Also, Elizabeth Kerr of the Scottish Meteorological Office.

In regards to the provision of remotely sensed data, I would like to thank John Cooke and Peter Purcell of the Natural Environmental Research Council (NERC) Airborne Remote Sensing Facility (ARSF) for collection of the data of the Scottish lakes, and Stuart White of the Rutherford Laboratory for supplying archived ATM data.

I would also like to express my thanks to Chris Place and Steve Dowers of the Geography Department at Edinburgh University for their support with computational matters involved in this thesis. Additionally, I would like to thank *Second Byte* of Edinburgh for their support in hardware maintenance.

Contents

Figures

Tables

1 Introduction

This thesis explores the spatial dynamics of phytoplankton within lakes. By way of introduction, this chapter will firstly describe what is meant by the term *spatial dynamics* as applied to a fluid system, describing how spatial dynamics are dependent upon the forces to which the system is subjected. The focus will then be on the spatial dynamics that occur within *lake systems*, as opposed to those of other fluid systems. This will involve a discussion of the environmental properties of lakes and the structural and physiological properties of phytoplankton that may determine the spatial dynamics of phytoplankton. There will then follow a short introduction on how the spatial dynamics of lakes affect the methodology by which these can be studied. This chapter will then finish with a statement of the precise objectives of this thesis.

1.1 Spatial dynamics

1.1.1 Forces, processes and properties in fluid environments

Fluid environments include atmospheres, oceans, rivers, estuaries and lakes. The nature of fluid environments may be defined by the properties of their fluid media, often referred to as *field properties* (Versteeg and Malalasekera, 1995). These, properties include density, pressure, temperature and velocity. Density is defined as mass per unit area, pressure by the force exerted per unit area, and temperature is an index of heat per unit area. Velocity quantifies the direction-dependent rate of mass displacement, or flow, within the medium. Velocity is usually broken-down into *convectional* and *turbulent* components (Hamill, 1995): convection refers to the average component of the velocity field, and turbulence refers to short scale spatio-temporal fluctuation in the velocity field. Additionally, any contaminants of the fluid medium (such as phytoplankton) may also be defined as field properties.

All fluid media are subject to several *forces*. These forces include radiative forces, gravitational forces and frictional forces (Houghton, 1986). Forces cause *processes* within the fluid media, a process being defined here as any physical agent that

contributes to the unfolding of the physical dynamics of the system (Fisher, 1994). Processes in fluid environments include conduction of heat and mass displacement.

1.1.2 Spatial distributions of processes and properties

Processes and resultant medium properties are realised with specific spatial distributions (Harris 1980a; Harris 1994). As used in this thesis, the spatial distribution may be quantified by two terms: *pattern* and *scale*. The term *pattern* refers to a scale-independent 'repeatable arrangement' (Platt and Sathyendranath, 1994). For example, the letter 'P' has a different pattern to the letter 'Q'. It is scale-independent because is has the same pattern whether it is the size that it is on this page, or has a maximum dimension of several kilometres. The term *scale*, in contrast, refers to the 'characteristic magnitude, either in space or time, of a particular process or pattern' (Platt and Sathyendranath, 1994). Different patterns may have equivalent scales. In this thesis, the terms *macro-scale*, *meso-scale* and *micro-scale* are used to characterise the spatial scale of variation. As defined here, macro-scale refers to distances of greater than 1 km, meso-scale variation refers to distances of between 10 m and 1 km, and micro-scale refers to distances of less than 10 m. The determination of these scales is purely arbitrary, but is useful because processes within lakes may be differentiated from one another according to these scales (Section 2.2.4.3 and Section 2.4.3).

Processes are occurring (and properties of the medium are changed) as temporally dependent functions, so processes and medium properties have *temporal distributions*. The focus of this thesis is on spatial distributions rather than temporal distributions, but there is reference to temporal distributions because the spatial and temporal dimensions are interrelated (Section 2.4.4): that is, fluid environments are *dynamic*.

1.1.3 Dynamic equilibria

Fluid media generally exist in a state of *dynamic equilibrium* with the forces acting upon them. The term *equilibrium* refers to the state of balance of the system, created by the forces controlling it, in which the state will remain unchanged through time unless the controlling forces change (Whittow, 1984). With a change in controlling

forces, there is a change in the state of the system. For example, the density of a parcel of water exists in dynamic equilibrium with the forces (such as heat flux and pressure of the overlying water column) acting upon it. The density changes in response to changes in acting forces (such as when heat is added or when there is an increase in the height of the overlying water column). The state of dynamic equilibrium allows for the existence of temporary disequilibria or '*contemporaneous disequilibria*' (Harris, 1983; Richerson, 1997) because there is a time lag between the response to the forcing function and the actual realisation as a new system state. The actual time lag varies greatly between different medium properties and acting forces. Because processes exist in a state of dynamic equilibrium with the forces applied to the medium, the patterns and scales of processes also exist in a state of dynamic equilibrium.

The term *spatial dynamics* as used in this thesis refers to the formation of a spatial distribution of medium properties (including phytoplankton) according to forces acting upon the medium, such that the spatial distribution is in dynamic equilibrium with the forces causing it.

1.2 Spatial dynamics in lakes

So far, a causal link has been established between forces, processes, and spatial distributions of field properties for general fluid environments. It is now the intention to introduce spatial dynamics for a specific fluid environment: that of lakes.

1.2.1 General features of lakes

A lake is defined here as a fresh water body, completely surrounded by land, where the hydraulic processes are predominantly a function of wind stress (the stress imparted by wind on the water surface) and heating exchange. Wind stress results in convection and turbulence, and heat exchange results in vertical changes in water density which may result in a complete overturn of the water at certain times of the year (Imberger and Hamblin, 1982). Other forces may initiate hydraulic processes, such as stream inflows and outflows, and gravitational changes (initiating tides), but these forces tend to have relatively little effect in comparison to wind stress.

Lakes are one realisation of what Margalef (1992) has referred to as the *epicontinental aquatic system*, the other realisations being surface streams and sub-surface waters. They form in surface depressions caused by glacial and riverine erosion and deposition, chemical weathering and dams. Freshwater bodies that are anthropogenic in origin are usually defined as being surface reservoirs. For the purposes of this study, no distinction is made between 'lakes' and 'surface reservoirs' because the hydrometry (the pattern and scale of current flows) of many lakes of non-anthropogenic origin is being affected increasingly by anthropogenic influence so the distinction between lakes and reservoirs is often arbitrary.

Lakes vary greatly in their *water quality properties*. A water quality property is defined here as any physical impurity within a water body. Water quality properties include suspended sediments (both organic and inorganic), dissolved compounds (both organic and inorganic) and living organisms (ranging in size from tens of centimetres, such as fish, to several micrometres, such as phytoplankton). The large number of water quality properties has led to many different classification procedures: Spence (1967) classified lakes according to calcium carbonate concentration; Vollenweider (1968) classified lakes according to nutrient loading; and Maitland (1978) classified lakes according to fish concentration. A classification system that has achieved dominance is that of the Organisation for Economic Co-operation and Development (OECD 1982). This classifies lakes according to the concentrations of total phosphorus (TP) and chlorophyll-*a* (chl-*a*) concentration, with lakes ranging from ultra-oligotrophic to hypertrophic (Table 1-1). This is the classification scheme used in this study.

Table 1-1. OECD lake classification scheme.

	Ultra-oligotrophic	Oligotrophic	Mesotrophic	Eutrophic	Hypertrophic
TP (mg m^{-3})	< 4	< 10	< 35	< 100	> 100
Chl-*a* (mg m^{-3})	< 1	< 2.5	< 8	< 25	> 25

Source: OECD (1982)

1.2.2 Types of lakes considered in this study

In this study, the lakes considered are typical of those of Western Europe. That is, their surface area is less than 100 km^2 and they show a monomictic annual

temperature regime (Section 2.2.1). There is great variation in properties between these lakes, but not of the same magnitude as exists within all lakes of the world. Relationships established between spatial dynamics and causative processes in this thesis are only applicable to lakes of similar characteristics, and extrapolation to lakes that are of a greatly different scale, such as the North American or East African Great Lakes, or have a different annual temperature regime, such as those in more equatorial or polar regions, is not appropriate. A discussion of some of the issued involved is found in Spigel and Coulter (1996).

1.2.3 Lake environmental properties and phytoplanktonic properties

Before an introduction to some of the specific spatial dynamics of lakes (that is, how lakes differ from oceans), it is necessary to detail what properties are involved in the interaction.

In this thesis, a lake environmental property is defined as any non-planktonic property of the lake environment that affects the functioning of the lake system. Properties can be categorised as being atmospheric, inflow- and outflow-based, morphometric and hydrometric (Table 1-2). There is strong interaction between individual lake environmental properties. For example, morphometric properties (such as depth) and atmospheric properties (such as wind speed and temperature) affect hydrometric properties (such as convection rates).

In this thesis, phytoplanktonic properties are categorised as being *structural* or *physiological* (Table 1-2). The former affect the rate of movement of phytoplankton towards or away from the surface in a still water column (Reynolds, 1973b) or affect the amount of displacement in a moving water body, and the latter affect the rate of expansion of the population according to reproduction (Vollenweider, 1968). These properties will be described in greater detail in Section 2.3. Other factors (senescence, grazing and flushing) are not considered (justification for their exclusion is shown in Section 9.3.2)

Table 1-2. Categorisation of lake environmental and phytoplanktonic properties used in this thesis.

	Property category	Individual property
Lake environmental properties	Morphometric	Area
		Depth
		Shape
	Atmospheric	Irradiance
		Heat
		Wind
	Inflows and outflows	Water inflows and outflows
		Nutrient inflows and outflows
	Hydrometric	Convection
		Turbulence
Phytoplanktonic properties	Structural properties	Density
		Radius
		Form resistance
		Presence or absence of flagella
	Physiological properties	Exponential specific growth rate
		Maximum specific growth rate
		Half saturation specific growth rate

Lake environmental properties and phytoplanktonic properties are interdependent. For example, phytoplankton rising velocities are affected by the phytoplanktonic property of density (mass over volume) which may depend upon the environmental property of irradiance; irradiance is affected by irradiance attenuation, which depends upon phytoplankton concentration among other factors, which in turn may be dependent upon net growth rates.

1.2.4 Spatial dynamics specific to lakes

Much of the initial work conducted on the spatial dynamics in lakes has been based upon oceanographic research. Kolmogorov (1941), for example, identified a turbulent energy spectrum in the ocean. At the largest scale, there is a general convectional circulation, which involves circulation occurring over the whole dimension of the fluid medium. At smaller scales, there is a turbulent mixing range, which involves interface behaviour and boundary layers. At even smaller scales, there is a transitional range, where the energy of turbulence is overcome by viscosity (a measure of internal friction). At the smallest scales, there is a viscous range, where molecular excitation is dominant. Kolmogorov's energy spectrum is applicable, with some modification, to lakes (Boyce, 1974).

Differences between the energy spectra of oceans and lakes (and by implication

difference in their spatial dynamics) result from the fact that lakes exist over smaller spatial scales (smaller surface area and volume). This results in three differences. Firstly, the small scale of a lake may create a physical barrier for the minimum size required for certain large scale processes to operate. For example, large and persistent circulation processes such as gyres cannot exist beneath scales of approximately 100 km. Secondly, less energy is imparted into lakes (a smaller surface area to absorb radiation or heat or to be affected by wind stress). With less energy, hydrometry will be more quiescent, and wave heights and depths of wave-induced mixing may be less. Harris (1986) showed that for a given scale, turbulent kinetic energy within lakes tended to be less than turbulent kinetic energy within oceans. Thirdly, the relative effect of friction between water flows and the bed is greater in lakes. Friction tends to have a great influence on spatial dynamics in lakes because all parts of the lake are relatively near to the morphometric boundary (this boundary may influence flows within the entire lake).

1.2.5 Justification for studying spatial dynamics

There are several reasons for studying spatial dynamics within lakes.

i. Implications for management

Lakes are under increasing anthropogenic pressure. They are commonly used as pollutant sinks, fishing grounds, wildlife reserves and recreational areas (Harper, 1992). Often, individual resource uses conflict with others. For example, entry of pollutants such as nitrates and phosphates from agricultural runoff may cause increased phytoplankton concentrations. Under certain atmospheric conditions, blooms of cyanobacteria (a type of phytoplankton) involving temporary surface 'scums' may result. Not only may blooms damage fisheries by causing oxygen depletion (Ayles *et al.*, 1976) but they may produce toxins: neurotoxins and heptatoxins. Neurotoxins may cause animal death by damage to the nervous system. Heptatoxins may cause liver damage and it is believed that prolonged exposure may be carcinogenic (Hallegraeff, 1993). Most reported instances in the USA and Europe have focused on neurotoxins. These have resulted in animal death and human sickness in the shallow reservoir, Rutland Water, UK (Harper, 1992; Howard, 1993a; Ferguson, 1997). Also, Carmichael (1994) has summarised numerous instances of

animal death, in both livestock and birds, in the USA. Globally, there is increased emphasis on heptatoxins, and there is currently research investigating links between this and high rates of liver failure in China.

Recreation activity, particularly the influence of boats, may greatly affect the hydrometry of the lake (Mosisch and Arthington, 1998). For example, wakes caused by boats may cause increased erosion of banks (Tivy, 1980).

The effect of one resource use of a lake on other resource uses is not spatially constant. For example, a cyanobacterial bloom may affect a specific shore to a greater extent than other shores. Knowledge of spatial dynamics may, therefore, aid in improving lake management (Harris, 1980a). Many management procedures exist for reducing nutrient concentrations in lakes (Harper, 1992) and some of these procedures (those that are conducted within the lake, rather than outside such as land-use controls) require a knowledge of spatial dynamics for proper implementation. For example, artificial impoundments may be produced near to stream inputs to localise sedimentation of phosphorous. Alternatively, artificial aeration may be implemented to keep the lake mixed throughout the year, and therefore ensure a more spatially homogeneous distribution of nutrients.

ii. Implications for understanding global environment

Lakes may be used to estimate properties of climates, both, global and local, and, past and present. This is because climates affect processes occurring within lakes, which may be seen by analysis of sediment layers at lake beds (Farmer, 1994). By taking cores through the lake bed and estimating the rates of sedimentation through dating it has been possible to indicate the rainfall of past climates (Muchane, 1996). However, spatial dynamics within lakes affect the spatial distribution of sedimentation rates (Larsen and Macdonald, 1993), and interpretation of past climates may be difficult if the position of core observations are not chosen correctly (for example, one part of the lake may be more prone to sedimentation than another). Knowledge of the spatial dynamics may allow the correct positioning of cores within lakes (for example, by avoiding stream plumes).

1.3 Modelling spatial dynamics in lakes

1.3.1 Modelling approaches

i. Describing and Understanding

A model is defined in this thesis as 'any rule that generates outputs from inputs' (Overton, 1977). This definition includes any relationship, whether defined qualitatively or quantitatively. Jakeman *et al.* (1993) state two perspectives for constructing a model: a *pragmatic* perspective and a *philosophical* perspective. The former perspective has modelling conducted with the aim of *describing* relationships between properties. For example, if it is desired to know the relationship between the maximum scale over which variation in phytoplankton concentration occurs and lake area, a simple statistical relationship may be established. The latter perspective has modelling conducted with the aim of *understanding* or *analysing* relationships between properties. Using the same example, to determine the relationship between maximum scale and lake area, the model might determine the causative effect of lake area on hydrometry, and determine how the interaction of hydrometry and phytoplankton buoyancy determines the maximum scale at which variation occurs.

The two perspectives are not diametrically opposed in their application because descriptive models may assist in identifying themes that can be addressed more rigorously in analytical modelling. Additionally, some degree of descriptive modelling will be necessary for inclusion in an analytical model because in no environmental system are all processes understood. For example, the exact pathways by which irradiance is converted into phytoplankton cell carbohydrate under the influence of nutrient assimilation are not fully known. However, if a statistical model can be produced describing the relationship between the accumulation of cell ballast and irradiance and nutrients, it may be possible to use this model in a much larger process-based model that focuses upon the interaction between cell ballast and hydrometry.

In this thesis, the emphasis is on modelling to gain understanding of spatial dynamics in lakes rather than simply describing them, although initially there is more emphasis on describing relationships. Modelling with the intention of understanding the

environment requires a critical interpretation of the means by which the model functions. This is because the outcome of any model is, by nature, dependent upon the way in which the model has been formulated.

ii. Reductionism and Holism

Two divergent approaches have dominated the analysis of lakes: reductionism and holism. The first approach, as applied to lakes, involves analysis of particular lake systems with an attempt at describing and understanding their complexity. Within the analysis it is implicitly assumed that generalisation from one system to another is not possible. The second approach, as applied to lakes, involves analysis of particular lake systems with the assumption that general features of these systems can be described and understood, leading to the formulation of theories that can be applied to other lake systems. This approach, referred to as *empirical limnology*, was advocated by Hutchinson (1957). More recent exponents of this approach include Vollenweider (1968) and Rigler (1982) who both studied the response of the eutrophic states of lakes to phosphorus loading. This approach is used throughout this thesis in addressing the objectives of the thesis.

iii. Modelling strategies

Modelling strategies, in terms of how the properties of a system may be characterised or parameterised, are numerous. These include statistical (Kneale and Howard, 1997), artificial neural network (Recknagel, 1997) and genetic algorithm-based (Bouchart and Hapartzoumian, 1999) strategies. The disadvantage of these three strategies is that, although they may describe adequately how a system behaves, they may not show the reason for that behaviour, being more akin to 'black-box' models. Alternatively, expert systems may be used, in which system components are represented through hierarchical data structures which have been produced through goal oriented production rules (Angel *et al.*, 1999). The dominant modelling strategy used throughout this thesis is deterministic, dynamic modelling (Section 2.7). In common with expert systems, the emphasis in dynamic modelling is based on heuristic knowledge of how a system behaves. However, with dynamic modelling, a greater range of system outputs may be simulated, ensuring the greater potential for understanding system characteristics.

1.3.2 Implications of lake spatial dynamics for modelling

The spatial dynamics of lakes determine the methods by which they can be modelled. To model spatial dynamics successfully, it is necessary to resolve their dimensionality, range of spatial and temporal scales, complexity and sensitivity.

i. Resolving the dimensionality

The three-dimensional aspect of lakes has long since been noted (Hutchinson, 1957). Data solely on surface spatial distributions of processes and water quality properties may not provide enough information on the three-dimensional dynamics of the system. When analysing existent spatial distributions, or generating new distributions through process modelling, it is necessary to include the vertical dimension.

Spatial dynamics, by definition, involve a temporal aspect. A proper understanding of the relationships between the spatial dynamics of phytoplankton and causative processes cannot be properly established if the past history of phytoplankton spatial distributions and causative processes is not fully known. The importance of considering the temporal domain has been stressed by Imberger (1985), when it was shown that mixed layers within lakes evolved to keep pace with changing wind stresses. System dimensions have been shown to be important in affecting the lag between wind event and system response (Lee and Mysak, 1979).

ii. Resolving the range of scales

Properties within lakes change through a great range of spatial and temporal scales. Phytoplankton communities are highly dynamic (Sakshaug, 1980), and vary over scales from several microseconds and micrometres to many years and kilometres (Reynolds, 1990). Velocities may vary by several orders over scales of metres and hours (Section 2.2.4). When modelling, it is necessary to ensure that the data used in the model are of a scale appropriate to the dynamics of the phenomena being modelled. For phytoplankton spatial dynamics, data of high spatial and temporal resolution are required to resolve small scale changes, and data covering large areas (and possibly long time periods) are necessary to resolve large scale changes.

High spatial and temporal resolution remotely sensed data may be appropriate for

resolving short scale variation. However, satellite remote sensing, at present, is inappropriate. Recent satellites, such as SeaWifs, may have the spectral resolution required to resolve water quality properties and the temporal resolution required to resolve spatial dynamics occurring over time periods of several hours to days (Siegel *et al.*, 1999). However, they do not have the spatial resolution required to resolve short scale spatial dynamics and do not have the temporal resolution to look at temporal scales over time periods of several minutes. Airborne-based remote sensing is the optimal remote sensing technique for this. If coupled with contact measurements of the lake (*in situ* sampling), high resolutions in the vertical dimension may also be derived.

Comprehensive coverage of the lake is necessary to ensure that large scale spatial dynamics can be resolved. Again, airborne remote sensing may be a suitable method of data collection. A sample of the lake will not necessarily be representative (Appendix F).

iii. Resolving the complexity and sensitivity

A fluid field has few physical properties: density, pressure, velocity and temperature. When non-biological contaminants (inorganic suspended sediments or dissolved compounds) are introduced there is an increase in the complexity of the system behaviour as there are interactions between the properties of the contaminant and the properties of the fluid. When biological contaminants are introduced, there is a further increase in complexity as there will be additional interactions between the biological contaminants themselves. Typically, hundreds of species of phytoplankton exist within a given lake, and ecological relationships between them and nutrients, irradiance, and the velocity field are very complex. Between these properties, feedback mechanisms are often in operation. These mechanisms are often non-linear, resulting in a variety of possible behaviours, including chaotic behaviour (Addison, 1997). This suggests that detailed measurements have to be made of lake environments, and that models of lake environments have to incorporate a great number of processes. These processes include convection and turbulence (as functions of wind speed), phytoplankton growth (as functions of irradiance, nutrient concentration and temperature) and phytoplankton buoyancy (as a function of

irradiance). However, as with all modelling, it is necessary to apply '*Ockham's Razor*': the model should be as simple as possible, only including parts of the system that it is essential to model. Attempts at modelling too many characteristics of the system may cause a decrease in model reliability because there are 'limits to our ability to mathematically characterise the complexity of nature' (Chapra, 1997).

So far, the complexity of spatial dynamics in lakes has been referred to. However, in comparison to terrestrial ecosystems, lakes have 'apparent simplicity' (Rigler and Peters, 1995). Firstly, lakes have definitive boundaries (water-air interface, water-land interface), through which the passing of living organisms is restricted. Secondly, lakes may be dissected into specific subsystems: epilimnion, metalimnion, hypolimnion (Section 2.2.1). The crossing from one subsystem to another is again restricted, but to a lesser extent. This compartmentalisation aids the modelling of spatial dynamics within lakes, and is utilised continually in this thesis.

1.4 Objectives, approaches and additional outcomes

1.4.1 Objectives

The main objective of this research was ***to determine the relationships between the spatial dynamics of phytoplankton and the interaction of lake environmental and phytoplanktonic properties.***

To achieve this objective, emphasis was placed upon analysing relationships between firstly, the spatial dynamics of phytoplankton and the lake hydrometry (which was itself the function of morphometric, atmospheric and inflow and outflow properties) and secondly, between the spatial dynamics of phytoplankton and phytoplanktonic properties:

i. The relationships between the spatial dynamics of phytoplankton and lake hydrometry

- **Properties that force hydrometry**

  Spatial dynamics of phytoplankton could be related to the wind environment. For example, different wind vectors could cause spatial dynamics such that spatial variation in phytoplankton concentration becomes scale-dependent, either

occurring at small or large horizontal scales.

Spatial dynamics could be related to the stream inflow and outflow configurations. For example, spatial dynamics initiated by stream inflows could cause nutrient gradients that result in phytoplankton gradients through differential population growth.

- **Properties that modify hydrometry**

Spatial dynamics of phytoplankton could be scaled to the surface area of lakes such that there is an increase in the magnitude of the variation in phytoplankton concentration and an increase in the spatial scale over which the variation occurs with an increase in lake surface area. Spatial dynamics could be scaled to the depth of lakes such that there is more heterogeneity in deep lakes. Additionally, spatial dynamics could be positively related to the complexity of lake shape, such that there are more complex spatial dynamics of phytoplankton in lakes with elongated and multi-basin morphometries and simpler spatial dynamics in lakes with rounded single-basin morphometries.

ii. The relationships between the spatial dynamics of phytoplankton and phytoplankton properties

- **Properties that affect rising velocity**

Species that have buoyancies that are greatly different to the buoyancy of water may have spatial dynamics that result in heterogeneous spatial distributions, and species with buoyancies similar to that of water may have spatial dynamics that result in homogeneous spatial distributions. Phytoplankton size and shape may affect the rate of development of spatial distributions, by affecting the rate of displacement of phytoplankton.

- **Properties that affect growth rates**

Species with high growth rates may cause different phytoplankton spatial dynamics than species with low growth rates. For example, an increase in the maximum specific growth rate may cause an increase in the magnitude of the spatial variation in phytoplankton concentration.

It is possible that specific properties cause specific spatial dynamics. However,

because all properties act concurrently, the emphasis in the analysis involved looking at the effect of interactions between all the properties involved. The requirement for modelling these interactions has long been established: 'The interplay between physical processes and water quality and the feedback mechanisms must be better understood if water quality models are to be used as a predictive tool' (Imberger and Hamblin, 1982). Attention in this thesis is focused on how the spatial dynamics of phytoplankton are affected by interactions between, firstly, phytoplankton motility or buoyancy and water flows in the horizontal and vertical domains, and secondly, population growth and the spatial distribution of nutrient concentration. Additionally, because this thesis is exploring spatial *dynamics*, an analysis of the temporal aspect of the formation and destruction of spatial distributions is necessary. It is possible that the effects of causative processes may be seen not solely in the spatial distributions that they produce, but in how long it takes for these spatial distributions to be produced.

1.4.2 Approaches used to attain objectives and structure of thesis

A modelling approach is used throughout this thesis. Use is made of models of varying data requirements and levels of scientific 'soundness' (in regards to their underlying assumptions). Model outputs are interpreted qualitatively and quantitatively.

Chapter 2 provides the background to the study. It initially describes the environmental properties that are characteristic of lakes, the properties that are characteristic of phytoplankton, and how these properties interact to cause specific spatial dynamics of phytoplankton. Attention is then focused on the background to some of the techniques that are used in this thesis to analyse the spatial dynamics of phytoplankton: how existent spatial dynamics in lakes can be detected and quantified, and how spatial dynamics can be generated using process modelling.

Chapters 3 and 4 introduce the lakes that are analysed in this study, and the methodology that is used. Two methods are used to link the spatial dynamics of phytoplankton to causative processes. Firstly, an exploratory analysis, involving qualitative interpretation of existent spatial distributions as revealed in remotely sensed images, is used to establish general relationships (Chapter 5). Then, using

some of the conclusions drawn from the exploratory analysis as a basis for further investigation, Computational Fluid Dynamic (CFD) process modelling (Chapters 6, 7 and 8) is used to simulate spatial dynamics. This enables a more robust investigation of spatial dynamics. Chapter 6 describes calibration of the process model, Chapter 7 describes the use of the process model for simulating spatial dynamics in real lakes, and Chapter 8 describes the use of the process model for simulating spatial dynamics in hypothetical user-determined basins. Outcomes are discussed and conclusions given in Chapter 9.

The main data source on the spatial distributions of phytoplankton is provided through remote sensing. Given the nature of remote sensing, emphasis is therefore on the spatial dynamics of phytoplankton at the surface rather than within the vertical domain. However, when data on the vertical distribution of phytoplankton are available, or the vertical distribution may be inferred through modelling, these are included because an understanding of what is occurring in the vertical dimension aids the understanding of what is occurring at the surface.

1.4.3 Additional outcomes

Although the primary objective of this thesis was to analyse how lake environmental properties and phytoplanktonic properties interact to cause spatial dynamics, there are additional outcomes of this research.

Firstly, the relative merits of the two modelling approaches used (qualitative interpretation and process modelling) are considered in terms of their relative merits. This involves analysis of what information the approaches can provide (in terms of dimensionality and resolution) and an analysis of how reliable this information is (in terms of the potential to which they contain error).

Secondly, because this thesis involves geostatistical techniques to quantify scales of spatial variation, it is relatively easy to use such techniques in optimising sampling strategies (Appendix F). Although production of such strategies does not aid in the understanding of spatial dynamics in this thesis, it is the intention of future research to use optimised sampling for the investigation of spatial dynamics (Section 9.7).

2 Background

2.1 Introduction

This chapter provides the background for this thesis. It can effectively be divided into two parts. The first part describes the general properties of lake environments and phytoplankton, leading onto a discussion of how these properties may interact to cause the spatial dynamics of phytoplankton. The second part focuses upon the techniques that are used in this thesis to analyse this interaction. This involves methods by which relative phytoplankton concentrations can be determined, methods by which phytoplankton spatial distributions can be analysed, and methods of simulating the spatial dynamics of phytoplankton through process modelling.

2.2 Lake environmental properties

2.2.1 Atmospheric properties

The main atmospheric properties considered in this thesis are irradiance, thermal and wind properties.

i. Irradiance properties

Irradiance on a lake surface has two main temporal periodicities: a diurnal periodicity with maximum irradiance exhibited around midday, and an annual periodicity with maximum irradiance exhibited on June 21 in the Northern Hemisphere (Spencer, 1971). Superimposed on these periodicities are the effects of the atmosphere's composition (particularly the presence of clouds) and the effects of surrounding topography (mountains may obscure the sun at low solar azimuths). The proportion of irradiance passing through the interface between the lake and the atmosphere to become sub-surface irradiance rather than being deflected depends on the solar azimuth (Appendix D) and the azimuth angle of the lake surface. The azimuth angle of the lake surface depends upon wave characteristics, which are a function of wind speed.

In biological modelling, it is common to consider in most detail that irradiance which is available for photosynthesis: *Photosynthetically Active Radiation* (PAR), which spans the wavelength range 380 nm to 750 nm (Parsons and Takahashi, 1973). In mid-latitudes during summer and in the absence of cloud, the maximum noon PAR sub-surface irradiance may be in the region of 1500 μE m^{-2} s^{-1} (Appendix D). For the same time of year, cloud cover may reduce this value by a factor of up to 10.

Within water bodies, irradiance decreases exponentially as a function of depth because of scattering and absorption in overlying water layers (Jerlov, 1976; Kirk, 1994). The decrease in irradiance with depth may be described by the Beer-Lambert model (used in the process model of this thesis as described in Section 3.3.3.2):

$$I_z = I_o \, e^{-\varepsilon z} \qquad (2\text{-}1)$$

where I_z is the irradiance at depth z, I_o is the sub-surface irradiance, and ε is the vertical extinction coefficient. The vertical extinction coefficient depends upon the combined extinction coefficients of all water quality properties involved: water itself, phytoplankton, dissolved organic carbon (also known as DOC, gilvin or aquatic humus) and non-planktonic suspended sediment. Therefore, inflow and outflow properties and hydrometric properties affect the spatio-temporal distribution of irradiance within a lake because they may affect the spatio-temporal distribution of water quality properties.

At a depth usually varying between 1 m and 10 m (depending upon the vertical extinction coefficient) irradiance becomes less than 1 % of that immediately beneath the surface. The part of the water column between the surface and this depth is referred to the euphotic zone, and defines where phytoplankton photosynthesis may occur (Section 2.3.3). The maximum depth of the euphotic zone for a given vertical extinction coefficient may be defined as follows (Scheffer, 1998):

$$Z_{eu} = \frac{4.6}{\varepsilon} \qquad (2\text{-}2)$$

where Z_{eu} is the depth of the euphotic zone. The rate of extinction of irradiant intensity with increasing depth is wavelength-specific (Reynolds, 1984). Blue irradiance (approximately 430 nm) is generally attenuated at a greater rate than red irradiance (approximately 630 nm) which is generally attenuated at a greater rate

than green irradiance (approximately 530 nm). The irradiance wavelengths that are most efficiently used in photosynthesis occur at the greater wavelengths within PAR (which are attenuated to a lesser extent) so the depth of the euphotic zone for PAR may be defined as follows:

$$Z_{eu} = \frac{3.5}{\varepsilon_{\min}} \qquad (2\text{-}3)$$

where ε_{min} is the minimum vertical extinction coefficient for PAR, which is approximately 75 % of ε.

ii. Thermal properties

The heat balance of a lake depends upon the radiative balance (incoming solar shortwave radiation, incoming atmospheric longwave radiation, and outgoing longwave radiation) and conduction and evaporation (Chapra, 1997). In most temperate lakes, the dominant cause of temporal variation in lake heat balance is caused by variation in irradiant intensity (that is, irradiance heats the lakes). Therefore, heat balances show similar periodicities to irradiance (greatest temperatures during daylight and summer). There is a lag between forcing function and response, so greatest diurnal temperatures are experienced up to several hours after maximum diurnal irradiance and greatest annual temperatures are experienced up to several weeks after maximum monthly irradiance.

Because absorption of this incoming radiation declines exponentially with depth and downwards conduction occurs from the surface, the greatest temperature changes are experienced near to the surface. Therefore, the vertical regime may vary vertically. As summer is approached, surface heating may result in a buoyant layer (the *epilimnion*) overlying a less buoyant layer (the *hypolimnion*). The epilimnion is separated from the hypolimnion by a layer referred to as the *metalimnion* (typically less than 1 to 2 m), which is defined by a thermal step (the *thermocline*) (Imberger, 1985). As winter is approached, loss of heat from the surface may result in the near-surface water becoming denser than water at greater depths. This may cause complete mixing of the water column (Imberger and Hamblin, 1982; Harris, 1983; Vincent, 1983). When this is the dominant annual pattern, the temperature regime is described as being monomictic.

The thermal regime of a lake also varies horizontally if the lake is subject to wind action. Wind stress causes horizontal currents that distort the thermocline, tilting it deeper downwind and shallower upwind (Smith, 1992). At the upwind end the decrease in the thermocline depth is associated with the rise of colder water. The horizontal density gradient generates a buoyancy force that is necessary to balance wind stress.

The thermal regime of a lake has a great effect on the spatial dynamics of phytoplankton. Firstly, the thermal regime determines patterns of convection and turbulence (Section 2.2.4) and so determines the interaction of these with phytoplanktonic properties. Secondly, annual variation in the thermal regime affects the spatial dynamics of nutrients, which in turn affect phytoplankton growth rates. Vincent (1983) and Stauffer and Armstrong (1984) have shown that during stratification nutrients can accumulate in the hypolimnion, and that on destratification in winter, these nutrients can be mixed upwards to the surface and allow the development of high concentrations of phytoplankton in spring.

iii. Wind properties

Wind regimes have similar periodicities to the diurnal and seasonal periodicities of radiance regimes. This is because near-surface wind speed is positively related to the rate at which air density changes with increasing elevation (the boundary layer thermal gradient) which in turn is a function of absorbed radiance. Most atmospheric heating occurs from radiance emitted by the terrestrial (or aquatic) surface so there is a time lag between maximum solar radiance and maximum wind speed resulting from the time lag for the terrestrial or aquatic surface to be heated (and to start emitting maximum amounts of radiance).

Wind vectors are greatly influenced by local factors, and diurnal and annual periodicities may be obscured. The topography and landcover surrounding lakes greatly influence wind speed and direction: for example, valleys can channel winds, and forested areas can reduce wind speeds (Oke, 1987).

2.2.2 Inflows and outflow properties

Inflow and outflow properties pertain to the exchange of water and water quality

properties (such as nutrients) between the lake and inflowing and outflowing streams. In addition to streams, there is exchange of both water and water quality nutrients with the surrounding lake walls and the atmosphere, but exchange between the lake and streams is generally by far the most important in terms of flux.

Inflow and outflow properties vary greatly between lakes, by both magnitude and spatial configuration. The term *magnitude* refers to the discharge of the streams into or out of the lake, but it is often more beneficial to quantify magnitude by fluvial flows relative to the volume of the lake. The term *spatial configuration* refers to how clustered or dispersed the stream inflow and outflows are. A clustered configuration may have stream inflows and outflows in one area of a lake shore, and a dispersed configuration may have stream inflows and outflows on opposite shores.

2.2.3 Morphometric properties

Lake morphometry may be defined as the size and shape of a lake in three dimensions. Temporal variations in morphometry generally occur over long time scales, and are ignored in this thesis. There is, however, great morphometric variation between lakes.

Morphometric properties commonly used in this study are based upon those established by Welch (1948) and Hutchinson (1957). These include *surface area*, *volume*, *maximum length*, *mean width* (surface area over maximum length), *elongation* (a ratio of the maximum length of the lake to the diameter of a circle with the same surface area), *maximum depth*, *mean depth* (volume over surface area), and *mean depth over maximum depth*. Morphometric properties have a great influence on hydrometric properties within lakes, either through being a direct control on hydrometric processes (morphometric boundaries act as a physical control on where flows can occur) or by influencing other environmental properties. For example, wind speed increases with distance from the shore because of the reduction in surface friction associated with a water surface, so large lakes typically experience greater wind speeds (Oke, 1987). Other morphometric effects in spatial dynamics of lakes include those on lake heat balances (Gao and Stefan, 1999), species composition (Keller and Conlon, 1994) and sedimentation (Blais and Kaleff, 1995)

2.2.4 Hydrometric properties

The hydrometry of a lake (that is, the spatio-temporal variation in water velocity) is the combined result of the atmospheric properties, inflow and outflow properties and morphometric properties of the lake. Stream inflows and outflows may initiate water flows and may even dominate the hydrometry under certain conditions, such as reservoir flushing. Additionally, spatial differences in water density (as a result of temperature or salinity) may initiate flows. Ferrandino and Aylor (1985) have identified both of these effects on hydrometry for the reservoir Lake Lillionah, USA. However, in most cases, the dominant cause of water flow within lakes is wind-forcing. The bulk of the following sections describe how wind-forcing causes convection and turbulence within lakes. Firstly, the relationship between wind stress and surface current velocities is described. Then the relationship between wind stress and current velocities as a function of depth is described. This will lead onto a description of the convection and turbulence properties that may be initiated by wind-forcing. Finally, there will be a short section in the hydrometry that results from inflows and outflows, as this is pertinent for some of the lakes considered in this thesis.

2.2.4.1 Wind-forced hydrometry

Wind initiates water flow because there is friction between the flowing air and water. This results in a shear stress which causes a displacement of surface water, approximately in a downwind direction. The shear stress may be estimated by many methods of varying complexity (for example, some models include the effect of the generation of waves). A generic empirically-derived model is that used by Smith (1979):

$$\tau_s = \left(W^2 + 0.07W^3\right) \times 10^{-4} \qquad (2\text{-}4)$$

where τ_s is the wind shear stress and W is the wind speed (m s^{-1}).

Many studies have examined empirically the relationship between lake surface current speeds and wind speed. At winds speeds of 4 m s^{-1} or less Haines and Bryson (1961) found the following relationship:

$$U_s = \frac{6.91W}{\bar{W}^{0.56}} \quad (2\text{-}5)$$

where U_s is the surface current speed. At wind speeds of approximately 4 m s^{-1}, the surface may develop waves so its friction properties will change, and the equation of Haines and Bryson (1961) cannot be used. However, at wind speeds of between 4 m s^{-1} and 10 m s^{-1}, the relationship described by Smith (1979) where the surface current speed is 1.5 % of the wind speed is often applicable. These two relationships are used in the exploratory analysis of this thesis (Chapter 5).

Surface currents are deflected from the wind axis because of *Coriolis acceleration*:

$$C = m2\Omega \sin\phi U_z \quad (2\text{-}6)$$

where C is the Coriolis parameter, m is the mass of the body of moving water, Ω is the angular velocity of the Earth about its axis, ϕ is the latitude, and U_z is the velocity at depth z. This effect is caused by the spherical geometry of the Earth, centripetal acceleration and the fact that objects in motion tend to stay in motion (Newton's First Law). It results in deflection to the right in the Northern Hemisphere and deflection to the left in the Southern Hemisphere. Coriolis acceleration is inversely related to the current speed, so the effects of this may be negligible when lakes are influenced by high wind speeds.

2.2.4.2 Ekman spirals

Ekman (1905) proposed that water flows in the Northern Hemisphere are increasingly deflected in a clockwise direction with increasing depth: the term used for this is the *Ekman spiral*. This spiral exists because of the combined effects of two relationships: the inverse relationship between flow speed and depth, and the inverse relationship between flow speed and Coriolis acceleration.

There is an exponential decline in flow speed with depth (Smith, 1979):

$$U_z = U_s e^{-Kz} \quad (2\text{-}7)$$

where K is the damping coefficient (which may be determined empirically). This exponential decline in flow speed occurs because of shearing between successive layers of water. There is an increase in deflection with increasing depth because

Coriolis acceleration is inversely related to flow speed. Ekman concluded that flows in an opposite direction to that at the surface occurred at the *depth of frictional resistance*. This depth may be defined as:

$$D_* = \frac{30.47\tau_s}{\sin\varphi U_s} \qquad (2\text{-}8)$$

where D_* is the depth of frictional resistance, below which flow velocities are negligible. Again, this relationship is used in the exploratory analysis of this thesis (Chapter 5). Return flows may occur above the depth of frictional resistance. For example, if the lake is shallow or is subject to temperature stratification (in which the thermocline may act as a boundary that may be the effective lake base with respect to circulation), return flows may occur nearer to the lake surface.

2.2.4.3 Convection: Macro-, meso-, and micro-scale convection cells

Because of the demands of mass conservation, a downwind displacement of mass through convection must have a compensatory return displacement of mass: that is, a convection cell must be occurring. In lakes, convection cells exist from macro- to micro-scales.

i. Macro-scale convection cells

Macro-scale convection cells occupy the whole horizontal dimension of the basin. In all cases, convection occurs in both horizontal and vertical dimensions, but for a given lake, one of these dimensions tends to dominate macro-scale convection cells. In both cases, changes in flow directions are caused by obstructions, such as the lake shore.

Horizontal macro-scale convection cells, in which the return flow occurs at the surface, often exist in shallow lakes. Livingstone (1954) proposed a simple two-dimensional 'conveyor belt' model in the horizontal dimension for a circular lake under conditions of constant wind direction and wind stress. A steady-state equilibrium may develop in which the wind-forced drift current transports water to the downwind shore, resulting in a surface slope both along and across the wind axis (due to the circular shape of the lake). This across-axis slope then drives drift currents at the perimeter of the lake, running in opposing directions to the wind.

Vertical macro-scale convection cells, in which the return flow occurs beneath the surface, often exist in deeper lakes. Banks (1975) proposed a simple two-dimensional 'conveyor belt' model to describe the velocity of horizontal currents associated with a vertical dimension convection cell. In this model, water at the surface flows in the same direction as the wind (the '*exponential drift current*'), water beneath the surface flows in the opposite direction to the wind (the '*gradient current*'), and water flows downwards at downwind parts of the lake and upwards at the upwind parts of the lake. In areas unaffected by downwelling and upwelling, current velocities could be described by the following formula:

$$\frac{U_z}{U_s} = 4\left\{\left(1-\frac{z}{D_L}\right)-\frac{3}{4}\left[1-\left(\frac{z}{D_L}\right)\right]\right\} \qquad (2\text{-}9)$$

where D_L is the depth of the lake. At the surface, current horizontal velocities are at a maximum and decrease exponentially until zero at D_L / 3. At depths greater than D_L / 3, velocities become negative (that is, sub-surface return flow) and reach an absolute maximum at D_L / 1.5. Velocities increase to zero at D_L, because of the friction effects of the bed. This model has been criticised by Smith (1992) because of its inability to model vertical flows, and its assumption that the profile will be the same at all wind speeds. Smith (1979) proposed a model in which the exponential drift current and the gradient current are treated separately. The velocity of the current at any depth is estimated as the difference between Equation 2-7 and the velocity of the gradient current:

$$U_z = -6.75u_* \log\left[30(D_L - z)/r_p\right] \qquad (2\text{-}10)$$

where u_* is the friction velocity (a measure of turbulence) and r_p is the roughness coefficient. This model is superior to that of Banks (1975) because it is able to simulate the changes in vertical profile that are associated with a change in wind velocity. Specifically, with an increase in wind velocity the depth of zero current velocity increases, resulting in a lesser exponential decay rate with increasing depth for the drift current, and a greater absolute horizontal velocity for the return gradient current. These models provide insight on general patterns of circulation within water. It is, however, accepted (Smith, 1992) that these models only describe patterns under 'ideal' conditions of constant wind stress, simple morphometry, and

the absence of Coriolis acceleration. Under real circumstances, these conditions will not exist: hence, the need for more advanced ('*dynamic*') approaches. Additionally, neither model takes into account the change in density exhibited at the thermocline. This density change may act as a barrier to vertical flows, and confine vertical dimension convection cells to the epilimnion.

ii. Meso-cells convection cells

Although the models describing macro-scale convection cells may help to describe properties of the overall circulation, they do not realistically describe flows occurring within lakes because of their assumption of simple morphometries and constant wind stress. Superimposed on the overall circulation will be meso-scale convection cells (typically with horizontal dimensions between 10 m and 1 km for the lakes under consideration in this thesis) that are associated with bays, promontories, islands, inflows and outflows. They tend to exist over smaller time scales than macro-scale convection cells (Harris, 1986).

iii. Micro-scale convection cells

Micro-scale convection cells include Langmuir cells and wave cells. Langmuir (1938) identified streaks along the surface that were separated by several metres and that were aligned with wind direction. These surface streaks were caused by the accumulation of DOC in the downwelling areas of convectional eddies that had widths and depths of several metres, and lengths of tens of metres. Surface waves cause micro-scale convection cells in the near-surface layer, the depth of which are approximately half the length of the surface waves.

There is usually spatial anisotropy in convection cells (that is, the horizontal scale of the convection cells is often different to the vertical dimension) because of the effect of boundaries. For example, lakes are generally wider than they are deep, so a macro-scale convection cell occupying the whole of the lake will have a greater horizontal dimension than vertical dimension. If there is stratification, the density boundary may further limit the vertical scale over which this macro-scale convection cell occurs, and return flows may be confined to the epilimnion (Imberger and Hamblin, 1982).

2.2.4.4 Turbulence

Turbulence may be defined as 'a state of continuous instability' in the velocity field in which 'successive instabilities have reduced the level of predictability so much so that it is appropriate to describe the flow statistically' (Triton, 1988). Flows in lakes are usually turbulent. The existence or absence of turbulence may be determined from the *Reynolds number*, R_e.

$$R_e = \frac{Ud}{\nu_k} \tag{2-11}$$

where ν_k is the kinematic viscosity of the water and U is the average velocity from the surface to depth d. At Reynolds numbers below approximately 500 flows will be laminar, and at Reynolds numbers above 2000 flows will be turbulent. Even at low current speeds and small depths, Reynolds numbers are typically several orders of magnitude greater than the threshold required for the existence of turbulence.

Turbulence is chaotic (Lorenz, 1963), and turbulent flow may be characterised by three properties (Imberger, 1994). Firstly, the velocity field consists of a mean and a random component. Secondly, the random component is three-dimensional. Thirdly, there is an infinite number of length scales (in comparison to a laminar flow where there is a single length scale of the basin dimension).

Although turbulence occurs in three dimensions, the mixing power as defined by the *coefficient of eddy viscosity* (also referred to as *the coefficient of eddy diffusivity*) is highly anisotropic, varying greatly between horizontal and vertical dimensions.

i. Turbulence in the horizontal dimension

The coefficient of eddy viscosity in the horizontal dimension (K_h) is related to the length scale (L') because of the energy spectrum. If a patch of particles is being diffused by turbulence, the rate of diffusion of the patch increases as the length scale increases because particles become entrained in larger and larger eddies. Lam and Simons (1976) estimated the horizontal eddy viscosity as follows:

$$K_h = 2.23 \times 10^{-4} (L')^{1.3} \tag{2-12}$$

Therefore, horizontal eddy viscosities approached 20 $m^2\ s^{-1}$ at distances of 5 km. Other authors have produced similar estimates (Okubo, 1971; Murthy, 1976).

ii. Turbulence in the vertical dimension

Banks (1975) has related the coefficient of eddy viscosity in the vertical dimension, K_z, to the wind speed and the effective depth of the lake, D_E, for unstratified lakes:

$$K_z = (4.29W - 15.45) \times 10^{-5} D_E \qquad (2\text{-}13)$$

From this it can be seen that for a wind speed of 5 m s^{-1} and a depth of 10 m, the coefficient of eddy viscosity in the vertical dimension is 0.0003 m^2 s^{-1}. Eddy viscosities in the vertical dimension are, therefore, many orders of magnitude less than in the horizontal dimension.

If density stratification exists, eddy viscosities in the vertical dimension may be even more reduced. Denman and Gargatt (1982) have empirically verified that the size of micro-scale eddies may be restricted in the vertical dimension and therefore stretched in the horizontal dimension under conditions of stratification.

As with the horizontal coefficient of eddy viscosity, the vertical coefficient of eddy visocity varies spatially. It is usually greatest near to the surface within the mixed layer, which may be defined as the layer which is actively turbulent (Imberger, 1994). The depth of this has been related empirically to the fetch, and the average wind speed over that distance (U.S. Army 1962). The wave period T_s is estimated as follows:

$$T_s = \left(0.46 \times \left[\frac{gF}{W^2} \right]^{0.28} \times W \right) / g \qquad (2\text{-}14)$$

where g is the gravitational force (N m^{-2}), and F is the fetch (m) and W is the mean wind speed over that distance. From this, the length of the surface waves, λ_s is estimated as follows:

$$\lambda_s = 1.56 T_s^2 \qquad (2\text{-}15)$$

The depth of the mixed layer is usually estimated as half the length of the waves. Fetch as a function of position within the lake is estimated as a weighted function of distances from that position to locations around the upwind shore (Hilton and Rigg, 1984). In the exploratory analysis of this thesis, the depth of the mixed layer is estimated from these equations (Chapter 5).

2.2.4.5 Inflows and outflows

So far, emphasis has been placed upon the role of wind-forcing in the determination of lake hydrometry. In parts of a lake, over meso- and micro-scales, the effect of inflows and outflows may be dominant. Inflows and outflows have both convectional and turbulent characteristics. The rapid movement of water relative to that within the lake results in a rolling vortex which disintegrates into fully turbulent flow at some position away from the position of inflow or outflow. The effect of an inflow on the hydrodynamics of a lake is often vertically-dependent. When the density of the inflow is less than that of the lake (which is usually the case in temperate lakes in summer because of the increased temperature of streams) the inflowing water remains on the surface. If the density of the inflow is greater than that at the surface of the lake (which may occur if the inflowing water contains greater concentrations of suspended sediment), the inflowing water sinks to a depth in the lake where the densities are equivalent.

2.3 Phytoplanktonic properties

2.3.1 Phytoplankton classification

Before a description of the two main groups of phytoplanktonic properties that are considered in this thesis (phytoplankton structural properties and phytoplankton physiological properties) it is necessary to introduce the phylogenetic classification of phytoplankton types.

Phytoplankton may be defined as 'the community of plants ... *adapted to suspension* in the sea or in fresh waters and which is *liable to passive movement by wind and current*' (Reynolds, 1984). Certain types of phytoplankton are motile, with propulsion caused by swimming or the excretion of mass (Heaney and Talling, 1980). Many types of phytoplankton exist. The phylogenetic classification of those most referred to in this thesis is shown in Table 2-1.

Table 2-1. Grouping of phytoplankton.

Kingdom	Phylum	Class	Order	Genus
Prokaryota		Photobacteria **(Cyanobacteria: 'blue-green' algae)**	*Choococcales*	*Microcystis*
			Nostocales	*Anabaena* *Oscillatoria*
Eukaryota	Cryptophyta			
	Pyrrhophyta **('Dinoflagellates')**	Dinophyceae		*Ceratium*
		Adinophyceae		
	Raphidophyta			
	Chrysophyta	Chryosphyceae		
		Haptophyceae		
		Xanthophyceae		
		Bacillariophyceae **('Diatoms')**	*Biddulphiales*	*Cyclotella* *Stephanodiscus*
			Bacillariales	*Asterionella* *Fragilaria*
		Craspedophyceae		
	Eugelophyta			
	Chlorophyta ('green algae')		*Chorococcales*	*Chlorella* *Kirchneriella*

Source: Reynolds (1984)

For the purpose of this study, attention will be focused on diatoms, cyanobacteria and dinoflagellates. Diatoms are associated with colder water, with their peak concentration generally occurring during colder months of the year, although they are not exclusive to cold water bodies. Cyanobacteria are associated with warmer water than diatoms, and their peak in concentration generally occurs during warmer months of the year. Some genera are associated with stable water columns, including, *Nostocales* such as *Anabaena* and *Aphanizomenon*, and some are associated with unstable water columns, including *Choococcales* such as *Microcystis* (Reynolds, 1984).

2.3.2 Phytoplanktonic structural properties

Phytoplankton structural properties as defined in this thesis include *density, radius, form resistance (shape)* and the *presence or absence of flagella*. The first three properties affect rising velocities (the velocity in the direction against that of gravitational acceleration) in phytoplankton species that are *passively buoyant*. That is, where phytoplankton are unable to swim. The presence of flagella affects rising velocities in phytoplankton species that are *actively buoyant*. That is, where phytoplankton can swim.

i. Rising velocities with passively buoyant species

Rising velocities for passively buoyant species are dependent upon density, radius and form resistance in the following ways. Cells (or flocculations of cells) less dense than water will rise, and those more dense than water will sink. The greater the radius, the greater the velocity of this movement (as a greater mass is involved). The greater the form resistance (which measures deviation from a spherical shape), the slower the velocity because frictional resistance to movement is increased.

- **Density**

  Diatom rising velocities are always negative (they sink in a still water column) because their density is greater than that of water as they have siliceous cell walls. Cyanobacteria may have positive or negative rising velocities depending upon whether their density is less than or greater then that of water. Cyanobacteria contain *gas vacuoles* (intracellular gas-filled organelles) which reduce their density to potentially less than that of water, but irradiance-induced photosynthesis may cause the accumulation of cell carbohydrate which may make them more dense than water. Cyanobacterial density changes with a diurnal periodicity according to irradiance levels (Section 3.3.3.2), often being greater than that of water at midday, and less than that of water at night. Reynolds (1972) has reported that rising velocities of *Anabaena cicinalis* vary between approximately 20 $\mu m\ s^{-1}$ and $-4\ \mu m\ s^{-1}$ depending upon the proportion of the cell that consists of gas-vacuoles.

- **Radius**

  Diatoms are relatively large and typically 0.1 – 0.2 mm in diameter. Certain species of diatoms may form into colonies of collected cells, the radii of which may have a great effect on sinking rates. Cyanobacteria are generally smaller than diatoms, but there is great variation in cell size between different species. Like diatoms, they often form into colonies of collected cells (*Microcystis* colonies may be up to 0.5 mm in diameter), and again their radii may greatly affect their rates of vertical movement.

- **Form resistance**

  Form resistance describes the extent to which the phytoplankton shape differs from that of a sphere (which has a form resistance of unity). Different species of phytoplankton have different shapes. For example, the diatoms *Stephanodiscus* and *Cyclotella* are squat cylinders, the cyanobacterium *Synedra acus* is an attenuate cylinder. Additionally, when cells flocculate together to form colonies, they form widely different shapes from chains to globular colonies (Davey and Walsby, 1985). Typical form resistances of cells or colonies range from 1.0 to greater than 5.0. When cells join together to form colonies, form resistances may be greatly increased. For example, colonies of 11 - 12 cells of the diatom *Fragilaria crotenensis* have an estimated form resistance of greater than 4.83, as opposed to single cells with a form resistance of 2.75 (Reynolds, 1984).

These structural parameters interact to determine rising velocity. An increase in colony size tends to increase sinking rates: single *Asterionella formosa* cells sink at a rate of approximately 2 $\mu m\ s^{-1}$, colonies of 16 cells sink at rates of approximately 10 $\mu m\ s^{-1}$ (Reynolds, 1973a; Smayda, 1974). Form resistance tends to increase as colony size increases (which reduces the rate of sinking), but the effect of an increase in radius (which increases the rate of sinking) is generally greater, so the net result of an increase in colony size is often to increase the rate of sinking.

Although there is great variation in rising velocities between species, the velocities typically experienced are less than 1 $m\ d^{-1}$. This velocity is of a comparable magnitude with the diffusion commonly induced by turbulence (Harris, 1986), and ensures that phytoplankton can exist throughout the water columns of lakes. In the absence of turbulence, it takes several days or weeks for a water column with vertical dimensions typical of lakes to be cleared of phytoplankton (by accumulation at the bed or surface) as a result of phytoplankton rising velocities. In the presence of turbulence, a near-even distribution of phytoplankton within the water column may be maintained.

ii. Rising velocities with actively buoyant species

Dinoflagellates, as the name implies, have flagellates that enable self-propelled movement. This motility is used to enable them to swim to optimal irradiance levels

(Section 3.3.3.2) and to avoid anoxic conditions, so dinoflagellates may have negative or positive rising velocities. Less research has been conducted on the rising velocities of flagellates. However, Heaney and Talling (1980) have described how flagellates swim to optimum light levels of 150 $\mu E\ m^{-2}\ s^{-1}$, so rising velocities may be either positive or negative depending upon irradiance levels.

2.3.3 Phytoplanktonic physiological properties

The phytoplankton physiological property of most interest in this thesis is the *exponential specific growth rate*, which is determined by the *maximum specific growth rate, half saturation specific growth rate*, nutrient concentration and irradiance levels. The maximum specific growth rate defines the maximum rate of exponential growth of a species under conditions of irradiance and nutrient saturation (irradiance is required for photosynthesis and nutrients are required in the generation of cell tissue). The half saturation specific growth rate relates growth rates to irradiance and nutrient levels. Depending upon the phytoplanktonic species and the lake environmental properties, either irradiance or nutrient concentration may be the limiting factor. Generally nutrient concentration is the limiting factor. However, even in oligotrophic lakes, it has been reported that irradiance may limit growth rates (Jones *et al.*, 1996). In both cases, growth is confined to the euphotic zone.

Both the quality and quantity of nutrients required to support growth vary between phytoplankton types, according to their physiology. For diatoms, silica is the most important nutrient (Paasche, 1980). For cyanobacteria and dinoflagellates, nitrogen and phosphorus are the most important nutrients, with phosphorus generally being the limiting nutrient in most temperate lakes of the Northern Hemisphere (Schindler, 1978). Maximum specific growth rates vary greatly between species: the dinoflagellate *Ceratium hirundinella* has a relatively low maximum specific growth rates of approximately 0.26 ln cells d^{-1} (Bruno and McLaughlin, 1977); the cyanobacterium *Oscillatoria agardhii* has a greater specific growth rate of approximately 0.82 ln cells d^{-1} (Foy *et al.*, 1976).

The net rate of population growth depends upon the balance between increases (predominantly according to the specific growth rate) and decreases (predominantly according to phytoplankton death rates but also from flushing of the lake system). In

most cases, it is differences in specific growth rates in eutrophic waters that determine differences in net population growth rates. Net population growth rates vary greatly according to both phytoplankton type and lake environmental conditions. Typically, maximum rates of net population increase vary between 0.1 and 0.4 ln cells d^{-1}, with mean values at approximately 0.25 ln cells d^{-1} (Reynolds *et al.*, 1982). However, net population growth rates will generally be less than these rates, and may be zero (when the population maximum has been reached) or negative. Although there is variation between phytoplankton types, under certain conditions a doubling of the population can occur over a period of several days.

2.4 Relationships between lake environmental properties and phytoplanktonic properties

2.4.1 Interaction mechanisms

So far, the general environmental properties of lakes and the general properties of phytoplankton have been defined. It is now the intention to describe how these properties interact, and how the spatial distribution with which the interaction occurs causes the spatial dynamics of phytoplankton.

Phytoplankton structural properties interact with the velocity field and the irradiance field. Flow of water causes phytoplankton displacement, the velocity of this displacement depending on phytoplankton density (which may be irradiance-dependent), size and shape as well as the velocity of the water flow. The spatial dynamics of the flow velocity will, therefore, affect the spatial dynamics of the displacement.

Phytoplankton physiological properties interact with irradiance, nutrients and heat to cause reproduction. The spatial dynamics of phytoplankton growth rates are dependent upon the spatial dynamics of irradiance, nutrient concentration and heat (which in turn are dependent upon morphometric, atmospheric, inflow and outflow, and hydrometric properties).

2.4.2 Phytoplankton convection and phytoplankton growth

Two main models have been used to analyse how rates of growth and convection

determine phytoplankton spatial distributions: the *critical patch size model* of Kierstead and Slobodkin (1953), and the *power spectra model* of Denman and Platt (1976).

i. Critical patch size model

Kierstead and Slobodkin (1953) proposed that the presence or absence of a phytoplankton patch in any given area was dependent upon the balance between phytoplankton growth (which contributed to sustaining the patch) and phytoplankton diffusion (which contributed to eroding the patch). They predicted a critical size, below which a phytoplankton patch could not be maintained, by a weighted ratio of diffusion over growth (the ratio now referred to as the 'KISS' model):

$$r_c = 2.4048(d / k) \qquad (2\text{-}16)$$

where d is the horizontal diffusivity, and k is the net rate of increase of the population. In lakes, the role of convection is increased, so the modification to the following model may be more appropriate:

$$r_c = c(U_s / k) \qquad (2\text{-}17)$$

where c is an empirically derived constant. The KISS model may be further adapted to include the effect of grazing by zooplankton (Wroblewski and O'Brien, 1976). Horizontal diffusivity is dependent upon wind speed, so these models have been confirmed empirically by several authors who found that high wind speeds tend to increase small scale structure by breaking up large scale patches (George and Edwards 1976; George and Heaney, 1978; Levasseur *et al.*, 1983).

ii. Power spectra model

Denman and Platt (1976) used power spectra analysis of a sample of surface chlorophyll-*a* concentration and surface temperature to show that two distinct scales of variation could be found: firstly, at spatial scales below a certain limit, the power spectra of chlorophyll concentration were similar to those of temperature; and secondly, at spatial scales above a certain limit, the power spectra diverged. Their conclusion was that beneath this limit phytoplankton were acting as a passive scalar of turbulence (hydrometry was the sole process responsible for determining spatial variation), but above this limit growth of the phytoplankton community was able to

overcome the dispersing effects of turbulence. From this, it is apparent that hydrometry alone does not determine spatial variation but that biological factors also have an influence.

Both the critical patch size and power spectra models are highly simplified, however, and only serve to show how scales of phytoplankton spatial variation may be dependent upon the interaction between lake environmental and phytoplanktonic properties: the scale-independent pattern of the variation has been ignored. Additionally, both models were developed using oceanic observations and therefore reflect the relatively simpler velocity field encountered in the ocean away from the shore. These models have less application to lakes because of the greater complexity of lake hydrometry.

2.4.3 Macro-, meso-, and micro-scale spatial distributions

Although there is a continuous spectrum of spatial variation within lakes, spatial variation in phytoplankton concentration is often categorised as existing at distinct spatial scales, from macro-scale down to micro-scale, with each scale having its own set of characteristic causative processes.

i. Macro-scale spatial variation

Macro-scale variation may be caused by two processes: differential growth rates, or the accumulation of phytoplankton in upwelling and downwelling areas.

Macro-scale spatial variation is often caused by differential growth rates within the lake (Reynolds 1984). Therefore, the interaction is largely between the physiological properties of the phytoplankton and the spatial dynamics of nutrients. These spatial dynamics are determined by the inflow and outflow properties (determining where the nutrients enter or leave the lake), and the morphometry which affects the hydrometry (specifically, the amount of obstruction to mixing that occurs, preventing homogenisation of the nutrient field). Spatial distributions resulting from differential growth have been reported in many lakes. For example, Leigh-Abbott *et al.* (1978) found a macro-scale phytoplankton distribution in Lake Tahoe, USA, and attributed this to differences in nutrient input and morphometry. On a much greater spatial

scale, increased phytoplankton concentrations have been linked to nutrient gradients in Lake Baikal, Russia (Bondarenko *et al.*, 1996).

Alternatively, spatial variation at macro-scales has been linked to negatively buoyant species accumulating in upwind areas of lakes, and positively buoyant species accumulating in downwind parts of the lake. Here, the interaction is between the structural properties of the phytoplankton and the hydrometry of the lake. Again, many studies have identified this distribution (Heaney, 1976; George and Edwards, 1976; George and Heaney, 1978). This variation tends to be less persistent than variation arising from nutrient growth, and has prompted George (1993) to describe this as *meso-scale* variation.

ii. Meso-scale spatial variation

As with convection cells, meso-scale spatial variation in phytoplankton concentration may be caused by bays, promontories, islands, stream inflows and stream outflows (George *et al.*, 1988). Variation at meso-scales tends to be less persistent than variation at macro-scales.

iii. Micro-scale spatial variation

Micro-scale spatial variation has been linked to several phenomena. Smayda (1970) showed how spatial distributions of phytoplankton occurred in Langmuir cells through the interaction being between phytoplankton buoyancy and the hydrometry of the Langmuir cell. Micro-scale spatial variation at smaller scales and showing no organised pattern has been linked to periods of intense mixing in Esthwaite Water, UK, (George, 1993), again the interaction being between the structural properties of the phytoplankton and the lake hydrometry. Micro-scale variation at scales of several millimetres has been associated with grazing and nutrient regeneration (Goldman *et al.*, 1979; McCarthy and Goldman 1979; Jackson, 1980).

Different scales of spatial variation may exist concurrently in the same lake. For example, Leigh-Abott *et al.* (1978) discriminated two distinct scales of patchiness in Lake Tahoe, USA. At large spatial scales, variation was caused by differences in nutrient input; at intermediate scales, variation was caused by differences in the

mixing regime.

2.4.4 Inter-relationship between spatial and temporal scales of variation

Spatial variation in hydrometric properties exists at specific spatial and temporal scales. Therefore, spatial variation in phytoplankton concentration exists at specific spatial and temporal scales.

The spatial and temporal scales of phytoplankton concentration are interrelated. Stommel (1965) identified that in oceanic environments, variation at great spatial scales occurred concurrently with variation at great temporal scales, and that variation at small spatial scales occurred concurrently with variation at small temporal scales. Harris (1986) described this inter-relationship in more detail as applied to phytoplankton ecology. Three scales were identified. Firstly, at the largest scales, climatological processes take place at time scales of a year or more and at horizontal scales of 10 km plus and vertical scales of 100 m plus. Secondly, at intermediate scales, ecological processes such as growth and community change typically take place at time scales of days to months and at horizontal scales of 100 m to 10 km and vertical scales of 1 m to 100 m. Thirdly, at the smallest scales, physiological processes such as nutrient uptake and photosynthesis typically operate at a time scale of one hour, at horizontal spatial scales of 1 m to 100 m and at vertical spatial scales of 1 mm to 1 m.

2.5 Detecting spatial distributions: remote sensing and surface sampling

For the spatial distribution of phytoplankton to be determined, it is necessary to have an index of phytoplankton concentration. Two methods are outlined here: *remote sensing* and *'surface' sampling*.

2.5.1 Remote Sensing

Optical remote sensing of lakes is able to provide information on lake water quality properties by detecting the spectral characteristics that are specific to these properties.

2.5.1.1 Spectral characteristics of lakes

Interactions of irradiance with a water body (in terms of altering the quality and quantity of irradiance) may be summarised as follows. Irradiance incident on a water surface is partially reflected back into the atmosphere, and partially penetrates the atmosphere - water interface (the exact proportions of reflection and penetration being a function of the wavelength of the irradiance, and the incident angle). There is a reduction in irradiance with increasing depth because as photons pass through the water they are either absorbed or scattered by water molecules or any substance within the water (such as phytoplankton). Absorption and scattering processes are wavelength-specific and depend upon the spectral characteristics of the water body, which in turn are determined by the combination of the spectral characteristics of pure water and any impurities within the water. Impurities are DOC, suspended sediments (both organic and inorganic) and phytoplankton.

Water absorbs a relatively small proportion of visible irradiance at low wavelengths, with its absorption coefficient increasing approximately exponentially with increasing wavelength. DOC absorbs greatly at short wavelengths, with an exponential decline with increasing wavelength (Kirk, 1994). Non-planktonic suspended sediment generally has a fairly constant spectral signature, although there is often a small decrease in reflectance with increasing wavelength (Iturriaga and Siegel, 1989).

Absorption by phytoplankton is wavelength specific (Daviescolly, *et. al.*, 1986; Daviescolly et al., 1988). Absorption coefficients are relatively great from 400 to 500 nm as a result of the pigments chlorophyll-*a*, β-carotene and zeaxanthin, and for cyanobacteria at 630 nm as a result of the pigment phycocyanin. Absorption coefficients are relatively small from 500 to 600 nm.

On the basis of their optical characteristics, water bodies may be classified as Case 1 or Case 2 (Jerlov, 1976). Case 1 waters contain low concentrations of other water quality parameters, so chlorophyll-*a* dominates the reflectance spectrum. Case 2 waters contain relatively greater concentrations of other optical water quality parameters, so chlorophyll does not dominate the reflectance spectrum. Methods of retrieving information on the chlorophyll-*a* content of a lake depends not only on the

absolute chlorophyll-*a* concentration, but also on chlorophyll-*a* concentration relative to the concentration of other water quality parameters.

2.5.1.2 Chlorophyll indices

Three different approaches may be used to determine water quality by remote sensing (Morel and Gorden, 1980): empirical; semi-empirical; and analytical. Empirical approaches, as used by Carpenter and Carpenter (1983) and Chacon-Torres *et al.* (1992), are based upon statistical relationships between irradiance and water quality. Semi-empirical approaches, as used by Stumpf and Tyler (1988) and Viscum Jørgensen (1999), are based upon a combination of statistical relationships and *a priori* knowledge of the reflectance characteristics of the water quality property. The semi-empirical method has proven most common because it remains fairly simple and yet has more scientific validity than the empirical approach in that it is less likely to produce spurious relationships. This approach often involves the use of spectral indices. Analytical approaches, as used by Dekker (1992a), are based upon knowledge of the optical water quality properties, and involve process modelling, such as solving of the radiative transfer equation, to link irradiance to water quality.

Relative chlorophyll-*a* concentration has commonly been estimated using spectral indices. These are ratios of the radiance in a waveband in which chlorophyll reflects greatly to a waveband in which chlorophyll absorbs greatly. Spectral indices have several advantages over single-waveband methods. Firstly, atmospheric effects are minimised because both channels are similarly affected to approximate extents, so atmospheric correction may not be necessary. Secondly, changes in the ambient light field are minimised, so comparisons between different images may be broadly applicable. Thirdly, variation of smaller magnitude may be resolved.

In deriving a chlorophyll index, it is necessary to take into account the presence of other water quality properties which may obscure the signal from chlorophyll-*a*, and the relationship between the spectral resolution of the sensor and the absorption and reflection features of the chlorophyll-*a*. Three areas of the electro-magnetic spectrum may effectively be used for detecting chlorophyll-*a* concentration (George 1997). Firstly, a *ratio of the phytoplankton reflectance peak to the phytoplankton*

absorption peak (550-570 nm / 430-450 nm) may be used. This was identified by Clarke *et al.* (1970), who found that as phytoplankton concentration increased, there was a relative reduction in irradiance in the blue part of the spectrum, and a relative increase in irradiance in the green part of the spectrum. However, because this may be noisy and may require atmospheric correction, a modification can be used: the ratio of the phytoplankton reflectance peak to the caretonoid absorption peak (550-570 nm / 480-500 nm) which is less sensitive to atmospheric effects. Secondly, the *amplitude of the main chlorophyll absorption peak* (550-570 nm / 660-670 nm) may be used. Thirdly, the *amplitude of the 'fluorescence' peak* (690-710 nm / 660-670 nm) may be used. The use of fluorescence has been criticised by Harris (1980b) because it is not strongly positively correlated with phytoplankton biomass, being also dependent upon other factors such as cell age. The optimal ratio is dependent upon both absolute chlorophyll-*a* concentration, and chlorophyll-*a* concentration relative to other lake water quality properties.

In analysing CASE 1 waters in the English Lake District with the Airborne Thematic Mapper (Appendix C1), George (1997) found that the optimal use of any index depended upon chlorophyll concentration. For lakes with less than 10 mg chlorophyll-*a* m^{-3}, waveband ratios based on the ratio of the phytoplankton reflectance peak to the phytoplankton absorption peak had the greatest correlation with chlorophyll concentration. For lakes with greater than 10 mg chlorophyll-*a* m^{-3}, waveband ratios based on the amplitude of the main chlorophyll absorption peak had the greatest correlation with chlorophyll concentration. Similarly, Gordon *et al.* (1983), using *Coastal Zone Color Scanner* data, found that for marine waters containing low chlorophyll concentrations the optimal ratio was that based on the phytoplankton reflectance peak to the phytoplankton absorption peak, but for greater chlorophyll concentrations the optimal ratio was that based on the amplitude of the 'fluorescence' peak.

In analysing CASE 2 water in the Netherlands with the Compact Airborne Spectrographic Imager (Appendix C2), Dekker (1993) used a chlorophyll index based on the amplitude of the fluorescence peak (706 nm / 676 nm) to determine chlorophyll concentrations in the Loosdrecht and Northern Vecht lakes (Netherlands) because greater concentration of DOC in these lakes made the use of waveband

ratios at short wavelengths ineffective.

2.5.1.3 Errors in remote sensing

Numerous sources of error exist with remote sensing of water quality. Surface waves alter the spectral characteristics of outgoing irradiance (Han and Rundquist, 1998). Reflectance of the lake bed (Ester and Holloway, 1992) or macrophytes (Armstrong, 1993) may also contribute to the outgoing irradiance. The atmosphere affects the irradiance reaching the sensor. The extent to which these errors affected the estimates of spatial distributions in this thesis is discussed in Section 9.2.1.

2.5.2 'Surface' sampling

Lake sampling involves physical contact measurement of properties of the lake. The main advantages of sampling are that it is possible to determine 'absolute' values of chlorophyll-*a* or phytoplankton concentration and that it is possible to determine the vertical distribution. Remote sensing when used alone cannot provide this information unless processed using analytically derived algorithms.

There are two main limitations to the information that may be provided by sampling. Firstly, achieving a spatially continuous coverage is not possible, so the sample estimate may be unrepresentative of the population (Hanna and Peters, 1991). Secondly, there is usually more error in determining the location of observations. Some of the issues concerning sampling in lakes have been referred to in George (1981b). The accuracy of estimates of the population from a sample can be increased with geostatistical modelling (Appendix F).

2.6 Analysing spatial distributions: geostatistics and qualitative interpretation

The detection of phytoplankton, by itself, does not provide information on the spatial distributions of phytoplankton without some further analysis. There are many approaches that may be used to analyse a spatial distribution (Davis, 1986), and a discussion of all is beyond the limits of this thesis. It is the intention now, however, to provide the background to the two main approaches which are used in this thesis:

geostatistical analysis and qualitative interpretation.

2.6.1 Geostatistics

Geostatistical analysis provides the ability to quantify scales of spatial variation using the coefficients of models fitted to functions of the variation. The key to geostatistics is the concept of the *regionalised variable* (Matheron, 1971). A regionalised variable is one realisation of a random function (a spatial set of random variables). Regionalised variables have properties intermediate between deterministic and random variables. That is, there is continuity from point to point, but this continuity is of such a complex nature that it may be difficult to identify and impossible to model deterministically. A statistical model is therefore required to model their spatial dependence.

Scales of spatial variation of a regionalised variable are quantified using the *variogram*. The variogram is a continuous function of the variance between the values of a variable separated by vectors (or *lags*) of distance and direction. If structure exists, then variances will be dependent on lag; if structure does not exist, then variances will be independent of lag. Modelling scales of spatial variation may be an end in itself. Alternatively, models of the scales of spatial variation may be used to estimate unknown values, simulate spatial variation or optimise sampling strategies (Atkinson 1991; Atkinson *et al.*, 1992; Atkinson et al., 1994; Simmard et al., 1992) (Appendix F).

To estimate the variogram it is necessary to have a sufficient number of data, a suitable algorithm for estimating a sample variogram from the data, a suitable mathematical model to describe the main features of the variogram, and a method of fitting the model that allows different weights to be applied to different parameters of the model.

i. Sufficient number of data

A sample of 200 observations may be sufficient if the variation is relatively isotropic, although a greater sample size is required if variation is anisotropic (Oliver and Webster, 1991).

ii. The sample variogram

The *sample variogram* is estimated as follows:

$$\hat{\gamma}(\mathbf{h}) = \frac{1}{2m(\mathbf{h})} \sum_{i=1}^{m(\mathbf{h})} \left\{ z(\mathbf{x}_i) - z(\mathbf{x}_i + \mathbf{h}) \right\}^2 \qquad (2\text{-}18)$$

where $m(\mathbf{h})$ is the number of pairs of observations, $\mathbf{h}$ is the lag and $z(\mathbf{x}_i)$ is the observed value at point $\mathbf{x}_i$. If the directional component of the lag is determined then it is possible to analyse the effect of direction as well as that of distance on variance.

iii. The variogram function

The sample variogram does not show continuously how semivariance varies as a function of lag, and so it may be necessary to fit a mathematical model: the *variogram* or *variogram function*. The model that is fitted must be conditional negative semi-definite (CNSD) in at least as many dimensions as there are dimensions in the data (McBratney and Webster, 1986). Models may be transitive such that a maximum variance is reached at a finite lag, or unbounded. Transitive models are so-called because the random function, from which the regionalised variable is a realisation, is based on a zone of transition of the overlap of two hypothetical blocks. The semivariance as a function of lag depends upon the proportion of overlap between the two blocks. A one-dimensional transitive model is the linear model with sill (in which the blocks are lines); a two-dimensional transitive model is the circular model (in which the blocks are circles); and three-dimensional transitive models include the spherical model (in which the blocks are spheres) and the exponential model (in which the blocks vary in size at random). Unbounded models are so-called because no maximum variance may be identified. Unbounded models include the linear model without sill and the power model.

iv. Fitting the model with different weighting parameters

Model parameters may include: the nugget variance, c_0, (the non-spatially dependent semivariance which, by definition, is constant at all lags); the spatially dependent variance, c_1, defining the difference between the maximum semivariance (at the sill) and the non-spatially dependent semivariance; and the range, a_1, defining the maximum spatial scale at which the data are spatially dependent. Further parameters

that may be derived are: the sill variance ($c_0 + c_1$) and the *signal-to-noise* ratio (c_0 / c_1). Values of these parameters may be determined by several techniques, including least-squares approximation and maximum likelihood estimation (McBratney and Webster, 1986). Alternatively, models may be fitted by eye.

If the intention is solely to determine at what scales spatial variation is occurring rather than the estimation of unknown values, simulation of spatial variation or the optimisation of sampling strategies, it may only be necessary to estimate the sample variogram and not fit a model.

The scale and shape of the variogram provide information on the scales at which variation occurs, but they do not provide definitive information on other characteristics of the spatial distribution, such as pattern. This is of benefit if the object of investigation is solely to investigate scales of spatial variation. However, if spatial distribution is being investigated, it is also necessary to look at pattern (as different patterns may have identical scales of spatial variation).

2.6.2 Qualitative interpretation

Interpretation of pattern qualitatively has been used in many different areas of remote sensing. Qualitative interpretation has particular relevance in looking at spatial distributions of fluid properties (atmospheres, oceans and lakes) because the patterns of some of these distributions may be extremely complex, and may not lend themselves to precise characterisation through statistics. Patterns that may be particularly informative are mushroom-like structures which may be indicative of surface eddying (Victorov, 1996), sharp gradients which may be indicative of shearing (Uncles *et al.*, 1999), and gentler gradients which may be indicative of upwelling (Bychkova *et al.*, 1985; Murty *et al.*, 1998). The exact methods of qualitatively interpreting remotely sensed images as used in this thesis are explained in more detail in Section 3.2 and their disadvantages are explained in Section 9.2.1.

Analysis of pattern may be very useful as a means of determining the processes by which scales of spatial variation are caused. For example, Langmuir circulation eddies will have little effect on the variogram as they are only found in certain parts

of lakes and their effect on the overall spatial distribution of surface chlorophyll-*a* concentration or temperature may be negligible. However, the orientation of Langmuir circulation 'streaks' may help in estimating surface current directions, which may help to explain anisotropy in the scales of spatial variation.

2.7 Producing spatial distributions: process modelling

2.7.1 CFD modelling

In the last half century, there has been a change in the approach used to describe and estimate hydraulic properties within lakes. Until the 1950s, *classical hydraulic* approaches were dominant. Here, specific properties of the system were described and estimated through the use of empirically derived relationships (some of the established relationships that have been described in Section 2.2). From the 1960s, *computational fluid dynamics* (CFD) approaches have been dominant. CFD may be defined as the 'analysis of systems involving fluid flow, heat transfer and associated phenomena such as chemical reactions by means of computer based simulation' (Versteeg and Malalasekera, 1995). Anything more than a cursory treatment of the subject is not possible here due to space-constraints (a detailed discussion is given by Ferziger and Peric, 1996). However, some description of the general procedure used in CFD to solve fluid problems is necessary because CFD forms such an intrinsic part of this thesis. The remainder of this section describes the main elements involved in the operation of a CFD model: firstly, the *formulation of the grid system* which contains the unknown field variables (such as velocity vectors); secondly, the *establishment of the governing flow equations*; thirdly, the *discretisation of the flow equations* by substitution of algebraic approximations; and fourthly, the *solution of the algebraic equations*.

i. Formulation of the grid system

In a CFD model, the fluid continuum is divided into an array (or *grid*) of between one and three dimensions (usually two or three), with the equations of the CFD model being solved for each grid cell. Two commonly used systems are the *finite difference scheme* and the *finite element scheme*. In the finite difference scheme,

grids are orthogonal; in the finite element scheme, grids are non-orthogonal (Figure 2-1). In the finite difference system, field properties are described by point observations at the node points of the grid; in the finite element system, piecewise functions are used on elements to describe the field properties. A newer system - *the finite volume scheme* – has the same grid characteristics as the finite element scheme, but involves a slightly different and more efficient method of discretisation.

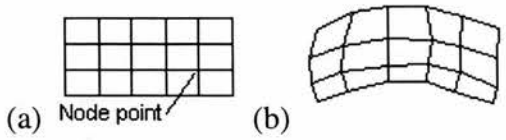

Figure 2-1. Grid systems used in CFD models: (a) orthogonal finite difference grid; (b) non-orthogonal finite element or finite volume grid.

ii. Establishment of the governing flow equations

A set of governing flow equations, based on the principles of mass, momentum and energy conservation, provide a mathematical basis for describing the fluid flow and heat transfer occurring within the fluid continuum:

- ***Mass Conservation (Newton's Law of Motion)***

  The law of mass conservation states that the rate of increase of mass in a fluid element is equal to the net rate of flow of mass into that element.

- ***Momentum Conservation (Newton's Second Law of Motion)***

  The law of momentum conservation states that the rate of increase of momentum of a fluid element is equal to the sum of forces acting on that fluid element. The momentum equation is divided into components corresponding to x, y and z dimensions.

- **Energy Conservation (First Law of Thermodynamics):**

  The law of energy conservation states that the rate of energy increase of a fluid element is equal to the sum of the net rate of heat added to that element and the net rate of work done on that fluid element:

From the combination of the governing flow equations, the Navier-Stokes equations are derived. These are a set of six partial differential equations describing the mass,

three momentum components, internal energy and equations of state of a fluid continuum. For conditions found in lakes, flow will almost certainly be turbulent, so it is common to use the Reynolds' averaged versions of the equations (that is, Navier-Stokes equations for turbulent flow).

iii. Discretisation of the flow equations to produce algebraic equations.

The main aim of discretisation is 'to transform the partial differential equation into a new equation where the variable in one cell is a function of the variable in the neighbouring cells' (Olsen 1997). Discretisation methods include the First-Order Upstream Scheme, the Power-Law Scheme, the Second-Order Upstream Scheme, and the Quick Scheme. Discretisation may produce errors if the flow is not aligned with the grid. These errors are termed *false diffusion* because they have a diffusion-like appearance.

iv. Solution of the algebraic functions.

The algebraic equations that have been produced by discretisation can be solved by a variety of methods: *direct* or *indirect* (iterative). Direct methods involve matrix inversion or Gaussian elimination. The principles of matrix inversion are relatively simple, but require greater computational power. Iterative methods involve the guessing of properties, solving the discretised equations with the guessed properties, and using estimated residual to refine the initial guesses (with the process continuing until convergence). Several methods exist for the solution of algebraic equations. Typical iterative schemes include the SIMPLE (Semi-Implicit Method for Pressure-Linked Equations) algorithm (Patankar, 1980).

CFD techniques have been applied to the study of hydrometry and water quality within many lakes. Two-dimensional depth-averaged models have been used effectively when sub-surface return flows are not dominant: John *et al.* (1995) have used a finite-difference model to simulate circulation in Long Lake, Canada, and Zacharias and Ferentinos (1997) have used a finite-volume model to simulate circulation in Lake Trichonis, Greece, with reasonable agreement between measured and simulated flows. When sub-surface return flows have made a significant contribution to flows, it has been necessary to use three-dimensional models.

Simons (1974) used a three-dimensional finite difference model to simulate circulation in Lake Ontario, Canada, and Falconer *et al.* (1991) have used a three-dimensional finite difference model of Esthwaite Water, UK.

Water quality components have been incorporated into some models. Carrick *et al.* (1994) used a three-dimensional finite difference model to simulate sediment circulation in Lake Okeechobee, USA, with the simulation being verified using National Ocean and Atmospheric Administration Advanced Very High Resolution Radiometer (NOAA AVHRR) imagery. Huttula *et al.* (1996) used a three-dimensional finite difference model to simulate oxygen, phosphorus and phytoplankton circulation in Lake Pyhaselka, Finland. However, the water quality components that have been used were relatively simplistic when recent advances in biological modelling are considered.

2.7.2 Biological modelling

As with CFD modelling, there have been advances in the nature of phytoplankton modelling within recent years. In most cases, the emphasis has been on process models although other approaches involving statistics or neural networks have been used (Whitehead *et al.*, 1997). Usually, process models are based around coefficients that have been determined by laboratory analysis.

Rising velocities are often estimated through Stokes' equation (Section 3.3.3.2). Several models for use with cyanobacteria estimate cell density, which is an integral part of Stokes' equation, as a function of irradiance (Kromkamp and Walsby, 1990; Howard *et al.*, 1995, Belov and Giles, 1997). More recently, estimates of cyanobacterial density have been based upon the conversion of photosynthetic products into cell growth, cell ballast and cell maintenance.

Several approaches have been used to model phytoplankton specific growth rates dynamically. Some approaches have related rates to irradiance or nutrient concentration according to Michaelis-Menton kinetics (Moloney and Field, 1991, Howard *et al.*, 1995). Some models have incorporated cell death as well as specific growth rates as a way of increasing the accuracy with which net population growth is estimated (for example, Belov and Giles, 1997).

Like CFD models, biological models also vary in dimensionality. Many are only one-dimensional, often looking at change in phytoplankton concentration as a function of depth. The SCUM series of models of Howard (1993b and 1997) approach three-dimensionality by allowing horizontal migration of phytoplankton from one cell into horizontally neighbouring cells. However, although the biological component of the model is relatively advanced, migration in the horizontal dimension occurs pseudo-randomly. This is unlikely to occur in lakes.

3 Method

3.1 Introduction

The relationships between the spatial dynamics of phytoplankton and the interaction between lake environmental and phytoplanktonic properties were analysed using a two-tiered approach. Firstly, *exploratory analysis* (largely qualitative) of measured spatial distributions was undertaken as a means of identifying some of the main relationships involved. Then, using the relationships identified from the exploratory analysis as general markers for further investigation, relationships were analysed by *process modelling*.

Exploratory analysis involved considering measured spatial distributions (largely from archived data, with distributions determined through remote sensing) and attempting to explain these in terms of prevalent lake environmental and phytoplanktonic properties. Use was made of a large number of Scottish, English and Dutch lakes, involving a wide range of conditions. These conditions were estimated from archived data and empirically derived models. Relationships between spatial distributions and properties were determined qualitatively. Although the qualitative analysis was used as a precursor to process modelling, its intrinsic value as a means of determining relationships is discussed in Section 9.2.

Process modelling involved a three-dimensional CFD model to analyse the relationships involved in determining the *spatial dynamics* (rather than just *spatial distributions*) of phytoplankton. Model formulation is discussed in Section 3.3. Before analysis, model validation through analysis of the sensitivity of its internal boundary conditions was necessary, however (Chapter 6). After calibration, the relationships between the spatial dynamics of phytoplankton and causative processes were investigated by process modelling of real lakes using measured spatial distributions and measured properties (Chapter 7) and hypothetical basins, using user-determined properties (Chapter 8). Process modelling was used because it enabled greater precision in the analysis of the relationships involved in determining

the spatial dynamics of phytoplankton. Process modelling of real lakes was undertaken to determine spatial dynamics in complex real environments, with the measurements of spatial distributions enabling the verification of the simulations. Process modelling of hypothetical basins was undertaken because it enabled greater control as to which features of the spatial dynamics were to be explored (that is, more control over external boundary conditions was possible). The value of this approach is discussed in Section 9.3.

3.2 Exploratory analysis

In the exploratory analysis of relationships, three stages were involved: firstly, the determination of spatial distributions of phytoplankton; secondly, the determination of lake environmental and phytoplanktonic properties; and thirdly, an attempt to relate the spatial distributions of phytoplankton to the interaction between lake environmental and phytoplanktonic properties.

3.2.1 Determination of spatial distributions of phytoplankton

As mentioned in Section 3.1, the dominant technique of determining the spatial distributions of phytoplankton was remote sensing. Spectrally-based indices for chlorophyll were used to estimate relative chlorophyll-*a* concentrations. The emphasis with this approach was that it was not necessary to provide an accurate estimation of absolute chlorophyll-*a* or phytoplankton concentrations. Rather, the emphasis was on determining when and where variation was occurring. The chlorophyll indices used were lake-specific (Section 4.2).

Spatial distributions of phytoplankton were characterised qualitatively. Where appropriate, the variogram was used to investigate scales of spatial variation. Appropriate uses of the variogram were, firstly, for comparing spatial distributions within the same lake at different times, and secondly, for comparing concurrent spatial distributions in different lakes. Variograms were computed using the *Geostatistical Software LIBrary (GSLIB)* (Deutsch and Journel, 1992). Omnidirectional variograms were used instead of directional variograms because directional variograms were much noisier (especially at greater lags), being based upon fewer observations for estimating semivariance for a given lag.

3.2.2 Determination of lake environmental and phytoplanktonic properties

Properties of the phytoplankton species were determined from the literature using archived data (when available). Lake environmental properties were determined from two sources: firstly, archived data were used, either alone or in empirical modelling to estimate new environmental properties; and secondly, lake environmental properties could be estimated qualitatively from the remotely sensed images.

i. Estimation of flow properties by empirical modelling

Data from weather stations provided approximate estimates of wind regimes at the lakes during the time around image acquisition. From this, it was possible to estimate flow properties of the water such as convection and turbulence from empirical models.

- ***Current speeds***

  With wind speeds less than 4 m s^{-1}, surface current speeds were estimated according to the formula of Haines and Bryson (1961) (Equation 2-5). With wind speeds of between 4 and 10 m s^{-1}, the surface current speed was estimated as 1.5 % of the wind speed (after the relationship determined by Smith, 1979). The depth of frictional resistance was estimated according to the method of Smith (1979) (Equation 2-6), although this could only be applied if the effective depth of the lake (the depth of the thermocline) was greater than the depth of frictional resistance.

- ***Depth of mixed layer***

  The depth of the mixed layer was estimated according to the formula of the U.S. Army (1962) (Equation 2-14). In this way it was possible to infer the vertical distribution of the phytoplankton.

ii. Estimation of flow properties by qualitative analysis of remotely sensed images

Pattern in the chlorophyll or thermal images of the lake were used to infer surface current directions. Patterns included: Langmuir circulation, diffusion of inflows, and

free turbulent flows and shearing patterns around morphometric obstructions (promontories and islands).

Thermal image data were used to delineate areas of downwelling and upwelling when thermal stratification was present: upwelling of colder water from deeper within the water column reduces surface temperatures.

Additionally, aerial photographs were acquired concurrently with several of the multispectral scanner images. From these, surface current directions were estimated from the alignment of waves and shearing fronts (if present), and a crude estimate of the surface velocity of the water was possible using the presence or absence of waves. Additionally, if clouds were present in the image, it was possible to attempt verification of wind directions as measured at the weather stations through qualitative analysis of the change in cloud positions between successive images.

3.2.3 Establishment of relationships

The relationships between spatial distributions of phytoplankton and causative processes were assessed qualitatively. The advantages and disadvantages of this approach are discussed in Section 9.2.3.

Initially, a lake-by-lake case-study approach was used, rather than one involving comparison between different lakes. Inter-lake comparisons were difficult for two reasons. Firstly, spatial distributions of phytoplankton depended on a great range of causative processes, and even though a fairly large sample of lakes was used, it was not possible to find lakes that shared enough similar properties to enable investigation of a change in a given property. For example, it may be difficult to quantify the effect of the size of a lake on phytoplankton spatial distributions by comparing the spatial distributions within large and small lakes as they may experience different irradiance environments or have different types of phytoplankton. Secondly, it was necessary to use different techniques for estimating spatial distributions of phytoplankton, so estimated spatial distributions will have had different errors, and exacting approaches for comparing lakes (for example, by comparing their variances) would have had little statistical 'soundness'. Images were acquired by different sensors (with different spatial and spectral resolutions),

different chlorophyll indices were used (because it was necessary to reduce the effect of other water quality properties), and atmospheric correction was not possible (because of a lack of concurrent data on atmospheric characteristics). For a given spatial distribution, a change in any one of the techniques by which the spatial distribution was estimated would result in a change in the estimate.

The exploratory analysis was therefore limited in the information that it could provide, and merely acted as a precursor to process modelling.

3.3 Process modelling

3.3.1 Introduction

For process modelling, it was necessary to have a model that was able to simulate a wide variety of lake environmental and phytoplanktonic properties. Most commercial CFD models have limited application for phytoplankton modelling, and do not include recent advances in phytoplankton modelling such as buoyancy changes. It was therefore decided to take an existing public domain package, and to modify it so that is was adequate for the purposes of this study. The model chosen was SSIIM1.5 (Simulation of Sediment In water Intakes with Multiblock option) (Olsen 1997), which had been designed to model flow velocities and distributions of inorganic suspended sediments in rivers and reservoirs under the influence of flushing (Olsen, 1998). With the assistance of its author, a more advanced model was produced: SSIIM2.0. The emphasis in model formulation was to create a model that was able to simulate a diverse range of hydraulic and biological properties, yet still retain enough simplicity to allow it to simulate such properties on the basis of the quality of the data available for establishing boundary conditions.

3.3.2 Characteristics of SSIIM1.5

The SSIIM1.5 model was based on a three-dimensional non-orthogonal multiblock grid. This, therefore, had optimal grid characteristics: a three-dimensional grid enabled modelling of field properties in both horizontal and vertical dimensions, and non-orthogonality (intersections did not have to be at right angles) and the multiblock option (the final grid was composed of a composite of smaller grids)

enabled detailed coverage of complex morphometries.

The motion of water was described by the Navier-Stokes equations for turbulent flow:

$$\frac{\partial U_i}{\partial t} + U_j \frac{\partial U_i}{\partial x_j} = \frac{1}{\rho_w} \frac{\partial}{\partial x_j} \left(P\delta_{ij} - \rho_w \overline{u}_i \overline{u}_j \right) \tag{3-1}$$

where U_i is the Reynolds-averaged velocity, u is the fluctuating velocity caused by turbulence, t is time, x is a space variable, P is pressure, ρ_w is water density i and j are the space dimensions (summed in all directions), and δ is the Kroneker delta term. The first term on the left is the transient term which is solved by an implicit method, the second term on the left is the convective term which is solved by the first-order upwind scheme, the first term on the right is the pressure term, and the last term on the right is the Reynolds stress term. This stress term was modelled by the Boussinesq approximation:

$$-\rho \overline{u_i u_j} = \rho \nu_T \frac{\partial U_i}{\partial x_j} + \frac{2}{3} k \delta_{ij} \tag{3-2}$$

where ν_T is the eddy viscosity which is estimated by the turbulence model. SSIIM1.5 provided several turbulence models for estimation of eddy viscosity. The default model was the standard k-ε model:

$$\nu_T = c_\mu \frac{k^2}{\varepsilon} \tag{3-3}$$

where k is the turbulent kinetic energy, ε is the rate of dissipation and c_μ is a constant (0.09). Additional models included the zero-equation model:

$$\nu_T = 0.11 D_L u_* \tag{3-4}$$

where u_* is the wind-induced shear velocity.

Suspended sediment transport was estimated by the convection-diffusion equation for sediment concentration, c:

$$\frac{\partial c}{\partial t} + U_j \frac{\partial c}{\partial x_j} + w \left(\frac{\partial c}{\partial x_z} \right) = \frac{\partial}{\partial x_j} \left(\Gamma \frac{\partial c}{\partial x_j} \right) \tag{3-5}$$

w is the rising velocity of the suspended sediment and Γ is the turbulent mixing coefficient. Γ was modelled as:

$$\Gamma = \frac{F / A}{dc / dx} \tag{3-6}$$

where $\bar{F}$ is the flux and A is the surface area of a cell.

Discretisation was performed by the second order upwind scheme (Middleman, 1998).

3.3.3 Modification of SSIIM1.5 to SSIIM2.0

Modifications to the SSIIM1.5 model in the creation of SSIIM2.0 as part of this thesis involved the inclusion of routines to model wind stress on the lake and Coriolis acceleration in the hydrodynamic component, and the addition of a biological component (the inclusion of routines to model phytoplankton rising velocities as a result of buoyancy or motility, and specific growth rates).

3.3.3.1 Modifications to the hydrodynamic component

i. Addition of a wind stress component

Wind shear stress was estimated as a function of friction coefficient (C_D), air density (ρ_a) and wind speed (W):

$$\tau = C_D \rho_a W^2 \tag{3-7}$$

The friction coefficient was calculated according to one of several formulae. The Bengtsson formula (Bengtsson, 1973) had a constant friction coefficient.

$$C_D = 1.1 \times 10^{-3} \tag{3-8}$$

The van Dorn formula (van Dorn, 1953) estimated the friction coefficient as a discontinuous function, taking into account the changing hydraulic properties of the water surface:

$$C_D = 1.1 \times 10^{-3} \qquad \text{for } W < 5.6 \text{ m s}^{-1} \tag{3-9}$$

$$C_D = 1.0 + 1.9 \times \left(1.0 - \left(\frac{5.6}{W}\right)\right)^2 \times 1.0 \times 10^{-3} \qquad \text{for } W > 5.6 \text{ m s}^{-1}$$

The Wu formula (Wu, 1969) had two discontinuities, again taking into account

changes in hydraulic properties:

$$C_D = \frac{1.25}{\sqrt{W}} \times 1.0 \times 10^{-3} \quad \text{for W} < 1.0 \text{ m s}^{-1} \qquad (3\text{-}10)$$

$$C_D = 2.6 \times 10^{-3} \quad \text{for } 1.0 \text{ ms}^{-1} < W < 15 \text{ m s}^{-1}$$

$$C_D 0.5 \times \sqrt{W} \times 1.0 \times 10^{-1} \quad \text{for } W > 15 \text{ m s}^{-1}$$

ii. Addition of a Coriolis term

The Coriolis parameter, U_i, was added to Equation 3-5 to form Equation 3-11.

$$\frac{\partial U_i}{\partial t} + U_j \frac{\partial U_i}{\partial x_j} + \int U_j = \frac{1}{\rho} \frac{\partial}{\partial x_k} \left(P\delta_{ij} - \rho \overline{u_i u_j} \right) \qquad (3\text{-}11)$$

3.3.3.2 Addition of a biological component

i. Phytoplankton rising velocities

Phytoplankton convection and diffusion rates in flowing water were estimated according to Equation 3-11. Phytoplankton rising velocity in a still water column was estimated according to Stokes' Law in the case of passively buoyant diatoms or cyanobacteria, or according to an empirically derived motility equation in the case of actively swimming dinoflagellates. The actual movement of phytoplankton within the grid depended upon both characteristics of the flow and the phytoplankton rising velocity.

- ***Stokes' Law for passive buoyancy***

  Stokes' law was used to estimate the rising velocity for passively buoyant phytoplankton:

$$w = -\frac{2gr^2(p_c - p_w)}{(9\varphi\eta)} \qquad (3\text{-}12)$$

  where w is the rising velocity (positive if the phytoplankton is rising, negative if it is falling), g is the gravitational acceleration, r is the colony radius (Table 3-1), φ is the form resistance, η is the water viscosity, p_w is the water density, and p_c is the phytoplankton density. With diatoms, cell density was assumed to be

constant (Table 3-1). With cyanobacteria, cell density was estimated as a function of cell carbohydrate concentration according to the method of Kromkamp and Walsby (1990):

$$p_{c2} = p_{c1} + t\left\{c_1\left[\frac{I_z}{K_i + I_z}\right]\right\} - c_2 I_p - c_3 \qquad (3\text{-}13)$$

where p_{c1} is the density at t_1 (time one), p_{c2} is the density at t_2 (time two), c_1 is the rate of constant density increase ($2.2*10^{-3}$ kg m^{-3} s^{-1}), $-c_2$ is the rate of constant density decrease ($2.78*10^{-7}$ kg m^{-3} s^{-1}), $-c_3$ is the minimal rate of density decrease ($3.83*10^{-4}$ kg m^{-3} s^{-1}), K_i is the half-saturation irradiance (units: μE m^{-2} s^{-1}) for a maximum rate of density increase (25 μmol^2 s^{-1}), I_p is the average irradiance (units: μE m^{-2} s^{-1}) experienced in the previous day and t is the time interval (s). According to this, cell density depended upon the balance between the rate of increase of carbohydrate due to photosynthesis (c_1), and the rate of decrease due to respiration (c_2 and c_3). In all cases, density was confined within maximum and minimum density limits, as determined from the literature (Table 3-1).

Table 3-1. Density and size parameters of phytoplankton species.

	Species	Mean density (Mg m^{-3})	Min. density (Mg m^{-3})	Max. density (Mg m^{-3})	Cell or colony radius (μm)
Diatoms	*Stephanodiscus astrea*	1.091	NA	NA	13
Cyanobacteria	*Microcystis aeruginosa*	0.994-1.004	0.955	1.07	250

Sources: Reynolds *et al.*, (1981), Reynolds (1984), Howard (1993a). Properties marked NA are not applicable.

Irradiance as a function of depth was estimated according to the Beer-Lambert law (Equation 2-1). The extinction coefficient was estimated as a function of cyanobacterial concentration, from a modification of an empirical relationship established by Bindloss (1976) for diatoms in Loch Leven:

$$\varepsilon = 0.69 + 0.0946c \qquad (3\text{-}14)$$

Sub-surface irradiance was either estimated from measurements (when available) or according to the method outlined in Appendix D.

- ***Motility equation***

  Dinoflagellate motility was modelled as a function of irradiance. Because dinoflagellate swimming velocities are typically two orders of magnitude less than those of water currents, it was decided to estimate swimming velocities for the vertical dimension only. Heaney and Furnass (1980) have shown that dinoflagellates migrate to optimal conditions of approximately 150 μE m^{-2} s^{-1}. Dinoflagellate rising velocities were determined in SSIIM2.0 according to what extent the irradiance at the depth at which they existed differed from the optimum irradiance. They swam towards the depth of optimum irradiance, and had a negative rising velocity if the depth of optimum irradiance was greater than their initial depth, and a positive rising velocity if the depth of optimum irradiance was lesser than their present depth:

$$w = abs\left(\frac{I_{opt} - I_z}{I_{ran}}\right) \times w_{\max} \qquad (3\text{-}15)$$

  where I_{opt} is the optimum irradiance (150 μmolar photons m^{-2} s^{-1}), I_z is the irradiance at the depth of the dinoflagellates, I_{ran} is an irradiance range parameter and $w_{\max}$ is the maximum swimming velocity (m s^{-1}).

  Additionally, dinoflagellates avoid anoxic conditions (Heaney and Talling, 1980), and their vertical movement is reduced by steep temperature or density gradients (Olsson and Edler, 1991). However, it was decided that it was not necessary to include either of these effects as they are only exhibited if dinoflagellates swim across the thermocline. For the lakes in this study, this would not occur because the irradiance environment beneath the thermocline would be unfavourable for their existence, and they would be confined to the epilimnion.

If phytoplankton came into contact with the bed, they were assumed to stay there unless resuspended. Resuspension was estimated as follows (Chapra, 1997):

$$\frac{dc}{dt} = a(\sigma_{bed} - \sigma_{critical})^b \quad (3\text{-}16)$$

where σ_{bed} is the bed shear stress, $\sigma_{critical}$ is the critical bed shear stress and a and b are coefficients.

ii. Phytoplankton specific growth rates

Phytoplankton concentration was estimated as a function of the exponential specific growth rate:

$$c_{t2} = e^{k'} c_{t1} \quad (3\text{-}17)$$

where c_{t1} is the phytoplankton concentration at time t = 1, c_{t2} is the phytoplankton concentration at t = 2, and k' is the exponential specific growth rate (ln units day^{-1}). The exponential specific growth rate was dependent upon several factors: irradiance, nutrient concentration and temperature.

It was assumed that either irradiance or nutrient concentration would be the limiting factor to further growth, so both the *irradiance specific growth rate*, k_i, and the *nutrient specific growth rate*, k_n, were calculated, and the smallest of these was used as a value for k'.

The irradiance specific growth rate was estimated according to Michaelis–Menton kinetics (Dugdale, 1967) as:

$$k_i = k_{\max}\left(\frac{I_z}{K_i + I_z}\right) \quad (3\text{-}18)$$

where $k_{\max}$ is the maximum specific growth rate given nutrient saturation and K_i is the half-saturation coefficient representing the concentration required to sustain a growth rate half the maximum under conditions of no nutrient limitation.

The nutrient specific growth rate was estimated as follows:

$$k_n = k_{\max}\left(\frac{n}{K_n + n}\right) \quad (3\text{-}19)$$

where k_{max} is the maximum specific growth rate given irradiance saturation, K_n is the half-saturation coefficient representing the concentration required to sustain a growth rate half the maximum under conditions of no irradiance limitation, and n is the nutrient concentration (phosphorus in the case of cyanobacteria, and silica in the case

of diatoms). When growth was dependent upon more than one nutrient, nutrient limitation on growth was estimated as the minimum of that for the source terms. The alternative approaches of multiplying the terms or combining the reciprocals of the terms were not used as the former approach produces excessively low growth rates if both terms are limiting, and the latter produces unrealistic results if one is limiting (Chapra, 1997). Nutrients were modelled as passive scalars of the velocity field.

Parameters affecting the growth dependency on irradiance under conditions of nutrient saturation, and growth dependency on nutrients under conditions of irradiance saturation, have been determined by many authors (Table 3-2).

Table 3-2. Growth rates of phytoplankton species.

Class	Species	K_{max}	K_I ($\mu E\ m^{-2}\ s^{-1}$)	K_n ($g\ m^{-3}$)
Diatoms	*Stephanodiscus*	1.18	11	0.73 (silica)
Cyanobacteria	*Microcystis*	0.48	46	0.060 (phosphorus)

Source: Foy et al., (1976), Bruno and McLaughlin (1977), Reynolds *at al* (1981) and Nicklisch and Kohl (1983)

Growth rates were multiplied by the *theta model* to invoke a temperature dependency (Chapra, 1997), using parameters determined by Eppley (1972):

$$k = k\left(k_{20}\theta^{T-20}\right) \tag{3-20}$$

where k_{20} is the growth rate at a 20 °C and $\theta = 1.066$.

4 Study areas and data

4.1 Study Areas

Lakes were chosen from three areas in northern Europe: Scotland, the English Lake District, and the Loosdrecht and Northern Vecht area of the Netherlands. These areas were chosen to provide a sample of lakes representative of the variation that exists between Western European lakes, with mean lake properties varying between areas and lake properties varying within a given area. In addition, a small eutrophic reservoir in Southern Wales (Eglwys Nynydd) was used in process modelling. This was included because there were some detailed archived data for this lake, enabling the establishment of external boundary conditions for running a process model. Characteristics of this lake are described in Section 7.3.

4.1.1 Scottish lakes

Four Scottish lakes were studied: Lochs Lomond, Ness, Awe and Leven (Figure 4-1).

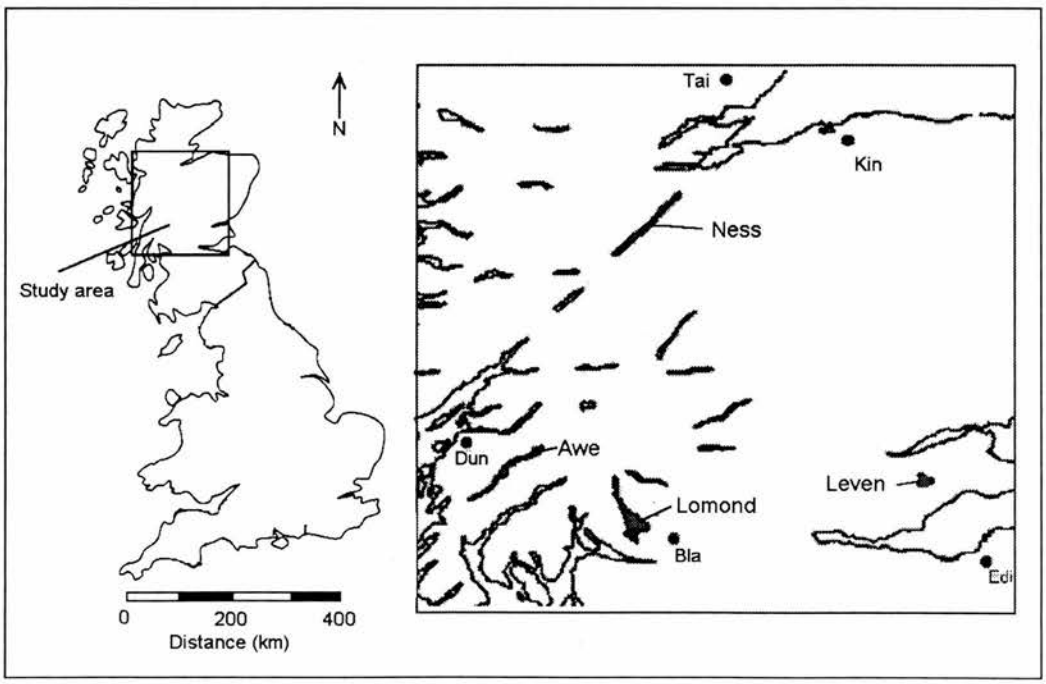

Figure 4-1. Location of selected Scottish lakes. Weather stations are: Tain (Tai), Dunstaffnage (Dun), Kinloss (Kin), Edinburgh Turnhouse (Edi) and Bla (Bairlinnans).

Three of these – Lochs Lomond, Ness and Awe - were formed in glacially eroded valleys in the North West Highlands, resulting in an orientation that reflects the north-east to south-west glacial erosional geomorphology (Curran and Poodle, 1994; Pierce, 1999). Loch Leven, located in the lower terrain of the east of Scotland, differed in that it was formed in a shallow depression amongst glacial deposits (Kirby 1972/1973).

Although there is great variation between Scottish lakes in terms of their morphometric and ecological characteristics, Scottish lakes generally are large and elongated (Table 4-1; Appendix B) and have low nutrient status (Table 4-2). An exception is Loch Leven, which has a higher nutrient concentration and a non-elongated morphometry.

Table 4-1. Morphometry of selected Scottish lakes.

	Area (km^2)	Volume (Mm^3)	Max. length (km)	Mean width (km)	Elongation	Max. depth (m)	Mean depth (m)
Lomond	71.7	2630	36.4	1.95	18.6	190	37
Ness	56.4	7450	39	1.45	26.8	230	132
Awe	38.4	1230	41	0.94	43.6	93.6	32
Leven	13.3	52	5.9	2.25	2.6	25.5	3.9
Mean	**44.9**	**2840**	**30.5**	**6.59**	**22.9**	**143.7**	**51.2**

Source: Murray and Pullar (1910) and Maitland *et al.* (1994)

Table 4-2. Biological status of selected Scottish lakes

	Trophic status	Mean chlorophyll-*a* concentration ($mg\ m^{-3}$)
Lomond	Oligotrophic	2
Ness	Oligotrophic	1.5
Awe	Oligotrophic	1.8
Leven	Mesotrophic	3.5

Source: Maitland (1981)

The Lochs Lomond, Ness and Awe are situated in deep valleys. These valleys often affect wind direction by forcing winds along the valley profile (Smith *et al.*, 1981). Because Loch Leven is situated in less variable topography, however, there is less influence on synoptic wind directions, so winds are more variable in direction.

Studies of the spatial distributions of chlorophyll-*a* and phytoplankton concentration within Lochs Lomond, Ness and Awe were undertaken by George and Jones (1987).

Emphasis was placed upon catchment characteristics, which resulted in the existence of long-term macro-scale gradients. Spatial distributions were attributed to differences in growth rates along the length of each lake, these differences resulting from geological and land-use differences in the surrounding sub-catchments. These conclusions have been confirmed by Bailey-Watts and Duncan (1981) and Best and Traill (1994). Other factors, however, including the wind environment, the distribution of stream inflows and outflows, and lake morphometry were seen to have an effect. Jones *et al.* (1995), in a study of Loch Ness, placed more emphasis upon wind regime, describing how different phytoplankton spatial distributions occurred according to the wind direction. There has been less study of the spatial distribution of phytoplankton in Loch Leven. However, Bailey-Watts (1981) has shown that this generally has very little spatial variation in phytoplankton concentration, this near-homogeneity being attributed to wind mixing of the unsheltered small lake.

4.1.2 English Lake District lakes

The English Lake District lakes are a group of lakes situated in the highlands of north-west England. They have a radial drainage pattern (Figure 4-2) that reflects the glacial erosional morphology of the area (Macan, 1970).

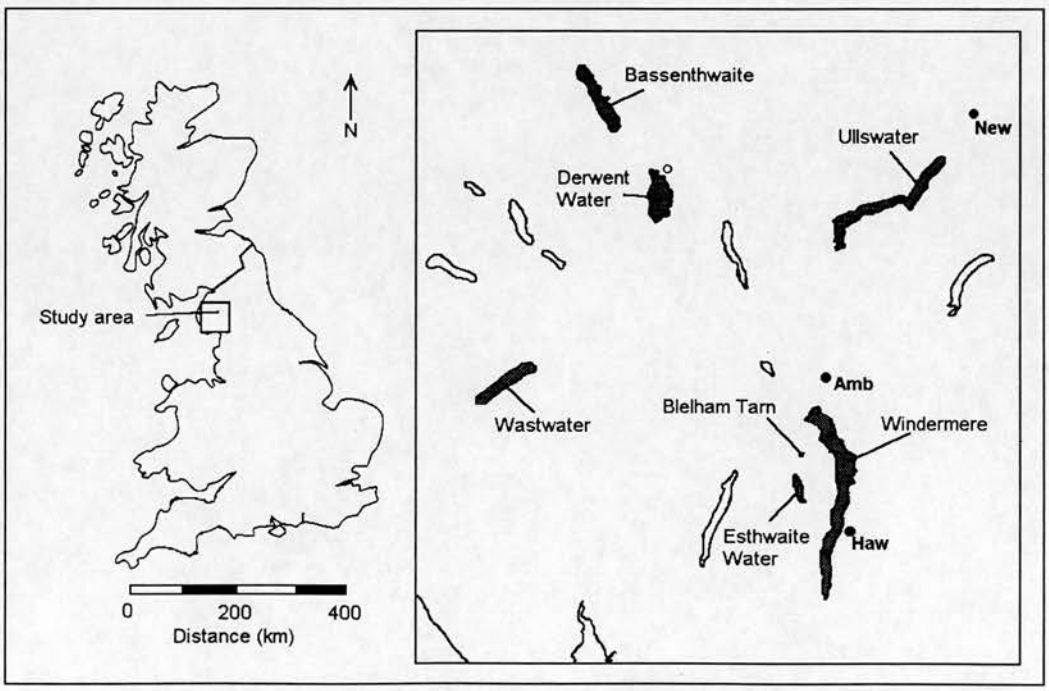

Figure 4-2. Location of selected English Lake District lakes. Weather stations are: Newton Rigg (New), Ambleside (Amb), Haws Wood (Haw).

The English Lake District lakes vary greatly in size (Table 4-3; Appendix B) and nutrient status (Table 4-4). On average, they are smaller than the Scottish lakes. Lakes of the south-eastern side of the district have higher nutrient concentration as this area is more affected by anthropogenic activity.

Table 4-3. Morphometry of selected English Lake District lakes.

	Area (km^2)	Volume (Mm^3)	Max. length (km)	Mean width (km)	Elongation	Max. depth (m)	Mean depth (m)
Windermere	14.79	347	17	0.869	19.5	66.8	23.8
Ullswater	8.087	223	11.8	0.756	15.6	62.5	25.3
Bassenthwaite	5.35	29	6.2	1.190	5.2	21.3	5.5
Derwent Water	5.35	29	4.6	1.160	3.9	22.0	5.5
Wast Water	2.91	117	4.8	0.595	8.1	78.6	41.0
Esthwaite Water	1.0	6.4	2.5	0.45	5.5	15.5	6.4
Blelham Tarn	0.102	0.7	0.8	0.133	6.0	15.1	6.6
Mean	**4.06**	**75.58**	**6.11**	**0.679**	**8.5**	**40.25**	**16.3**

Source: Mill (1895) and Macan (1970).

Table 4-4. Biological status of selected English Lake District lakes.

	Trophic status	Mean chlorophyll-a concentration (mg m^{-3})
Windermere (N)	Mesotrophic	7.0
Windermere (S)	Eutrophic	11.5
Ullswater	Mesotrophic	7.0
Bassenthwaite	Mesotrophic	20-40
Derwent Water	Oligotrophic	NA
Wast Water	Oligotrophic	NA
Esthwaite Water	Eutrophic	25
Blelham Tarn	Eutrophic	12.5

Source: Macan (1970) and George (1997). Properties marked NA are not available.

Most investigation of the spatial distributions of chlorophyll-*a* and phytoplankton concentration in lakes of the English Lake District, has centred on Lake Windermere Ullswater and Esthwaite Water. Long term phytoplankton gradients have been caused by differential growth between basins resulting from different geological and land use characteristics in Lake Windermere (George 1981a; George 1981b) and Ullswater (George *pers. com*). Wind regimes, rather than nutrient gradients, have a

greater effect in Esthwaite Water, with positively buoyant phytoplankton species accumulating downwind, negatively buoyant species accumulating upwind, and vigorous mixing causes macro-scale variation to disintegrate into micro-scale variation (George and Heaney, 1978; George, 1981b; George, 1993).

There has been much less investigation of the spatial distributions within other lakes of the English Lake District: exceptions being George and Charlton (1996), who found very little evidence of spatial variation in Lake Bassenthwaite.

4.1.3 Dutch Loosdrecht and Northern Vecht Lakes

The Loosdrecht and Northern Vecht lakes are a group of lakes situated in close proximity to one another in the central-west Netherlands (Figure 4-3). All the lakes are either anthropogenic in origin or under strong anthropogenic interference (Van Liere et al., 1992; Hofstra and Van Liere, 1992).

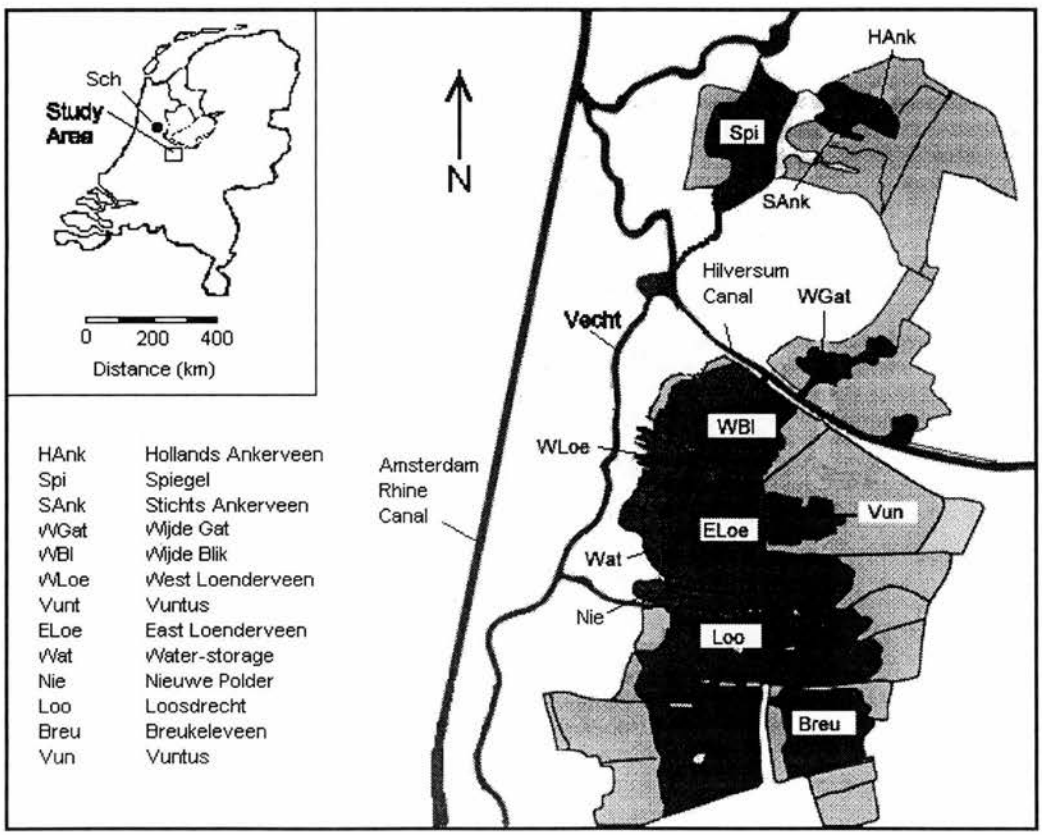

Figure 4-3. Location of selected Dutch Loosdrecht and Northern Vecht lakes. Weather station: Schiphol airport (Sch).

The seven Loosdrecht lakes are adjacent, being separated by dykes. For the purposes of this study the Loosdrecht lakes are divided into two groups. Firstly, there are the central lakes, consisting of the Lakes Loosdrecht, Breukeleveen, Vuntus and Nieuwe Polder. These are interconnected and relatively shallow. Secondly, there are the peripheral lakes, consisting of the Lakes Water-storage, East Loenderveen and West Loenderveen. These are not all interconnected, and range greatly in depth. In this study, the lakes north of the Loosdrecht lakes, which are fed by the River Vecht (Lakes Spiegel, Stichts Ankerveen and Hollands Ankerveen) and the Hilversum Canal (Lakes Wijde Blik and Wijde Gat) are classified as the Northern Vecht lakes. On average, the Loosdrecht and Northern Vecht lakes (Table 4-5; Appendix B) are smaller, less elongated and shallower than the English Lake District lakes. With the exception of Water-storage and Lake Spiegel, the lakes have high trophic status (Table 4-6).

Table 4-5. Morphometry of selected Dutch Loosdrecht and Northern Vecht lakes.

	Area (km^2)	Volume (Mm^3)	Max length (km)	Mean width (km)	Elongation	Mean depth (m)
Loosdrecht lakes						
Loosdrecht	9.79	17.9	5.07	1.93	3.0	1.85
East Loenderveen	2.18	5.1	2.25	0.96	2.3	2.35
Breukeleveen	1.79	2.6	1.77	1.01	2	1.45
Water-storage	1.23	9.8	2.00	0.61	4.1	8
Vuntus	0.88	1.3	1.45	0.60	2.4	1.45
WestLoenderveen	0.6	0.9	1.35	0.44	3.0	1.5
Nieuwe Polder	0.30	0.5	1.19	0.25	7.9	2.1
Northern Vecht lakes						
Wijde Blik	2.9	20	2.16	1.34	1.6	20
Spiegel	2.7	40.0	2.24	1.20	2.4	40
Stichts Ankerveen	1.36	2.0	0.64	2.12	2.7	1.30
Wijde Gat	1.11	1.7	0.89	1.24	2.5	1.15
Hollands Ankerveen	0.97	1.5	1.02	0.95	1.0	1.2
Mean	**2.15**	**8.6**	**1.83**	**1.05**	**2.7**	**6.86**

Source: Dekker *et al.* (1992b)

Table 4-6. Biological status of selected Dutch Loosdrecht and Northern Vecht lakes.

	Trophic status	Secchi depth (m)	Seston dry weight (mg l^{-1})	Mean chlorophyll-a concentration (mg m^{-3})
Loosdrecht Lakes				
Loosdrecht	Eutrophic	0.35	35	125
East Loenderveen	Eutrophic	0.45	23	59
Breukeleveen	Highly eutrophic	0.4	40	125
Water-storage	Oligotrophic	2.25	3	6
Vuntus	Highly eutrophic	0.4	35	130
West Loenderveen	Eutrophic	0.5	17	58
Nieuwe Polder	Highly eutrophic	0.50	18	95
Northern Vecht Lakes				
Wijde Blik	Mesotrophic-eutrophic	1.7	3	30
Spiegel	Oligo-mesotrophic	2.7	3	10
Hollands Ankerveen	Eutrophic	0.45	19	114
Wijde Gat	Highly eutrophic	0.35	28	177
Stichts Ankerveen	Mesotrophic	0.85	7	24

Source: Dekker *et al.*, (1992a)

Although there has been much study of temporal changes in mean phytoplankton concentration (Gons et al., 1992; Van Tongeren et al., 1992), there has been comparatively little study of the spatial distributions of phytoplankton within the Dutch lakes. Dekker *at al.* (1992a) have linked basin-wide trends in Lake Wijde Blik to the inflow of water from the Hilversums Canal, and basin-wide gradients in Lake Water-storage to the inflow of iron-rich water from a dephosphorisation plant. Other lakes were seen to have a more homogeneous spatial distribution. Hydrometry in these lakes, which determined the spatial distributions of phytoplankton, is the combined result of fluvial-forcing and wind-forcing (Engelsen *et al.*, 1992).

4.2 Remotely sensed data

Data from two sensors were used in this thesis: the Daedalus AADS 1268 Airborne Thematic Mapper (ATM); and the Compact Airborne Spectrographic Imager (CASI) (Wilson, 1995). The ATM has eleven channels: five channels in the optical region of the electro-magnetic spectrum (EMS), five channels in the near-to mid-infrared region, and one channel is in the thermal-infrared region. Optical channels are

approximately 50 nm in width, near- to mid-infrared channels are approximately 100 nm in width, and the thermal channel is 4500 nm in width. Channel wavelengths are fixed (Appendix C1). Although this sensor has relatively high spectral resolution in comparison to most satellites, and images created from this sensor often have strong correlations with water quality properties, wavebands are not positioned for optimal remote sensing of water quality (Malthus, 1996). Additionally, the ATM has only 8-bit or 10-bit radiometric resolution (so can gauge irradiant intensity in only 256 or 1024 levels). The CASI has fourteen channels from optical to near-infrared regions of the EMS (Appendix C2). It is superior to the ATM for detecting water quality because of three reasons. Firstly, the CASI wavebands are approximately 20 nm wide, resulting in less averaging of the spectral signature of a surface property. Secondly, channel wavelength ranges are user-determined, and can be positioned for optimal remote sensing of water quality. Thirdly, the CASI has a 16-bit radiometric resolution (so can gauge irradiant intensity in 65536 levels) and can therefore detect variation of smaller magnitude.

All images were geometrically rectified using second-order polynomial transformations between images and 1:50,000 scale maps. Polynomial transformations were established from approximately 50 ground control points for each lake. Nearest-neighbour resampling of pixels was used because this technique retains the original pixel values (Mather, 1987). When statistics were to be obtained from the images, images were degraded to an equivalent spatial resolution (8 m).

i. Remotely sensed images of the Scottish lakes

Images of the Scottish lakes were obtained from NERC archives (acquired by the NERC ATM in 1985) or as part of the NERC Airborne Remote Sensing Campaign in 1997 (Table 4-7). The original intention with the 1997 Campaign was to use CASI data to produce chlorophyll indices because of the greater spectral and radiometric resolution of the CASI sensor. However, the CASI images were affected by severe geometric distortion, considerably affecting their utility for the analysis of structure within the lakes. ATM data, collected concurrently with the CASI, were used because the ATM data were much less affected by geometric distortion. Images were acquired at ground spatial resolutions varying from between 5 and 10 m. Images were acquired for summer dates so that chlorophyll concentrations would be

at a maximum and signal-to-noise ratios maximised, and as near to midday as possible to minimise look-angle effects.

Table 4-7. Remotely sensed images of the Scottish lakes.

Lake	Date	Sensor	Ground spatial resolution (m)	Flightline orientation (°)	Radiometric Resolution
Lomond	29 May 1985	ATM	8	345	8-bit
Ness	3 June 1997	ATM	5	35	10-bit
Awe	23 May 1997	ATM	5	65	10-bit
Leven	11 May 1985	ATM	10	35	8-bit

The four Scottish lakes were Case 1 waters because they contained relatively low concentrations of dissolved organic carbon (DOC) and suspended sediments (SS) so their optical properties were mainly determined by phytoplankton. It was therefore possible to use chlorophyll indices based-upon short wavelength bands to estimate chlorophyll concentrations. Thus, chlorophyll indices were derived from a waveband ratio of ATM 3 (520 – 600 nm) over ATM 2 (450 – 520 nm). This ratio was chosen because it has been found to be the optimal ratio in waters containing low chlorophyll-*a* concentrations and low concentrations of other optical water quality properties (George, 1997).

ii. Remotely sensed images of the English lakes

Images of the English Lakes were obtained from NERC archives (acquired by the NERC ATM in 1987, 1988 and 1994) and obtained from Environmental Agency archives (acquired by the Environment Agency CASI in 1995) (Table 4-8). The 1995 CASI data were less affected by geometric distortion than the 1997 NERC Airborne Remote Sensing Campaign CASI data so could still be used in this thesis. Images were acquired at ground spatial resolutions of between 2 and 4 m.

Table 4-8. Remotely sensed images of the English lakes.

Lake	Date	Sensor	Ground spatial resolution (m)	Flightline orientation (°)	Radiometric Resolution
Ullswater	30 May 1994	ATM	4	Variable	8-bit
	13 July 1994	ATM	4	Variable	8-bit
	26 June 1995	CASI	4	25	16-bit
Wast Water	22 June 1995	CASI	4	45	16-bit
Bassenthwaite	15 June 1995	CASI	4	345	16-bit
Derwent Water	15 June 1995	CASI	4	345	16-bit
Esthwaite Water	24 July 1987	ATM	2	0	8-bit
Blelham Tarn	7 Aug. 1988	ATM	4	20	8-bit

All of the English lakes studied in this thesis were Case 1 waters, again enabling the use of chlorophyll indices based on short wavelengths. For the ATM images, two chlorophyll indices were used. Firstly, a chlorophyll index derived from a waveband ratio of Channel 3 (520 – 600 nm) over Channel 2 (450 – 520 nm) was used for the mesotrophic and oligotrophic lakes. Secondly, a chlorophyll index derived from a waveband ratio of Channel 3 (520 – 600 nm) over Channel 5 (630 – 690 nm) was used for the eutrophic lake Esthwaite Water. These waveband ratios were established as being optimal for these lakes by George (1997). CASI images were acquired using the *Default SeaWifs / Ocean Colour* bandset (Appendix C2). For the CASI images, chlorophyll indices were derived from a waveband ratio of Channel 5 (545 - 565 nm) over Channel 3 (480 – 499 nm).

iii. Remotely sensed images of the Dutch lakes

CASI images of the Dutch lakes were obtained from the Arnold Dekker, of REmote sensing WAterquality NETherlands (REWANET) (Table 4-9).

Table 4-9. Remotely sensed images of the Dutch lakes.

Lake	Date	Sensor	Ground spatial resolution (m)	Flightline Orientation (°)	Radiometric resolution
Loosdrecht Lakes					
Loosdrecht	18 Aug. 1992	CASI	4 m	360	16-bit
East Loenderveen	18 Aug. 1992	CASI	4 m	360	16-bit
Breukeleveen	18 Aug. 1992	CASI	4 m	360	16-bit
Water-storage	18 Aug. 1992	CASI	4 m	360	16-bit
Vuntus	18 Aug. 1992	CASI	4 m	360	16-bit
West Loenderveen	18 Aug. 1992	CASI	4 m	360	16-bit
Nieuwe Polder	18 Aug. 1992	CASI	4 m	360	16-bit
Northern Vecht Lakes					
Wijde Blik	18 Aug. 1992	CASI	4 m	360	16-bit
Spiegel	18 Aug. 1992	CASI	4 m	360	16-bit
Hollands Ankerveen	18 Aug. 1992	CASI	4 m	360	16-bit
Wijde Gat	18 Aug. 1992	CASI	4 m	360	16-bit
Stichts Ankerveen	18 Aug. 1992	CASI	4 m	360	16-bit

Most of the Dutch lakes used in this thesis were Case 2 waters because they contained high concentrations of DOC, which greatly contributed to their spectral characteristics. Therefore, for remote sensing of chlorophyll-*a*, it was necessary to use wavelengths where the effects of DOC were minimal (that is, at greater wavelengths). CASI images of the Dutch lakes were acquired using a bandset determined by Dekker (1993) (Appendix C2). A waveband ratio of Channel 9

(centred on 705 nm) over Channel 7 (centred on 664 nm) was used as a chlorophyll index. In Channel 9 there is a peak in radiance reflectance due to a minimum in the combined absorption curves of algae and water; in Channel 7 there is less upwelling radiance due to an *in vivo* chlorophyll absorption peak. A ratio of the two wavebands has been shown to correlate highly with chlorophyll-*a* concentration (Dekker, 1993).

4.3 Other data

Wind data for around the time of image data acquisition of lakes in the UK were obtained from weather stations supported by the UK Meteorological Office and the Institute of Freshwater Ecology. In most cases, data were obtained from archives at the British Atmospheric Data Centre. Wind data for the Dutch lakes were obtained from the Netherlands Meteorological Institute. Details of the weather data are given in Appendix E, and their locations relative to the lakes are shown in Figure 4-1, Figure 4-2, and Figure 4-3.

Data on phytoplankton spatial distributions, dominant phytoplankton species, thermal profiles, and bathymetry were obtained from the Institute of Freshwater Ecology for the lakes in the UK and the Centre for Limnology for lakes in the Netherlands. Data on the inflows and outflows of Loch Leven were obtained from the Scottish Environmental Protection Agency.

5 Exploratory analysis

5.1 Introduction

This chapter of the thesis involves exploratory analysis of the relationships between the spatial distributions of phytoplankton concentration, as evident in airborne remotely sensed images acquired between 1988 and 1997, and the interaction between lake environmental and phytoplanktonic properties. The three study areas of the Scottish lakes, the English lakes, and the Dutch lakes provide examples of a wide range of causative processes, where spatial distributions of phytoplankton have been linked to basin-wide nutrient gradients, wind events and inflows, respectively.

As a conceptual framework, this chapter is divided into three parts: patchiness as a result of nutrient gradients; patchiness as a result of wind-forced hydrometry; and patchiness as a result of inflow-forced hydrometry. In the first case, macro-scale phytoplankton patchiness is created by differential growth; in the latter two cases, phytoplankton patchiness (at scales from macro to micro) is created by differential displacement. It should be noted, however, that for most of the lakes considered in this thesis, patchiness is the result of a combination of these environmental processes. For example, in a lake where differential growth causes macro-scale patchiness, wind-forcing may still cause patchiness at scales from macro to micro. The identification of a main cause (be it nutrient growth, or wind-forced or inflow-forced hydrometry) does not imply the absence of other causes.

5.2 Patchiness and nutrient gradients

Patchiness caused by nutrient gradients was seen in images of Loch Lomond and Ullswater.

5.2.1 Loch Lomond

Loch Lomond was imaged by the NERC ATM on 29 May 1985 (Figure 5-1 and Figure 5-2).

As seen in Figure 5-1, the mean chlorophyll index values were greater in the southern basin (approximately 0.8) than in the northern basin (approximately 0.7).

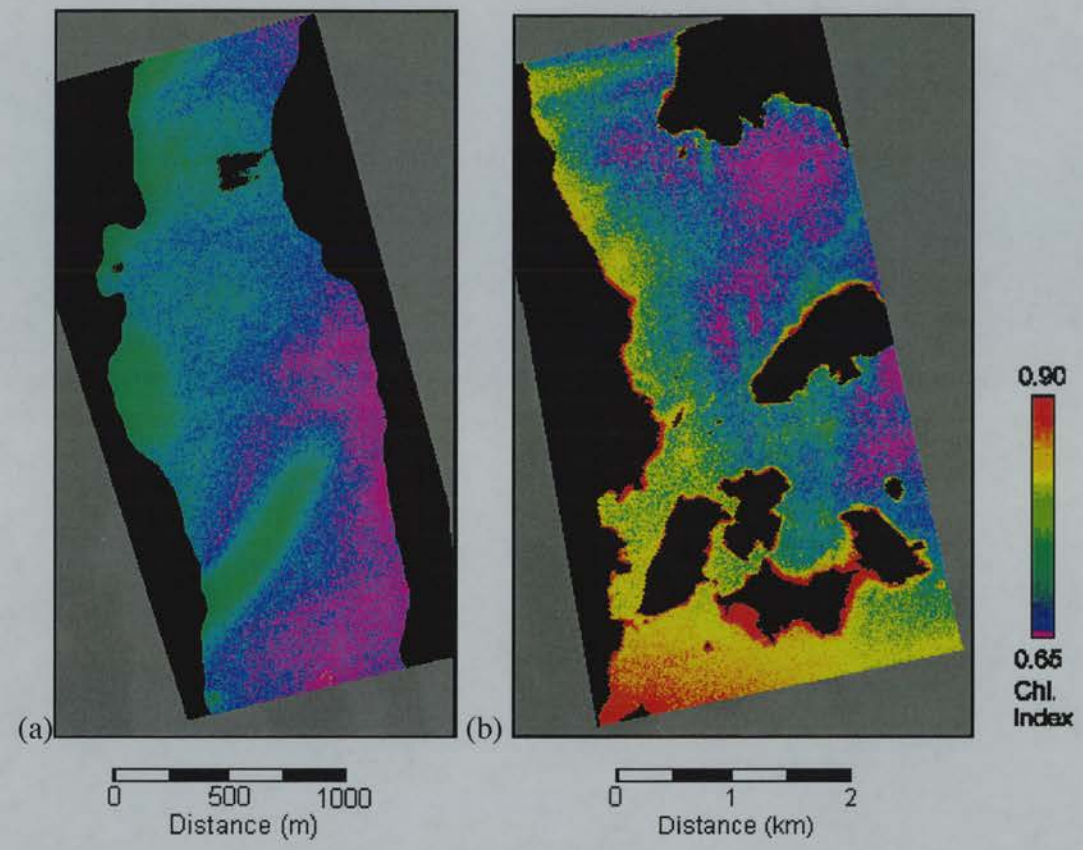

Figure 5-1. Chlorophyll index of Loch Lomond (29 May 1985) from an ATM image: (a) northern basin; (b) southern basin. North is at the top of this image and for all subsequent images.

The existence of greater values in the southern basin may be attributed to the effect of increased growth rates, resulting from an increased nutrient input there. This concurs with the work of George and Jones (1987), Bailey-Watts and Duncan (1981), and George (1993). The morphometry of this lake contributes towards maintaining nutrient gradients, because the presence of a shallow island-occupied area (part of which may be seen in Figure 5-1b) obstructs diffusion and therefore reduces rates of homogenisation. Additionally, along much of the northern basin, turbulent diffusion is limited by the northern basin's maximum width of approximately 1 km. Curran (1986) suggested that the maximum horizontal eddy viscosity for the northern basin will not exceed 1 $m^2 s^{-1}$.

The thermal image of the southern basin also indicated the obstructions to flow at the

islands (Figure 5-2b), with the presence of fronts separating waters of different temperature in areas near to the islands. By contrast, the northern basin (Figure 5-1a) exhibited much gentler gradients because of its near-absence of islands.

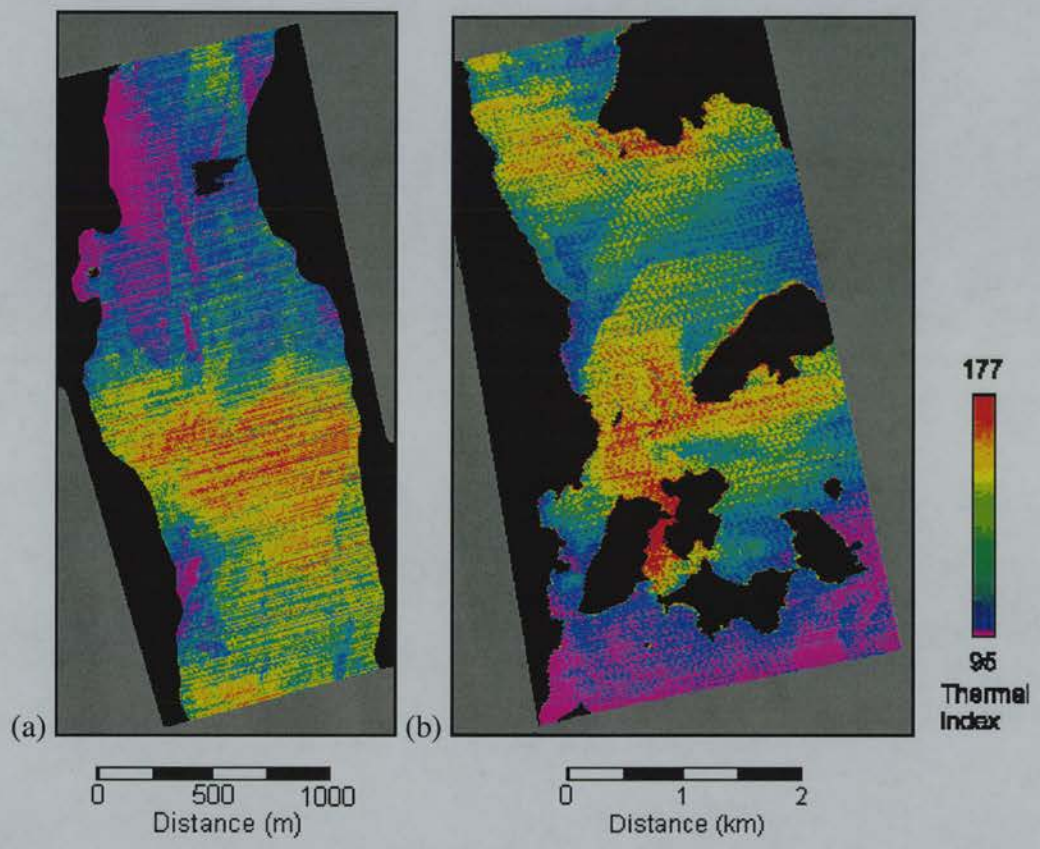

Figure 5-2. Thermal index of Loch Lomond (29 May 1985) from an ATM image: (a) northern basin; (b) southern basin.

There were sharper shearing edges in the thermal image of the southern basin than in the chlorophyll image because skin temperatures more effectively defined flow properties occurring at the instant of image acquisition. This was because skin temperatures acted as passive scalars of the velocity field (Denman and Platt, 1976). In contrast, chlorophyll gradients were gentler because phytoplankton, although obviously affected by flows, do not act as a passive scalar of the velocity field. Their spatial distribution was also the result of, firstly, the interaction between their structural properties and water flow properties, and secondly, their growth rates.

Superimposed on this macro-scale structure was a structure that was created by wind-forcing. Wind data from Blairlinnans weather station indicated a relatively

quiescent wind environment leading up to the time of image acquisition, with wind speeds varying between 1 m s^{-1} and 6 m s^{-1}. Winds were flowing predominantly from the south. From this, a general circulation pattern can be estimated as follows. Firstly, a surface current, deflected by Coriolis acceleration, would have flowed in a south-west to north-east direction, with a flow speed varying between 1.5 and 9 cm s^{-1} (from Equation 2-5). Downwelling on the eastern shore and upwelling on the western shore would then have ensued. This would have caused a sub-surface return current at a depth of approximately 20 m (from Equation 2-8) between these shores. Verification evidence within the images is, however, difficult to find. The northward deflection of the plume in the northern basin suggests a surface flow in a south-west to north-east direction. Likewise, the presence of shearing fronts behind the islands in the southern basin suggests a similar flow direction. However, the thermal images (Figure 5-2) do not show clear evidence of upwelling on the western shore (which would be exhibited as lower thermal index values). Although there were patches, of lower thermal index values near to the shore, there was not a thermal front passing consistently along this shore.

Without more data on this lake, it was impossible to determine the causes of the patches of higher chlorophyll index values in the northern basin. If water was circulating northward, it was probable that there would be upwelling on the western shore, which could possibly be indicative of negatively buoyant species accumulating in upwelling areas.

5.2.2 Ullswater

ATM images of Ullswater were acquired on 30 May 1994, 13 July 1994 and a CASI image was acquired on 26 June 1995.

In all images, chlorophyll index values in the northern basin were greater than in the southern basin (Figure 5-3a-c). In both the May 1994 and the July 1995 images, greater chlorophyll index values existed on the eastern shores (Figure 5-3a and c).

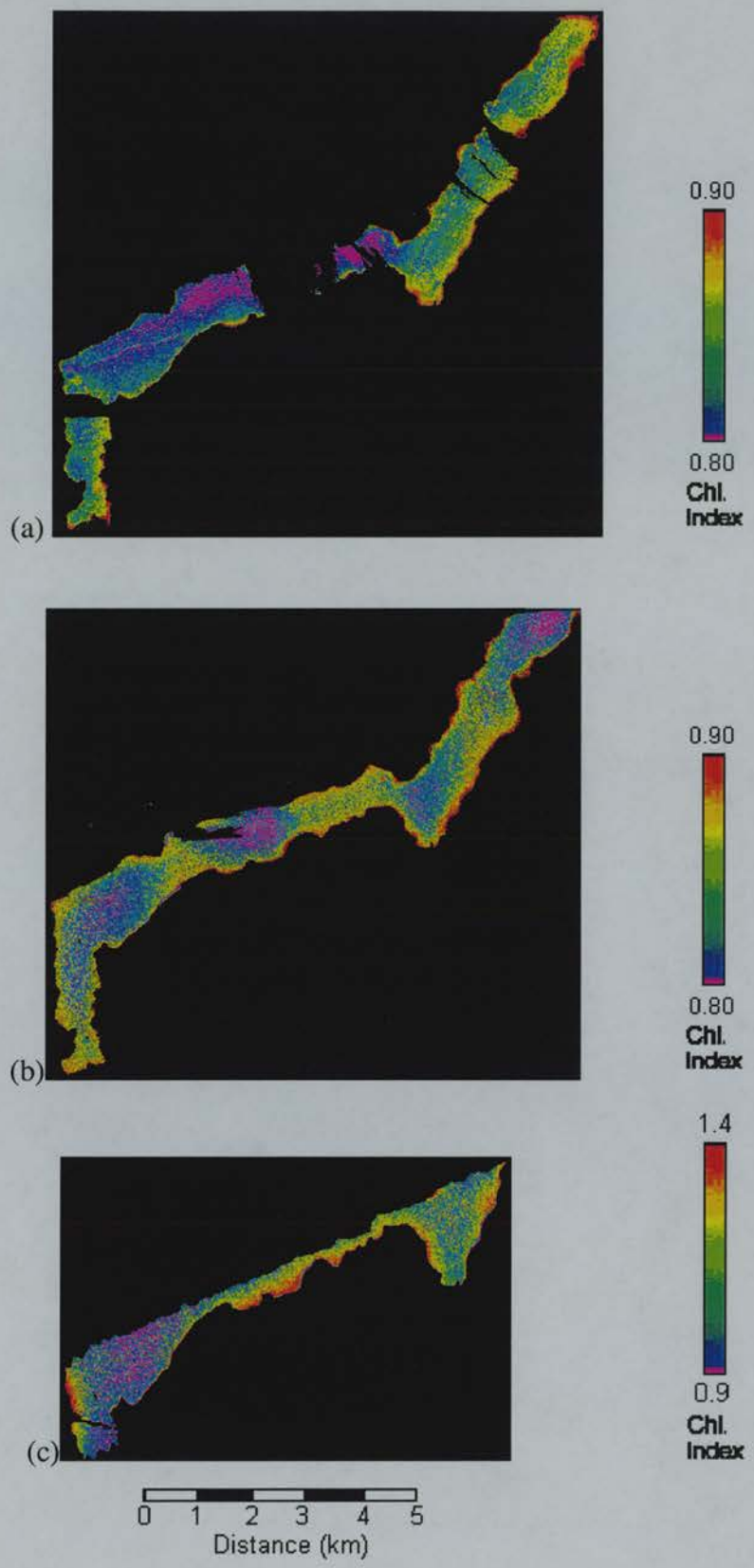

Figure 5-3. Chlorophyll indices of Ullswater: (a) 30 May 1994 from an ATM image; (b) 13 July 1994 from an ATM image; (c) 26 June 1995 from a CASI image.

As with Loch Lomond, the most noticeable characteristic of the spatial distribution of the chlorophyll index in Ullswater was the difference in mean values between the basins. This was particularly evident in the May 1994 and July 1994 images, which both had similar scales of spatial variation (Figure 5-4). Again, it may be assumed that differential growth was occurring, with a restriction of convection and diffusion between the two basins preventing homogenisation.

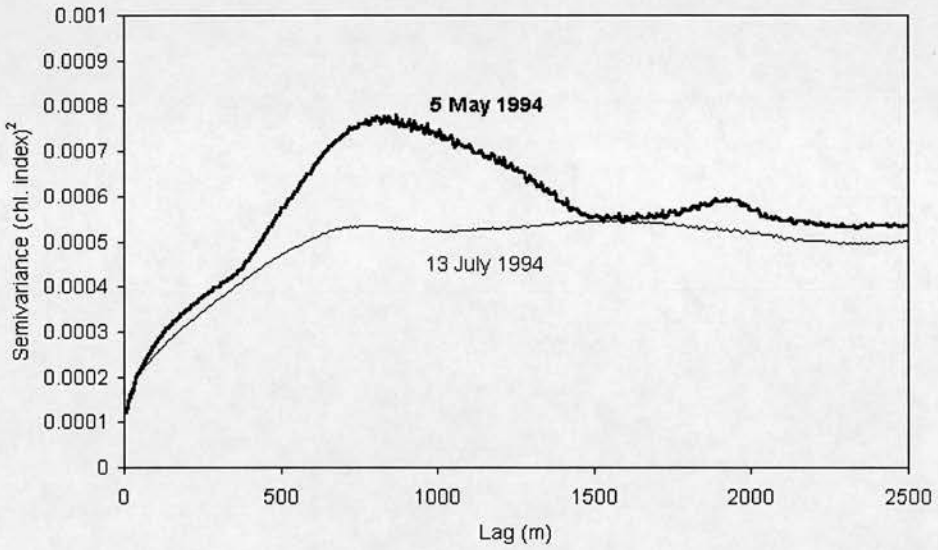

Figure 5-4. Omnidirectional variograms of chlorophyll indices in Ullswater (5 May 1994 and 13 July 1994).

The other characteristic, that of a west to east gradient in the May 1994 and June 1995 images may be attributed to wind-induced currents. Both dates had similar wind profiles, with the wind direction being from the south and south-west, with mean daily speeds of approximately 5 m s^{-1}. A surface current flow towards the east of approximately 8 cm s^{-1} will have been initiated, with downwelling occurring at the eastern shore. A sub-surface return current at the depth of frictional resistance (approximately 15 m) will also most likely have occurred. The greater chlorophyll index values on the south-eastern side of Ullswater may be attributed to displacement of phytoplankton away from the upwelling area. The effect of this on the scales of spatial variation was exhibited as an increased semivariance at lags of approximately 1000 m (Figure 5-4), which corresponded to the across-axis distance. On 13 July 1994, wind speeds were less than 1 m s^{-1}. It is possible that convection rates were

not great enough to allow the formation of an east-west gradient in phytoplankton concentration within the basins.

5.3 Patchiness and wind-forced hydrometry

Patchiness caused by wind-forcing occurs at macro- to micro-scales. In the former case, convection is the dominant cause; in the latter case, turbulence is the dominant cause.

5.3.1 Macro-scale patchiness and convection

Lakes in which wind-forced macro-scale patchiness existed were Loch Ness, Loch Awe, Esthwaite Water, and Blelham Tarn.

5.3.1.1 Loch Ness

At ATM image of Loch Ness was acquired on 3 June 1997 (Figure 5-5 and Figure 5-6). The greatest chlorophyll index existed along the eastern shore and at the southern end of the basin (Figure 5-5). However, it is probable that the high chlorophyll index values on the eastern shore were the result of look-angle effects. This is likely for Loch Ness because it is so oligotrophic that there is a low signal to noise ratio, and therefore images are likely to be disproportionally affected by such effects. The greater chlorophyll index values at the southern end of the lake were probably indicative of a change in water quality, but not necessarily of chlorophyll concentration: DOC may have had an impact on the chlorophyll index (Glen George *pers. com*).

There was a macro-scale trend in thermal index values from low values in the north to high values in the south (Figure 5-6). Additionally, there was a plume of high chlorophyll index values halfway along the basin on the eastern shore.

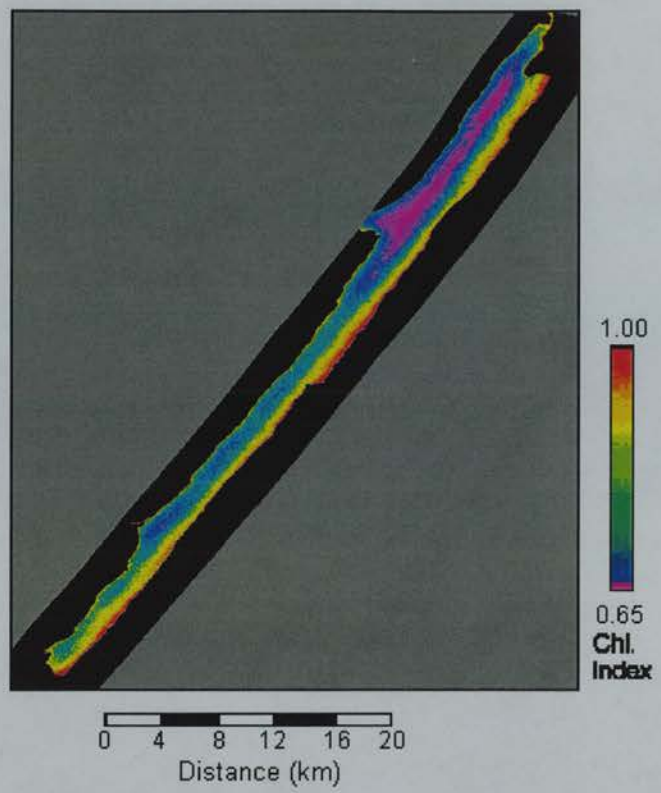

Figure 5-5. Chlorophyll index of Loch Ness (3 June 1997) from a CASI image.

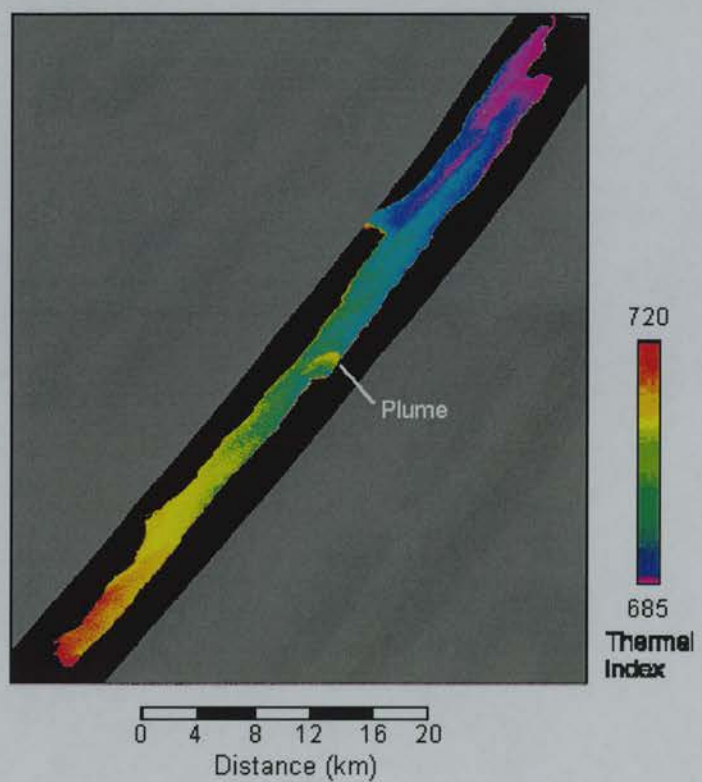

Figure 5-6. Thermal index of Loch Ness (3 June 1997) from a CASI image.

This horizontal thermal profile could be indicative of the upwelling of water in the north of the basin. Such upwelling would have caused a southward displacement of surface water. In addition to evidence in the thermal waveband, meteorological data suggest that such a southward displacement occurred. Although there was some difference between the wind directions measured at the nearest weather stations on 3 June 1997, wind environments were relatively similar: at Tain, winds were predominantly from the north-east; at Kinloss, winds were predominantly from the north-north-east; and at Dunstaffnage, winds were predominantly from the north. From this can be inferred that a northerly wind direction was probable, and it can therefore be expected that there was some southward displacement of surface water. Additionally, the plume halfway along the basin (that can be seen as greater thermal index values) was displaced towards the south with increasing distance away from the eastern shore. This again suggested a southward convection in the lake. In all cases wind speeds were less than 4.4 m s^{-1}, which should have caused surface current speed approaching 6 cm s^{-1}. This would be insufficient to cause enough mixing to disintegrate the basin-wide macro-scale patchiness into micro-scale patchiness.

The spatial distribution of chlorophyll index values in this lake is consistent with a southward displacement of surface water. Phytoplankton could be entrained in the flow and therefore accumulate in the south, particularly if positively buoyant. This concurs with the work of Jones *et al.* (1995). Wind-forcing appears to have had a greater effect than differential growth in Loch Ness, on the basis of this image, as the gradient in chlorophyll index values opposed that of the gradient in nutrient inputs.

5.3.1.2 Loch Awe

An ATM image of the northern basin of Loch Awe was acquired on 23 May 1997. Macro-scale variation in chlorophyll index values of the northern basin was evident (Figure 5-7), with greatest values in the far north, at approximately two thirds of the way down the axis, and at the intersection between the northern and southern basins (Appendix D). However, these latter two patches could be attributed to the influence of cloud shading. There was an across-axis gradient in thermal index values in the northern basin from low values at the southern shore to high values at the northern shore (Figure 5-8).

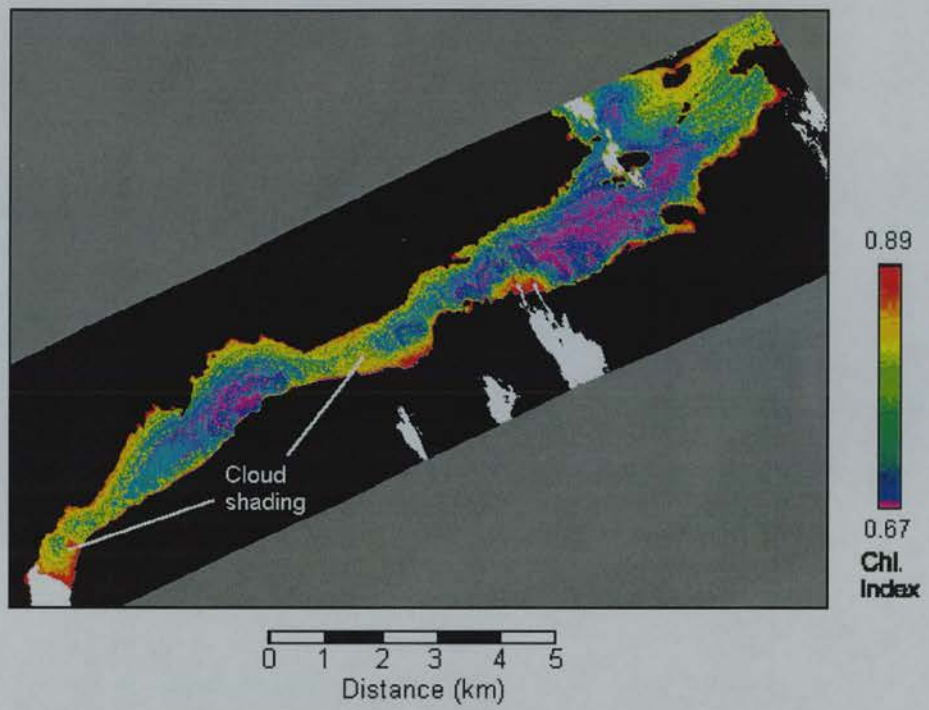

Figure 5-7. Chlorophyll index of the northern basin of Loch Awe (23 May 1997) from an ATM image.

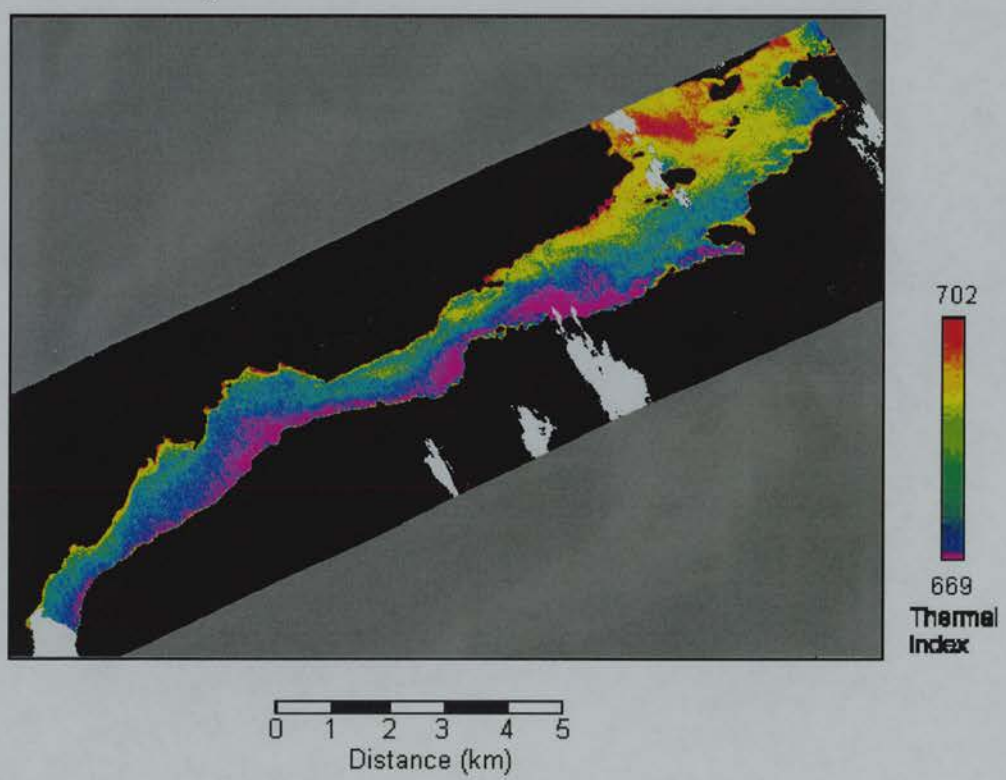

Figure 5-8. Thermal index of the northern basin of Loch Awe (23 May 1997) from an ATM image.

From the across-axis gradient in chlorophyll index values, it may be inferred that phytoplankton at the surface were being displaced towards the north. Wind data, aerial photographs acquired concurrently, and the thermal image support this hypothesis. On 23 May 1997, at Blairlinnans weather station, wind direction was from the south-east with wind speeds varying between 1.5 m s^{-1} and 3.5 m s^{-1}. A similar regime was measured at Dunstaffnage weather station. For the measured wind speeds, surface current speeds would have varied between approximately 2 cm s^{-1} and 5 cm s^{-1}. General wind directions, as determined through the change of cloud patterns in successive aerial photographs showed similar wind directions. No surface waves were present in the aerial photograph, again supporting the hypothesis of there being a relatively quiescent wind environment. These data suggest that an across-axis convection cell had been initiated, with upwelling at the southern shore and downwelling at the northern shore. This is verified by the thermal image, which exhibitted a relatively cold band of water along the southern shore.

5.3.1.3 Esthwaite Water

Nine ATM images of Esthwaite Water were acquired on 24 July 1987 from 11:00 to 14:00 at approximately 20 minute intervals. However, cloud shading occurred in most of the images, and greatly affected the chlorophyll indices of the images within six of the nine images (these were excluded from subsequent analysis). Additionally, there were look-angle effects in the western side of the final image, which were exhibited as low values, so this part of the lake was also excluded from subsequent analysis.

Chlorophyll and thermal indices were standardised by division by their respective means to enable a comparison of the relative scales of spatial variation. Without standardisation, changes in mean properties such as the increase in temperature throughout the period of imaging, would have greatly affected the variograms and partially obscured more subtle scales of spatial variation.

Spatial variation at macro- to micro-scales was present in both chlorophyll index (Figure 5-9) and thermal index images (Figure 5-10).

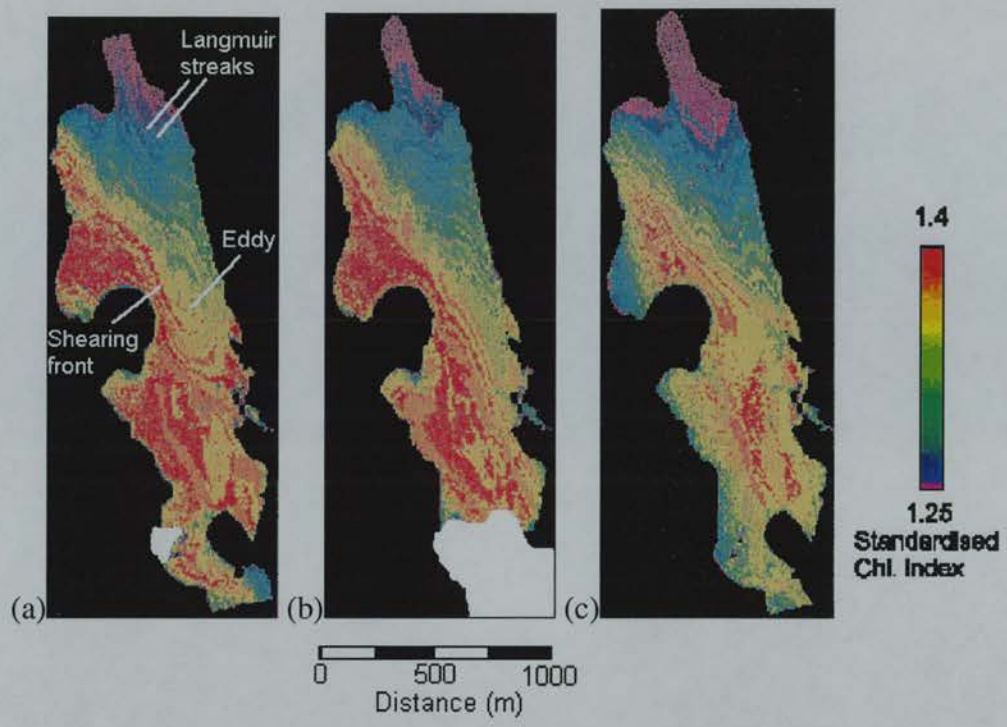

Figure 5-9. Standardised chlorophyll indices of Esthwaite Water (24 July 1987) from ATM images: (a) 12:40 Hrs; (b) 13:00 Hrs; and (c) 14:00 Hrs.

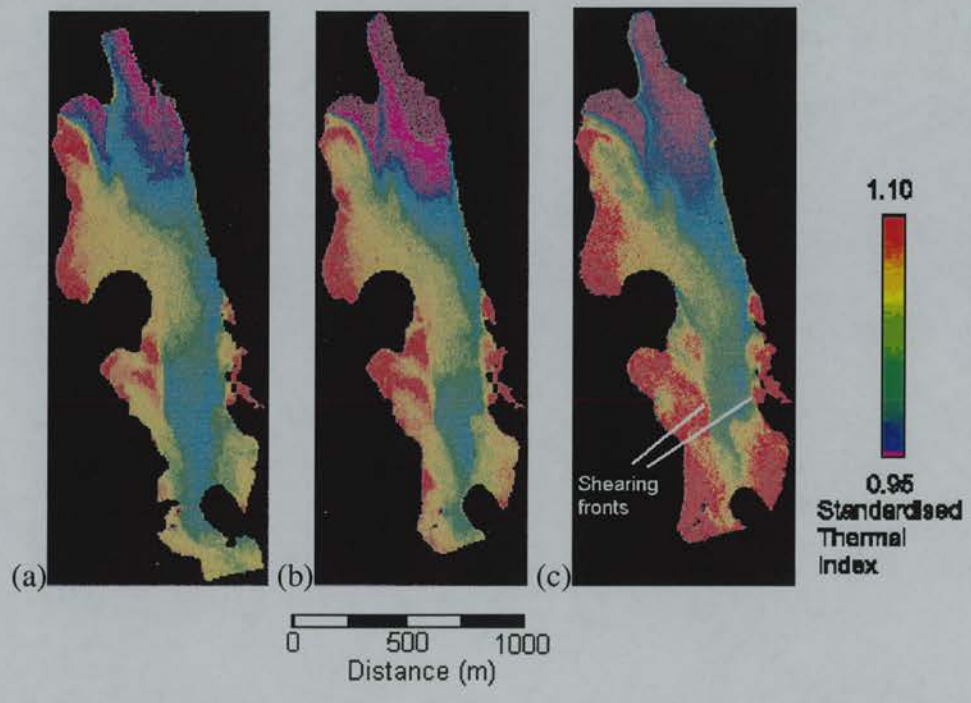

Figure 5-10. Standardised thermal indices of Esthwaite Water (24 July 1987) from ATM images: (a) 12:40 Hrs; (b) 13:00 Hrs; and (c) 14:00 Hrs.

The standardised chlorophyll index images (Figure 5-9) exhibited a macro-scale

spatial distribution that included a gradient from relatively low values in the north to relatively higher values in the south, and meso- to micro-scales spatial distributions including shearing fronts, eddies, and Langmuir circulation. The standardised thermal index images (Figure 5-10) exhibited a macro-scale spatial distribution that included a gradient from lower values in the north to higher values in the south. Meso- to micro-scale spatial distributions included higher values in the west and east of the lake in the shallow areas and smaller values in the central channel of the lake. These areas were separated by shearing fronts that were more pronounced than in the chlorophyll images.

Throughout the series of chlorophyll and thermal images, there was a progressive movement of values towards the south. For example, the low standardised thermal index values apparent in the north of the image acquired at 12:40 Hrs extended a third of the lake length towards the south in the image acquired at 14:00 Hrs.

George and Allen (1987) summarised the processes occurring within the lake. In response to a northerly wind of 5 m s^{-1}, surface currents flowed towards the south-west because of wind stress and Coriolis deflection. This forced surface water into the western shore, resulting in downwelling and a sub-surface return current. With the dominant species being positively buoyant *Oscillatoria limnetica*, there was downwind accumulation on the western shore. George and Allen (1987) further cited the existence of thermal fronts, particularly in the south–western and eastern shallow areas, as indicating the compartmentalisation of circulation within the lake.

Variograms of the standardised chlorophyll images (Figure 5-11a) differed greatly from those of the standardised thermal images (Figure 5-11b), and at all spatial scales the semivariance of the standardised skin temperature index was greater than the semivariance of the standardised chlorophyll index.

The semivariance in the standardised thermal index increased with time at all spatial scales (Figure 5-11b). The general structure was to some extent, however, retained. The first sill was reached at approximately 400 m, corresponding to the distance from the inlet to the north–west bay, and the second sill was reached at approximately 1200 m, corresponding to the distance between the inlet and the south–west basin. The continuous increase in semivariance with time was caused by

the progressive forcing of the thermal front in a southward direction which resulted in a greater difference between standardised thermal index values in the north and south of the lake. In contrast, there was much less change in the semivariance of the standardised chlorophyll index through time. This was because the spatial distribution of the phytoplankton population was remaining relatively static. That is, the position of the phytoplankton was determined by the position of downwelling areas, and these did not move as horizontal currents were of relatively constant direction.

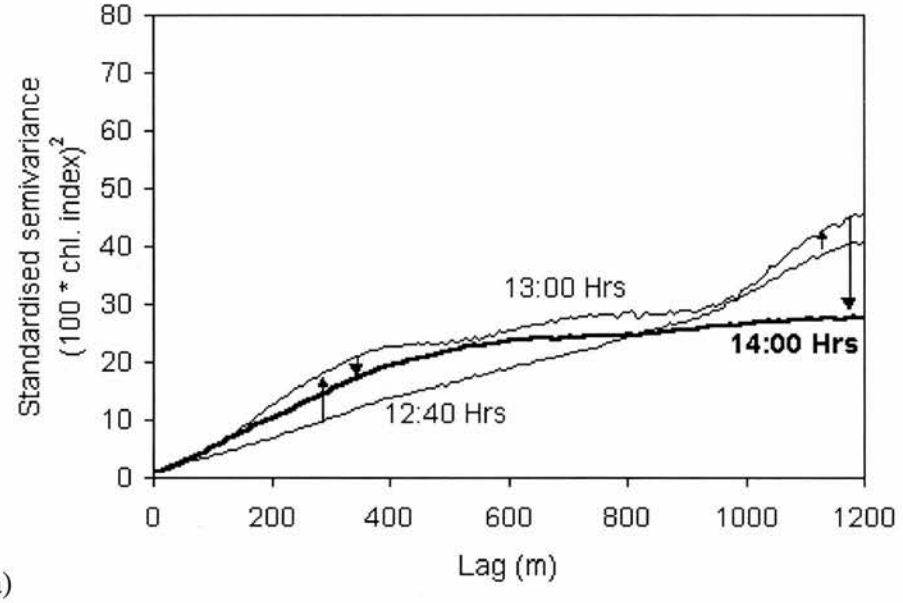

(a)

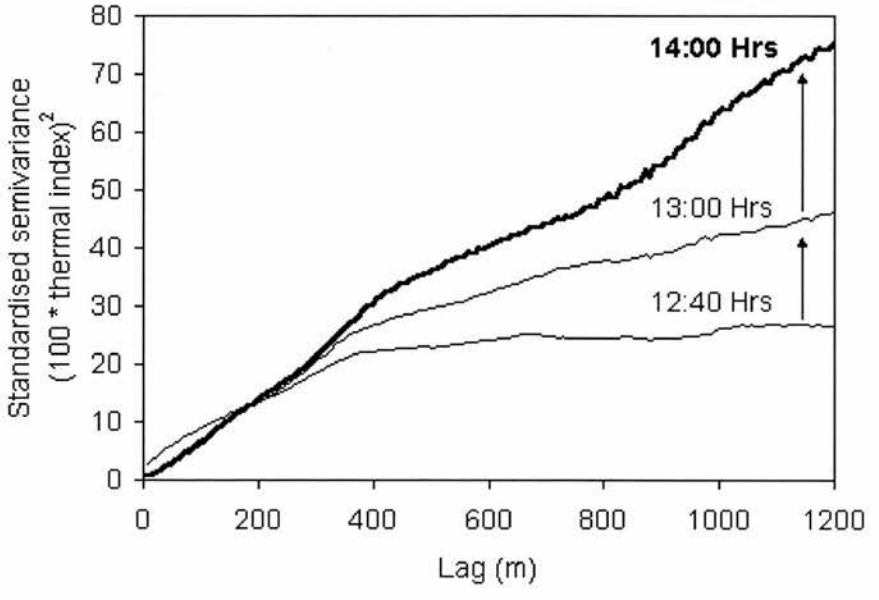

(b)

Figure 5-11. Omnidirectional variograms of Esthwaite Water: (a) standardised chlorophyll index; (b) standardised thermal index.

5.3.1.4 Blelham Tarn

An ATM image of Blelham Tarn was acquired on 7 August 1988. Greater chlorophyll index values existed in the north east of the lake (Figure 5-12), and greater skin temperature index values existed at the sides of the lake (Figure 5-13).

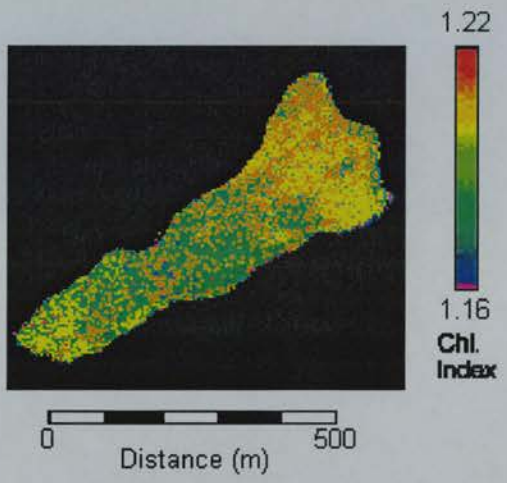

Figure 5-12. Chlorophyll index of Blelham Tarn (7 August 1988) from an ATM image.

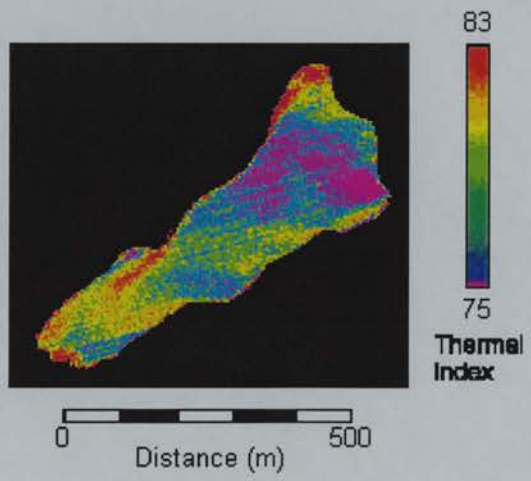

Figure 5-13. Thermal index of Blelham Tarn (7 August 1988) from an ATM image.

On the day of image acquisition, the dominant wind direction was from the south–west, with wind speeds of less than 5 m s^{-1}, and the dominant phytoplankton species was the cyanobacterium *Aphanizomenon flos-aquae*. From this, it can be inferred that a vertical dimension convection cell had been initiated, resulting in a surface accumulation of *Aphanizomenon* over the downwelling area in the north–east.

It was not possible, however, to use the thermal image to support this inference. Even if the lake was not strongly stratified at this time, some thermal stratification would be expected as a result of heating that occurred thoughout the day. With even slightly colder sub-surface water upwelling in upwind areas, there should have been lower surface temperatures in the south–west. These were not evident in the image. A possible explanation for the spatial distribution in the thermal image would be the conduction of heat from the shores, which would have had a relatively greater affect for this lake because it was comparatively small.

5.3.2 Micro-scale patchiness and turbulence

Lakes in which micro-scale patchiness existed were Bassenthwaite, Derwent Water and Wast Water. CASI images of these lakes were acquired on 15 June 1995 (Figure 5-14, Figure 5-15 and Figure 5-16).

All lakes were greatly affected by image noise (which was particularly apparent in near true-colour combinations), including cloud shading, look-angle effects and sunglint. Cloud shading was exhibited as lower values in the near true-colour images and higher values in the chlorophyll index images. Look-angle effects were exhibited as higher values in the near true-colour images and lower values in the chlorophyll index images. Sunglint was exhibited as higher values in near true-colour images and higher values in the chlorophyll index images.

There was no macro- or meso-scale spatial variation in the chlorophyll index for any of the images. The lack of this spatial variation cannot be attributed to image noise because at the time of remote sensing (approximately 14:00 Hrs), Fresnel scattering accounted for very little of the reflected radiance. Solar elevation was approximately 51°24' at the latitude of the lakes at the time of image acquisition, and for this elevation surface reflectance will have been less than 5% (Gordon, 1989). Additionally, bed features were apparent in certain images, indicating that light was penetrating the water to a depth of several metres beneath the surface. It can therefore be inferred that the absence of macro- to meso-scale structure in the images was caused by an absence of this structure in the lake.

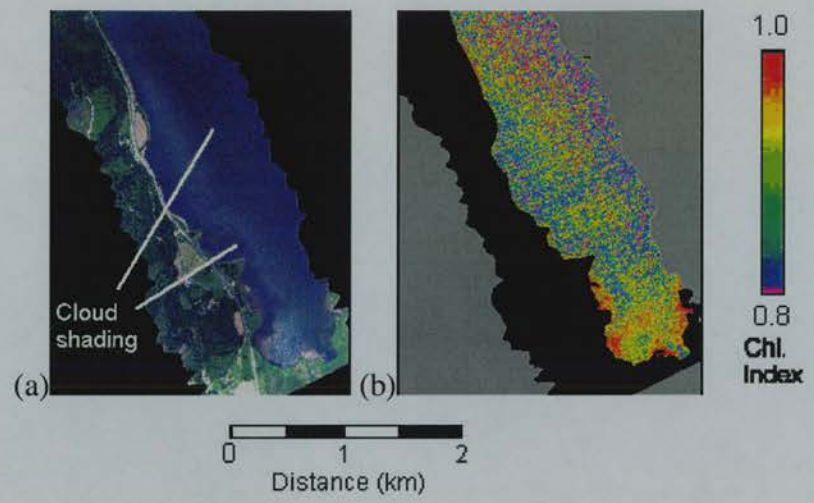

Figure 5-14. Water quality of Bassenthwaite (15 June 95) from a CASI image: near true-colour; (b) chlorophyll index.

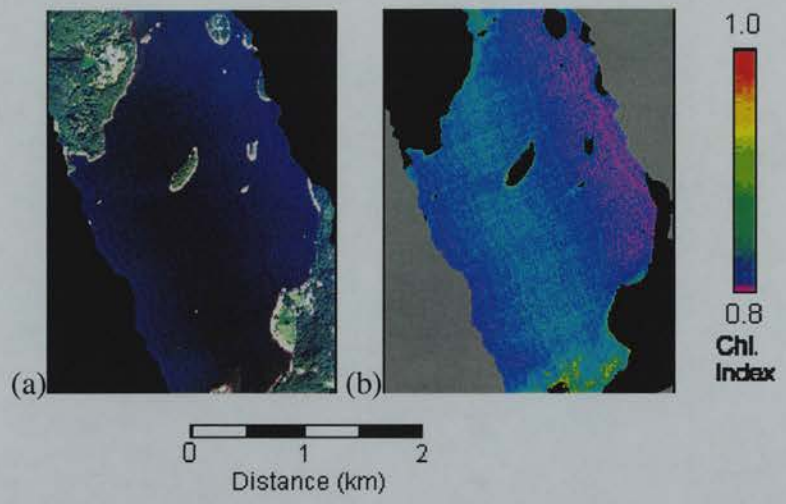

Figure 5-15. Water quality of Derwent Water (15 June 1995) from a CASI image: (a) near true-colour; (b) chlorophyll index.

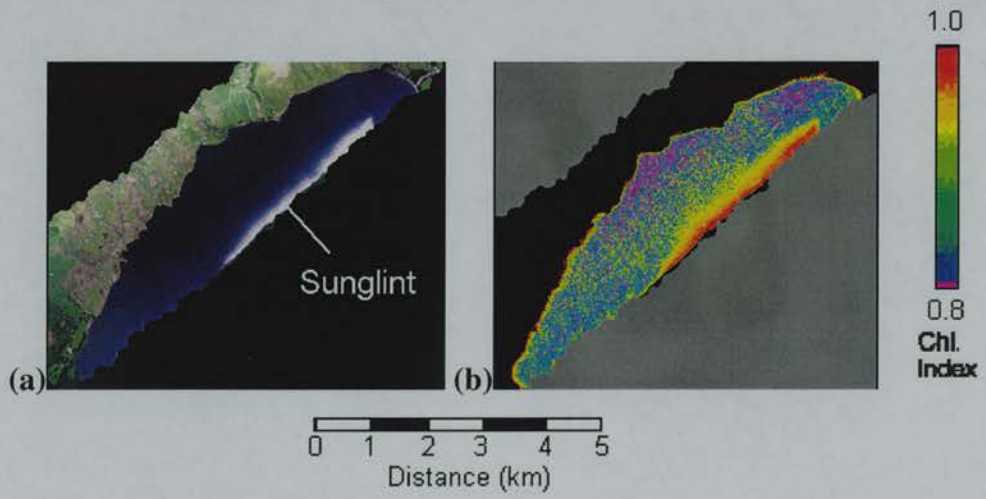

Figure 5-16. Water quality of Wast Water (15 June 1995) from a CASI image: near true-colour; (b) chlorophyll index.

The lack of macro-scale spatial distributions may be attributed to a strong wind environment, and a morphometry that does not reduce mixing. Mean daily wind speeds were greater than 11 m s^{-1} on 15 June 1995, and in the preceding week were consistently greater than 6 m s^{-1}. It can be expected that wind-induced mixing will have homogenised the lakes in the vertical and horizontal dimensions. Morphometry would have contributed towards this homogenisation. Firstly, none of the lakes were elongated (in comparison to lakes such as Ness and Ullswater), so there would be relatively high fetches, and depths of wave-induced mixing, for a given distance from the shore. Secondly, none of the lakes contained obstructions (such as islands) which would restrict the maximum scale of eddying. Finally, Bassenthwaite and Derwent Water were relatively shallow, increasing the propensity for surface return flows.

For Bassenthwaite and Derwent Water, vertical homogeneity was almost assured. A wind speed of 11 m s^{-1} will have caused enough wave-induced mixing to have homogenised the phytoplankton concentration within the lakes to depths of 3.5 m and 3 m, respectively. Additionally, if vertical convection was occurring, vertical convection rates will have been of such a magnitude that they will have reduced the effect of the buoyancy characteristics of phytoplankton species to determine phytoplankton accumulation in upwelling or downwelling areas. Finally, for lakes with an average depth of less than 6 m (which restricted the depth at which sub-surface return flows could occur) some phytoplankton will have been entrained in sub-surface return flows (if present), regardless of their buoyancy characteristics. It can be expected that any upwelling that did occur on upwind shores, will be of water containing concentrations of phytoplankton that were similar to those at the surface. Again, this will have retarded the development of macro-scale horizontal heterogeneity.

For Wast Water, the situation was slightly different because of the relatively great depth of the lake. Wave-induced mixing will not have homogenised the lake in the vertical dimension, because the lake is relatively deep. Vertical heterogeneity can be assumed, so upwelling of relatively phytoplankton-free water should reduce surface concentrations in upwind areas. It is possible that gradients existed, but could not be detected by the algorithms used.

5.4 Patchiness and inflow-forced hydrometry

5.4.1 Introduction

CASI images of the Loosdrecht and Northern Vecht lakes were acquired on 18 August 1992 (Figure 5-17).

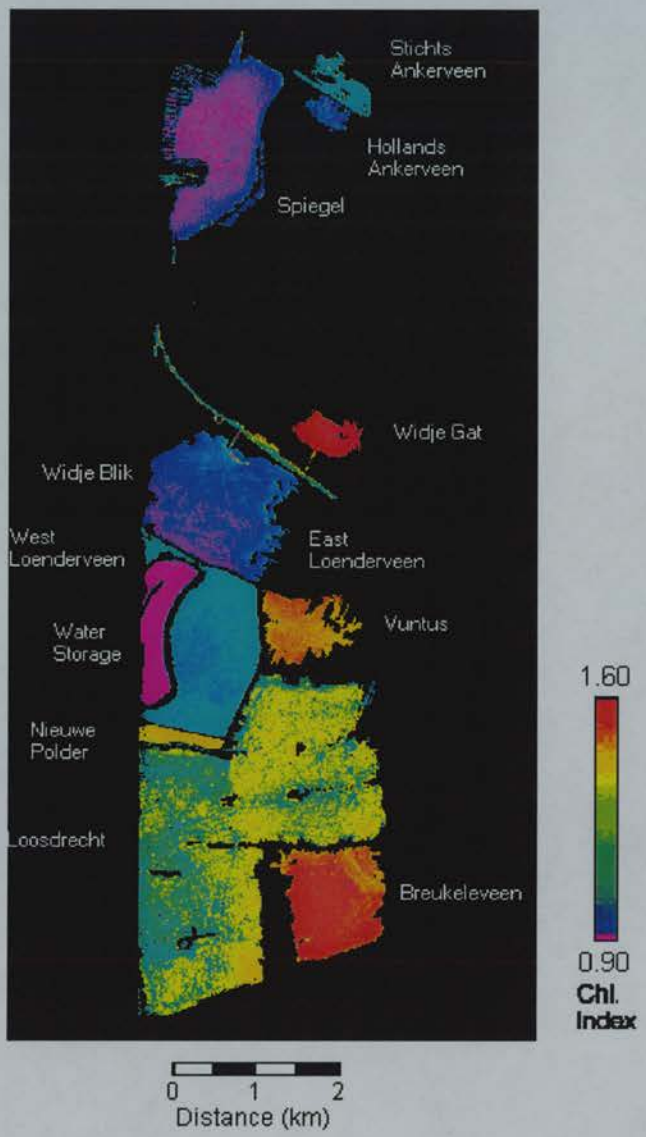

Figure 5-17. Chlorophyll index of the Dutch lakes (18 August 1992) from a CASI image.

Contact measurements, concurrent with the remotely sensed images, were not made. However, mean chlorophyll index values were positively correlated with mean pigmentation of the lakes from a sample acquired previously by Dekker (1992a) as

shown in (Figure 5-18).

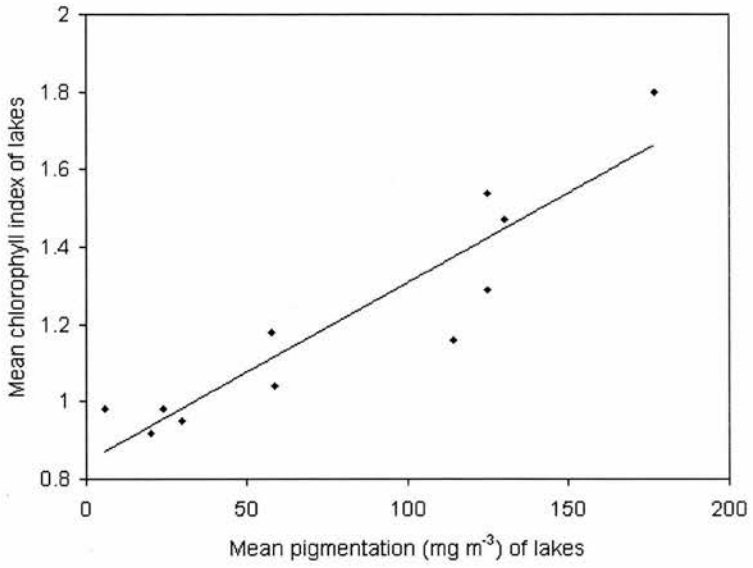

Figure 5-18. Comparison of mean chlorophyll index values with mean pigmentation (after Dekker, 1988) of the Dutch lakes. Mean pigmentation is the sum of chlorophyll-*a* concentration and phaeopigments.

The dominant cause of patchiness in these lakes is usually inflows from the streams and flows between lakes under the influence of wind-forcing (Wasser, 1988; Dekker, 1992a). From interpretation of spatial distributions of chlorophyll in the images and comparison with archived data, it is inferred that these were the causes of patchiness on 18 June 1992.

5.4.2 Meso-scale patchiness and stream inflows

The Lakes Loosdrecht, Spiegel, Nieuwe Polder, Hollands Anderveen, Stichts Ankerveen, Wijde Blik and Wijde Gat experienced inflows (either from the Hilversum Canal, the Amsterdam-Rhine Canal or the River Vecht). However, only in Lake Wijde Blik (Figure 5-19) and Lake Widje Gat (Figure 5-20) were basin-wide chlorophyll gradients created. The spatial distributions in these two lakes were consistent with an inflow from the Hilversum Canal. Greatest chlorophyll index values in Lake Wijde Blik (which is one of the less nutrient-rich lakes of the Northern Vecht lakes), and smallest chlorophyll index values in Lake Widje Gat (one of the most nutrient rich lakes) were found near to their connections with the

Hilversum Canal. From the images, it appears that a flow from the Hilversum Canal into the lakes was causing an increase in chlorophyll concentration of Lake Wijde Blik and a decrease in concentration of Lake Wijde Gat.

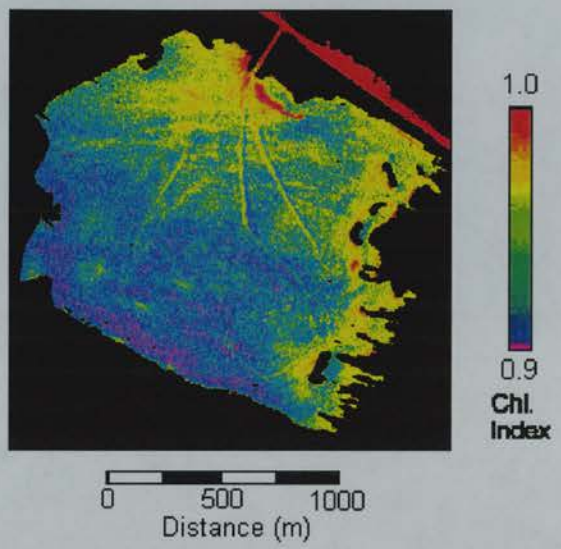

Figure 5-19. Chlorophyll index of Lake Wijde Blik (18 August 1992) from a CASI image.

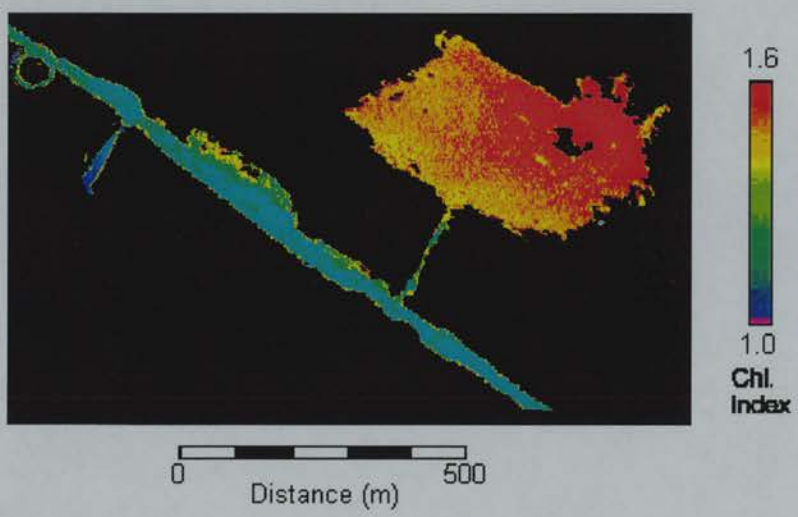

Figure 5-20. Chlorophyll index of Lake Wijde Gat (18 August 1992) from a CASI image.

Flows between the Hilversum Canal and the lakes connected to it are controlled by the flow of water in the canal by the influence of gravity and the wind direction. In the absence of wind, there is a flow from the canal into Wijde Blik and Wijde Gat under the influence of gravity. If winds originate from the south, there is a flow from

Lake Wijde Blik into the canal and from the canal into Lake Wijde Gat; if winds originate from the north, there is a flow from the canal into Lake Wijde Blik (Marteen Ouboter *pers.com*).

Over the several weeks previous to the time of image acquisition, winds had predominantly originated from the south-west, reaching wind speeds approaching 8 m s^{-1}. On the day of image acquisition, however, there was a change in wind regime to one that was more quiescent, with winds originating from the south east (Figure 5-21). Also shown on Figure 5-21 is the approximate displacement of surface water that would have occurred on 17 and 18 August 1992.

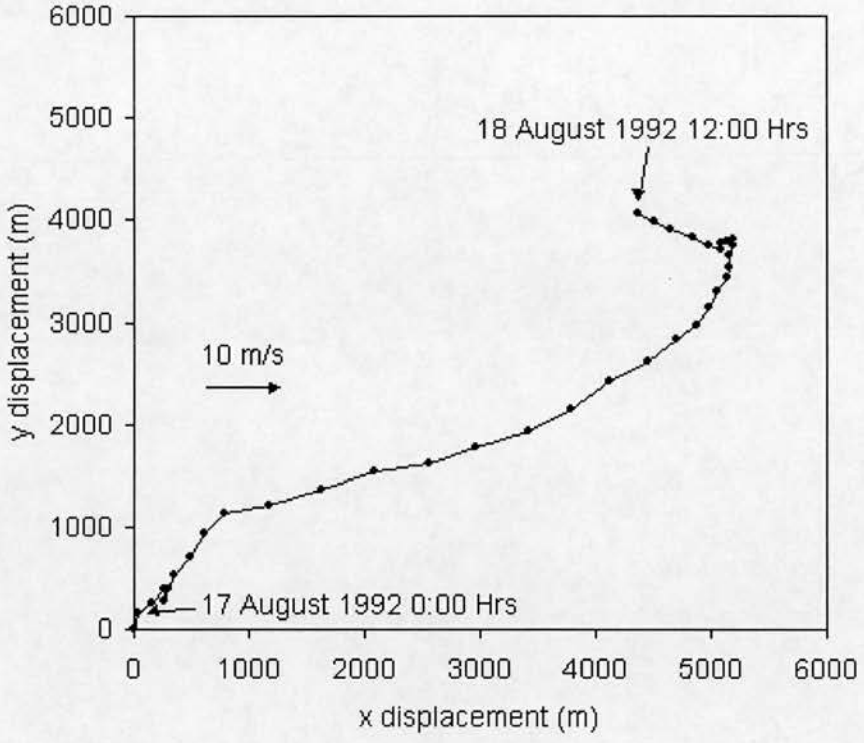

Figure 5-21. Wind vectors affecting the Loosdrecht and Northern Vecht lakes. Each point represents an hour.

Preceding 18 August 1992, the wind direction would have caused a displacement of surface water towards the north-east. This would concur with the spatial distribution of phytoplankton in Wijde Gat but would not concur with the spatial distribution in Wijde Blik. For there to be an absence of preferential displacement of phytoplankton into either of these lakes, it is necessary for it to be flowing along, rather than across, the axis of the canal, as on 18 August 1992. It may therefore be inferred (although

without more data it cannot be verified) that the spatial distributions in both of these lakes had been created on 18 August 1992.

5.4.3 Meso-scale patchiness and inter-lake flows

In Lake Breukeleveen, a basin-wide chlorophyll gradient existed from lower chlorophyll index values near to the input from Lake Loosdrecht to greater chlorophyll index values at the opposing bank and at the western shore (Figure 5-22).

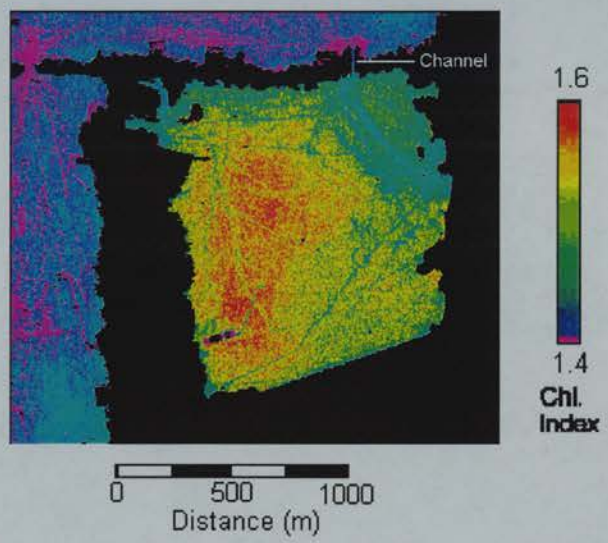

Figure 5-22. Chlorophyll index of Breukeleveen (18 August 1992) from a CASI image.

Two main hypotheses may be proposed to explain the spatial distribution in Lake Breukeleveen. Firstly, that the spatial distribution in Lake Breukeleveen was caused by flows from Lake Loosdrecht to Lake Breukeleveen under the influence of inflow-induced hydrometry within the Loosdrecht lake system as a whole, with the Amsterdam-Rhine Canal and the River Vecht being the main driving forces. Secondly, that the spatial distribution in Lake Breukeleveen was caused by flows from Lake Loosdrecht to Lake Breukeleveen in the preceding days due to wind-forced displacement. For both hypotheses, flows from Lake Loosdrecht (which has a lesser mean chlorophyll concentration than Lake Breukeleveen) resulted in a reduction in chlorophyll concentrations in Lake Breukeleveeen near to the connecting channel: in effect, inflowing waters from Lake Loosdrecht were diluting waters in Lake Breukeleveen.

The first hypothesis, that of a discharge between lakes under the influence of inputs from the River Vecht and Amsterdam-Rhine Canal, is supported by data on discharged between the Loosdrecht lake system and surrounding sources and sinks. Data on amounts of water entering the Loosdrecht lake system in 1992 were unavailable, but a study of circulation between 1982 and 1987 showed that in the summer months an inflow into the system occurs from the Amsterdam-Rhine Canal and the River Vecht in order to compensate for natural seepage to lower polder areas to the south of the lake system (Figure 5-23). Patterns of exchange between the River Vecht, the Hilversum Canal, and the Loosdrecht lake system have not changed greatly between 1987 and 1992 (Ouboter *pers. com*).

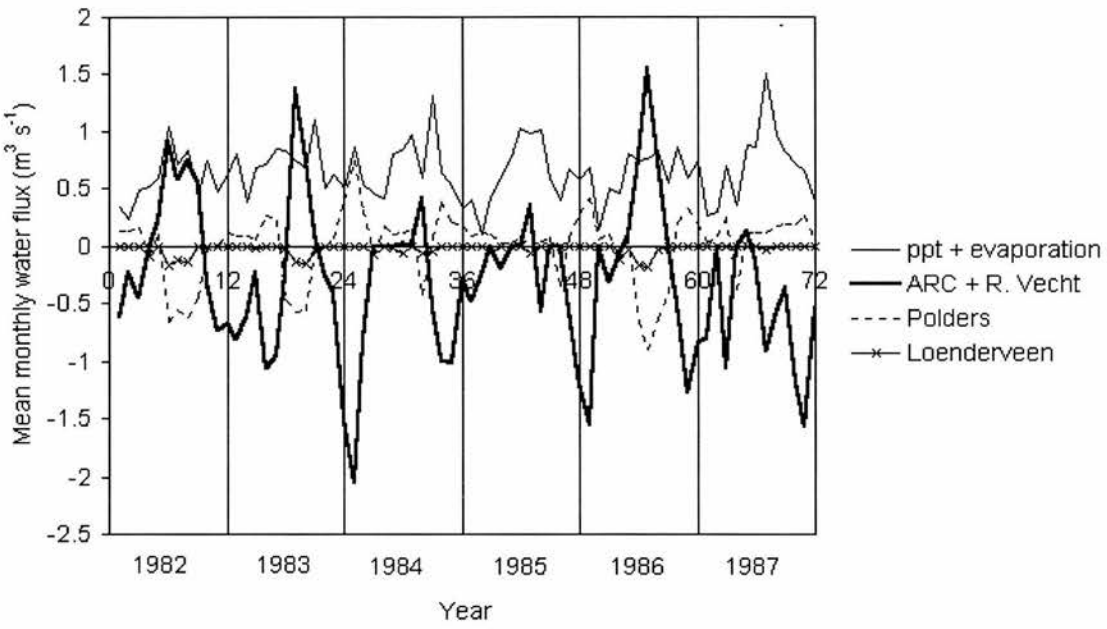

Figure 5-23. Water exchanges affecting the Loosdrecht lake system: exchanges with atmosphere through precipitation and evaporation (ppt+evaporation); exchanges with the Amsterdam-Rhine Canal and River Vecht (ARC + R. Vecht); exchanges between the lake system and surrounding polders (Polders); exchanges between Lake Loosdrecht and East Loenderveen (Loenderveen).

At the time image of acquisition, it was probable that water was entering the system from the Amsterdam-Rhine Canal and River Vecht. Wasser (1988), through the use of physical modelling of the lake system, had shown that inflows of water from these sources cause a circulation between lakes, with flows from Lake Loosdrecht into Lake Breukeleveen.

The second hypothesis, that of flows between Lake Loosdrecht and Lake Breukeleveen under the influence of wind-forcing is supported by wind data. Wasser's model showed that south-west winds cause flows from Lake Loosdrecht into Lake Breukeleveen. If the spatial distribution in Lake Breukeleveen had been produced on the day previous to the day of image acquisition, it is possible that wind-induced flows from Lake Loosdrecht into Lake Breukeleveen may have been responsible for the spatial distribution of chlorophyll in Lake Breukeleveen.

It is not possible to infer which hypothesis is correct without more data for verification. Additionally, it is not possible to determine the effect of other factors, such as the change in wind direction that occurred subsequent to image acquistion.

5.4.4 Inter-lake comparison

The effects of inflows in the Lakes Wijde Blik, Widje Gat and Breukeleveen were to cause chlorophyll gradients that were much greater than in the other Loosdrecht and Northern Vecht Lakes. A comparison of omnidirectional variograms of the lakes (Figure 5-24) reveals greatly different properties.

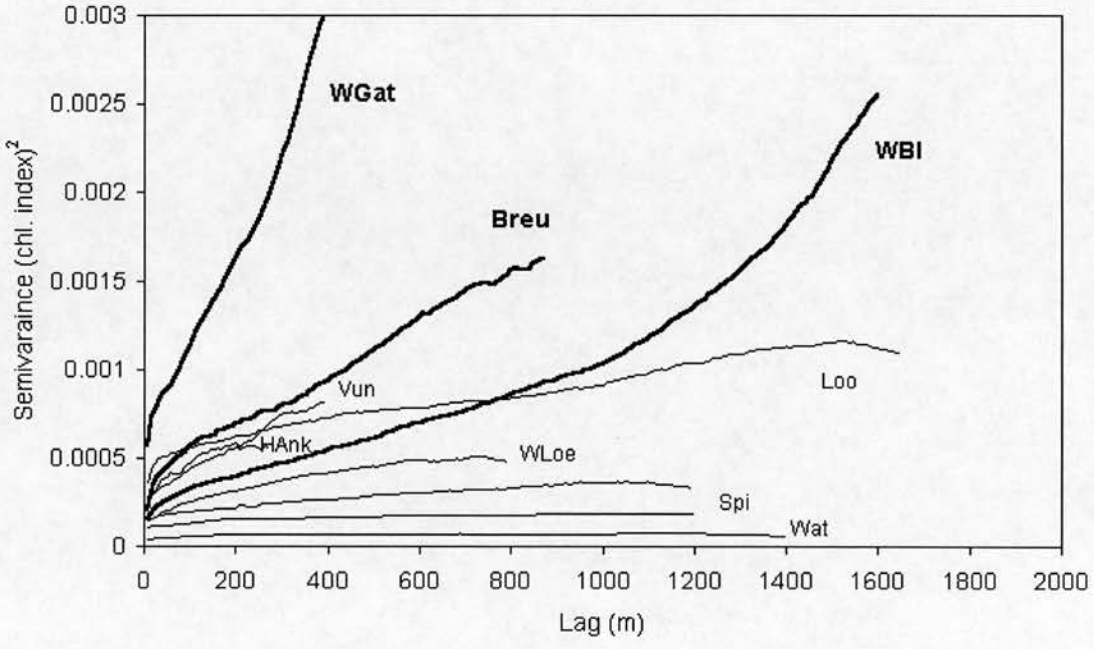

Figure 5-24. Omnidirectional variograms of surface chlorophyll index of the Loosdrecht and Northern Vecht lakes. Name abbreviations are shown in Figure 4-3. An omnidirectional variogram of Stichts Ankerveen was not estimated because there was reflection from lake macrophytes.

The Lakes Wijde Blik, Wijde Gat and Breukeleveen experienced unbounded spatial variation (semivariance increased as a function of lag with no limit) and the other lakes experienced bounded variation (semivariances reached a limit). Additionally, the Lakes Wijde Blik, and Breukeleveen tended to greater semivariances at all lags.

The Loosdrecht and Northern Vecht lakes that exhibited relatively little spatial variation in chlorophyll will still have been affected by inflows from rivers and other lakes. It is proposed here than the lack of variation in these lakes was caused because inflowing water had similar water qualities to the lake into which it was discharging. That is, there was a near-steady equilibrium between water quality in a given lake and its inflowing streams. Unfortunately, there were no available data to verify this. The problem of a lack of verification will be discussed in Section 9.2.

5.5 Conclusion

The approach used in this chapter was greatly reliant on the use of remotely sensed data. In regards to investigating the spatial dynamics of phytoplankton, such data have two main disadvantages. Firstly, the data lack a vertical aspect, only providing information on what occurs at the surface. Secondly, the data have a very limited temporal aspect, only providing snap-shots of *spatial distributions* rather than *spatial dynamics*. In addition, various problems existed with the quality of the archived data used: the spectral resolutions of the sensors were too coarse to infer phytoplankton types from the images alone; and look-angle effects, sun glint and bed reflectance were often present. These limitations are discussed in more detail in Section 9.2. Although these limitations prevented the establishment of conclusive relationships between the spatial dynamics of phytoplankton and causative processes, the analysis has identified areas that may be investigated more rigorously through process modelling. The main conclusions are as follows:

i. Spatial distributions and nutrient gradients

Nutrient gradients greatly affected spatial distributions of phytoplankton in Loch Lomond and Ullswater. It may be inferred that in these lakes, much of the spatial distribution resulted from lake-wide differences in the phytoplankton growth rates. It is probably not coincidental that these lakes were large and had complex shapes

(Table 4-1 and Table 4-3). For a given wind stress, it would have been harder to homogenise the nutrient gradient horizontally, as surface eddies would have had a greater distance to travel, and obstructions to flow would have limited the maximum intensity of the eddying. It may, therefore, be inferred that morphometry had a role in maintaining nutrient gradients, and resultant patterns of differential growth

ii. Spatial distributions and wind-induced hydrometry

Wind had a role in lakes where spatial distributions have traditionally been attributed to nutrient gradients (such as Loch Ness). Winds determined the spatial distributions because they controlled scale-dependency and anisotropy. Scale-dependency depended upon wind speeds. Under relatively weak wind-forcing (speeds less than 5 m s^{-1}), it is inferred that macro-scale gradients were caused by the displacement of phytoplankton from upwelling areas. Under stronger wind-forcing (speeds greater than 5 m s^{-1}), macro-scale variation in phytoplankton did not exist in the absence of nutrient gradients. It is inferred that this was because wind-induced mixing in the horizontal and vertical domains caused the disintegration of macro-scale structure into micro-scale structure. Wind direction determined the direction of displacement of the phytoplankton, often resulting in greater variance in the direction along rather than across the wind axis. Morphometry influenced hydrometries. In Esthwaite Water, surface spatial distributions were caused by wind-induced flows being forced from the surface domain into the vertical domain at shores, allowing phytoplankton buoyancies to interact with vertical velocities. In lakes were obstructions to mixing were less, spatial distributions of phytoplankton were more homogeneous.

iii. Spatial distributions and inflow-forced hydrometry

Inflows had a great effect on spatial distributions in lakes when the inflowing water contained greatly different phytoplankton concentrations to those in the lakes. In affecting the spatial distributions, this inflow-forced hydrometry had greatest importance when lakes were relatively small with respect to inflows. For instance, although inflows determined spatial distributions of phytoplankton in Loch Ness and Ullswater by causing long-tem nutrient gradients, their affect on spatial distributions through the displacement of phytoplankton was relatively small and localised.

6 Process model validation

6.1 Introduction

For the SSIIM2.0 process model to be used in the analysis of the spatial dynamics of phytoplankton, it was necessary for it to be able to model accurately the responses of hydrometric and phytoplanktonic behaviour to external boundary conditions. Thus, some form of model validation was required. Validation may involve several stages, including calibration, beta testing and sensitivity analysis (Chapra, 1997).

Calibration involves 'tuning' the parameters (or internal boundary conditions) of the model so that it simulates results (such as spatial distributions of phytoplankton) that have been measured empirically. After calibration, the model should be able to produce accurate results when running under similar external boundary conditions. SSIIM2.0 was based on existing models that had already been calibrated. SSIIM was calibrated by Olsen (1997). The cyanobacterial buoyancy model was calibrated by Kromkamp and Walsby (1990). Stokes' equation (Equation 3-12) has been empirically verified by McNown and Malaika (1950). Michaelis-Menton kinetics models have been calibrated from *in vitro* studies by Foy (1976), Reynolds (1981), and Nicklish and Kohl (1983). Therefore, calibration as part of this thesis was unnecessary

Beta testing involves running the model under a range of different boundary conditions. This is necessary because calibration only shows the model functioning for one set of boundary conditions, and model limitations (and 'bugs') may only appear when functioning under greatly different boundary conditions. Beta testing of SSIIM has been conducted by several authors (Bowles *et al.*, 1998; Seed, 1997; and Stoesser, 1998).

Sensitivity analysis involves examining model sensitivity to boundary conditions. This was necessary in this thesis because there has been little research on SSIIM's sensitivity, and it was likely that some aspects of model structure (such as grid resolution) would change between simulations. The main components on which

sensitivity analysis was performed were the *grid resolution*, the *time step*, the *wind friction coefficient model* and the *turbulence model* (Table 6-1).

Table 6-1. Properties undergoing sensitivity analysis.

	Property undergoing sensitivity analysis				
Boundary condition	Vertical cell Dimension	Horizontal cell dimension	Time step	Wind friction coefficient model	Turbulence model
Vertical cell dimension (m)	2.5, 3, 3.5	90	90	90	90
Horizontal cell dimension (m)	90	70, 90, 110	90	90	90
Time step (s)	900	900	900, 1800, 3600	900	900
Wind friction coefficient model	Bengtsson	Bengtsson	Bengtsson	Bengtsson van Dorn Wu	Bengtsson
Turbulence model	k-ε	k-ε	k-ε	k-ε	k-ε zero-equation

6.2 Validation basin: Lake Windermere

The lake chosen for performing sensitivity analysis of SSIIM2.0 was Lake Windermere, in the English Lake District. This is the largest English lake, with a surface area of greater than 14 km^2 and a maximum depth of greater than 60 m (the southern basin has a maximum depth of 44 m). It is highly elongated, and is divided into two basins, the southern basin of which is shown in Figure 6-1.

This lake was chosen because there was some similarity, in terms of climate and morphometry, between this lake and the real lakes (Chapter 7) and hypothetical basins (Chapter 8) that were subsequently studied. Sensitivity to internal boundary conditions could therefore be gauged using external boundary conditions that were typical of the lakes for which the model had been devised.

Only the southern basin was used in model validation because of computational limits. It was intended to maintain the horizontal grid cell dimension at approximately 100 m, and the vertical grid dimension at approximately 2 m (it was believed that these would be the maximum dimension for which physically realistic

results would be produced). This resulted in approximately 30,000 grid cells. Producing a grid for the whole of Lake Windermere would have resulted in more than double this number, and would have exceeded the maximum number of cells that the model was capable of simulating.

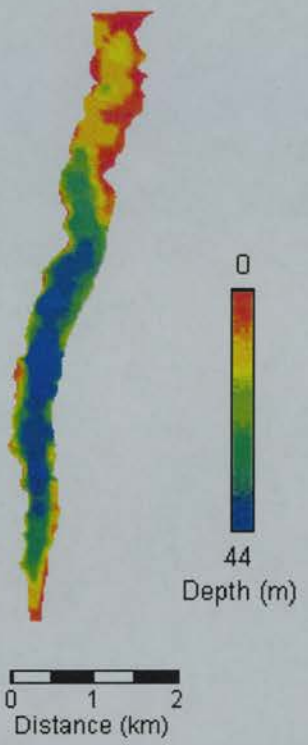

Figure 6-1. Bathymetry of the southern basin of Lake Windermere.

In all cases, simulations were of the effect of wind-forcing on a stratified lake (a thermocline at 10 m). 24 hours were simulated, with a wind from the south that varied from a minimum of 1 m s^{-1} (at 0:00 Hrs) to a maximum of 5 m s^{-1} (at 12:00 Hrs). This wind profile was chosen because, firstly, it was typical of that experienced at Lake Windermere and, secondly the use of a forcing function that varied in intensity allowed an analysis of the effect of both increases and decreases in stress applied to the system. The Coriolis parameter was set at 1.117×10^{-4}, which corresponded to the latitude of Lake Windermere.

For comparing the effects of internal boundary conditions, calculations were made of mean flow velocities in the surface cell layer at hourly intervals, and flow velocities as a function of depth at the centre of the lake (O.S. B.N.G. 238800 494000).

6.3 Hydrometric sensitivity to spatial resolution

Simulations had vertical cell dimensions at 2 m, 2.5 m and 3 m, and horizontal cell dimensions at 70 m, 90 m and 110 m (Figure 6-2). Dimensions of these magnitudes were chosen as a compromise between the requirement for modelling small scale processes and the requirement for computational efficiency, and were typical of those reported in the literature (Falconer *et al.*, 1991; Huttula *et al.*, 1996).

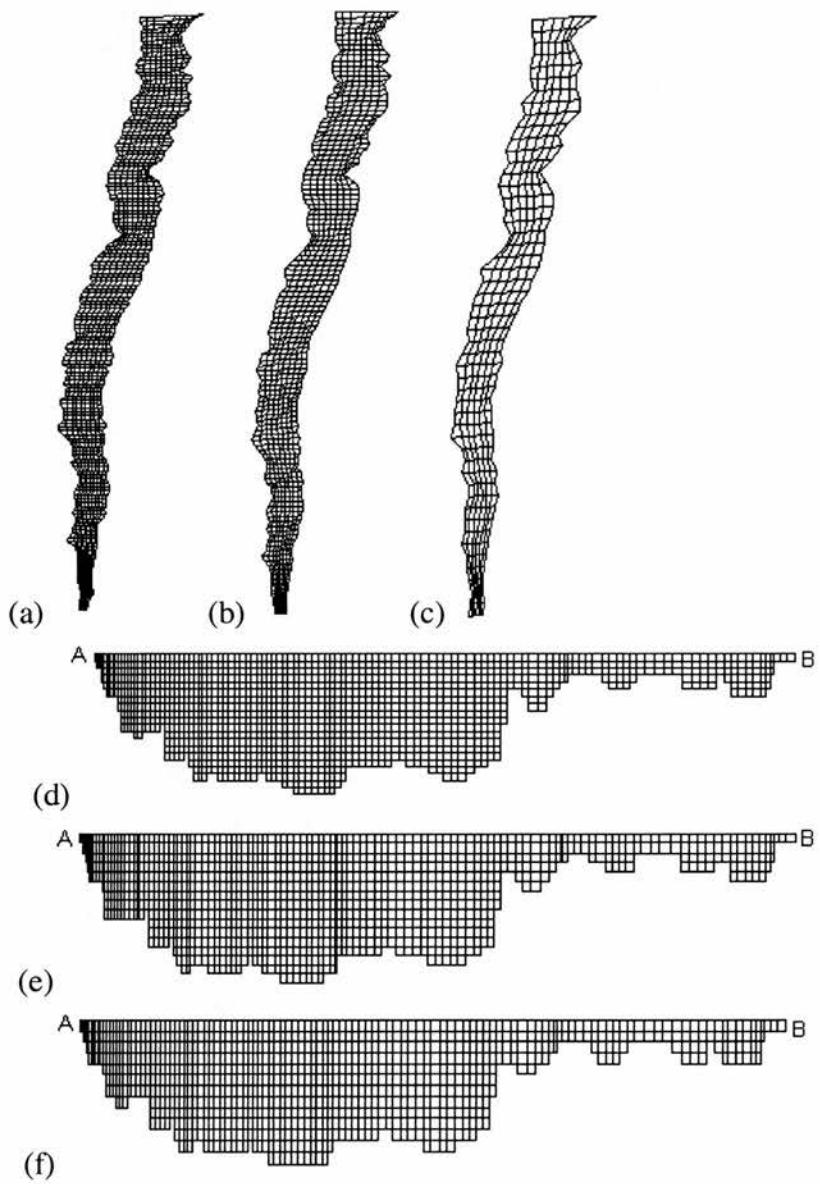

Figure 6-2. Grids used in sensitivity analysis: (a) horizontal dimension = 70 m; (b) horizontal dimension = 90 m; (c) horizontal dimension = 110 m; (d) vertical dimension = 2.5 m; (e) vertical dimension = 3 m; (f) vertical dimension = 3.5 m.

i. Vertical cell dimension

Increasing the vertical cell dimension caused two effects on the mean velocity of the surface layer (Figure 6-3). Firstly, the magnitude of the temporal variation in the mean velocity decreased, with a fall in maximum mean velocity (at approximately 12:30 Hrs) and a rise in minimum mean velocity (at approximately 24:00 Hrs). Secondly, the lag between the change in wind stress and the change in mean velocity increased (that is, there was an increase in response lag to the forcing function).

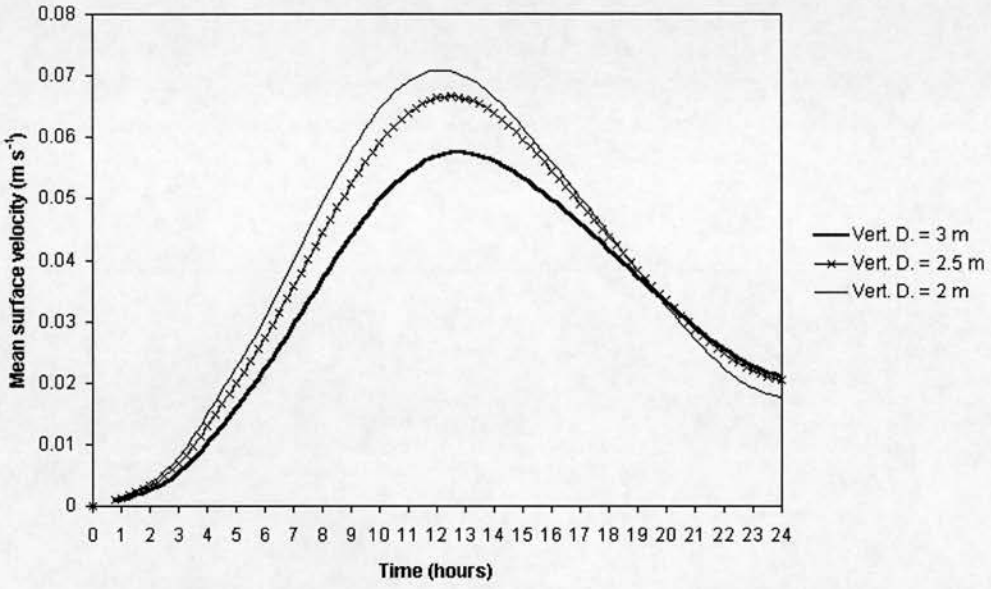

Figure 6-3. Mean surface velocities for different vertical cell dimensions.

With an increase in depth beneath the surface in lakes, there is an exponential decline in velocity (Section 2.2.4). This depth-dependent change is a continuous function, but in the model this continuous function was represented by a step function, with the step size being equal to the vertical cell dimension. By increasing the surface cell layer's vertical dimension, a greater length of the continuous function was included within the surface cell layer, and a greater amount of averaging occurred as the continuous function was converted into a step function of increasingly coarse resolution. For example, with a vertical dimension of 3 m, the surface layer included characteristics of the velocity field of up to 1 m beneath that when the vertical dimension was 2 m, causing a reduction in the velocity of the surface layer.

This conversion of a continuous function to a step function was responsible for the

increase in response lag and decrease in magnitude of the temporal variation in mean velocity with an increase in vertical cell dimension. In response to a change in wind stress, the surface (rather than sub-surface) of a lake experiences greatest change in flow velocities because this layer is in immediate contact with the wind. With an increase in depth beneath the surface, a change in wind stress has less effect on flow velocities, involving an increase in the response lag. By increasing the vertical cell dimension, the surface cell layer included a greater depth of the lake, and resulted in an increase in response lag. When wind stress decreased towards the end of the simulation, the increase in response lag with increasing cell size, caused mean velocity to decrease at a lesser rate, resulting in a decrease in the magnitude of the temporal variation of mean velocity of the surface layer.

The effect of representing a continuous function by a step function again became apparent when analysing the effect of vertical cell dimension on angular deflection as a function of depth (Figure 6-4). With vertical cell dimensions of 2 and 2.5 m, rates of angular deflection with increasing depth were relatively similar. However, with a vertical cell dimension of 3 m, deflection patterns suggested that nearly two 360° rotations had occurred within the upper 10 m of the water column.

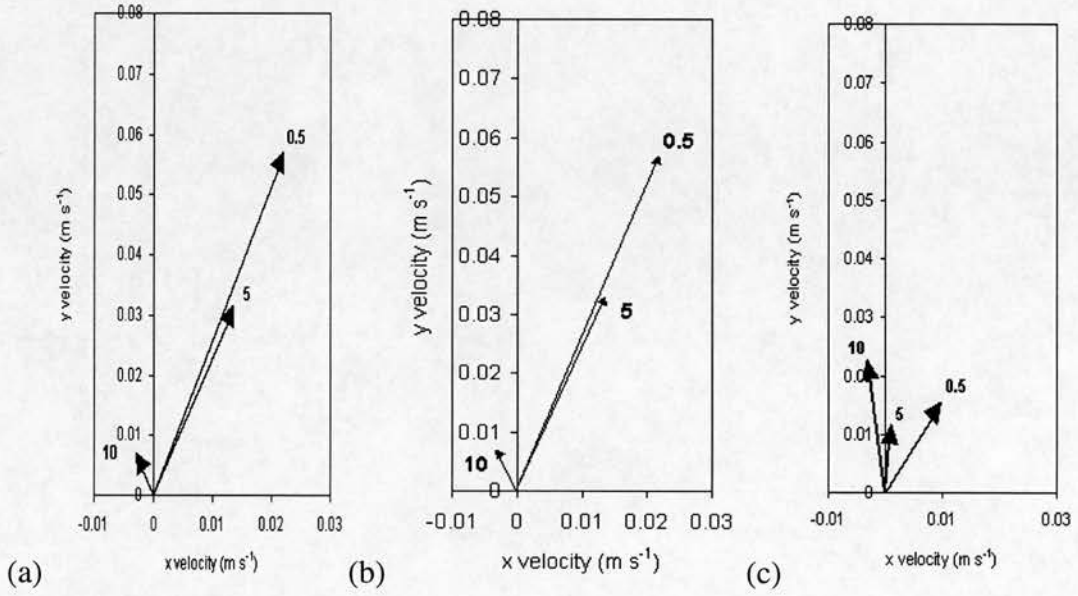

Figure 6-4. Angular deflection as a function of depth for different vertical cell dimensions: (a) vertical cell dimension = 2 m; (b) vertical cell dimension = 2.5 m; (c) vertical cell dimension = 3 m. Values at the end of each arrow are the depth of the velocity vector (m).

ii. Horizontal cell dimension

Increasing the horizontal cell dimension produced very different effects to decreasing the vertical cell dimension. Firstly, an increase in horizontal cell dimension resulted in an increase in the magnitude of the variation in mean velocity of the surface later (Figure 6-5). Secondly, the change in magnitude was much smaller. For example, increasing the horizontal cell dimension from 70 m to 110 m (which resulted in approximately doubling the horizontal areas of each cell) resulted in a increase in maximum velocity by less than 5 %. Thirdly, there was no measurable effect on the response lag to the forcing function. Finally, a increase in horizontal cell dimension had very little effect on the rate of angular deflection as a function of depth (Figure 6-6).

The relatively insensitivity to horizontal cell dimension was expected. Because the forcing function was from the surface, changes in the grid geometry which were perpendicular to the surface (and therefore lay across the axis of most change in velocity field properties) should have had greatest effect. Changing the grid geometry parallel to the surface will only have had the effect of averaging between areas horizontally, along an axis in which there was relatively little change in horizontal velocity field properties.

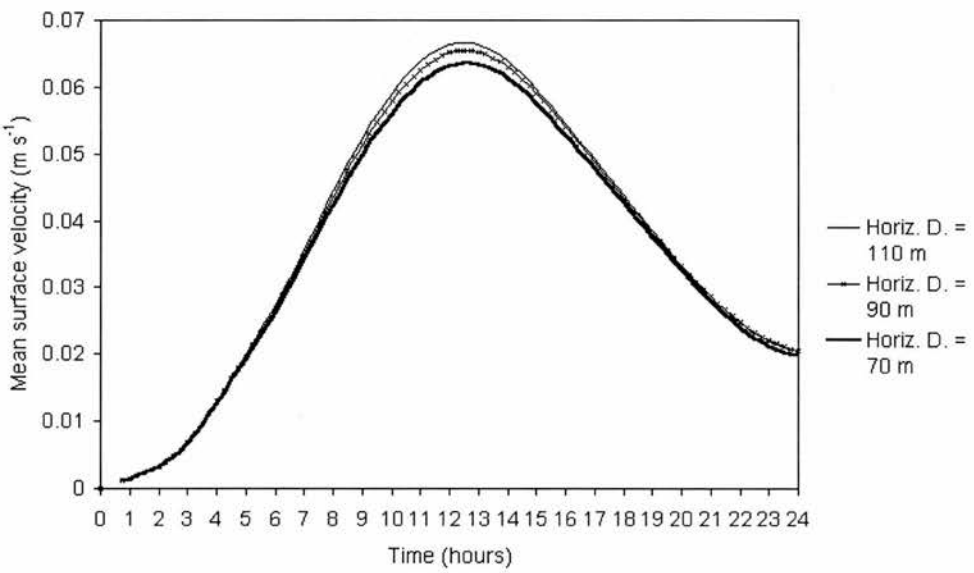

Figure 6-5. Mean surface velocities for different horizontal cell dimensions.

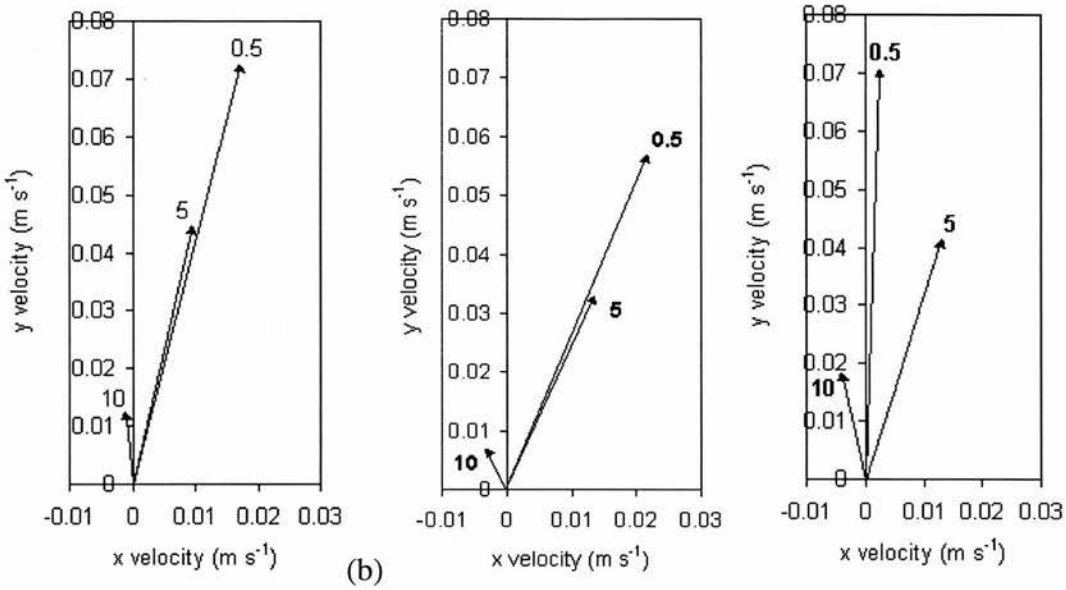

Figure 6-6. Angular deflection as a function of depth for different horizontal cell dimensions: (a) horizontal cell dimension = 70 m; (b) horizontal cell dimension = 90 m; (c) horizontal cell dimension = 110 m. Values at the end of each arrow are the depth of the velocity vector (m).

6.4 Hydrometric sensitivity to temporal resolution

With a increase in the time step, a similar pattern to that of decreasing vertical cell dimension occurred. There was an increase in the magnitude of the variation in surface velocity, and an increase in the response lag to the forcing function (Figure 6-7).

However, the effect of time step on the response lag was much greater (the model was greatly sensitive to the time step). Increasing the time step from 900 seconds to 3600 seconds resulted in a delay of the time at which maximum wind speed was reached by several hours, and an increase in the maximum velocity of the surface layer by approximately 10 %.

The time step also had a great effect on the rate of increase of angular deflection with increasing depth (Figure 6-8). With a time step of 3600 s, there was very little angular deflection, and flows at the depth of the thermocline were only deflected approximately 40° from those at the surface. Given that George (1981a) found sub-surface return flows at the thermocline deflected approximately 270° from those at

the surface for similar wind conditions, and that it is preferable to keep the time step as small as possible (Olsen, 1997) is it probable that the velocity field with a time step of 3600 s was unrealistic.

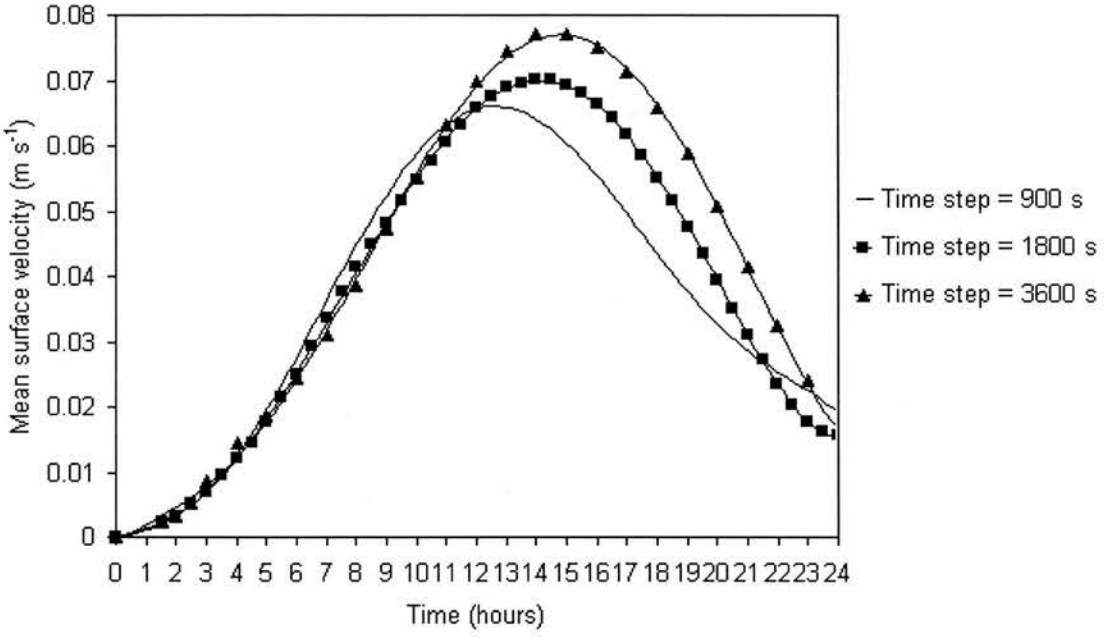

Figure 6-7. Mean surface velocities for different time steps.

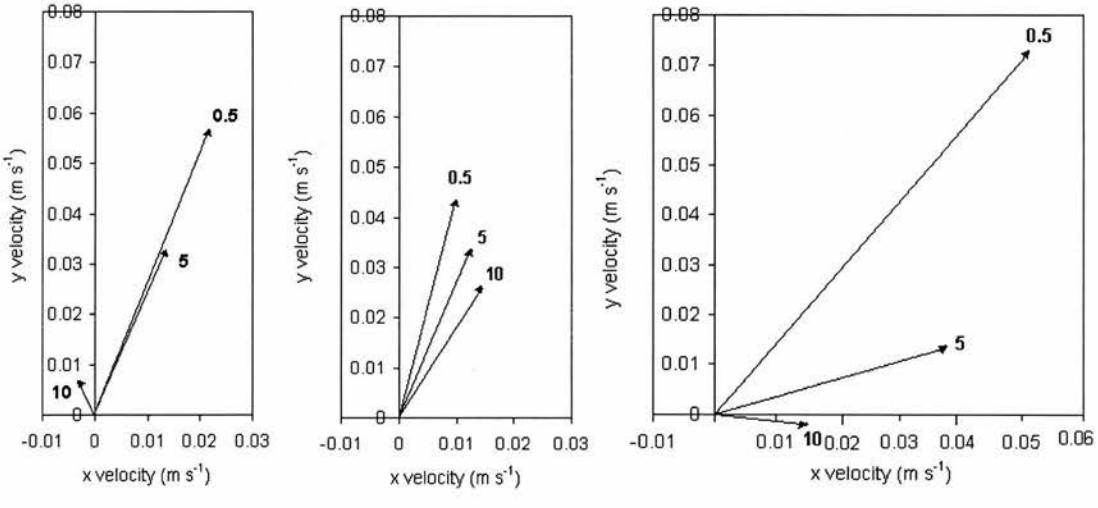

(a) (b) (c)

Figure 6-8. Angular deflection as a function of depth for different time steps: (a) time step = 900 s; (b) time step = 1800 s; (c) time step = 3600 s. Values at the end of each arrow are the depth of the velocity vector (m).

6.5 Hydrometric sensitivity to wind friction coefficient model

Simulations were run with one of three wind friction coefficient models, which in order of increasing complexity were the Bengtsson (1953), van Dorn (1973) and Wu (1969) models (Section 3.3.3.1).

Similar mean surface velocities were estimated by all wind friction coefficient models (Figure 6-9). This was because all the models produced similar wind friction coefficients at the wind speeds encountered in the simulations. However, mean surface velocities produced by the van Dorn model were approximately 10 % less than those produced by the Bengtsson and van Dorn models.

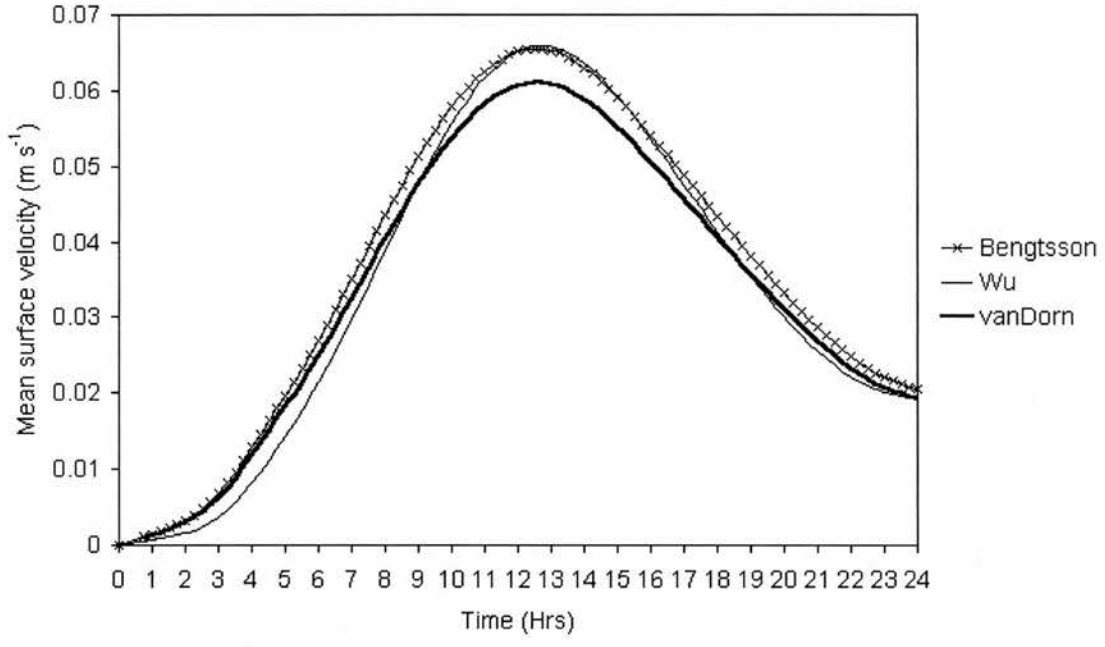

Figure 6-9. Mean surface velocities for different wind friction coefficient models.

Additionally, the rate of angular deflection with increasing depth was similar between all models (Figure 6-10). Again, this was because the models produced similar wind friction coefficients for the wind speeds with which the simulations were run.

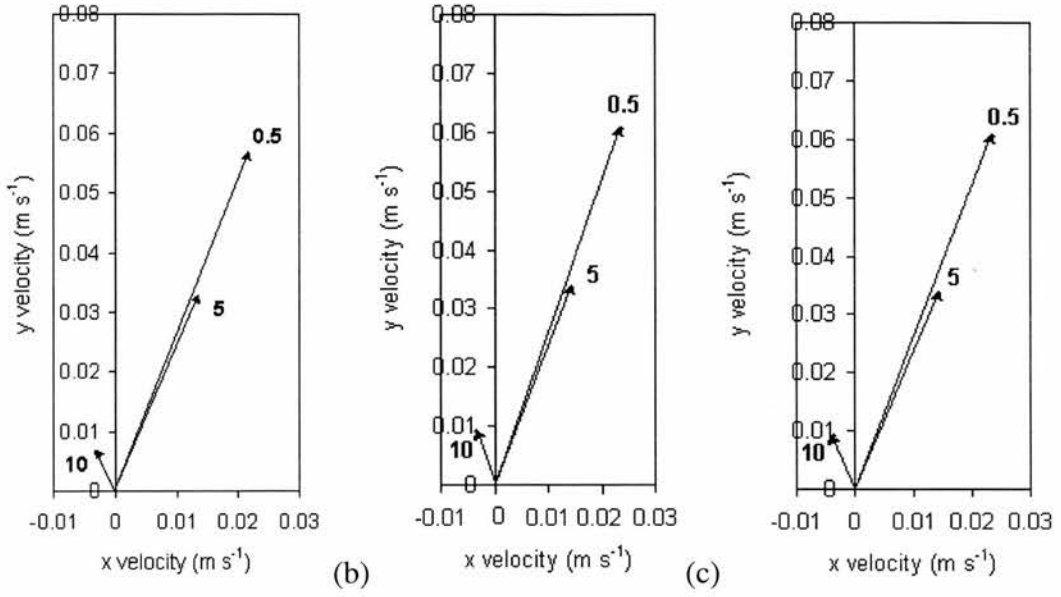

Figure 6-10. Angular deflection as a function of depth for different wind friction coefficient models: (a) Bengtsson; (b) Wu; (c) van Dorn. Values at the end of each arrow are the depth of the velocity vector (m).

6.6 Hydrometric sensitivity to turbulence model

Simulations were run with the turbulence estimated by the standard k-ε model and the zero-equation turbulence model (Section 3.3.2).

Greatly different hydrometries were created. The zero-equation model produced much lower mean surface velocities than the k-ε model (Figure 6-11) and produced much less angular deflection as a function of depth (Figure 6-12).

The zero-equation model caused a reduction in the mean velocity of the surface cells and a reduction in the rate of angular deflection because it increased the amount of turbulence. This increase in turbulence caused, firstly, a decrease in convection for a given energy input, and secondly, homogenisation of velocities in overlying and underlying layers (in effect, causing overlying and underlying layers to 'stick' together). As a result of this homogenisation of velocities in the vertical dimension, the zero-equation model was more likely to produce surface return flows than the k-ε model.

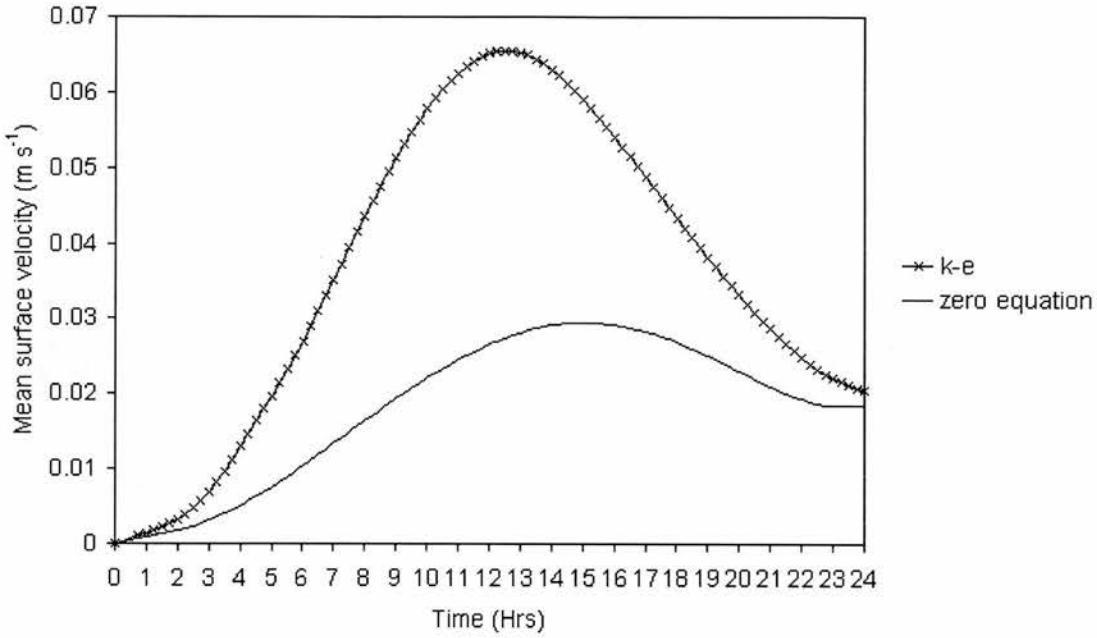

Figure 6-11. Mean surface velocities for different turbulence models.

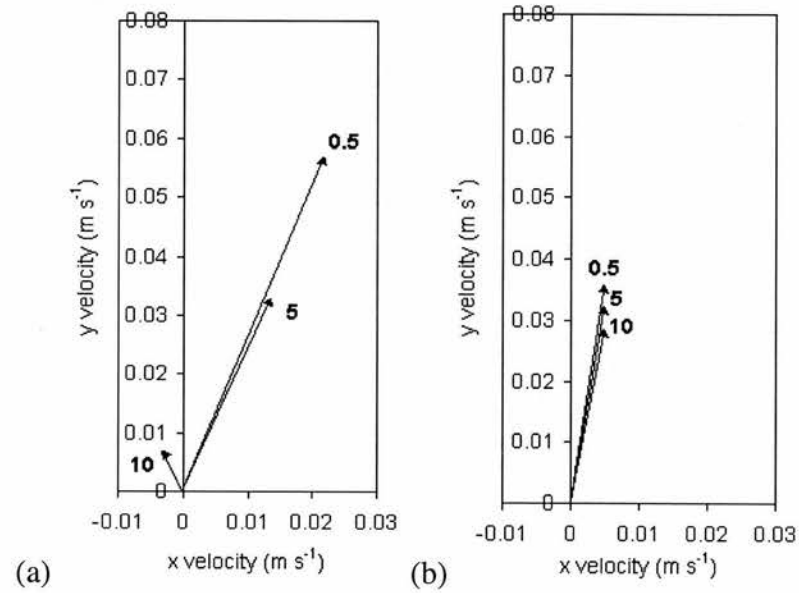

Figure 6-12. Angular deflection as a function of depth for different turbulence models: (a) *k*-ε model; (b) zero-equation model.

6.7 Effect of hydrometric sensitivities on the spatial dynamics of phytoplankton

So far in this chapter, emphasis has been upon the effect of a change of internal boundary conditions on the hydrometry. This section explains how this change in hydrometry may cause a change in the spatial dynamics of phytoplankton, by comparison of the spatial distributions created after simulating 24 hours of time (under the same external boundary conditions as those of Section 6.3 to Section 6.6).

Simulations were initiated with a surface layer of cyanobacteria (from 1 g m^{-3} at the surface to 0 g m^{-3} at a depth of 5 m), with an initial density of 0.965 Mg m^{-3}. The light climate was relatively dull (maximum irradiance = 600 μE m^{-2} s^{-1}), ensuring that the cyanobacteria were positively buoyant throughout the simulation. Cyanobacterial radius was set at 250 μm, which is a typical colony size for *Microcystis* (Howard, 1997).

Despite the changes in hydrometry from changes in internal boundary conditions, there was much similarity between the spatial distributions of cyanobacteria at the end of the simulations (Figure 6-13, Figure 6-14, Figure 6-15 and Figure 6-16). In all cases there was an accumulation of cyanobacteria on the eastern side of the lake. This was the result of Coriolis acceleration deflecting surface currents towards the north-east, so that cyanobacteria were displaced in that direction, and accumulated over the downwelling areas long the eastern side. A reduction in cyanobacterial concentration at the western side was experienced because of the upwelling of relatively cyanobacterial-free water.

Slight differences in spatial distributions did exist, however. There was an increase in across-axis variation in cyanobacterial concentration with a decrease in cell vertical dimension, an increase in cell horizontal dimension and an increase in time step, because these changes caused greater flow velocities and therefore greater rates of displacement of cyanobacteria at the surface. After the simulation of 24 hours, the zero-equation turbulence model produced greatest concentrations of cyanobacteria at some distance from the eastern wall along much of the basin. This was the result of a reduced rate of displacement at the surface.

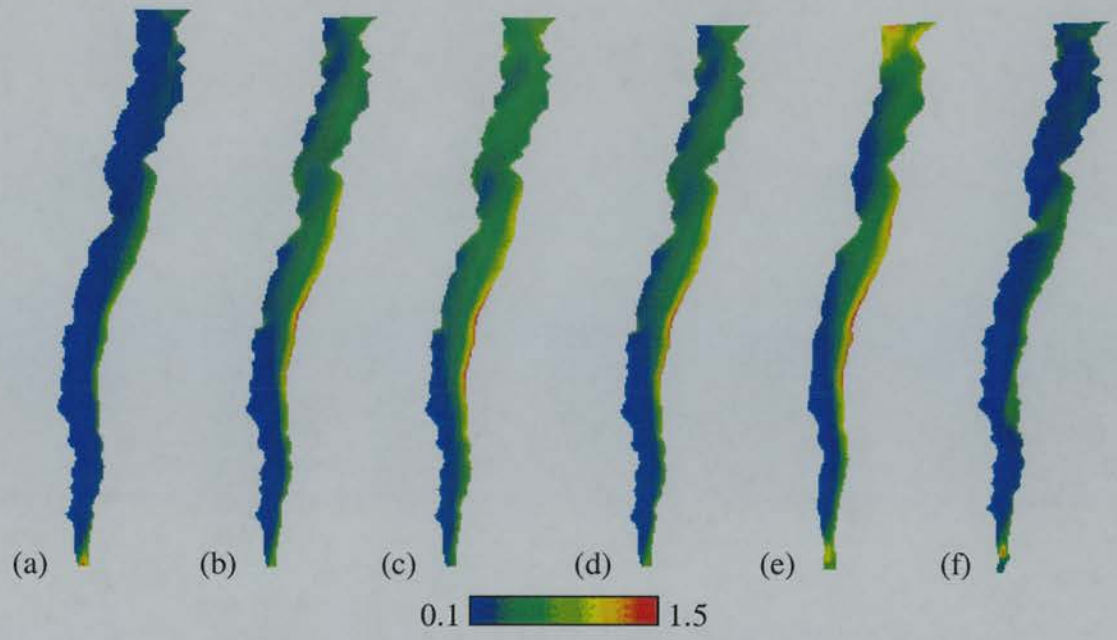

Figure 6-13. Spatial distributions of cyanobacteria in Lake Windermere generated with different grid resolutions: (a) vertical cell dimension = 2.5 m; (b) vertical cell dimension = 3 m; (c) vertical cell dimension = 3.5 m (d) horizontal cell dimension = 70 m; (e) horizontal cell dimension = 90 m; (f) horizontal cell dimension = 110 m.

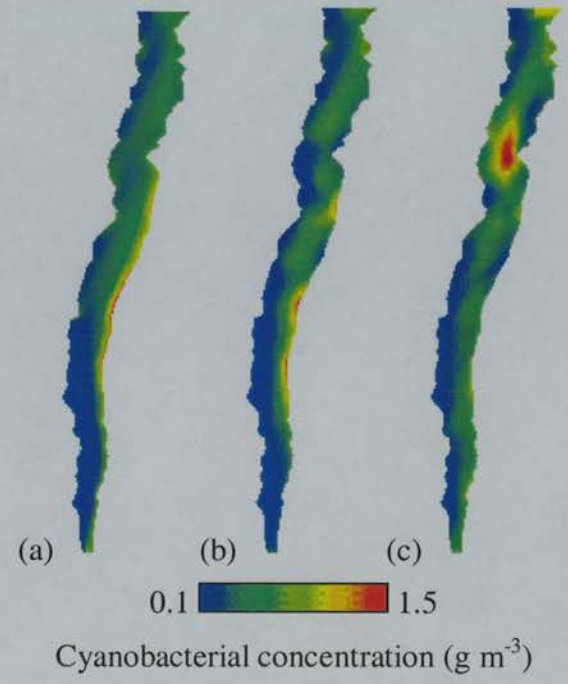

Figure 6-14. Spatial distributions of cyanobacteria in Lake Windermere generated with different time steps: (a) time step = 900 s; (b) time step = 1800 s; (c) time step = 3600 s.

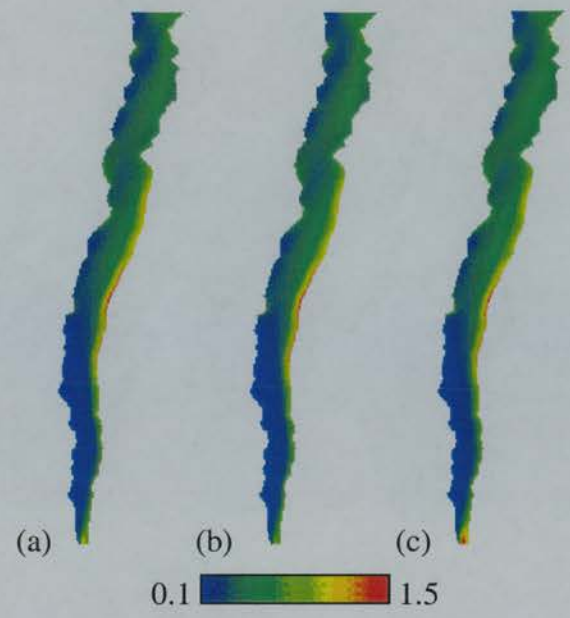

Figure 6-15. Spatial distribution of cyanobacteria in Lake Windermere generated with different wind friction coefficient models: (a) Bengtsson; (b) van Dorn; (c) Wu.

Figure 6-16. Spatial distribution of cyanobacteria in Lake Windermere generated with different turbulence models: (a) standard k-ε model; (b) zero-equation model.

6.8 Conclusion

i. Sensitivity to spatial resolution

SSIIM2.0 was highly sensitive to vertical grid resolution, although relatively insensitive to horizontal grid resolution. The effect of the sensitivity to vertical resolution on the simulated spatial dynamics of phytoplankton was that rates of development of horizontal macro-scale structure in the surface layer increased with an increase in vertical grid resolution.

ii. Sensitivity to temporal resolution

SSIIM2.0 was highly sensitive to temporal resolution. The effect of this sensitivity on the simulated spatial dynamics of phytoplankton was that rates of development of horizontal macro-scale structure in the surface layer increased with an increase in time step. In CFD modelling, the aim is generally to reduce the time step to as small as possible to minimise the effect of compounded errors experienced when converting differential equations into equations that can be solved computationally (Ferziger and Peric, 1996). Therefore, in Chapters 7 and 8, a time step of 900 s is used.

iii. Sensitivity to wind friction coefficient model

SSIIM2.0 was relatively insensitive to the wind friction coefficient model at the wind speeds applied, so the choice of model has little effect on the spatial dynamics of phytoplankton in the surface layer. In Chapters 7 and 8, the Bengtsson model is used because it is the simplest, and therefore most computationally efficient.

iv. Sensitivity to turbulence model

SSIIM2.0 was highly sensitive to the turbulence model. The k-ε model caused greater mean surface velocities and rates of deflection as a function of depth than the zero-equation model. This resulted in greater rates of development of macro-scale structure at the surface. The k-ε model is dominant within CFD modelling (Versteeg and Malalasekera, 1995) so is the model used in most simulations in Chapter 7 and 8. However, in one simulation, the zero-equation model is used because its increased turbulence satisfies the requirements of the simulation (Section 7.2).

7 Process modelling: real lakes

7.1 Introduction

To understand the causes of the spatial dynamics of phytoplankton in complex environments, CFD simulations of processes and resulted spatial distributions were made of three lakes in the UK: Loch Leven, Esthwaite Water, and Eglwys Nynydd. These were selected as a compromise between the amount of information that could be provided on the relationships between the spatial dynamics of phytoplankton and causative processes, and the availability of data to act as external boundary conditions for executing the SSIIM2.0.

The chosen lakes represented great differences in lake environmental properties (with great differences existing in morphometry, thermal structure, wind regime, and light regime) and great difference in phytoplankton characteristics (with dominant species being diatoms, dinoflagellates or cyanobacteria). A complex set of relationships could therefore be analysed.

Of all the lakes referred to in this thesis, there was more information on lake environmental and phytoplanktonic properties (to provide external boundary conditions) and more information on the spatial distributions of phytoplankton (to provide verification of the simulated spatial distributions) for these lakes than for any others. In all cases, however, model simulation was limited by the quality and quantity of available data, as often necessary data sets were either non-existent or of an unsuitable spatial or temporal scale. In such cases, estimation was required which increased the potential for discrepancy between simulated and measured spatial distributions.

The first simulation was relatively simple: merely the simulation of a spatial distribution of phytoplankton in Loch Leven from estimates of a single set of external boundary conditions. The second two simulations - of Esthwaite Water and Eglwys Nynydd - considered the same basins under different sets of external boundary conditions (different meteorological conditions or different phytoplankton species).

7.2 Loch Leven: the effect of turbulence on the spatial dynamics of phytoplankton

7.2.1 Introduction

Loch Leven differs from most other large Scottish lakes in that it is less elongated and it is relatively shallow. Bathymetrically, the lake has a shallow rim (extensive in the north) with two central areas of deeper water.

The hydraulic characteristics of the lake are greatly affected by the meteorology of the area, which varies over short time scales due to the passage of frontal systems. The lake is generally mixed (with no horizontal or vertical variation in water quality) as a result of these frontal systems. Mixing is pronounced because of the lake's morphometry (Smith 1972/1973). Firstly, most of the lake is relatively shallow, so the depth of the wave-mixed layer may extend to the bed (Smith and Sinclair, 1972). Secondly, the lake is non-elongated and contains few obstructions to flow so the largest energy-bearing eddy will occupy a long scale (maximum horizontal eddy viscosity for a length of 5 km will be approximately 20 $m^2 s^{-1}$). Thirdly, over much of the lake, current direction is generally constant at all depths with return currents occurring at the surface (Smith, 1972/1973). This will mean that the effect of buoyancy characteristics of phytoplankton in influencing the horizontal spatial dynamics of phytoplankton will be minimised. As a result of mixing, the lake is generally unstratified, although transient stratification may occur for short periods in the two deeper parts of the lake in warm calm weather (Smith 1972/1973).

Of the 50 species of phytoplankton most often found in the lake, there is large seasonal and annual variation in which species achieve dominance. Diatoms are generally dominant (Bailey-Watts, 1986; Bailey-Watts, 1992), particularly in winter and spring, (the major genus is *Stephanodiscus)*, but blue-green algae and green algae are also present (Bailey-Watts, 1992), particularly in the summer. Although mixing in the lake tends to homogenise the phytoplankton concentration (Bailey-Watts, 1981), gentle and non-persistent gradients have been found.

7.2.2 Measured spatial distributions

Many data exist on the spatial distribution of phytoplankton from a programme of intensive sampling conducted in May 1985. These data include an ATM image acquired at 10:00 Hrs on 11 May 1985, with concurrent surface measurements of chlorophyll-*a* concentration and temperature.

The ATM image was processed to show chlorophyll-*a* concentration using a regression relationship between radiance in Channels 3 and 5 of the ATM image and surface measurements (Bennet, 1994) as follows:

$$c = -1.5450 + 6.984\frac{ATM3}{ATM5} \qquad \textbf{(7-1)}$$

where c is the chlorophyll concentration. Although empirically derived, this relationship makes intrinsic sense: there is a chlorophyll reflectance feature in Channel 3 and a chlorophyll absorption feature in Channel 5. To aid comparison with the hypothetical basins (Chapter 8) in which the unit of measurement was in *g phytoplankton* m^{-3}, chlorophyll-*a* concentration was converted into the concentration of the diatom *Stephanodiscus* (the dominant species of phytoplankton at the time) using appropriate conversion factors (Reynolds, 1984). Mean *Stephanodiscus* concentration was estimated at 0.359 g m^{-3}.

A gradient in *Stephanodiscus* concentration from low concentrations in the east to high concentrations in the west was evident on 11 May 1985 from the ATM image (Figure 7-6a). Not only was the existence of a trend atypical for this lake, but greater concentrations were found in downwind areas which was an unusual spatial distribution for negatively buoyant diatoms.

7.2.3 Model objectives

The objective of the modelling was to simulate the spatial distribution in *Stephanodiscus* concentration that was evident in an ATM image acquired on 11 May 1985, in an attempt to understand why a negatively buoyant species was found in a downwind area.

7.2.4 Boundary conditions

The simulation was begun at 00:00 Hrs 9 May 1985. This was because this was the most likely time for spatial homogeneity in *Stephanodiscus* concentration to have existed. Previously, wind speeds had been relatively high, and it may be inferred that these speeds would have caused spatial homogeneity. The justification for this assumption is explained when describing the internal boundary conditions of the thermal profile and water quality.

i. Turbulence and wind-friction coefficient models

The zero-equation turbulence model was used as this generally causes greater turbulence than the standard k-ε model. This was a requirement because increased turbulence in the vertical dimension results in a smaller vertical change in convection properties (mean speed and direction), which should result in current flows more similar to those observed by Smith (1972/1973). The disadvantages of using this model, as relating to continuity between simulations are discussed in Section 9.3.3. The Bengtsson wind friction coefficient model was used.

ii. Bathymetry and grid morphometry

Transect data (Kirby, 1972/1973) were used to estimate bathymetry (Figure 7-1).

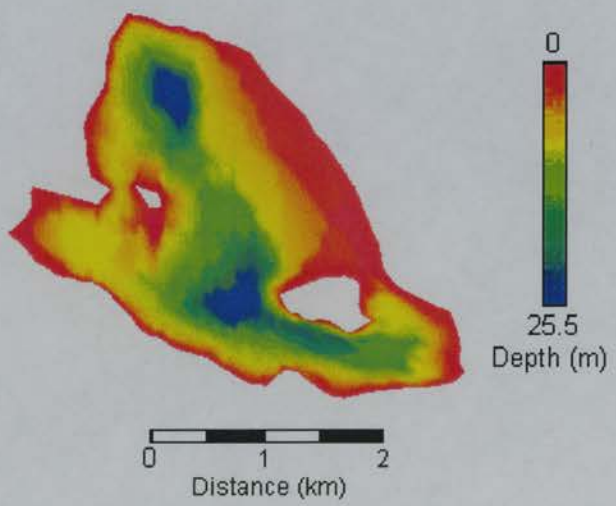

Figure 7-1. Bathymetry of Loch Leven.

A finite volume grid was generated from the bathymetry (Figure 7-2). Grid cells approximated 100 m in the horizontal dimension and 2 m in the vertical dimension.

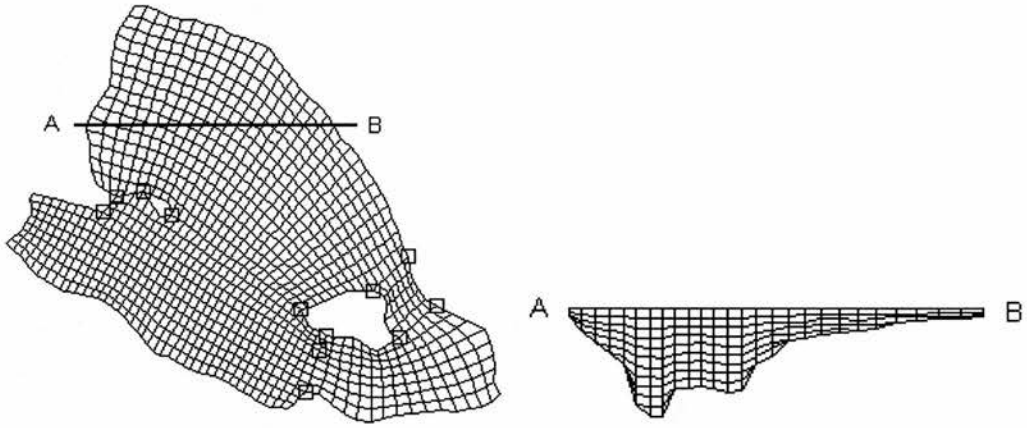

Figure 7-2. Grid of Loch Leven: (a) grid at surface (squares indicate connections between blocks); (b) transect.

iii. Irradiance

No measurements of sub-surface irradiance for the time of simulation at this site existed, so it was necessary to estimate this from the solar elevation, atmospheric conditions, and surface reflectance conditions (Kirk, 1994; Appendix D). The sky was overcast on 9 and 10 May, resulting in low levels of irradiance relative to 11 May when the sky was cloud-free (Figure 7-3).

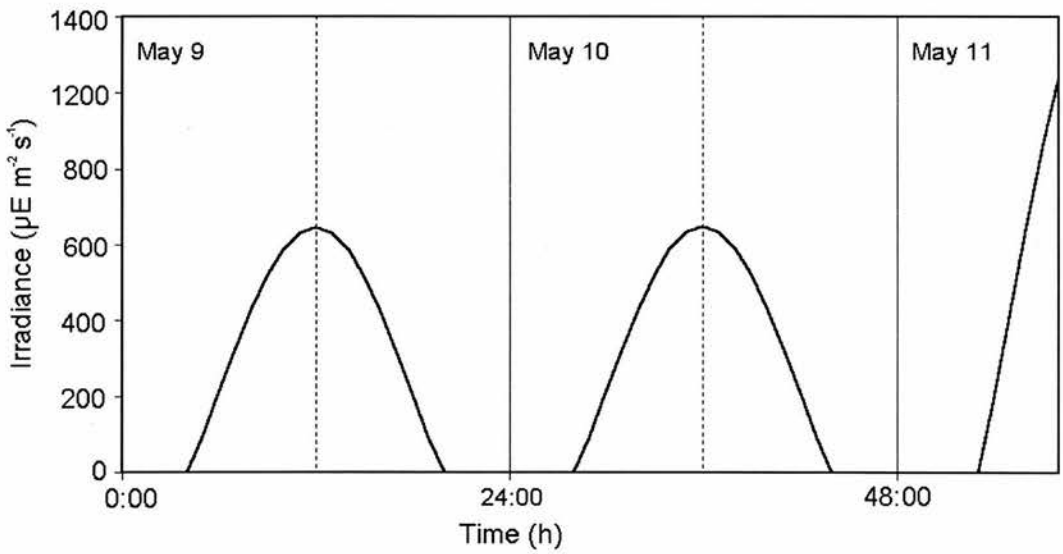

Figure 7-3. Time-series of irradiance for Loch Leven.

Thus, for a diatom concentration of 0.5 g m^{-3}, the extinction coefficient would be 0.73. For this, the depth of the euphotic zone would approach 7 m.

iv. Wind

A time-series of wind speed and direction from a meteorological station at Edinburgh Turnhouse (55057' N, 03021'W), 35 km south of the site, was used to drive the model (Appendix E). Prior to 9 May 1985, wind speeds had been consistently high (the mean daily wind speed was greater than 5 m s^{-1}) and of varying direction. This was followed on 9 May 1985 by a period of very low wind speeds (the mean daily wind speed was approximately 1 m s^{-1}). Finally, on 10 and 11 May, there was a period of higher wind speeds (the mean daily wind speed approached 4 m s^{-1}) with a relatively constant direction from the north-east and east.

The low wind speeds on 9 May 1985 were atypical for this lake. On only six days throughout 1985 were the mean daily wind speeds less than that experienced on 9 May 1985.

v. Thermal profile

No data existed on the horizontal or vertical variation in temperature for the few weeks preceding the time of image acquisition. As it has been established empirically that long periods of wind-induced mixing in this lake cause both horizontal and vertical homogeneity in temperature, and that wind speeds had been consistently high preceding 9 May 1985, the model was initiated at the beginning of 9 May 1985 with the assumption of thermal spatial homogeneity. As a result of wind-speeds preceding 9 May 1985, the depth of the wave-mixed layer can be estimated as being between 1 and 4 m (Smith and Sinclair, 1972). This will ensure that water quality within most of the lake will be homogeneous in the vertical dimension: exceptions being the two deep troughs. With the added effect of mixing from sub-surface gradient currents, it may be assumed that some mixing had occurred even at these depths.

Water temperature was estimated as being 11°C from the mean of a surface sample of 9 observations.

vi. Stream inflows and outflows

Although stream inflows and outflows affect phytoplankton species composition over long time scales in this lake, stream inflows and outflows were not included in the simulation because they have a negligible effect on the large scale convection patterns in the lake over a short-time period (Bailey-Watts *et al.*, 1990). The flushing rate is 7 x 10^{-3} volumes per day, or 2.57 lake volumes per year (Bailey-Watts *et al.*, 1989) so, over a simulation lasting for several days, this will not affect macro-scale spatial dynamics of nutrients or phytoplankton because of the comparatively greater effect of wind-induced circulation. Additionally, at the time of simulation, nutrient concentrations in the inflowing streams were of a similar level to those in the lake (Dick Jater *pers. com*).

vii. Water quality

Water quality was assumed to be spatially homogeneous on 9 May 1985 for the same reason that temperature was homogeneous. That is because of wind-induced mixing.

- ***Nutrient concentration***

  Silica concentration was modelled because this was the most well-documented nutrient affecting diatom growth in this lake. Bailey-Watts (1978) has reported silica depletion concurrent with diatom growth, and Bailey-Watts *et al.* (1989) have shown a positive correlation between diatom concentration and dissolved silica concentration in February, March, April and May 1985 (that is, high concentrations of silica support high concentrations of diatoms). Silica concentration was relatively low in May 1985 (approximately 7 g m^{-3}), so silica concentration was limiting diatom production.

  Phosphorus concentration was not simulated as it has been shown that there is a lack of correlation between diatom concentration and phosphorus concentration for this lake (Holden and Caines, 1972/1973) and a correlation would be expected if phosphorus concentration was a limiting factor. Nitrogen concentration was not simulated as it has been shown that diatom net population growth is not limited by low nitrate concentrations (Holden and Caines, 1972/1973).

- *Stephanodiscus concentration*

  Stephanodiscus concentration at the beginning of 9 May 1985 was estimated at 0.36 g m^{-3} (from interpolation between point observations at the main outflow on 2 May 1985 and measurements made in the lake on 11 May 1985).

7.2.5 Simulation

Surface currents were deflected approximately 40° to the right of the wind direction (Figure 7-4a), and a typical lake-wide vertical dimensional convection cell was initiated, with downwelling at downwind areas, and upwelling at upwind current areas. Downwelling and upwelling were of the order of ±0.1 mm s^{-1} (Figure 7-4b).

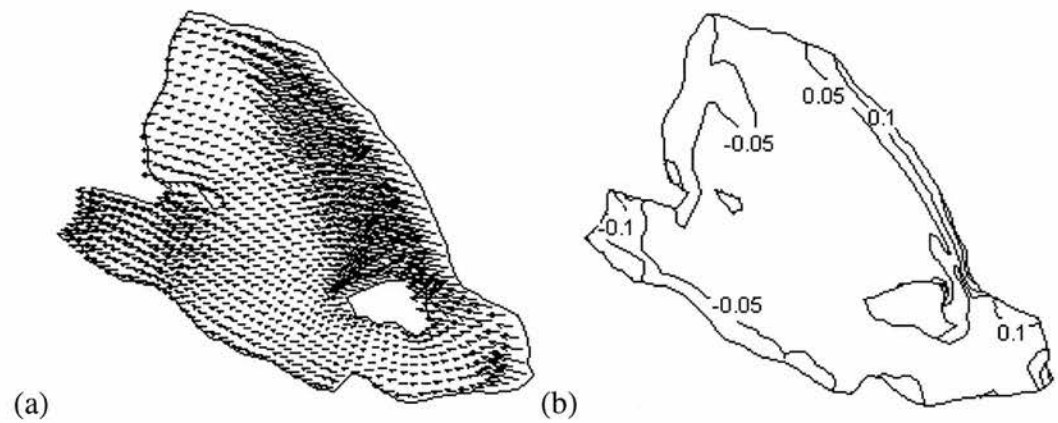

Figure 7-4. Simulated currents of Loch Leven (10:00 11 May 1985): (a) surface current vectors; (b) vertical velocity at surface (values are in mm s^{-1}).

A compensatory displacement of water through surface return flows was generally not experienced until towards the end of the simulation, with the bulk of return flows occurring beneath the surface. This contradicts the findings of Smith (1972/1973).

From the simulation, *Stephanodiscus* settling, combined with relatively low growth rates in the morning of 9 May 1985, caused a reduction in surface concentration (Figure 7-5). At approximately 12:00 Hrs, the increase in wind speed caused some resurfacing of *Stephanodiscus* which, coupled with greater irradiance-induced growth, caused a short-term increase in surface concentration. As wind speeds decreased during the evening, *Stephanodiscus* sinking rates increased, and by the end of 9 May 1985 the surface was greatly depleted of *Stephanodiscus*, with the concentration near the surface being much less than that at greater depths.

Additionally, some settling had occurred at the lake bed. During 10 May 1985 and 11 May 1985, wind-induced turbulence caused upwelling of *Stephanodiscus* from the deeper part of the lake.

Figure 7-5. Simulated mean surface *Stephanodiscus* concentrations in Loch Leven.

Wind-induced currents (predominantly from the north and north-east) caused an increase in surface *Stephanodiscus* concentration in the west and south-west. The simulated spatial distribution of surface *Stephanodiscus* concentration at 10:00 on 11 May 1985 was similar to that measured (Figure 7-6).

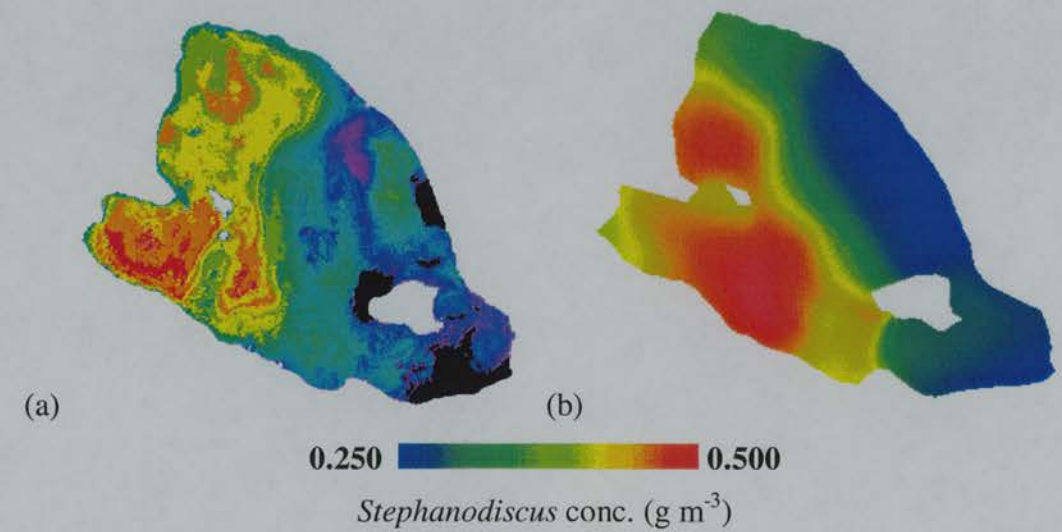

Figure 7-6. Surface *Stephanodiscus* concentration in Loch Leven (10:00 11 May 1985): (a) measured (from an ATM image); (b) simulated.

Discrepancies between the simulated and measured surface spatial distributions existed by the end of the simulation, however. The model underestimated mean surface *Stephanodiscus* concentration (the model estimate was 0.295 g m^{-3} as opposed to the outflow measurement of 0.359 g m^{-3}) and the estimated pattern was different with greater underestimation in the north-east of the lake. These differences may be attributed to errors in the data for establishing external boundary conditions and errors in the terms of the biological model (Section 9.3). However, if the model was allowed to simulate *Stephanodiscus* concentration for several hours of simulated time after that of the remotely sensed image, a mean concentration and spatial distribution more similar to that of the ATM image were produced.

7.2.6 Summary

The spatial dynamics of diatoms in Loch Leven were caused by two processes. Firstly, there was the upwelling of diatoms from deeper parts of the lake caused by wind-induced turbulence. Secondly, there was a westward wind-induced convection of diatoms close to the water surface. The CFD modelling used here has shown that it is possible to simulate the downwind accumulation of a negatively buoyant species of phytoplankton. A simpler non-dynamic approach would have been unable to explain the patterns found in this lake.

7.3 Eglwys Nynydd: the effect of wind speed on the spatial dynamics of phytoplankton

7.3.1 Introduction

Eglwys Nynydd is a small, shallow reservoir (a surface area of 1.01 km and a mean depth of 3.5 m) in South Wales. The bathymetry is relatively flat, although there is a deeper area in the south (Figure 7-7). Despite its small size, it has a relatively large retention time of approximately five months (George and Edwards 1976) as stream inflows and outflows are of small magnitude.

As with Loch Leven, the hydraulic characteristics are affected greatly by the lake's meteorology. Wind–induced mixing often results in a thermal homogeneity in both

horizontal and vertical dimensions. Unlike Loch Leven, sub-surface return flows dominate over surface return flows.

The lake is eutrophic. Diatoms dominate the spring months, green algae become dominant in April, and dense blooms of cyanobacteria (including *Microcystis* and *Anabaena*) occur in summer. It has been concluded that the dominant cause of variation in phytoplankton concentration is differential surface accumulation resulting from wind-forcing rather than inflow- and outflow-induced nutrient gradients, as tracer studies have shown that throughflows of water quickly lose their distinct identities (George and Edwards, 1976).

7.3.2 Measured spatial distributions

In 1969, a series of measurements were made of the horizontal and vertical distributions of phytoplankton concentration under conditions of different wind speeds by George and Edwards (1976). It was found that, firstly, macro-scale gradients of the cyanobacterium *Microcystis* existed with higher concentrations in downwind areas and near to the surface under the influence of wind speeds of less than 4 m s^{-1}, and secondly, greater homogeneity in *Microcystis* existed under the influence of wind speeds of greater than 4 m s^{-1}. These two spatial distributions were attributed respectively to positive buoyancy that was overcoming downwelling currents and wind-induced mixing that was disintegrating macro-scale spatial distributions.

7.3.3 Model objectives

The objective of the simulation was to analyse the effect of the wind regime, on the horizontal and vertical dynamics of *Microcystis*. The model was parameterised using data from 1969 to simulate distributions for *Microcystis* under, firstly, wind speeds of less than 4 m s^{-1} (with winds from the south) and, secondly, wind speeds of greater than 4 m s^{-1} (with winds from the north-west) (Appendix E).

7.3.4 Simulation with relatively low wind speeds

Processes were simulated for 12 hours before the measurements of phytoplankton spatial distributions had been acquired (the simulation was begun at 0:00 Hrs). This

was because wind data were unavailable for previous times. However, it is believed that the wind history in previous days has little effect on spatial distributions of phytoplankton (George and Edwards, 1976) as the lake responds relatively quickly to a change in wind conditions.

7.3.4.1 Boundary conditions

i. Turbulence and wind friction coefficient models

The model was run with the standard k-ε turbulence and the Bengtsson wind friction coefficient models.

ii. Bathymetry and grid morphology

Transect data from the British Steel Corporation were used to estimate bathymetry (Figure 7-7).

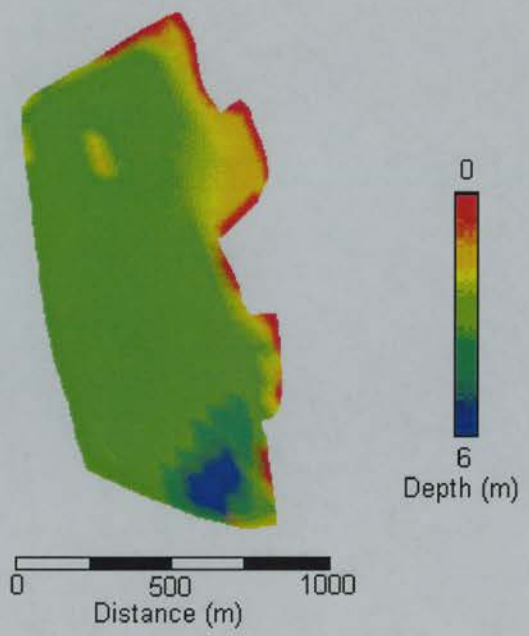

Figure 7-7. Bathymetry of Eglwys Nynydd.

A finite volume grid was generated from this, with cells of average dimensions of 100 m in the horizontal domain and 1 m in the vertical domain (Figure 7-8). Although it had been the initial intention to keep grid resolutions constant between the simulations of different lakes, it was necessary to use this finer grid in the vertical

dimension for Eglwys Nynydd because any coarser grid produced non-physical results (it was found that a minimum of approximately 10 cells was required by SSIIM2.0 to successfully characterise hydrometries involving sub-surface return flows).

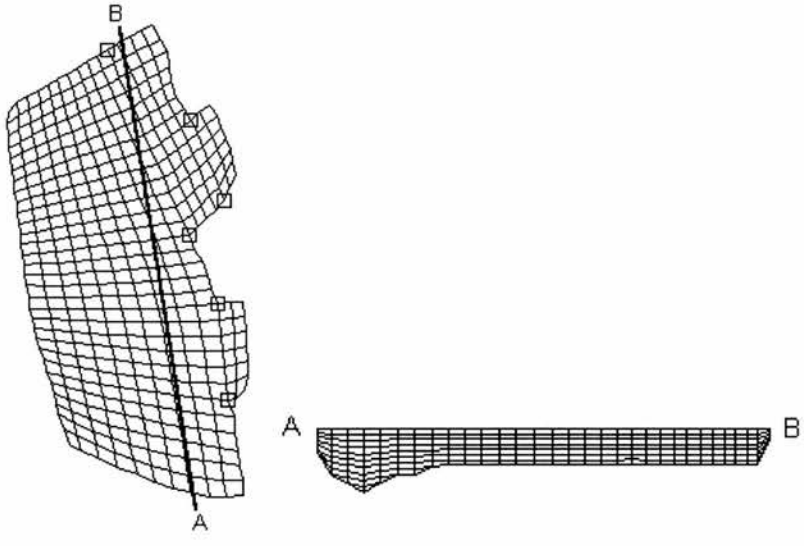

Figure 7-8. Grid of Eglwys Nynydd: (a) grid at surface (squares indicate connections between blocks); (b) transect.

iii. Other boundary conditions

Inflows and outflows were not modelled as it was believed that these would have a negligible effect on the spatial dynamics of phytoplankton (the mean flushing rate was only 0.57 percent of the lake volume per day and negligible compared to the volume of water displaced by wind-forcing). No data existed on irradiance, so this was estimated according to the method outlined previously (Appendix D), with the time of sunrise occurring at 5:00 Hrs.

Population growth was set to zero because the simulation was run for a time when the *Microcystis* concentration had reached its peak. The simulation was started with a homogeneous distribution of *Microcystis* in the horizontal dimension and a heterogeneous, vertically stratified profile. The initial mean *Microcystis* concentration in the simulation was set to be equal to that measured (that is, the simulation was run with the assumption that no population growth had occurred). The starting *Microcystis* density was set at 0.96 Mg m^{-3}.

7.3.4.2 Simulation

Simulated circulation patterns were similar to those measured by George and Edwards (1976). Surface currents were deflected to the right of the wind direction by Coriolis acceleration (Figure 7-9a), and Ekman spirals with vertical dimensions equal to those of the lake depth were initiated. Lake-wide convection cells were also initiated, with downwelling in the downwind parts of the lake (Figure 7-9b), and upwelling in the upwind parts of the lake. The magnitude of the upwelling and downwelling velocities was of the order of ± 0.1 mm s^{-1}.

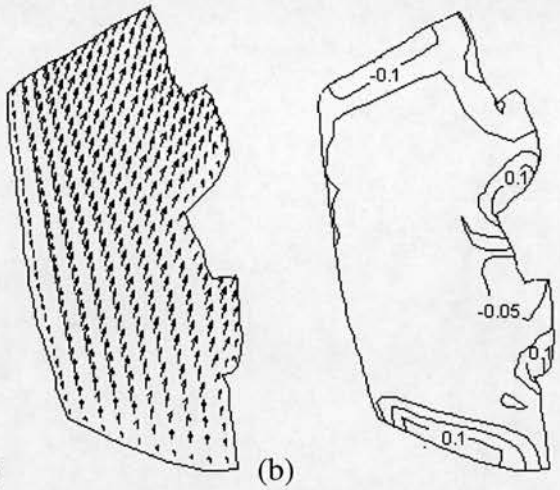

Figure 7-9. Simulated currents of Eglwys Nynydd (15:00 2 August 1973) of Esthwaite Water: (a) surface current vectors; (b) vertical velocity at surface (values are in mm s^{-1}).

Surface *Microcystis* density decreased from 0:00 Hrs to 5:00 Hrs because of carbon loss resulting from respiration, and there was a general upward movement as the cyanobacteria became more positively buoyant. From 5:30 Hrs, irradiance-induced photosynthesis caused an increase in density, and by 12:00 Hrs, the cyanobacteria had nearly become neutrally buoyant.

There was some similarity between the measured horizontal *Microcystis* distribution (Figure 7-10a) and the simulated horizontal *Microcystis* distribution (Figure 7-10b), with greater concentrations accumulating at the surface in the downwind area. This was because the *Microcystis* had been positively buoyant for most of the simulation, so the positive rising velocity was partially overcoming downwelling. Discrepancies existed however. Firstly, a small area of greater surface concentration was created

downwind of the first promontory because of the downwelling occurring there. This was not found by George and Edwards (1976) but it is a physically feasible phenomenon, and it is possible that their sampling regime had been unable to resolve this small scale variation. Secondly, the model greatly underestimated the magnitude of the variation in *Microcystis* concentration. This can be attributed to an inadequate knowledge of the prevalent environmental conditions for executing the model. The horizontal gradient could be increased by either running the model for a longer time period, or assuming a greater mean surface concentration at the initiation of the simulation.

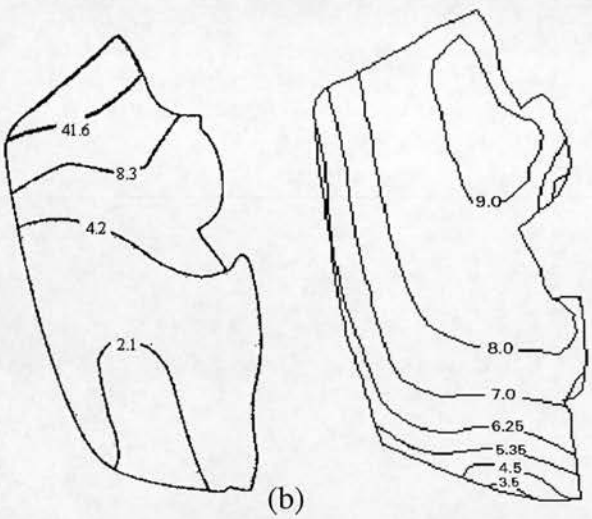

Figure 7-10. Surface *Microcystis* concentration of Eglwys Nynydd under weak SSW winds: (a) measured; (b) simulated (values are in g *Microcystis* m^{-3}).

The vertical distribution of *Microcystis* after 12 hours was similar to that measured (Figure 7-11). The vertical dynamics of *Microcystis* also showed some similarity to those that have commonly been modelled (Kromkamp and Walsby, 1990; Howard, 1997). The initial rise of the *Microcystis* towards the surface was consistent with a decrease in cell density, and the fall away from the surface around midday was consistent with an increase in cell density. The pattern deviated somewhat from those of Kromkamp and Walsby (1990) and Howard (1997) because of the affect of the vertical dimension convection cell. For example, partial downwelling of *Microcystis* from the surface by 6 hours into the simulation caused a downwards movement of the population as a whole even though the *Microcystis* was positively buoyant. In addition, discrepancies may also be attributed to an inaccurate initial

vertical *Microcystis* profile, and an inaccurate estimate of initial *Microcystis* density.

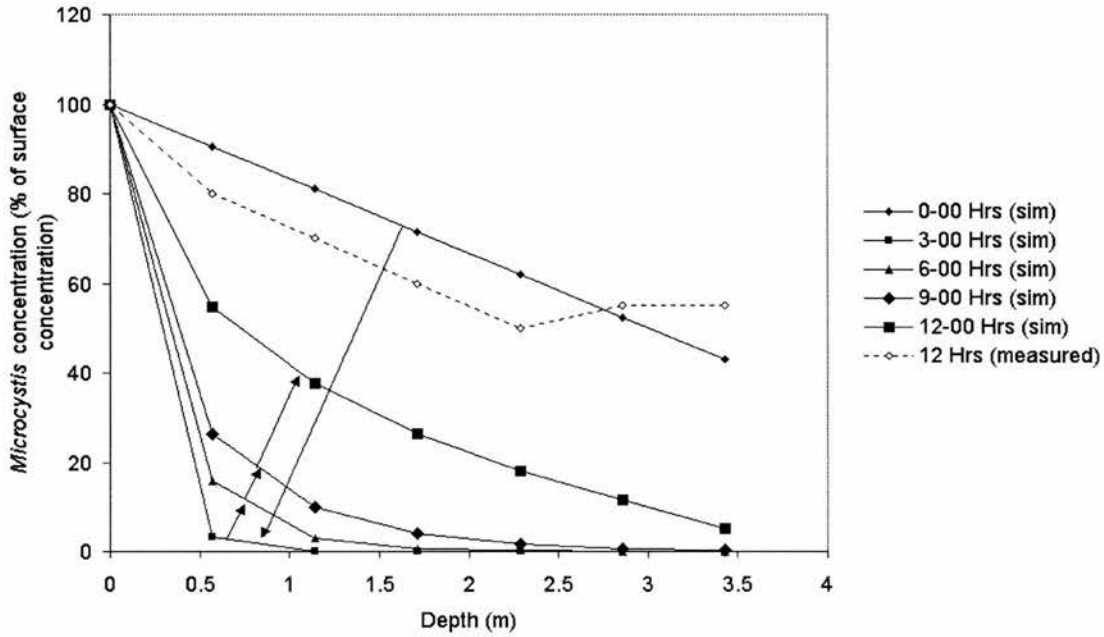

Figure 7-11. *Microcystis* concentration as a function of depth of Eglwys Nynydd under weak SSW winds.

7.3.5 Simulation with relatively high wind speeds

Processes were again simulated for 12 hours before the measurements had been made.

7.3.5.1 Boundary conditions

The only change in boundary conditions from the last simulation was that this simulation had winds of greater speed originating from the north to north-west (Appendix E).

7.3.5.2 Simulation

Surface currents were deflected clockwise of the wind direction (Figure 7-12a), but the magnitude of the deflection was less because surface current speeds were greater. A lake-wide vertical dimension convection cell was initiated, but the magnitude of the vertical velocities was greater and of the order of 0.2 m s^{-1} (Figure 7-12b) because of the increased wind stress.

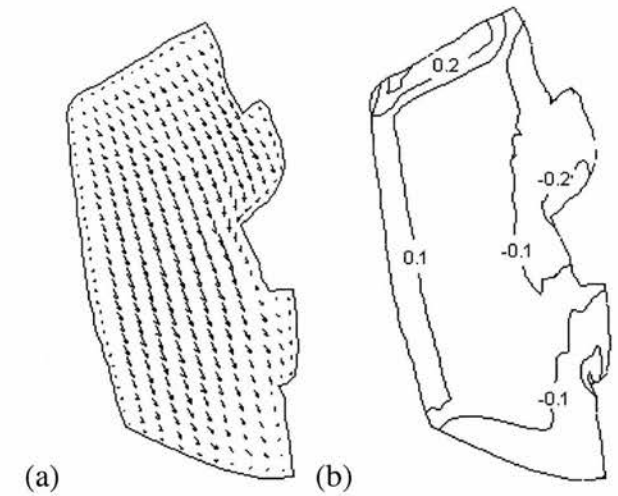

Figure 7-12. Vertical velocity at surface of Eglwys Nynydd: (a) surface current vectors; (b) vertical velocity at surface (values in mm s^{-1}).

Buoyancy followed a similar pattern to that of the simulation with relatively low wind speeds. The simulated horizontal distribution of surface *Microcystis* (Figure 7-13b) was different to that measured (Figure 7-13a), with a much greater gradient towards higher concentrations in the south.

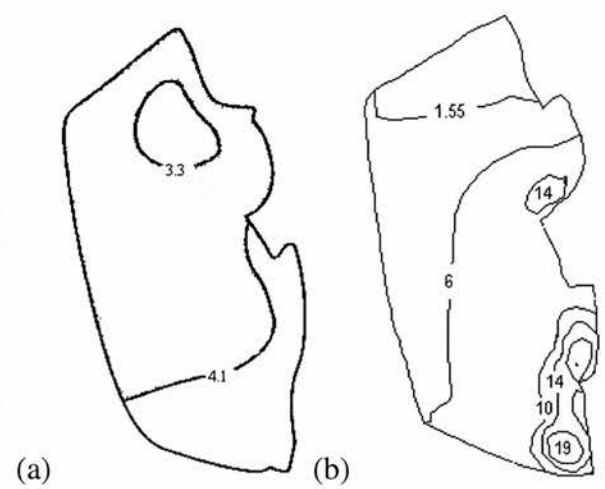

Figure 7-13. Surface *Microcystis* concentration of Eglwys Nynydd under strong NE winds: (a) measured; (b) simulated (values are in g *Microcystis* m^{-3}).

There was less discrepancy between the measured and simulated vertical distributions, however (Figure 7-14). Initially, there was a rise of *Microcystis* towards the surface because of their positive buoyancy. A downward movement of

the phytoplankton profile occurred after 6:00 Hrs, however, and resulted in a vertical distribution very similar to that measured at 12:00 Hrs.

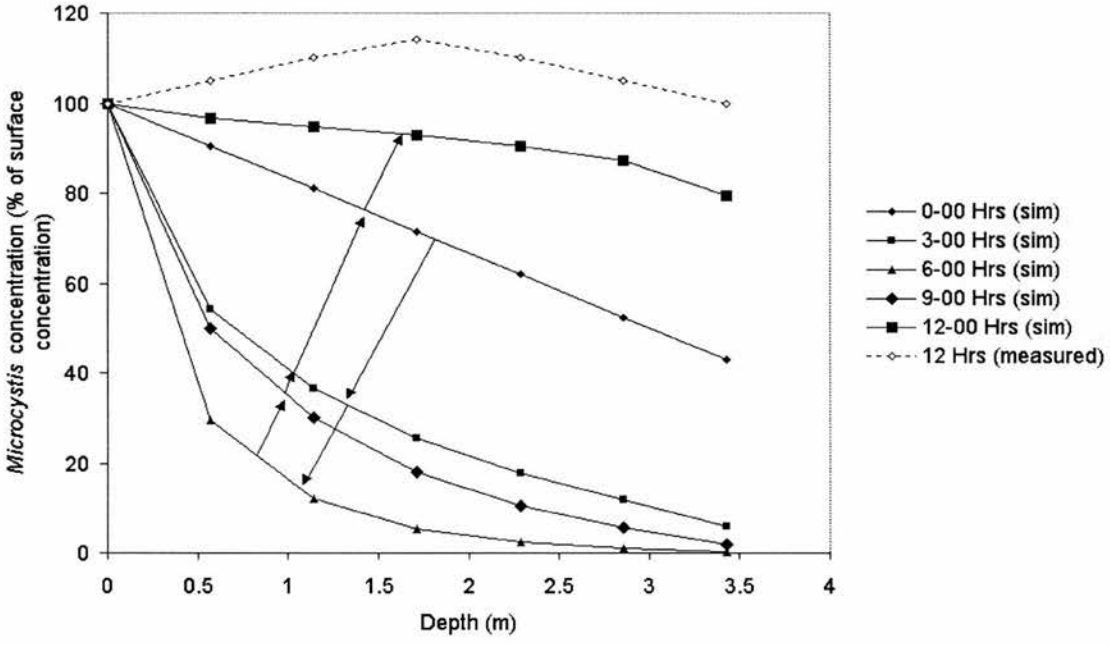

Figure 7-14. *Microcystis* concentration as a function of depth of Eglwys Nynydd under strong NE winds.

7.3.6 Summary

These two simulations have shown the importance of convection and turbulence in determining the spatial dynamics of cyanobacteria.

The spatial dynamics of cyanobacteria in Eglwys Nynydd were caused by the interaction between the velocity field and the buoyancy characteristics of the cyanobacteria. Because cyanobacteria were positively buoyant, they accumulated at the surface and were displaced downwind through convectional processes. In downwelling areas, their positive buoyancy was partially (although not totally) able to overcome downwelling flows, resulting in a basin-wide gradient in cyanobacterial concentration. When running the model under relatively weak winds, the simulated spatial distribution was similar to that measured.

Turbulent mixing also had an effect on spatial dynamics. With an increase in wind speed, there was an increase in vertical homogeneity (although there was an increase

in horizontal heterogeneity, which conflicted with the measured distribution, and may be attributed to a limitation of the model). Additionally, some of the increase in vertical homogeneity will have been cause by basin-wide mixing in the vertical domain through the vertical dimension convection cell.

7.4 Esthwaite Water: the effect of phytoplankton structure on the spatial dynamics of phytoplankton

7.4.1 Introduction

General features of the morphometry and hydrometry of Esthwaite have been described in Section 5.3.1.3. Phytoplankton species achieving dominance during the summer include the dinoflagellate *Ceratium hirundinella* and the cyanobacterium *Microcystis*. Temporal variation in phytoplankton concentration follows a pattern of exponential growth during May to July, relatively constant population levels in August and rapid decline in September and October (Heaney and Talling, 1980). Because net growth of the population is slow in August, it can be inferred that during this time basin-wide variation in phytoplankton concentration is the result of the redistribution of the phytoplankton by the interaction between wind-forcing and phytoplankton structural characteristics (Heaney, 1976) rather than differential growth caused by nutrient gradients.

There has been much research on the effects of the interaction between phytoplankton structure (with regard to its ability to regulate its position within the water quality) and hydrometry on the spatial dynamics of phytoplankton in this lake. Heaney and Talling (1980), conducting research on dinoflagellates, found that the spatial distributions were related to the wind speeds. Under low wind speeds (< 3 m s^{-1}), maximum densities of the dinoflagellate *Ceratium hirundinella* occurred at depths of 3 to 4 m (surface-avoidance was occurring). Under slightly greater wind speeds (approximately 3 m s^{-1}) surface currents flowed downwind with a sub-surface return current which caused upwelling of sub-surface *Ceratium* at the upwind area of the lake, and downwind transport of near-surface *Ceratium*. Under relatively strong winds (> 4 m s^{-1}) turbulence destroyed vertical stratification of *Ceratium*. George *et*

al. (1988), conducting research on cyanobacteria, found that surface accumulations of the cyanobacterium *Oscillatoria agardhii* were pushed downwind and accumulated over downwelling areas.

7.4.2 Measured spatial distributions

At 14:30 Hrs on 2 August 1973, a transect sample showed an upwind accumulation of chlorophyll-*a* concentration, with greater concentrations existing at the surface. The dominant type of phytoplankton identified from cell counts in a point sample acquired on 31 July 1973 was the dinoflagellate *Ceratium hirundinella*, from which it can be inferred that the chlorophyll-*a* gradient was the result of a *Ceratium* gradient. Approximately 15 other species of phytoplankton were also identified, but *Ceratium* concentration was approximately an order of magnitude greater that that of the other species. George and Heaney (1978) proposed that the spatial distribution found on 2 August 1972 was caused by the entrainment of surface-avoiding dinoflagellates in sub-surface return flows.

At 14:30 Hrs on 9 August 1973, a transect sample showed a downwind accumulation of chlorophyll-*a*. The dominant type of phytoplankton that was identified from cell counts in a point sample acquired on 7 August 1973 was the cyanobacterium *Microcystis*, from which it can be inferred that this chlorophyll-*a* gradient was the result of a *Microcystis* gradient. Again, other species were found, but in much smaller numbers. George and Heaney (1978) proposed that the spatial distribution found on 9 August 1973 was caused by the entrainment of positively buoyant phytoplankton in surface flows.

7.4.3 Model objectives

The objective of modelling the spatial dynamics of Esthwaite Water was to analyse the effect of the interaction between the structural characteristics of individual species and the environmental properties of the lake, particularly irradiance and current vectors. The model was parameterised to simulate horizontal and vertical dynamics for two species of phytoplankton under similar wind conditions: firstly, the dinoflagellate *Ceratium* (2 August 1973) and, secondly, the cyanobacterium *Microcystis* (9 August 1973).

7.4.4 Dinoflagellates dominant with greatest concentration at the thermocline

The simulation was initiated at 09:00 Hrs on the day of the measurements. This time of initiation was chosen because wind data for previous times were unavailable.

7.4.4.1 Boundary Conditions

i. Turbulence and wind friction coefficient model

The model was run with the standard k-ε turbulence and Bengtsson wind friction coefficient models.

ii. Bathymetry and grid morphometry

Bathymetry (Figure 7-15) was estimated from transect data collected by Mills (1895).

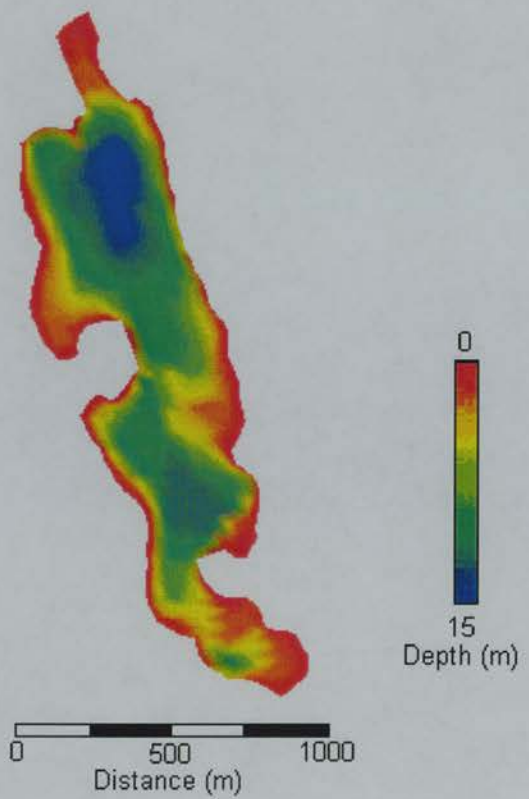

Figure 7-15. Bathymetry of Esthwaite Water

A finite volume grid was fitted to the bathymetry (Figure 7-16), with average cell dimensions of 30 m in the horizontal dimension and 2 m in the vertical dimension. It

was necessary to use a fine horizontal grid resolution because of the complexity of the morphometry: coarser grids produced non-physically realistic hydrometries.

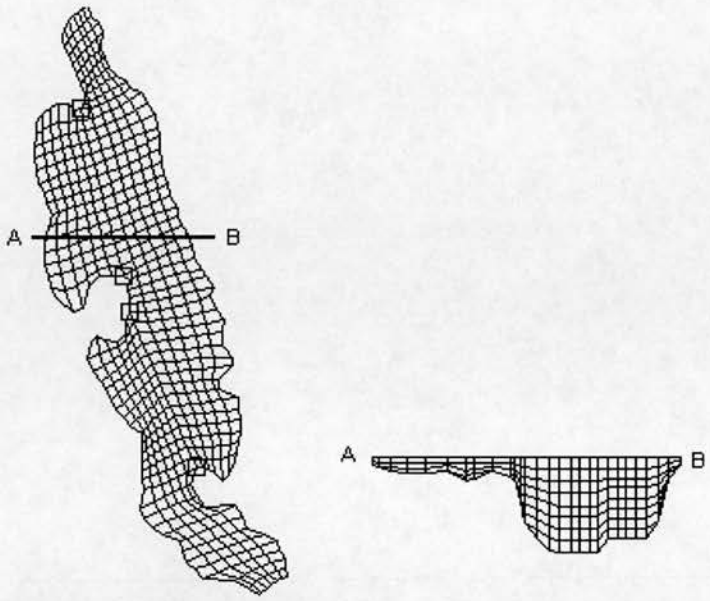

Figure 7-16. Grid of Esthwaite Water: (a) grid at surface (squares indicate connections between blocks); (b) transect.

iii. Irradiance

Data on irradiance were unavailable so these were estimated using the method outlined by Kirk (1994) (Appendix E). Estimates were reduced according to the cloud conditions measured at the Institute of Freshwater Ecology (O.S. B.N.G. 339000 495500). On 2 August 1973, there was only one octar of cloud. Therefore, irradiant intensities were relatively great (maximum irradiance of 1260 $\mu E\ m^{-2}\ s^{-1}$).

iv. Wind

Wind velocity data were obtained from a weather station 5 km to the south-south-east on the east side of Lake Windermere at Haws Wood (B. N. G. 338500 490500). Wind speeds varied between 2.5 m s^{-1} and 5 m s^{-1} (a mean of 2.75 m s^{-1}) with the dominant direction being from the south-south-west.

v. Thermal Profile

The lake was strongly stratified at this time, with a surface temperature of 18 °C, and a temperature of 10 °C at a depth of 12 m, and a thermocline at a depth of 6 m

(George and Heaney, 1978).

vi. Stream inflows and outflows

Stream inflows and outflows were not simulated as they usually have a negligible effect on circulation and nutrient gradients in Esthwaite Water.

vii. Water quality

- ***Nutrients***

  No data were available on nitrogen and phosphorus concentrations. However, since the dominant cause of spatial variation in phytoplankton concentration was wind-redistribution rather than differential growth due to nutrient gradients it is doubtful whether modelling spatial variation in nutrient concentration was necessary. For the short amount of time that was to be simulated (less than 12 hours) it was assumed that there was no great change in mean phytoplankton concentration (because a steady-state had been achieved for the summer), so the exponential growth rate was set to zero.

- ***Phytoplankton***

  No data were available on the horizontal or vertical distribution of *Ceratium* at 9:00 Hrs. The initial vertical distribution was set with a maximum at a depth of 4 m, with a decrease to near zero concentration at the surface and a depth of 9 m, this distribution being chosen to satisfy requirements for light and oxygen. For the relatively high levels of sub-surface irradiance that were estimated to exist at the start of the simulation, optimal levels would correspond to a depth of approximately 3 to 4 m for Esthwaite Water. Mean *Ceratium* concentration at a depth of 4 m was set at set to 3.6 g m^{-3} (corresponding to a chlorophyll-*a* concentration of approximately 40 mg m^{-3}).

7.4.4.2 Simulation

Surface currents were deflected clockwise from the wind direction by Coriolis acceleration (Figure 7-17a). This caused downwelling at the downwind area of the lake, particularly in the east and north (Figure 7-17b) and upwelling at the upwind area of the lake, particularly in the west and south. Vertical current speeds were of

an order of magnitude of ±0.2 mm s^{-1}.

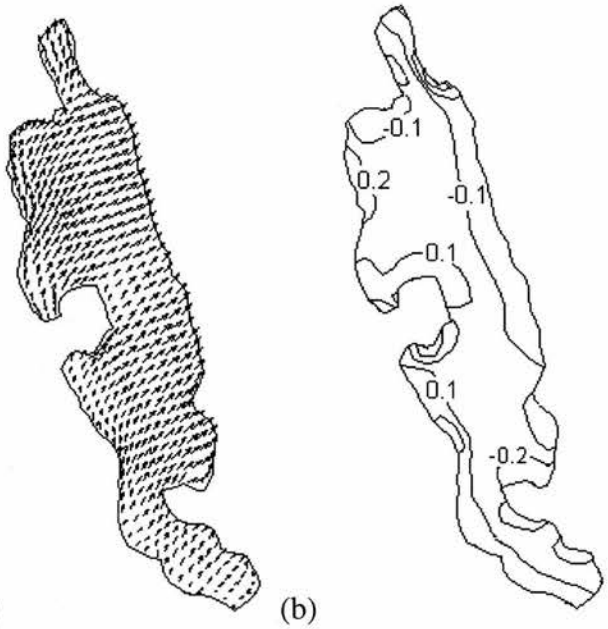

Figure 7-17. Simulated currents of Esthwaite (15:00 2 August 1973) of Esthwaite Water: (a) surface current vectors; (b) vertical velocity at surface (values are in mm s^{-1}).

There was a progressive rotation in current direction with increasing depth beneath the surface as the thermocline was approached (Figure 7-18).

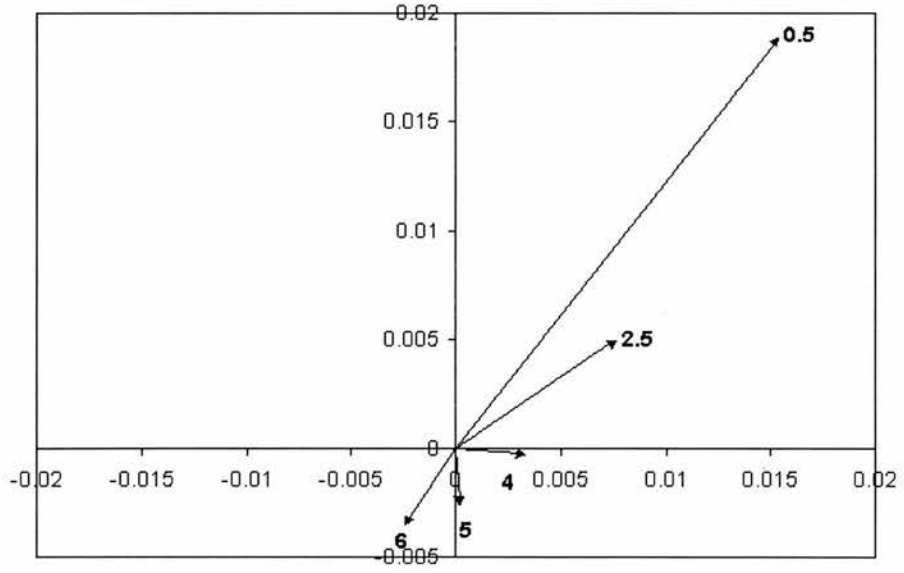

Figure 7-18. Current vectors for Esthwaite Water (15:00 2 August 1973) as a function of depth: values at the end of each arrow are the depth (m), values on *x* and *y* axis are *u* and *v* velocity component (m s^{-1}).

Simulated and measured surface *Ceratium* distributions were similar (Figure 7-19), although there was a simulated east-west trend that was not measured.

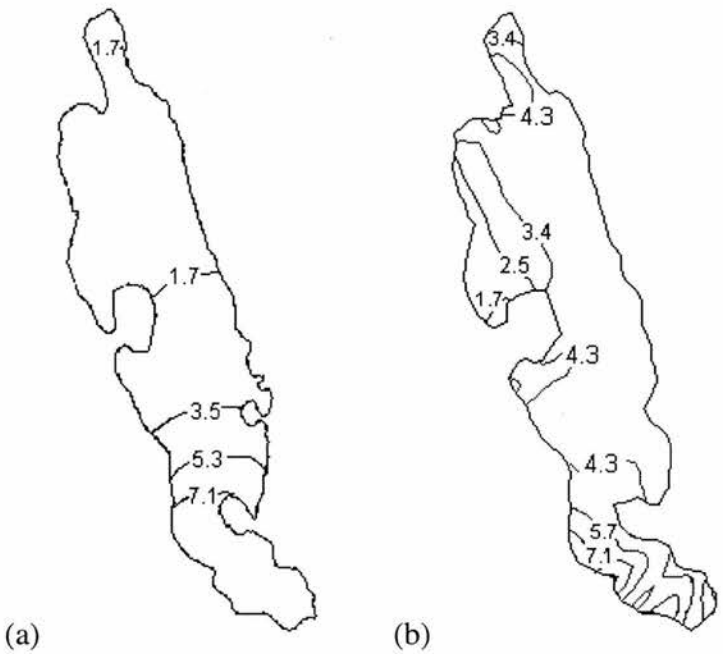

Figure 7-19. Surface *Ceratium* concentration (15:00 2 August 1973) of Esthwaite Water: (a) measured; (b) simulated (values are in g *Ceratium* m^{-3}.).

The discrepancy between the simulated and measured horizontal distributions may be attributed to the model over-estimating the rate of downwards momentum transfer through the thermocline. The simulated vertical velocity profile (Figure 7-18) had flows occurring at a depth of approximately 3 m that were hardly deflected from the wind direction, and return flows occurring beneath the thermocline. The model was, therefore, overestimating the depth at which the return flows occurred (by overestimating the rate of downwards momentum transfer). With a peak in *Ceratium* concentration occurring at 3 m depth (Figure 7-20), *Ceratium* would be entrained in downwind drift currents, resulting in the east-west gradient.

The simulated vertical distribution of *Ceratium* was similar to that measured (Figure 7-20), although the depth of the peak *Ceratium* concentration was underestimated. This underestimation of the depth may be attributed to the errors in the estimates of irradiance and initial *Ceratium* vertical distribution.

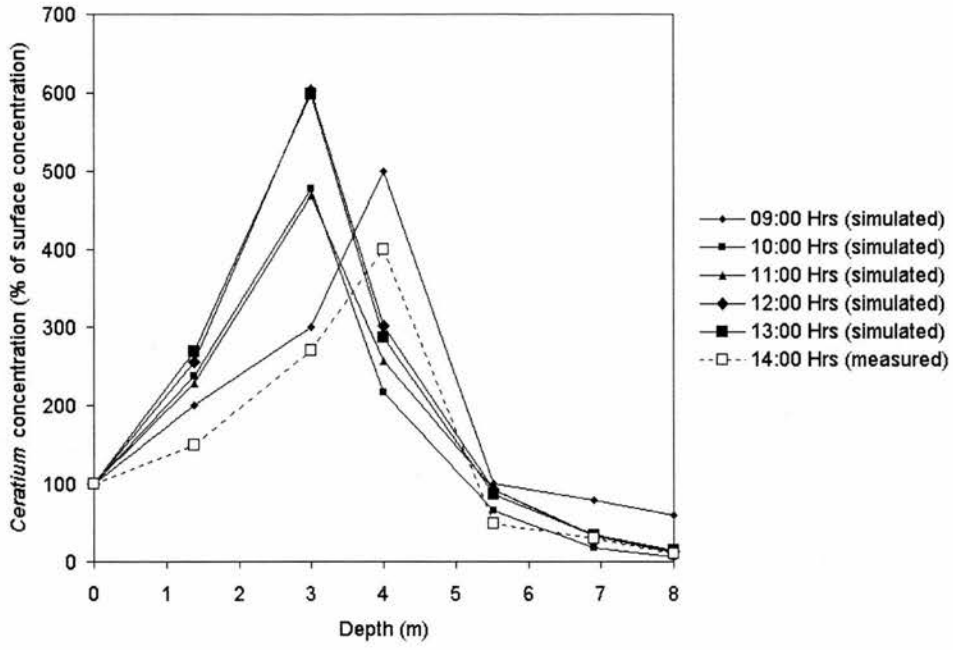

Figure 7-20. Ceratium concentration as a function of depth of Esthwaite Water.

7.4.5 Cyanobacteria dominant with greatest concentration at the surface

The simulation was initiated at 09:00 Hrs on the day of the measurements. Again, wind data for previous times were unavailable.

7.4.5.1 Boundary conditions

Boundary conditions were the same as for the *Ceratium* simulation, except for the following:

i. Irradiance

On 9 August 1973, the sky was totally overcast resulting in low irradiant intensities (maximum irradiance of 770 μE m^{-2} s^{-1}).

ii. Wind

On 9 August 1973 wind speeds varied between 2.5 m s^{-1} and 7 m s^{-1} (a mean of 3.5 m s^{-1}). Again, the dominant direction was from the south-south-west.

iii. Phytoplankton

No data were available on the initial horizontal or vertical distribution of the

Microcystis at 9:00 Hrs. The initial vertical distribution of *Microcystis* was set with a maximum at the surface and a minimum at a depth of 8 m. This distribution was determined according to the estimated change in irradiance levels that had occurred over the previous week. Mean surface *Microcystis* concentration was 7 g m^{-3} (corresponding to a chlorophyll-*a* concentration of 80 mg m^{-3}).

7.4.5.2 Simulation

Surface currents were deflected clockwise from the wind direction by Coriolis acceleration, but the deflection was less than on 2 August 1973 because of the greater wind speed (Figure 7-21a). Downwelling again occurred at the downwind area of the lake in the east (Figure 7-21b) and upwelling again occurred at the upwind area of the lake in the west, but the rate of vertical flow was greater (±0.3 mm s^{-1}) than for the *Ceratium* simulation because of the increased displacement of water by wind.

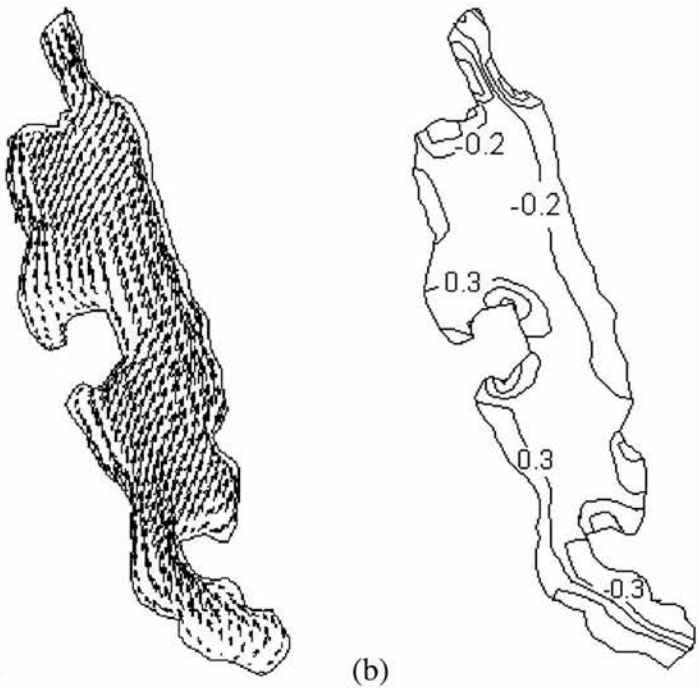

Figure 7-21. Simulated current of Esthwaite Water (15:00 9 August 1973): (a) surface current vectors; (b) vertical velocity at surface (values are in mm s^{-1}).

Microcystis increased in density but remained positively buoyant throughout most of the simulation (Figure 7-22). The rate of density increase was inversely proportional to distance from the surface (as irradiance, and therefore photosynthesis, decreased

with depth).

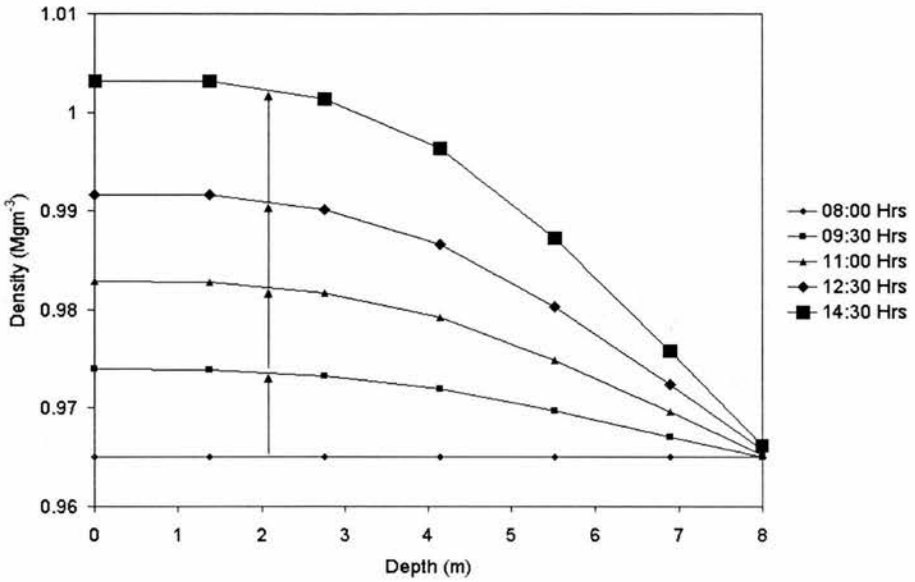

Figure 7-22. *Microcystis* density of Esthwaite Water.

The positively buoyant *Microcystis* accumulated over downwelling areas, resulting in a similar surface distribution to that measured (Figure 7-23), although with a greater magnitude of meso-scale and micro-scale variation.

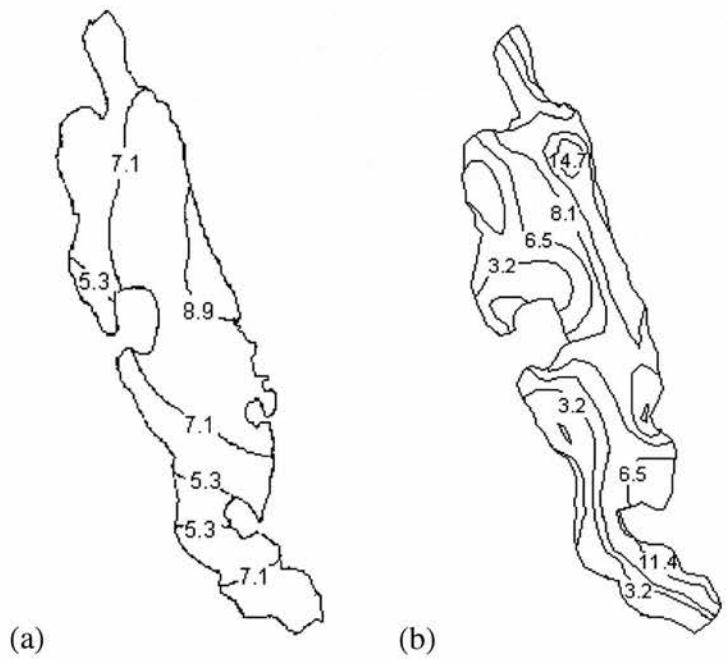

Figure 7-23. Surface *Microcystis* concentration of Esthwaite Water (15:00 9 August 1973): (a) measured; (b) simulated (values are in g *Microcystis* m^{-3}).

The simulated vertical distribution of *Microcystis* was also similar to that measured. The low initial density caused high rates of *Microcystis* to migrattion to the surface within the first 90 minutes of simulated time (Figure 7-24). From 9:30 Hrs, there was a downwards redistribution, resulting in a vertical distribution that was similar to that measured at 14:30 Hrs.

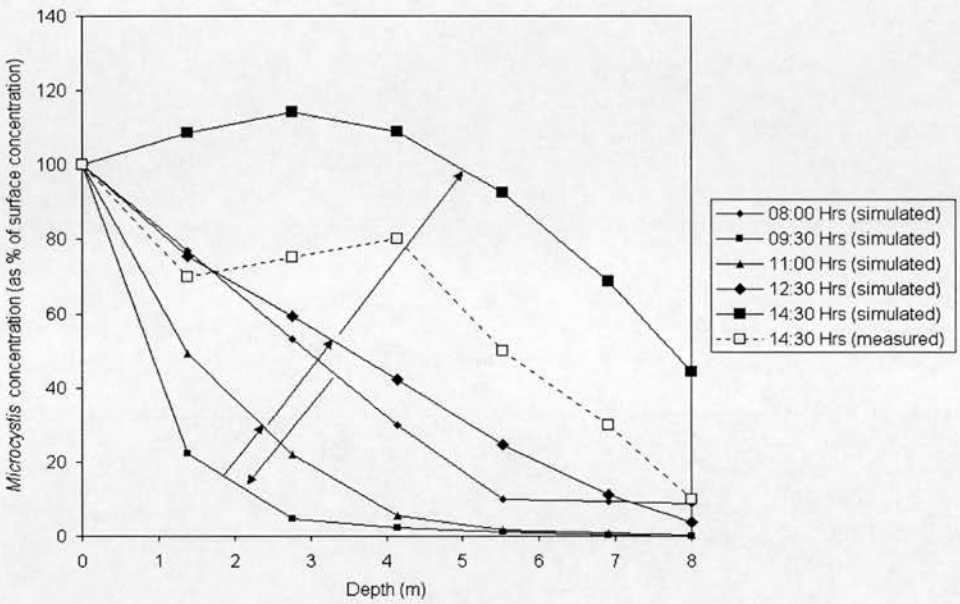

Figure 7-24. *Microcystis* concentration as a function of depth of Esthwaite Water.

Some of the discrepancies between the simulated and measured surface distribution of *Microcystis* may be related to the sampling regime, which in the north missed the area of simulated high concentration and near to the south missed the areas of simulated low and high concentrations at the west and east shores, respectively. Use of high resolution remote sensing data (George *et al.*, 1988) has shown patterns consistent with those simulated, so the simulated variation is not atypical for this lake. However, the position of the simulated peak concentration several hundred metres north of that measured suggests that the simulated eastward component of the near-surface velocity vector was too small relative to the northward component in the north-east part of the lake. Also, the underestimation of surface concentration in the north-west bay may likewise be attributed to an inaccurate estimation of the velocity field - a problem that has been encountered in past CFD modelling of Esthwaite Water (Falconer *et al.*, 1991).

The initial rise of the population towards the surface was due to the initially large positive buoyancy. *Microcystis* remained positively buoyant for most of the simulation, but by 14:00 Hrs there was a negligible difference between the density of *Microcystis* and that of water, so they was acting as a near-passive scalar of the velocity field. The downwards redistribution was therefore caused by wind-induced downwelling of *Microcystis* from the surface, and upwelling of water with lower *Microcystis* concentrations from near to the thermocline.

7.4.6 Summary

These two simulations have shown the importance of the interaction between the velocity field and species characteristics in determining the spatial dynamics of phytoplankton. Dinoflagellates accumulated upwind because they avoided the surface and were entrained in sub-surface return currents; cyanobacteria accumulated downwind because they migrated to the surface (through being positively buoyant) and were entrained in downwind surface currents.

The discrepancies between the measured and simulated distributions, particular with the dinoflagellate simulation, highlight the sensitivity of the functioning of the model to the way in which it has been formulated. This will be discussed in greater detail in Section 9.3.

7.5 Conclusion

From the CFD modelling of Loch Leven, Eglwys Nynydd and Esthwaite Water, various conclusions can be made about the spatial dynamics of phytoplankton in lakes.

i. Convection causes macro-scale spatial dynamics through displacement

Convection causes macro-scale gradients of phytoplankton concentration through the displacement of phytoplankton. Displacement may be divided into two components. Firstly, there is the differential displacement associated with the interaction between the phytoplankton rising velocities and the velocity field. For example, cyanobacteria in Eglwys Nynydd and Esthwaite Water had positive rising velocities so cyanobacterial concentration increased at shores where there were downwelling

flows (they were displaced less in the vertical dimension as their positive rising velocities overcame the negative vertical velocities of the water flow) and cyanobacterial concentration decreased at shores where there were upwelling flows (they were displaced more in the vertical dimension as their positive rising velocities added to the positive vertical velocities of the water flow). Secondly, there is the displacement from the vertical to the horizontal dimension (or *vice versa*). For example, in the simulations of cyanobacteria in Eglwys Nynydd and Esthwaite Water, there was an initial vertical heterogeneity with greater cyanobacterial concentration at the surface. Some of the reduction in phytoplankton concentration in upwind areas was the result of upwelling of relatively cyanobacterial-free water.

ii. Turbulence causes micro-scale spatial dynamics through mixing, but macro-scale variation in the intensity of turbulence may cause macro-scale spatial dynamics

Turbulence causes micro-scale spatial dynamics through mixing. This was shown adequately in the vertical dimension of Eglwys Nynydd when simulating under high wind speeds (although, this was not seen in the horizontal dimension, and can be attributed to a limitation of the SSIIM2.0 model). Turbulence, however, was also seen to contribute towards macro-scale spatial dynamics in Loch Leven because there was macro-scale spatial variation in the intensity of turbulence. That is, the zero-equation turbulence model estimated turbulence locally as a function of depth (because the amount of turbulence is related to the spatial scale of the system) so the rate of diatom vertical movement was spatially dependent. For example, when wind speeds increased, the rate at which diatoms were pushed towards the surface by turbulence was greater over the deeper areas. This contributed towards the macro-scale gradient at the surface.

iii. The scale of the spatial dynamics of phytoplankton is determined by lake scale

In all cases, lake-wide convection cells were initiated, so the scale over which hydraulic processes occurred was determined by the scale of the lake. Because the spatial dynamics of phytoplankton were determined by the interaction between phytoplanktonic properties and these hydraulic processes, generated spatial

distributions of phytoplankton were scaled to those of the lake basins. For example, the spatial scale of spatial distributions in Loch Leven was greater than those in Eglwys Nynydd and Esthwaite Water.

From the simulations, several conclusions may be made with regard to the modelling process.

i. Model external boundary conditions must be determined from appropriate measurements

The boundary conditions used in the simulations of this chapter were determined from approximate estimates, using data that had not been acquired with the intention of supporting CFD simulations. For example, in the simulation of Loch Leven, wind data were obtained from a weather station approximately 35 km to the south, and this will be one of the reasons that the simulated spatial distribution of Loch Leven differed to that measured. With more comprehensive data on the initial boundary conditions, it is expected that the lake systems can be described with greater accuracy.

ii. Verification data must be appropriate to those produced by the model

The verification data used in these simulations lacked a temporal aspect, in that there was only one measured spatial distribution for each simulation. This greatly limited the analysis, making the determination of spatial *dynamics*, rather than spatial *distributions*, more difficult. The only archived multi-temporal images – Esthwaite Water on 24 July 1987 (Section 5.3.1.3) – could not be used because there were no data on vertical distributions of phytoplankton for Esthwaite Water at this time.

For the lakes where verification data on spatial distributions of phytoplankton were acquired through samples (containing a limited number of observations), two potential problems existed. Firstly, there was the potential underestimation of the variation, which would be manifested as a general smoothing of the interpolated spatial distribution. Secondly, there was the potential error associated with inaccuracies in determining the exact positions of the observations. Verification through the use of remotely sensed data is a superior method because remote sensing

can provide comprehensive coverage of geo-registered data.

iii. Simple process models may be used to estimate spatial distributions

The outcomes of these simulations have shown that even without comprehensive data on the environment, with the use of simple deterministic models and some approximate estimates of boundary conditions, accurate simulation of spatial distributions of phytoplankton was possible. It is possible that recent trends in phytoplankton modelling towards the used of more complex models (for example, incorporating the variation in physiological states of specific species) are unnecessary if the intention is to simulate general features of the spatial dynamics over short time scales.

8 Process Modelling: hypothetical basins

8.1 Introduction

i. Rationale

This chapter explores the relationships between the spatial dynamics of phytoplankton and causative processes using process modelling of hypothetical situations. This is achieved through the application of hypothetical but physically realistic events, such as wind-forcing or fluvial-forcing, to basin models that are user-determined and do not exist in the real world (but have similarity to real lakes). Two reasons necessitated the use of hypothetical situations. Firstly, hypothetical situations enabled analysis of processes and resultant spatial dynamics for which data were unavailable. For example, there were not enough data for any of the real lakes considered in this thesis to model hydrodynamically the effect of inflows and outflows on spatial dynamics. Secondly, hypothetical situations enabled greater control of the lake environmental and phytoplanktonic properties (as represented by the external boundary conditions of the model) that affect spatial dynamics. The effects of certain properties could mask the effects of others, and only through the use of hypothetical basins was it possible to control the states of all properties. For example, when analysing the effects of the irradiance environment on the spatial dynamics of cyanobacteria (by irradiance-induced buoyancy changes) it was necessary to ensure that circulation-induced mixing within the lake was not too great to have obscured the effect of changes in buoyancy.

ii. Procedure

The spatial dynamics of phytoplankton are determined by the interaction between hydrometry (determined by atmospheric, morphometric and inflow and outflow properties) and phytoplanktonic properties. The procedure of this chapter was therefore to alter certain hydrometric and phytoplanktonic properties (while keeping all others constant) between different simulations, and to analyse how spatial dynamics differed, mainly through quantification of the spatial distribution of

phytoplankton after a given time period. When analysing the effect of hydrometry, both the forces causing flows (wind stress, and pressure from stream inflows and outflows) and the modification of these flows by morphometry were considered. When analysing the effect of phytoplanktonic properties, both structural and physiological properties were considered. As a means of determining the relative effects of a change in properties, comparison was made with a control simulation (Section 8.2).

More emphasis in this chapter was placed on quantifying the scale of spatial dynamics through use of the variogram. Previously, the variogram had little application because either, methods used in estimating spatial distributions were inconsistent between lakes (Chapter 5) or, simulations were initiated with different initial spatial distributions of phytoplankton and run for different lengths of time (Chapter 6). It was only in this chapter, where the method of determining the spatial dynamics of phytoplankton was consistent between simulations and where complete control over initial spatial distributions and simulation running times was achieved, that it was possible to use the variogram to compare the effects of a change in hydrometric and phytoplanktonic properties.

iii. Internal boundary conditions

Internal boundary conditions were kept as constant as possible between all simulations because it was necessary to minimise the effect of the model sensitivity to these conditions (see Chapter 6).

Grids were established with octagonal or sheared-octagonal basin shapes in the horizontal dimension as a compromise between the requirement for maintaining enough orthogonality to minimise false diffusion and the requirement to provide a grid shape that, to some extent, approximated those of natural lakes. For example, although a four-sided grid would have caused less false diffusion, this grid shape does not represent a 'typical' lake shape. An octagon or sheared-octagon, however, has a shape approximating those of real lakes.

Grid cells had horizontal dimensions of approximately 100 m and vertical dimensions of approximately 2 m. The time step was 900 s. The model was run using the Bengtsson wind friction coefficient model and the standard k-ε turbulence

model.

iv. Simulation time scales

The time scale over which processes were simulated was specified so that near-stable spatial distributions (that is, spatial distributions that were not changing quickly) could be achieved within the time scale for each simulation. For this, it was necessary to fulfil two criteria. Firstly, it was necessary to relate the time scale over which the simulation was run to the period of the forcing function(s). Spatial dynamics are dependent upon the period, phase and amplitude of forcing functions. If the phase and amplitude remain constant, then spatial dynamics for a given position in a cycle should be equivalent to the spatial dynamics for an equivalent position in preceding or succeeding cycles. Therefore, it should only be necessary to simulate the time scale of the first cycle of the forcing function (the period). Secondly, it was necessary to keep the time scale great enough for processes to result in stable spatial distributions over the spatial scale of the basins. Temporal scales of approximately 24 hours are typically associated with horizontal scales of approximately 1-2 km (Harris 1980a).

When running the model under the influence of wind-forcing, simulations were run for 24 hours. This satisfied both criteria: the period of the forcing function was 24 hours and the lakes were of a scale where stable spatial distributions could be produced within 24 hours (Section 8.3.2.1). When running the model under the influence of inflow- and outflow-forcing, however, it was necessary to increase the time scale to 7 days to satisfy the second criterion: that the processes would result in stable spatial distributions within that time scale. This is discussed in greater detail in Section 8.3.2.2.

8.2 The control simulation

i. Rationale

The control simulation was established to aid in determining the relative effects that a change in hydrometric or phytoplanktonic properties had on the spatial dynamics of phytoplankton.

ii. Boundary conditions

The control basin had an area of 6 km, a depth of 20 m and an elongation of 1 (elongation being calculated as the ratio of the maximum length of the lake to the diameter of a circle with the same area).

The irradiance regime had a diurnal periodicity, reaching a maximum of 800 $\mu E\ m^{-1}\ s^{-1}$ at 12:00 Hrs and a minimum at 0:00 Hrs and 24:00 Hrs. The average irradiance received in the previous day was 150 $\mu E\ m^{-2}\ s^{-1}$. The wind regime had a similar diurnal periodicity to the irradiance regime, although involving a time lag of 1 hour, reaching a maximum of 5 m s^{-1} at 13:00 Hrs and a minimum of 0 m s^{-1} at 1:00 Hrs. Winds were westerly. The thermal profile was horizontally homogeneous, but vertically heterogeneous, with a thermocline at a depth of 10 m. The Coriolis parameter was set to $1.3*10^{-4}$. These conditions are typically of those experienced in mid- to high-latitude Western European lakes in summer conditions.

The phytoplankton population consisted entirely of cyanobacteria, which was horizontally homogeneous at the surface (1 g m^{-3}), and vertically heterogeneous with no cyanobacteria beneath 5 m. This was typical of a mesotrophic-eutrophic lake. Cyanobacterial colony radius was 200 μm and form resistance was 1. Initial cyanobacterial density was 0.975 Mg m^{-3}, and maximum and minimum cell density were 1.065 and 0.92 Mg m^{-3} respectively. Nutrient concentration was zero.

The extinction coefficient was estimated as a function of phytoplankton concentration using the model of Bindloss (1973) adapted for cyanobacteria. This modification ensured that the initial extinction coefficient was approximately 2.

iii. Spatial dynamics of phytoplankton

Wind stress initiated a downwind surface flow, which was deflected approximately 40^{o} clockwise by Coriolis acceleration (Figure 8-1a). The requirement for mass conservation was satisfied by a vertical dimension convection cell, which involved downwelling in downwind areas, upwelling in upwind areas (Figure 8-1b) and a sub-surface return flow above the thermocline. There was an increase in horizontal and vertical flow velocities from the time of simulation initiation to a maximum at approximately 30 mins after maximum wind speed was reached (because of the time

lag in the response to the forcing function). There then followed a decrease in horizontal and vertical velocities as wind stress decreased.

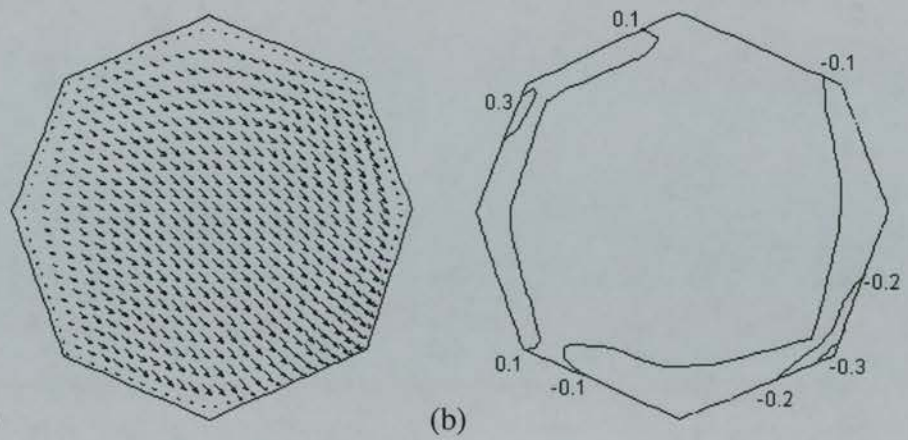

Figure 8-1. Hydrometry of the control basin: (a) surface flow vectors; (b) vertical velocity (values are in m s^{-1}). In this, and subsequent figures in this chapter, outputs are from the termination of the simulation.

Surface flows resulted in a downwind displacement of cyanobacteria at the surface (Figure 8-2). In downwelling areas, cyanobacteria accumulated at the surface because the positive rising velocity of the cyanobacteria was partially able to resist the downwelling velocities in these areas. In upwelling areas, cyanobacterial diminished at the surface because the upwelling flows contained lower concentrations of cyanobacteria than the surface layer.

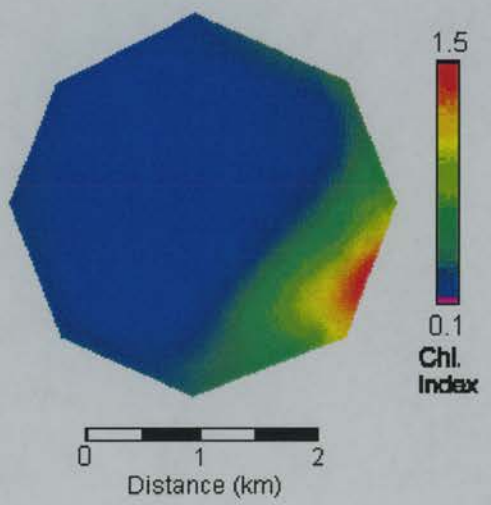

Figure 8-2. Surface cyanobacterial concentration of the control basin.

Semivariance of surface cyanobacterial concentration increased as a function of lag, reaching a maximum semivariance at approximately 2500 m (Figure 8-3). This lag was equivalent to the distance between the upwelling and downwelling areas. The south-west to north-east directional variogram had smaller semivariances for a given lag than the south-east to north-west directional variogram. This was because Coriolis acceleration had caused the downwelling and upwelling areas to be in the south-west and north-east respectively. The gradient in surface cyanobacterial concentration along this axis was much greater than the gradient perpendicular to this axis.

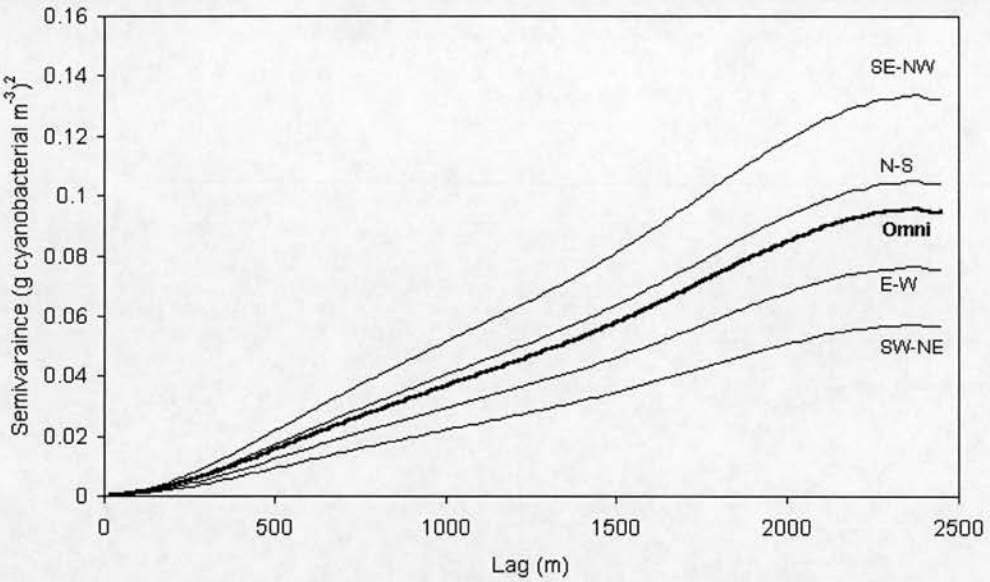

Figure 8-3. Variograms of surface cyanobacterial concentration for the control basin: south-east to north-west directional variogram (SE-NW); north to south directional variogram (N-S); omnidirectional variogram (Omni); east to west directional variogram (E-W); south-west to north-east directional variogram (SW-NE).

By the end of the simulation, vertical profiles of cyanobacteria were dependent upon the horizontal position within the basin (Figure 8-4). At the downwelling area, there was a nearly homogeneous vertical profile resulting from downwelling of cyanobacteria. As the upwelling area was approached, there was an increase in vertical stratification of cyanobacteria, with greater concentrations nearer to the surface than at greater depths. In all cases, cyanobacteria extended down to a depth of greater than 10 m. Flows were, therefore, only partially restrained by the density

gradient at the thermocline.

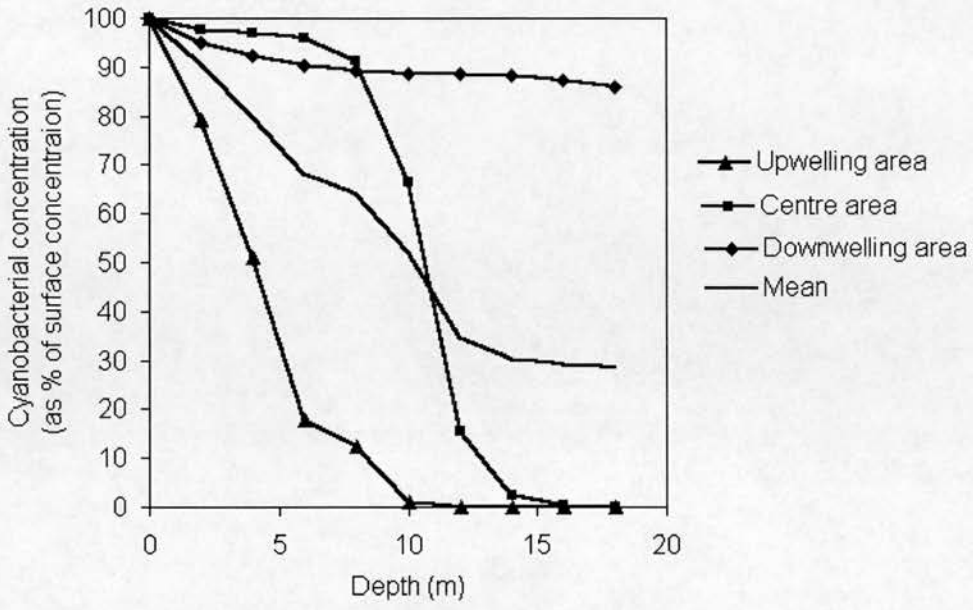

Figure 8-4. Cyanobacterial concentration as a function of depth.

In the control simulation, therefore, there was a basin-wide redistribution of cyanobacterial homogeneity within the horizontal dimension at the surface into the vertical dimension, and a likewise transfer of cyanobacterial heterogeneity within the vertical dimension into the horizontal dimension. Mixing within the vertical dimension was occurring, but this was predominantly mixing as a result of convection rather than turbulence.

8.3 Hydrometric properties and the spatial dynamics of phytoplankton

8.3.1 Hydrometric boundary conditions

Only the properties influencing hydrometry that it was believed would have greatest effect on the spatial dynamics of phytoplankton were altered between simulations. These included properties that forced the hydrometry (wind and inflows and outflows) and properties that modified the hydrometry (the morphometric properties of area, depth elongation and obstructions) as shown in Table 8-1. External

boundary conditions were typical of the lakes that have been considered throughout this thesis. For example, wind regimes followed a diurnal pattern, varying from relative quiescent (2 m s^{-1}) to relatively strong (8 m s^{-1}) and lake area varied between relatively small (2 km^2) and relatively large (12 km^2).

Table 8-1. Properties influencing spatial dynamics by affecting hydrometry.

	PROPERTY BEING TESTED					
	Forcing function		Morphometric modification			
Boundary condition	Wind	Inflows and outflows	Area	Depth	Elongation	Complexity
Maximum wind speed (m s^{-1})	2 (westerly) 5 (westerly) 8 (westerly) 5 (rd)	0	5	5	5	None
Fluvial network	N/A	Clustered Dispersed	N/A	N/A	N/A	None
Area (km^2)	6	1	2, 4, 6, 8, 10, 12	6	6	None
Depth (m)	20	10	20	5, 20	20	None
Elongation	1	1	1	1	1, 2, 4, 6	None
Complexity	1	1	1	1	~1	None Islands Promontories

Notes: N/A = not applicable; rd = random direction.

Unless stated otherwise, all other properties were kept constant between simulations.

8.3.2 Forcing of hydrometry

8.3.2.1 Wind-induced hydrometry

To test the effect of the wind regime on the spatial dynamics of cyanobacteria, simulations were run with wind regimes of different speed and directional consistency (that is, how much the wind direction remained constant). To test the effect of wind speed, simulations were run with wind speeds that reached a maximum of 2 m s^{-1}, 5 m s^{-1} (the control simulation) and 8 m s^{-1} at 13:00 Hrs, with the wind flowing from a constant direction (the west). To test the effect of wind directional consistency, a simulation was run with a wind profile that approached a maximum of 5 m s^{-1} with the wind flowing from a random direction that changed every 15 minutes.

i. Wind speed

Hydrometries were comparable to the control simulation. The only difference was that flow velocities for the 2 m s^{-1} and 8 m s^{-1} wind profiles were lesser and greater than from the control simulation, respectively.

With an increase in wind speed profile, three changes in the spatial distribution of cyanobacteria became apparent. Firstly there was a decrease in the mean surface cyanobacterial concentration from 1.2 g m^{-3} for the simulation with maximum wind speeds of 2 m s^{-1} to 1.03 g m^{-3} for the simulation with maximum wind speeds of 8 m s^{-1} (Figure 8-5). Secondly, there was an increase in the magnitude of horizontal variation of surface cyanobacterial concentration between the 2 m s^{-1} and 5 m s^{-1} wind profile but little change between the 5 m s^{-1} and 8 m s^{-1} profile, as shown by the variogram (Figure 8-6). Thirdly, there was a decrease in the magnitude of the vertical variation in cyanobacterial concentration (Figure 8-7).

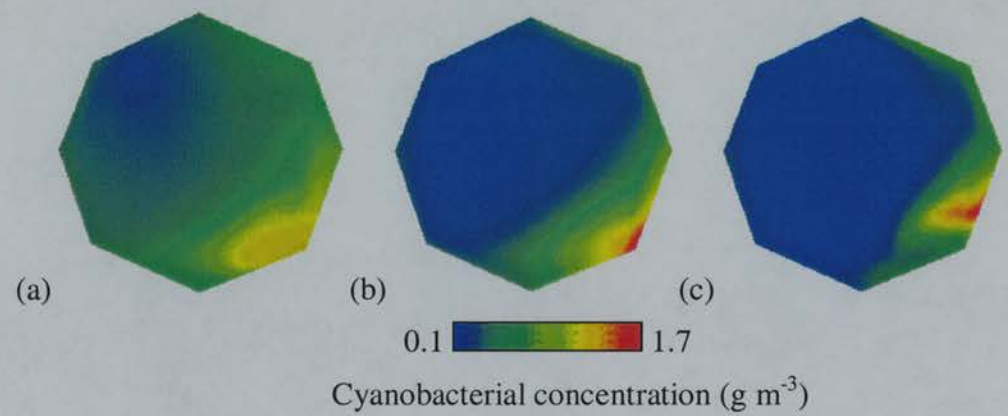

Figure 8-5. Surface cyanobacterial concentration for basins with different wind speed profiles: (a) W_{max} = 2 m s^{-1}; (b) W_{max} = 5 m s^{-1} (control basin); (c) W_{max} = 8 m s^{-1}.

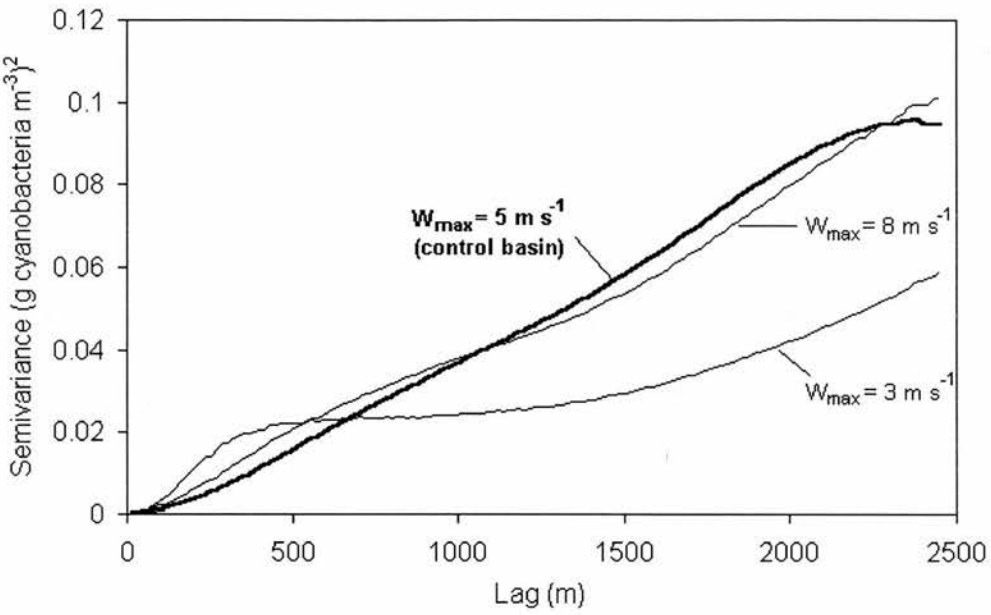

Figure 8-6. Omnidirectional variograms of surface cyanobacterial concentration for basins with different wind profiles.

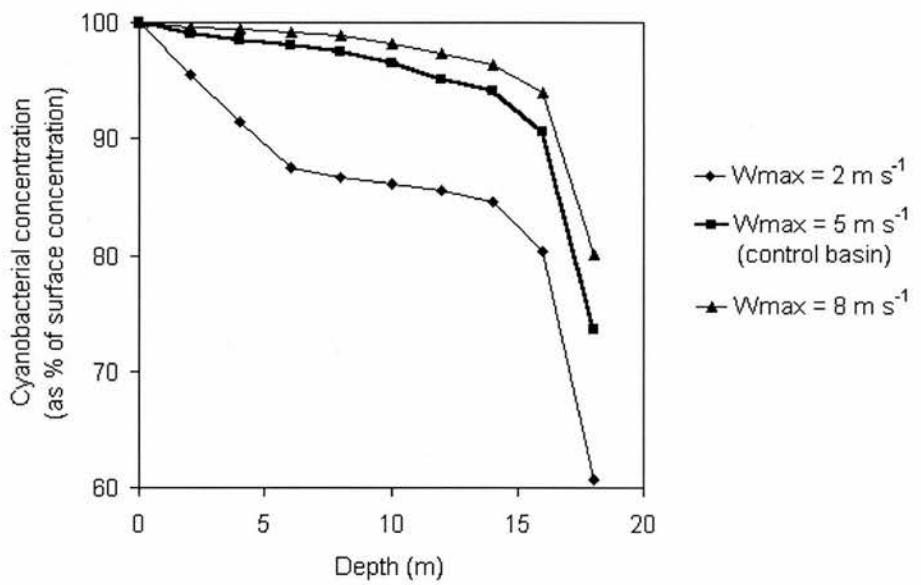

Figure 8-7. Cyanobacterial concentration as a function of depth for basins with different wind profiles.

The spatial dynamics of cyanobacteria in all three simulations were determined by the same processes. That is, cyanobacteria were partially resisting downwelling flows at downwelling areas and were displaced away from upwelling areas by flows that contained lower concentrations of cyanobacteria. The differences between the simulation outcomes depended upon the rate at which these processes occurred.

The simulation with the 2 m s^{-1} wind profile caused less mixing within the vertical dimension than that with the 5 m s^{-1} wind profile (the control simulation) because of the reduced upwelling and downwelling velocities. Less upwelling of relatively cyanobacterial-free water occurred in upwelling areas, and cyanobacteria were more able to resist downwelling in downwelling areas. Reduced velocities, therefore, caused greater surface concentrations and a greater rate of decrease of cyanobacterial concentration with increasing depth. The simulation with the 2 m s^{-1} wind profile caused less semivariances at lags near to the basin scale than the simulation with the 5 m s^{-1} profile because downwelling areas were less depleted of cyanobacteria as there was decreased upwelling of relatively cyanobacterial-free water.

The simulation with the 8 m s^{-1} wind profile produced a similar spatial distribution of cyanobacteria to that with the 5 m s^{-1} wind profile because the lake was already largely homogenised in the vertical dimension. Thus, upwelling flows contained concentrations of cyanobacteria similar to those of the surface (Figure 8-7), so cyanobacterial surface concentrations in upwind areas were not reduced greatly.

ii. Wind directional consistency

A wind regime of random direction caused three changes to the resultant spatial distribution. Firstly, there was a greater mean surface cyanobacterial concentration (Figure 8-8). Secondly, there was a decrease in the magnitude of horizontal variation in surface cyanobacterial concentration (Figure 8-9). Thirdly, there was a greater rate of decrease in cyanobacterial concentration as a function of depth (Figure 8-10).

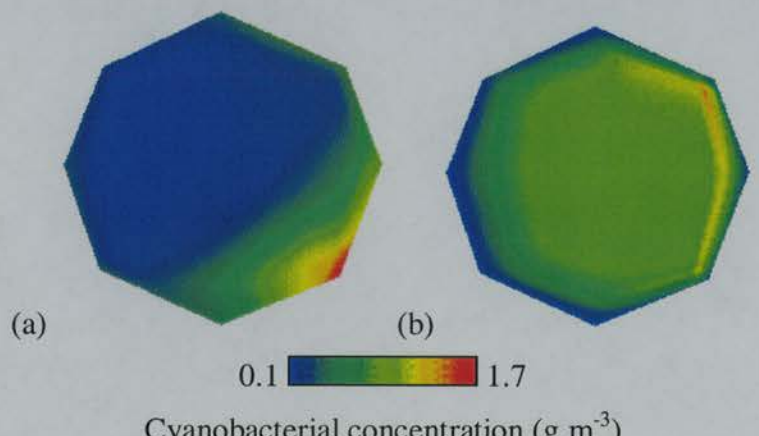

Figure 8-8. Surface cyanobacterial concentration for basins with different wind directional consistencies: (a) constant (control basin); (b) random direction.

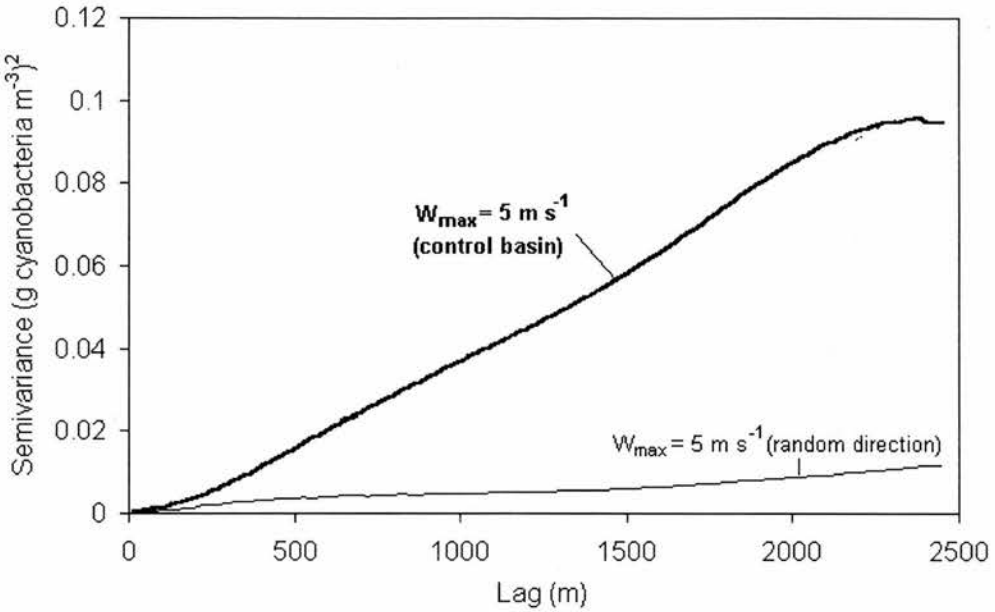

Figure 8-9. Omnidirectional variograms of surface cyanobacterial concentration for basins with different wind profiles.

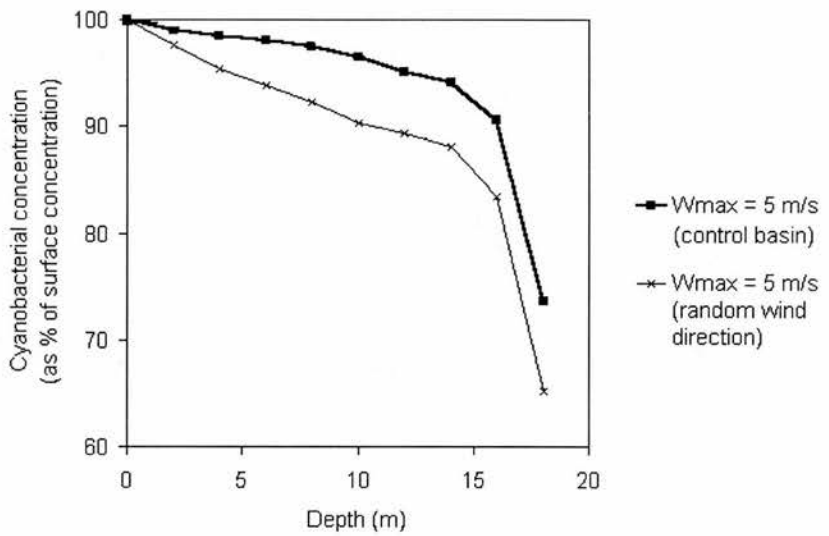

Figure 8-10. Cyanobacterial concentration as a function of depth for basins with different wind profiles.

A wind profile of random directions resulted in reduced horizontal and vertical flow velocities. This was because there was a horizontal change in the position of upwelling and downwelling areas throughout the simulation. With reduced upwelling rates of relatively cyanobacterial-free water, and with the area of

upwelling changing throughout the simulation, the amount of depletion of cyanobacteria at the surface was nearly spatially constant. This resulted in a more homogeneous spatial distribution of cyanobacteria at the surface. The greater rate of decrease of cyanobacteria with depth was the result of less mixing in the vertical dimension.

8.3.2.2 Inflow- and outflow-induced hydrometry

Simulations were run with both clustered and dispersed inflow and outflow configurations. Unlike all the other simulations in this chapter, these simulations were run over a time scale of 7 days. This was to ensure that relatively stable spatial distributions would be exhibited within the simulation time scale.

In most cases, the effect of inflows and outflows on hydrometry is relatively small because lakes generally have large ratios of lake volume to stream discharge (Smith, 1992). Therefore, residence time was set to be relatively short (approximately 5.78 days) by setting the lake volume to be small (an area of 1 km^2 and a depth set to 10 m) in comparison to stream discharge (10 m^{-3} s^{-1}). Although this was unusually short, it ensured that the effects of the discharges were manifested within the time constraints of the simulation. Simulations were run with no wind-forcing, so that the spatial dynamics of phytoplankton would solely be the result of the interaction between inflow- and outflow-induced hydrometry and phytoplankton characteristics.

Hydrometries of both simulations were very similar, regardless of the configuration of inflows and outflows (Figure 8-11). For both simulations, convection cells occurred within the horizontal dimension rather than the vertical dimension. Discharge into each basin initiated flows away from the point of inflow. This flow was progressively rotated clockwise in response to Coriolis acceleration, initiating a horizontal eddy in the north-west part of each basin which lasted for the week of simulated time. The convection cell was slightly stronger in the basin with the clustered inflow and outflow configuration. For both basins, there was shearing where the eddying flow reached the western wall, with some flows towards the north maintaining the eddy, and some flows towards the south maintaining a counter eddy (of a greater area but of lesser velocity).

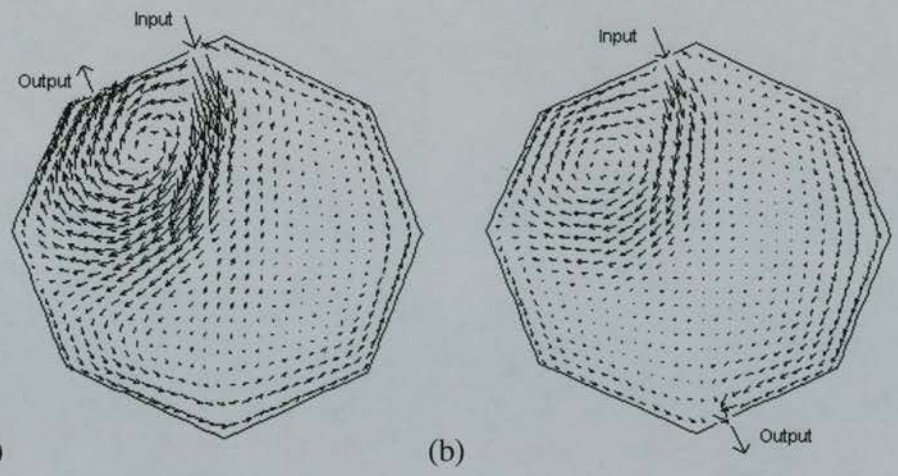

Figure 8-11. Surface velocity vectors for basins with different inflow and outflow configurations: (a) clustered inflow and outflow configuration; (b) dispersed inflow and outflow configuration.

For both simulations, relatively similar spatial distributions of cyanobacteria were created (Figure 8-12). In all cases, greatest cyanobacterial concentrations were found away from the source of water inflow because displacement away from there had occurred. For the simulations with a dispersed inflow and outflow configuration, there was a slightly more dispersed spatial distribution of cyanobacteria, with an increase in cyanobacterial concentration in the south-west.

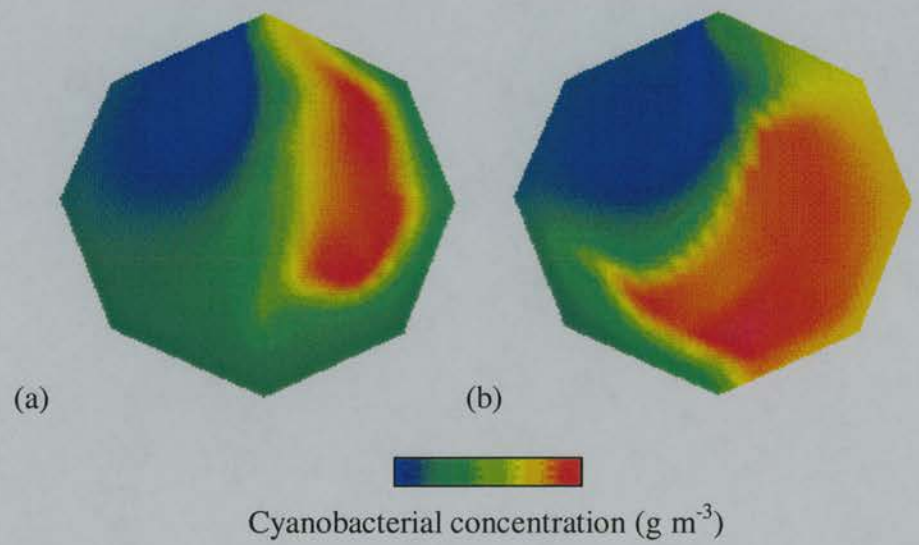

Figure 8-12. Surface cyanobacterial concentration for basins with different inflow and outflow configurations: (a) clustered inflow and outflow configuration; (b) dispersed inflow and outflow configuration.

Omnidirectional variograms of surface cyanobacterial concentration were similar regardless of inflow and outflow configuration, and were nearly identical until a lag of approximately 200 m to 300 m (Figure 8-13). The similarity was caused by the similarity of the hydrometry. The effect of the increased southward displacement of cyanobacteria with the dispersed inflow and outflow configuration did increasingly become apparent at lags approximating the length of the basin.

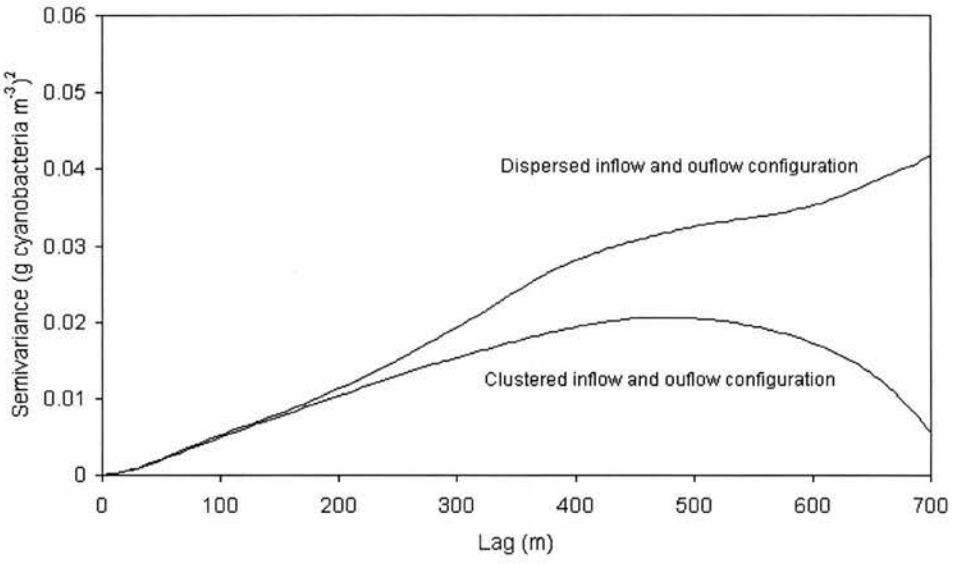

Figure 8-13. Omnidirectional variograms of surface cyanobacterial concentration for basins with different inflow and outflow configurations.

Semivariances were much less than experienced with the control basin (Figure 8-3) even though the residence time was relatively small and the time simulated was increased by a factor of 7. This suggests that in the creation of a basin-wide short-term gradient, the role of wind-forcing is much greater than that of forcing by inflows and outflows.

8.3.3 Morphometric modification of hydrometry

The morphometric properties studied were size-based (area and depth) and shape-based (elongation and complexity). In analysing the effect of morphometric properties, the objective was to understand how morphometry affected hydrometry and, therefore, influenced the specific spatial dynamics.

8.3.3.1 Area

To test the effect of basin area on the spatial dynamics of phytoplankton, simulations were run with areas of 2, 4, 6, 8, 10 and 12 km^2. Simulations were run with the same wind and irradiance regimes as used in the control basin (Table 8-1).

The general hydrometry was similar to that of the test basin: downwelling occurred downwind, upwelling occurred upwind, and Coriolis acceleration caused a clockwise deflection of flows. However, flow velocities were dependent upon basin area. With an increase in area, there was an increase in velocities because the amount of wind stress applied was positively related to basin area.

An increase in basin area resulted in an increase in mean surface cyanobacterial concentration (Figure 8-14) and an increase in the range over which variation occurred, but resulted in a decrease in the semivariance for a given lag as shown by omnidirectional variograms (Figure 8-15).

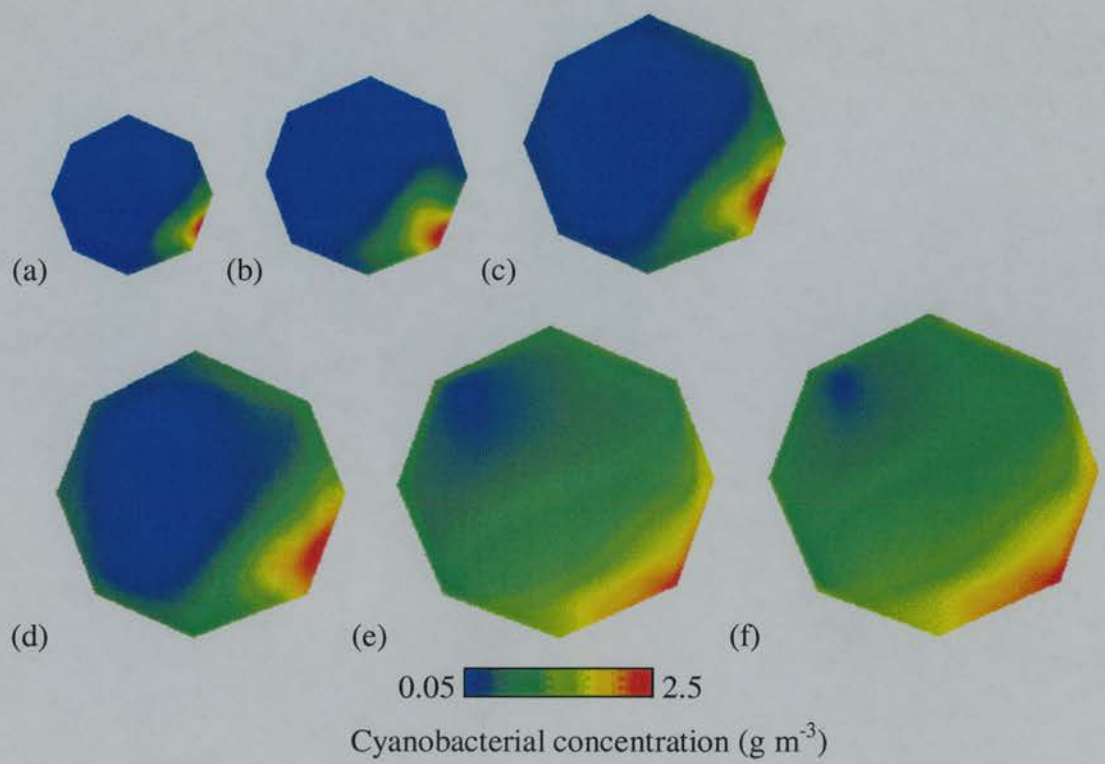

Figure 8-14. Surface cyanobacterial concentration for basins of different area: (a) A_L = 2 km^2; (b) A_L = 4 km^2; (c) A_L = 6 km^2 (control basin); (d) A_L = 8 km^2; (e) A_L = 10 km^2; (f) A_L = 12 km^2.

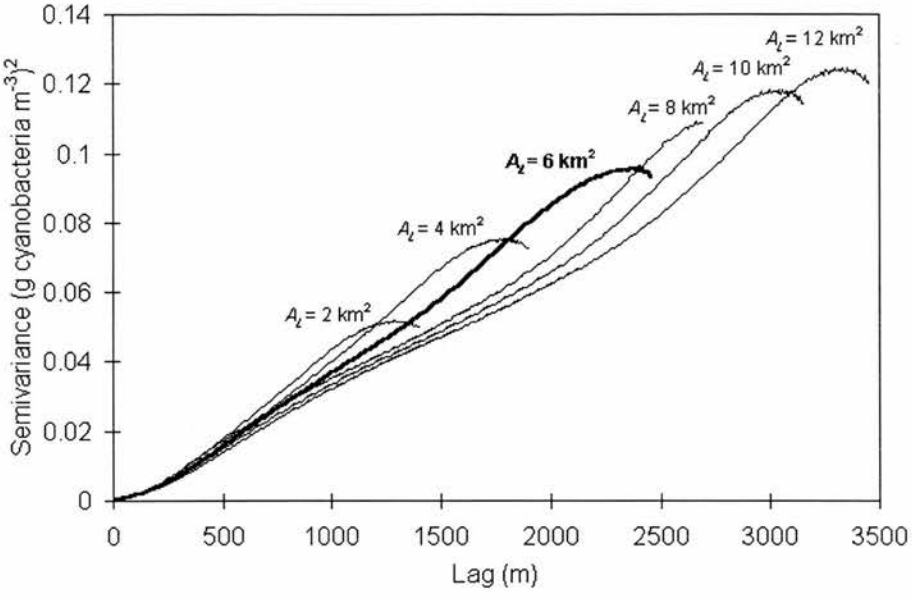

Figure 8-15. Omnidirectional variograms of surface cyanobacterial concentration for basins of different area.

Mean surface cyanobacterial concentration decreased with increasing basin area because basin area determined the relative proportion of the basin that was affected by upwelling of relatively cyanobacterial-free water. The wind regime resulted in a displacement of surface water by approximately 3000 m over the 24 hours of simulated time. This displacement almost completely mixed smaller basins. For example, the basin with an area of 2 km^2 had a maximum diameter of 1800 m, so upwelled cyanobacterial-free water will have reached to the downwelling wall (where there will have been partial but not total accumulation of cyanobacteria). In comparison, the basin with an area of 12 km^2 had a maximum diameter of 4000 m, so upwelled cyanobacterial-free water will not have reached the downwelling wall. A greater proportion of the surface of the larger basin, therefore, had cyanobacterial concentrations that were more similar to initial concentrations.

Semivariance for a given lag decreased with increasing basin area because the proportion of the surface affected by the upwelling (which reduced upwind surface cyanobacterial concentration) decreased with increasing basin area. With a decrease in the proportion of the surface affected, there was a decrease in the semivariance for a given distance.

The range over which variation of cyanobacteria occurred was positively related with

the horizontal scale of the basin because the horizontal distribution of vertical flows was determined by the positions of basin walls (vertical flows only occurred where horizontal flows were deflected into the vertical dimension). The spatial dynamics of cyanobacteria at the surface was therefore controlled by morphometry because the spatial distribution of these areas was controlled by basin morphometry.

8.3.3.2 Depth

To determine the effect of basin depth on the spatial dynamics of cyanobacteria, simulations were run on basins with depths of 5 m and 20 m (the control basin).

The hydrometry was greatly different between the two simulations. In the shallower basin, surface return flows were dominant, although there was some ephemeral vertical convection (Figure 8-16a). The surface return flow acted in a clock-wise direction because of Coriolis acceleration: running the model with no Coriolis acceleration produced two surface convectional eddies that ran in directions contrary to one another, according to the model of Livingstone (1954). The control basin, in contrast, experienced no surface return flow (Figure 8-16b).

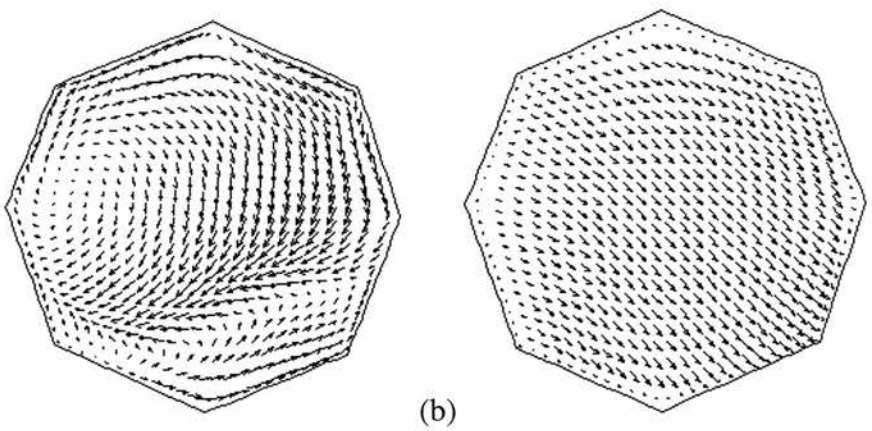

Figure 8-16. Surface velocity vectors for basins of different depth: (a) D_L = 5 m; (b) D_L = 20 m (control basin).

Greatly different spatial distributions of cyanobacteria were created. The shallower basin had a much greater mean surface cyanobacterial concentration. Additionally, in the shallower basin cyanobacteria actually accumulated upwind (Figure 8-17), which was contrary to expectations. For both basins, there was an increase in semivariance with increasing lag, although the rate of increase was less for the

shallower basin (Figure 8-18). Cyanobacterial concentration decreased as a function of depth in both basins (Figure 8-19). The shallow basin showed similar vertical profiles of cyanobacteria across the lake (in Figure 8-19 only the mean vertical profile is shown because the deviation from this pattern is negligible) in contrast to the deeper basin, were the vertical profile was dependent upon horizontal position within the basin.

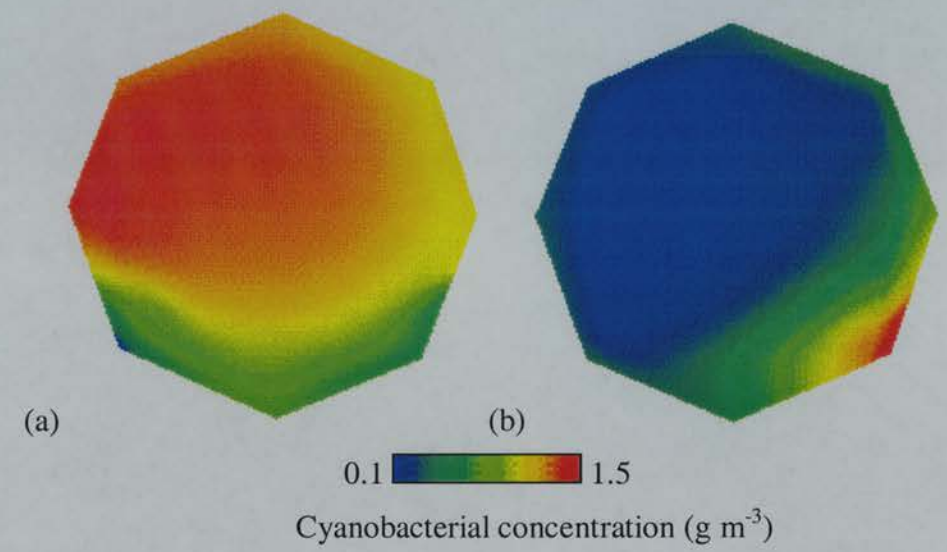

Figure 8-17. Surface cyanobacterial concentration for basins of different depth: (a) D_L = 5 m; (b) D_L = 20 m.

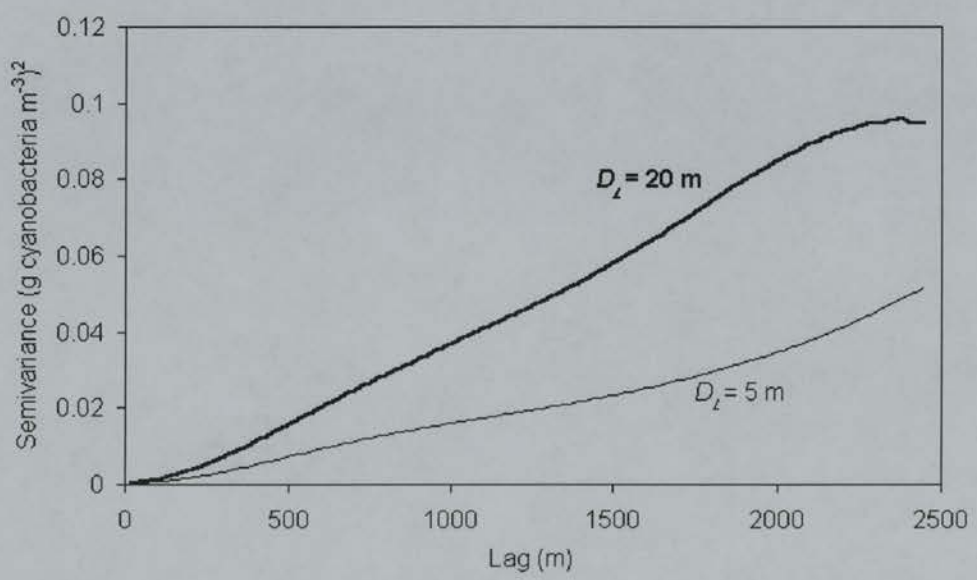

Figure 8-18. Omnidirectional variograms of surface cyanobacterial concentration for basins of different depth.

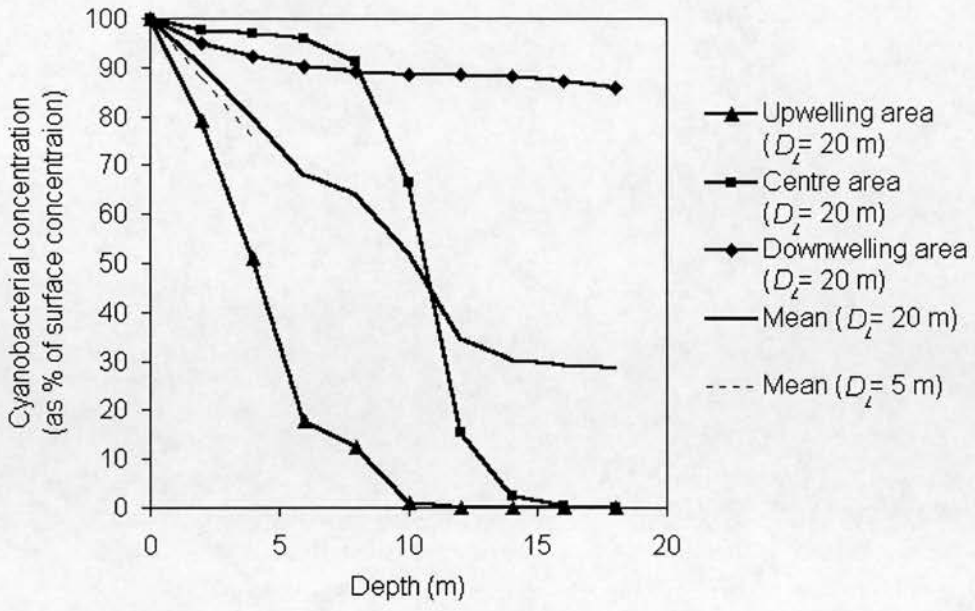

Figure 8-19. Cyanobacterial concentration as a function of depth for basins of different depth: D_L = 5 m; (b) D_L = 20 m (control basin).

Greater surface cyanobacterial concentration existed in the shallower basin because the basin's hydrometry reduced, both, downwelling of surface cyanobacteria, and upwelling of flows with lesser concentrations of cyanobacteria. The lesser semivariance in the shallower basin was due to two causes. Firstly, there was no clear vertical dimension convection cell in the shallower basin and surface return flows were dominant. Differential displacement (accumulation of cyanobacteria in downwelling areas and expulsion from upwelling areas) was, therefore, limited. Secondly, any upwelling that did occur in the shallower basin was confined to near-surface depths, which contained cyanobacterial concentrations that were relatively similar to those at the surface, so did not deplete surface concentrations.

The upwind accumulation of cyanobacteria in the shallower basin was probably ephemeral. With surface return flows being dominant, surface homogeneity should have been maintained. However, upwelling did occur upwind at periods throughout the simulation, which slightly reduced upwind cyanobacterial concentrations at approximately 12 hours into the simulation. This area of low concentration was then horizontally transferred around the basin by the surface flows, resulting in lower downwind concentrations by the end of the simulation. It is possible, therefore, that

a stable solution had not been achieved within the time scale of the simulation.

The equivalent horizontal scale over which cyanobacterial variation occurred may be attributed to the same cause as that of area. That is, basin walls defined the spatial scale of the surface variation by determining where upwelling and downwelling areas occurred. As horizontal dimensions were equivalent, so were the positions of these upwelling and downwelling areas (even if they were ephemeral in the shallow lake).

8.3.3.3 Elongation

To test the effect of elongation, simulations were run on basins with elongations of 1 (control basin), 2, 4 and 6. Area was kept constant between simulations at 6 km^2.

The hydrometries of the simulations were similar to that of the control simulation (Section 8.2) with the exception that an increase in elongation resulted in an along-axis elongation of the vertical dimension convection cell, and an across axis shortening of this convection cell. Spatial distributions of surface cyanobacteria showed this same along-axis elongation and across-axis shortening (Figure 8-20).

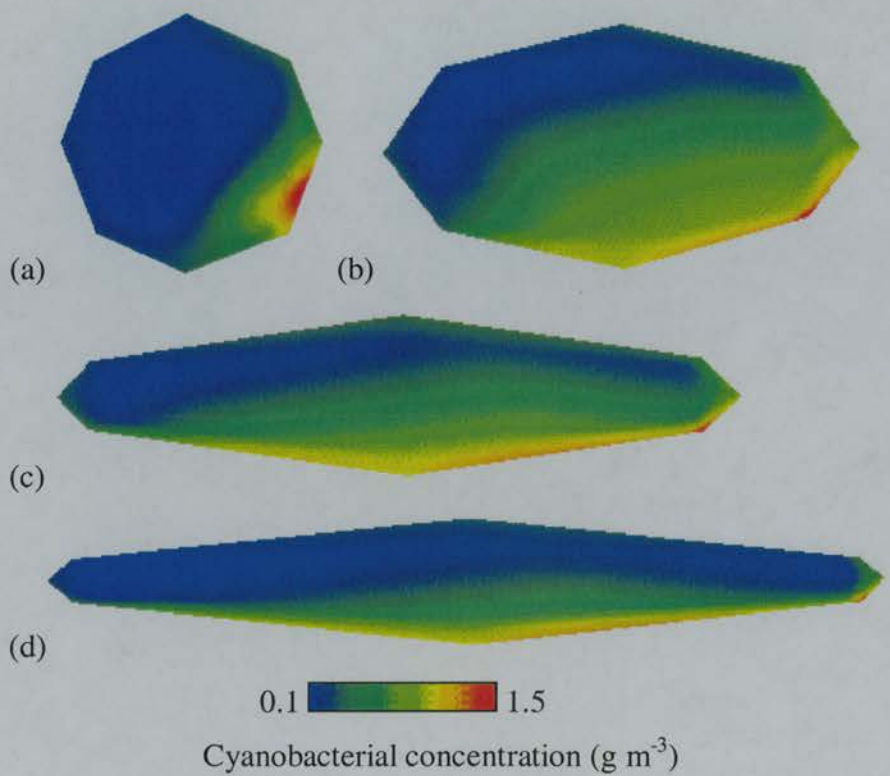

Figure 8-20. Surface cyanobacterial concentration for basins of different elongation: (a) E_L = 1 (control basin); (b) E_L = 2; (c) E_L = 4; (d) E_L = 6.

The more elongated the lake, the greater the geometric and zonal anisotropy as shown by the directional variograms (Figure 8-21). With an increase in elongation, the rate of increase of semivariance in the along-axis direction decreased, and the rate of increase in the across-axis direction increased. That is, variance in the across–axis direction was pushed to smaller spatial scales (as the lake became smaller in this dimension) and variance in the along–axis dimension was pushed to larger spatial scales (as the lake became larger in this dimension).

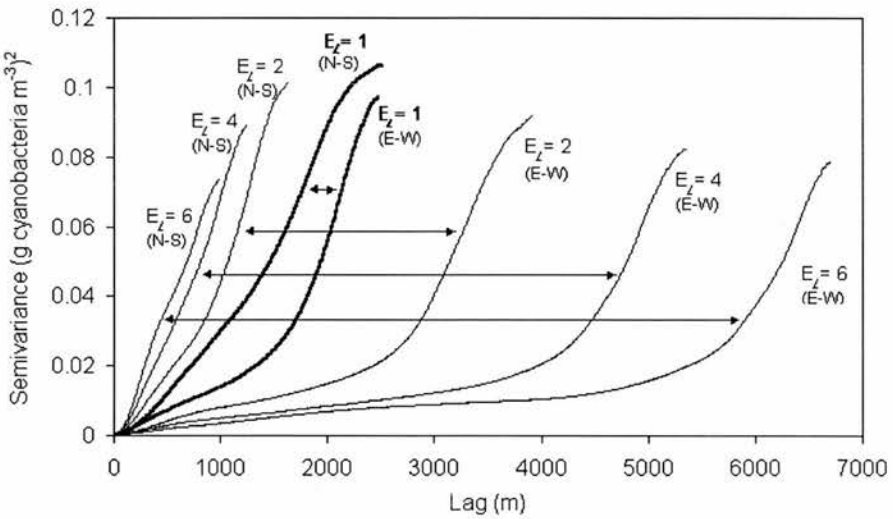

Figure 8-21. Directional variograms of surface cyanobacterial concentration for basins of different elongation: E-W variograms runs along-axis; N-S variograms run across-axis.

Again, the surface spatial distribution of cyanobacteria was caused by the effect of morphometry on the spatial distribution of surface flows. In the along-axis dimension, upwelling and downwelling areas were at relatively large distances. In the across-axis dimension, upwelling and downwelling areas were at smaller distances. Across-axis, there was a greater variance in vertical velocity for a given scale, which caused a greater variance in surface cyanobacterial concentration for a given spatial scale.

8.3.3.4 Complexity

To test the effect of basin complexity on the spatial dynamics of cyanobacteria, the

control simulation was compared with simulations where there was the presence of obstructions to flow (islands or promontories) in the centre of the basins.

Hydrometries were greatly altered by the presence of obstructions. Downwelling areas were created immediately upwind of the obstructions, and upwelling areas were created immediately downwind of the obstructions. That is, obstructions increased the number of vertical dimension convection cells operating within the basins. These small cells were superimposed on a larger vertical dimension convection cell operating over the whole of the basin.

With an increase in the complexity of the hydrometry, there was an increase in the complexity of the spatial dynamics of the cyanobacteria. Cyanobacteria were displaced away from upwelling areas and accumulated at the surface over the downwelling areas (Figure 8-22). However, because there were more upwelling and downwelling areas, there was greater micro- and meso-scale variation in cyanobacterial concentration.

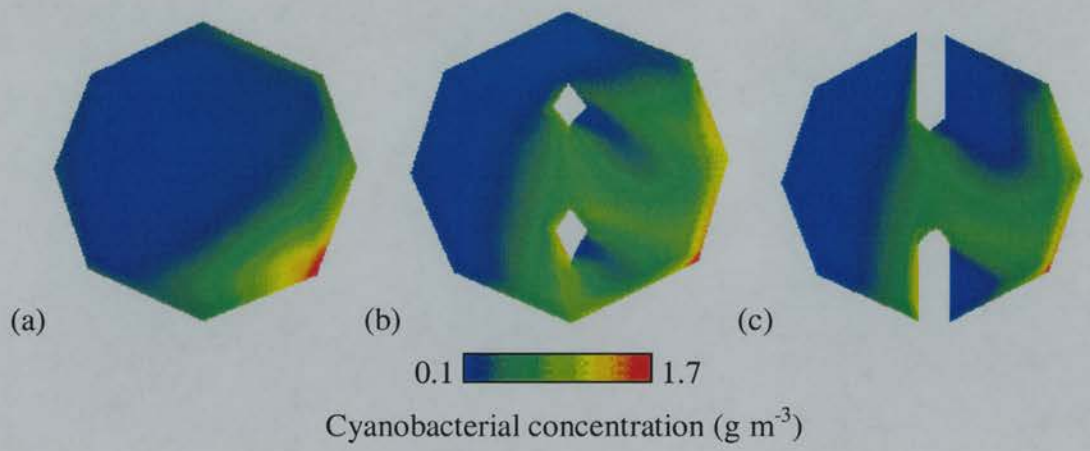

Figure 8-22. Surface cyanobacterial concentration for basins with different complexities: (a) simple basin (control basin); (b) basin with islands; (c) basin with promontories.

Omnidirectional variograms of the basins were relatively similar beneath a scale of approximately 1000 m (Figure 8-23). This corresponded to the distance from the western wall (where upwelling was occurring) to the beginning of the obstructions in the centre of the basins. At scales greater than 1000 m, the basins that contained obstructions had decreased semivariances than the control basin. This was because the meso-scale convection cells that were created by the obstructions produced

similar surface cyanobacterial concentrations around them to those at the basin walls. Cyanobacterial concentrations on the upwind side of the obstructions were similar to those on the downwind wall of the basin; and cyanobacterial concentrations on the downwind side of the obstructions were similar to those on the upwind wall of the basin. Obstructions, therefore, decreased semivariances at lags greater than 1000 m.

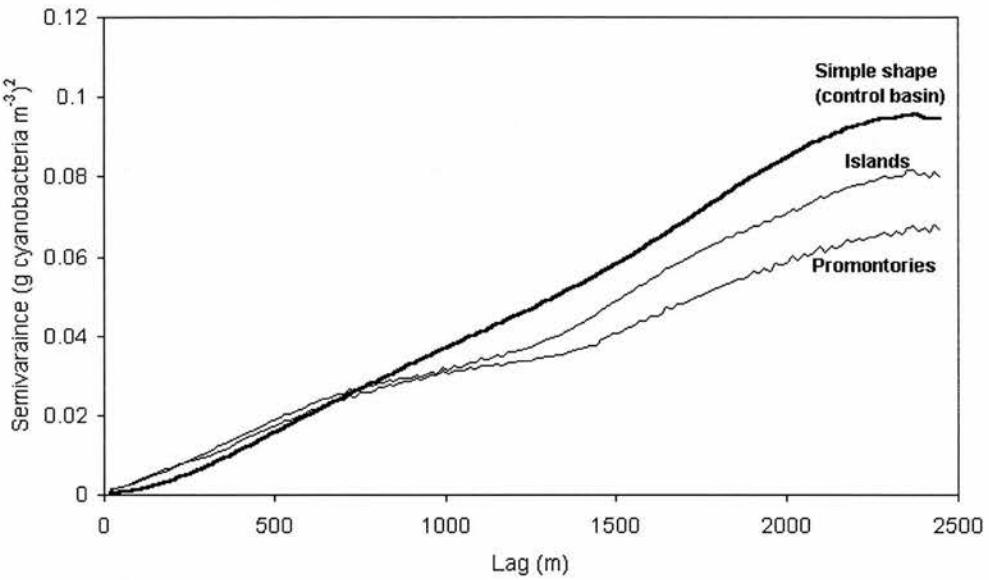

Figure 8-23. Omnidirectional variograms for basins with different complexities.

8.4 Phytoplanktonic properties and the spatial dynamics of phytoplankton

8.4.1 Phytoplanktonic boundary conditions

As with testing the effect of hydrometric properties, only phytoplanktonic properties that it was believed would have had most effect on the spatial dynamics of phytoplankton were altered between simulations, and all other properties remained constant. External boundary conditions affecting hydrometry were the same as those of the control simulation, so simulated hydrometries were also similar.

Cyanobacterial properties that were tested are shown in Table 8-2. Firstly, structural properties affecting the rising velocity were tested. Rising velocity was estimated for cyanobacteria as a function of density (which in turn was a positive function of

irradiance), cell radius and form resistance. Secondly, the physiological property of the maximum specific growth rate was tested. For this, nutrient concentration was set so that it would not limit cyanobacterial growth, so the only limits on growth were the maximum specific growth rate and irradiance.

Table 8-2. Phytoplanktonic properties influencing spatial dynamics.

	PROPERTY BEING TESTED			
	Cyanobacterial rising velocity			Growth rates
Boundary condition	Density-dependent	Radius-dependent	Form resistance-Dependent	
Irradiance ($\mu E\ m^{-2}\ s^{-1}$)	400 , 800, 1200	800	800	800
Radius (μm)	200	100, 200, 300	200	200
Form resistance	1	1	1, 2, 3	1
Maximum specific growth rate (ln units d^{-1})	NA	NA	NA	0, 0.5, 1.0

Notes: NA = not applicable

8.4.2 Density-dependent cyanobacterial rising velocity

To test the effect of cyanobacterial density on the spatial dynamics of cyanobacteria, simulations were run with irradiance regimes of different intensity (cyanobacterial density being positively related to irradiance levels). These varied from a low intensity irradiance regime (a maximum irradiance of 400 $\mu E\ m^{-2}\ s^{-1}$) to a high intensity irradiance regime (maximum irradiance of 1200 $\mu E\ m^{-2}\ s^{-1}$). The former was typical of overcast conditions and the latter was typical of clear atmospheric conditions for a summer day at mid-latitudes.

An increase in the intensity of the irradiance regime caused a decrease in surface cyanobacterial concentration (Figure 8-24) and a decrease in semivariance for a given lag (Figure 8-25). Increased irradiant intensities caused increased densities (Figure 8-26) and therefore decreased rising velocities. Decreased rising velocities caused the decreased mean concentrations. Decreased rising velocities caused greater downwelling in downwind areas, resulting in downwind concentrations more similar to those associated with the upwind concentrations caused by the upwelling of relatively cyanobacterial-free water. Thus, smaller semivariances resulted.

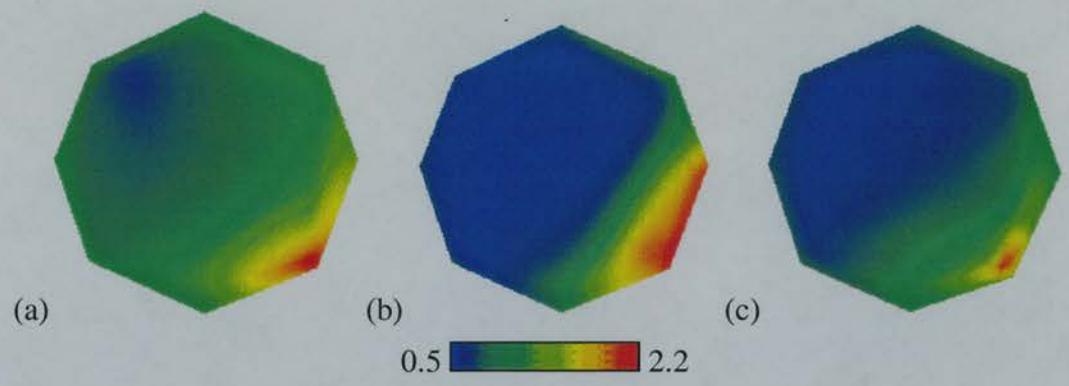

Figure 8-24. Surface cyanobacterial concentration for basins with different irradiance regimes: (a) I_{max} = 400 µE m^{-2} s^{-1}; (b) I_{max} = 800 µE m^{-2} s^{-1} (control basin); (c) I_{max} = 1200 µE m^{-2} s^{-1}.

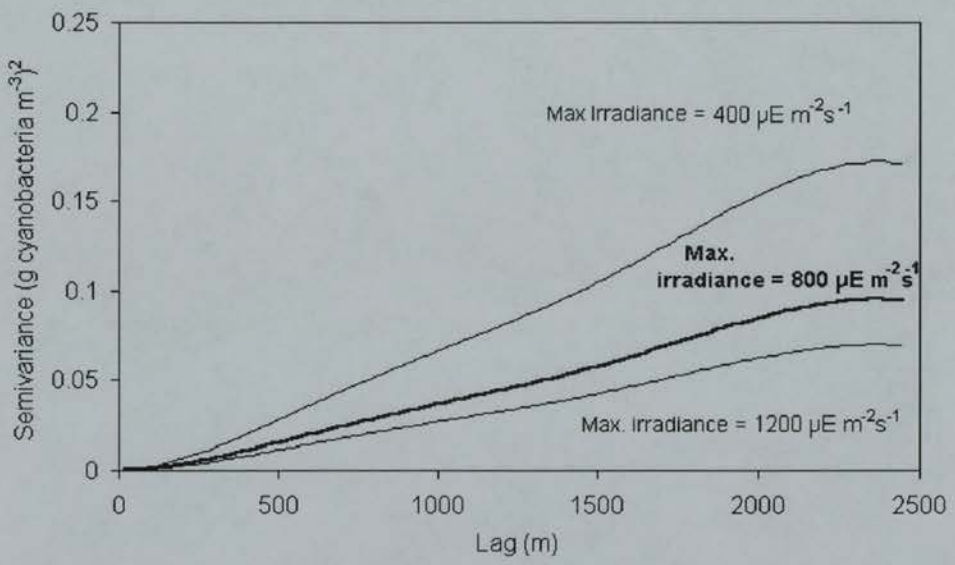

Figure 8-25. Variograms of surface cyanobacterial concentration for basins with different irradiance regimes.

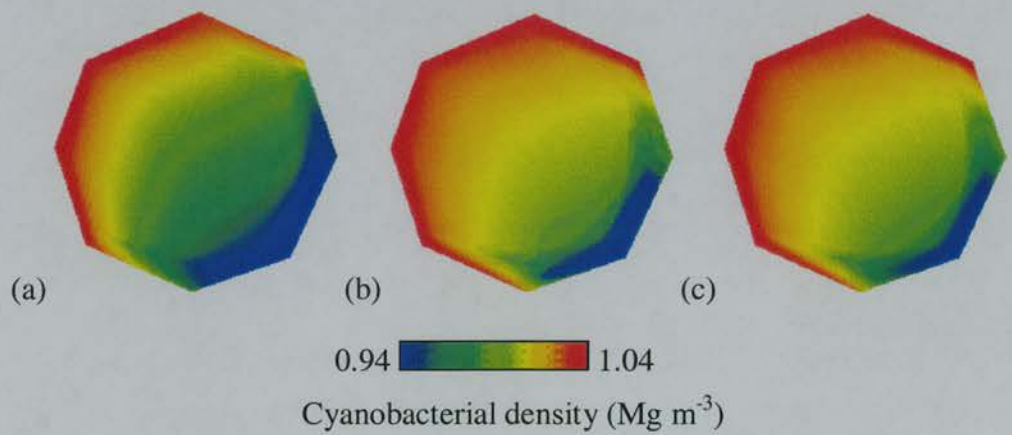

Figure 8-26. Surface cyanobacterial density for basins with different irradiance regimes: (a) I_{max} = 400 µE m^{-2} s^{-1}; (b) I_{max} = 800 µE m^{-2} s^{-1}; (c) I_{max} = 1200 µE m^{-2} s^{-1}.

8.4.3 Radius-dependent cyanobacterial rising velocity

To test the effect of cell radius on the spatial dynamics of cyanobacteria, simulations were run with colony radii varying from 100 μm to 300 μm. The former is typical of small flocculations of cyanobacteria such as *Oscillatoria* and the latter is typical of larger flocculations of cyanobacteria such as *Microcystis*.

An increase in colony radius resulted in an increase in mean surface cyanobacterial concentration (Figure 8-27) and an increase in semivariance at all lags (Figure 8-28).

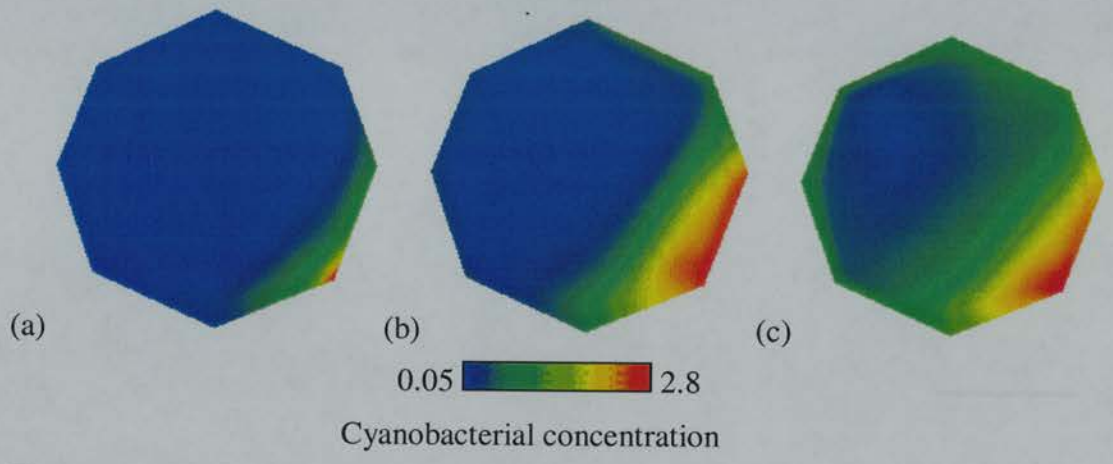

Figure 8-27. Surface cyanobacterial concentration for basins with cyanobacteria of different colony radii: (a) r = 100 μm; (b) r = 200 μm (control basin); (c) r = 300 μm.

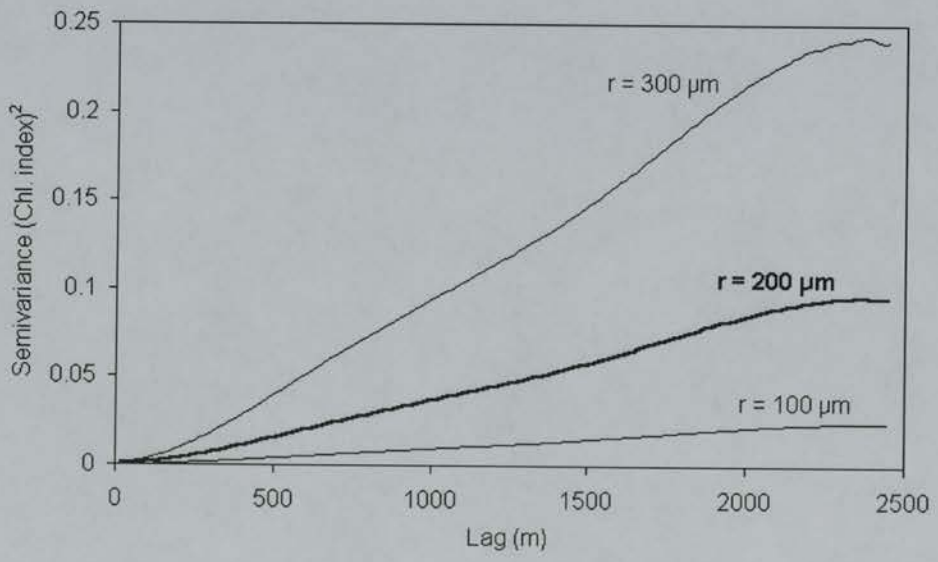

Figure 8-28. Variograms of surface cyanobacterial concentration for basins with cyanobacteria of different colony radii.

The increase in both mean cyanobacterial concentration and semivariance as a function of lag was caused by an increase in the rising velocity of the cyanobacteria. The integral of cyanobacterial density throughout the simulation was positive so the overall vertical direction of movement was upward. The velocity of vertical movement was positively related to the colony radius, according to Stokes' Equation (Equation 3-12). Therefore, the surface cyanobacterial concentration was increased because of increased floating towards the surface, and the semivariance was increased because cyanobacterial were more able to resist downwelling flows.

8.4.4 Form resistance-dependent rising velocity

To test the effect of cell form resistance on the spatial dynamics of cyanobacteria, simulations were run with form resistances varying from 1 to 3 (Table 8-2).

An increase in form resistance resulted in a decrease in surface cyanobacterial concentration (Figure 8-29) and a decrease in the semivariance of surface cyanobacterial concentration as a function of lag (Figure 8-30).

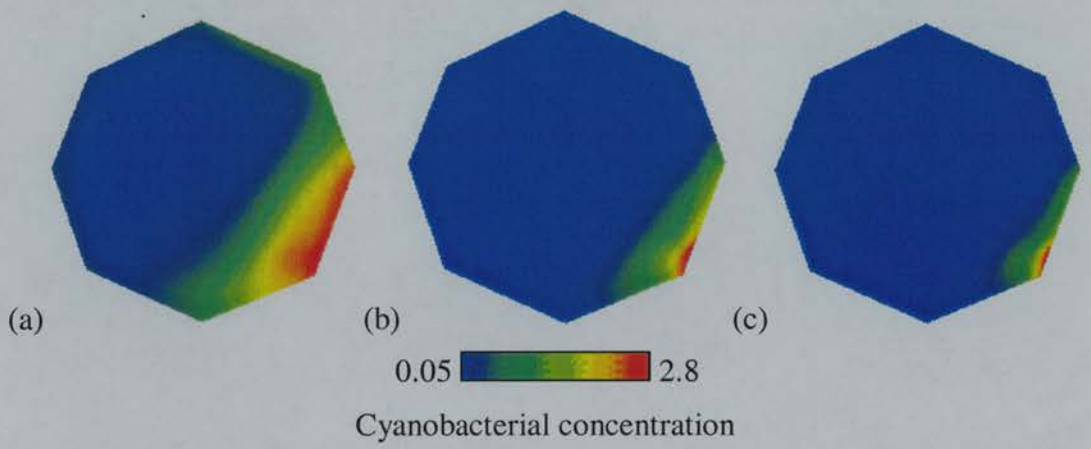

Figure 8-29. Surface cyanobacterial concentration for basins with cyanobacteria of different cell form resistances: (a) φ = 1 (control basin); (b) φ = 2; (c) φ = 3.

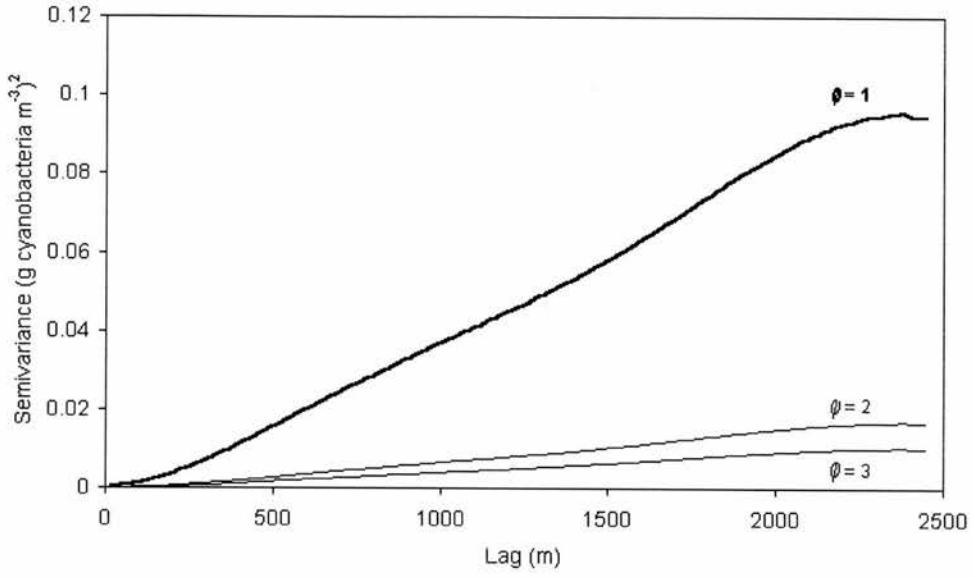

Figure 8-30. Variograms of surface cyanobacterial concentration for basins with cyanobacteria of different form resistances.

An increase in form resistance caused a decrease in the rising velocity and, therefore, a decrease in the rate of cyanobacterial migration toward the surface (thus, the lesser mean surface cyanobacterial concentration). Additionally, an increase in form resistance increased the extent to which cyanobacteria were entrained in the flows of the vertical dimension convection cell because a greater surface area was presented to the oncoming flow. This resulted in increased downwelling rates in the downwelling areas at the downwind side of the basin, and therefore lesser semivariances.

8.4.5 Maximum specific growth rates

To test the effect of the maximum specific growth rate on the spatial dynamics of cyanobacteria, simulations were run with maximum specific growth rates of 0 (the control simulation), 0.5 and 1.0 ln units d^{-1}.

An increase in maximum specific growth rate caused an increase in mean surface cyanobacterial concentration (Figure 8-31) and an increase in semivariance for a given lag (Figure 8-32).

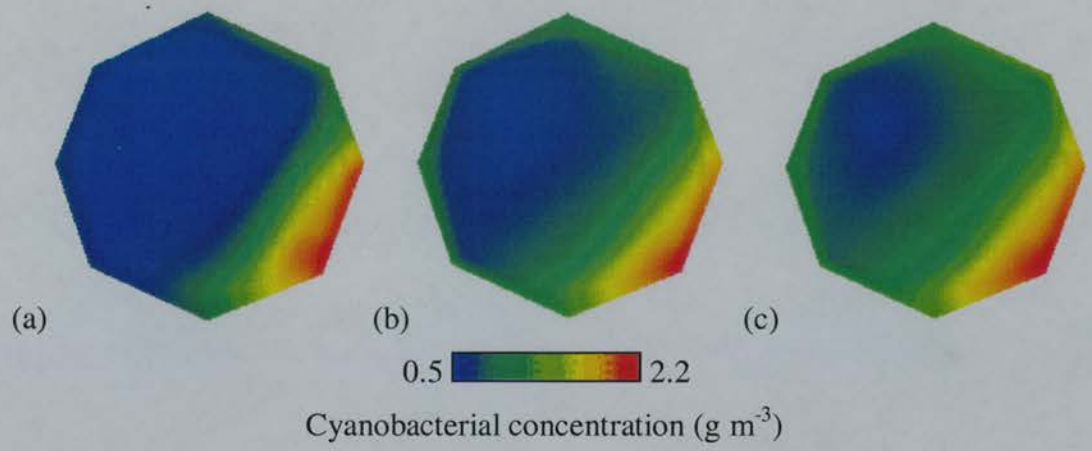

Figure 8-31. Surface cyanobacterial concentration for basins with cyanobacteria of different maximum specific growth rates: (a) k_{max} = 0 ln units d^{-1} (control basin); (b) k_{max} = 0.5 ln units d^{-1}; (c) k_{max} = 1.0 ln units d^{-1}.

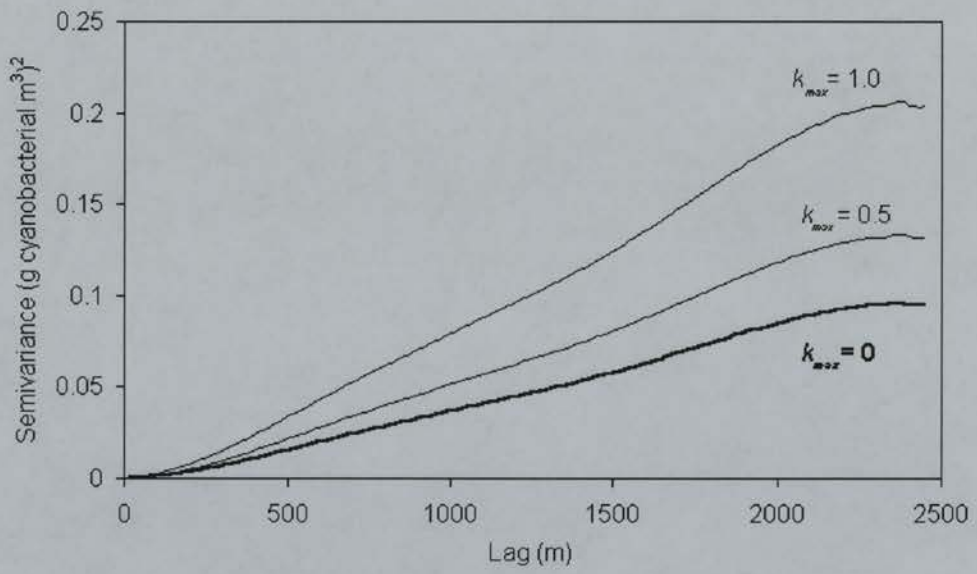

Figure 8-32. Surface cyanobacterial concentration for basins with cyanobacteria of different maximum specific growth rates: (a) k_{max} = 0 ln units d^{-1} (control basin); (b) k_{max} = 0.5 ln units d^{-1}; (c) k_{max} = 1.0 ln units d^{-1}.

The increase in semivariance for a given lag occurred because the net rate of growth was the product of population density and the maximum specific growth rate. Net growth rates were highest in downwelling areas because there were greater population densities there (as cyanobacteria had partially resisted downwelling flows). Thus, the increase in semivariance was caused by positive feedback mechanisms: any area where cyanobacterial concentrations were greater than the

mean concentration would have higher growth rates and therefore greater rates of increase in concentration. Negative feedback mechanisms will also have been in operation. For example, with an increase in population density, there will have been a decrease in irradiant intensity for a given depth because of shading. However, in these simulation, the effects of negative feedback mechanisms were less than those of positive feedback mechanisms.

8.5 Conclusion

The simulations of the spatial dynamics of phytoplankton resulting from wind-induced hydrometries and inflow- and outflow-induced hydrometries followed similar patterns to, and verified some of the conclusions of, the exploratory analysis (Chapter 5) and the modelling of real lakes (Chapter 7). Firstly, spatial dynamics were caused by the interaction between the species buoyancy properties and the hydrometry. Secondly, spatial dynamics were caused through the translocation of heterogeneity in one dimension into the other dimension (for example, vertical heterogeneity produced horizontal heterogeneity).

i. Hydrometric properties

Hydrometry affected the spatial dynamics of phytoplankton through displacement. Three types of displacement were involved. Firstly, there was differential displacement associated with the interaction between the phytoplankton buoyancy and the velocity field. With positive rising velocities, cyanobacteria were displaced to a lesser extent in parts of the basin where their rising velocities partially negated the flow velocities (downwelling areas) and were displaced to a greater extent in parts of the basin where their rising velocities added to the flow velocities (upwelling areas). Secondly, there was displacement associated with the translocation of vertical heterogeneity into the horizontal dimension at the surface. Thirdly, in simulations where inflows and outflows were the forces behind hydrometry, there was differential displacement associated with the great horizontal change in the velocity field. That is, phytoplankton were pushed away from the inflow.

Wind-induced hydrometry caused much greater spatial variation in phytoplankton than inflow- and outflow-induced hydrometry. This was because wind stress had a

comparatively greater effect over the whole of the basin in comparison to inflows and outflows where effects were localised to discharge areas. With wind-induced hydrometry, a threshold existed between 5 m s^{-1} and 8 m s^{-1} beyond which an increase in wind stress did not cause an increase in spatial variation. This was because, firstly, increased flow velocities overcame the absolute buoyancy of the phytoplankton, and secondly, increased mixing in the vertical dimension meant that upwelling flows contained similar phytoplankton concentrations to those at the surface.

Morphometry greatly modified the spatial dynamics of phytoplankton in all cases. This was because, firstly, morphometry controlled the relative positions of the upwelling and downwelling areas, secondly, morphometry affected the amount of wind stress applied to the basins, and thirdly, morphometry determined whether convection cells occurred within the horizontal or the vertical dimension. The magnitude of the variation was positively related to basin dimensions, with an increase in semivariances within increasing area and depth. The complexity of the spatial distribution was related to the basin shape.

ii. Phytoplanktonic properties

Phytoplanktonic properties had little effect on the spatial scale over which variation occurred. That is, maximum semivariances were achieved at spatial scales approximating those of the basins. This was because the spatial scale at which maximum semivariances occurred depended upon the relative locations of the upwelling and downwelling flows, which in turn were dependent upon the basin morphometry. Phytoplanktonic properties, however, had a great effect on the magnitude of the spatial variation. The greater the rising velocity (which was inversely related to the density, and directly related to the radius), the greater the semivariance for a given lag. Similarly, the greater the specific growth rate, the greater the semivariance for a given lag.

With respect to rising velocity, spatial dynamics were more sensitive to form resistance and cell radius than the irradiance environment. Decreasing the form resistance by a factor of 3 (from 3 to 1) or increasing the cell radius by a factor of 3 (from 100 μm to 300 μm) caused maximum semivariance to increase by a factor of

10. Increasing the irradiant intensity by a factor of 3 (from a maximum of 400 $\mu E\ m^{-2}\ s^{-1}$ to a maximum of 1200 $\mu E\ m^{-2}\ s^{-1}$) caused maximum semivariance to decrease by only a factor of 2.

The maximum specific growth rate of the cyanobacteria had a comparatively small effect on the maximum semivariance. Changing the maximum specific growth rate from having 0 to 1.0 ln units d^{-1} (which is the maximum experienced for many fast growing species) only resulted in increasing the semivariance by a factor of 2. What is perhaps more important, however, is that even with an initially spatially homogeneous nutrient distribution, phytoplankton growth will increase the variation in phytoplankton concentration under the presence of wind-forcing.

9 Discussion and Conclusions

9.1 Introduction

This chapter initially discusses the abilities and limitations of the approaches employed in this thesis (the exploratory analysis of the spatial distributions observed in the remotely sensed images, and the generation of spatial distributions through process modelling) for studying the spatial dynamics of phytoplankton within lakes. Involved in this will be the determination of the extent to which both approaches were able to produce information on the relationships between spatial dynamics and causative processes and the extent to which both processes were liable to errors and user-subjectivity. Only through such a discussion, is it possible to have reasonable confidence that conclusions made in this thesis have application to the real world.

The relationships between the spatial dynamics of phytoplankton and causative processes that have been shown throughout this thesis are then discussed. This leads on to a discussion on how the spatial dynamics are caused by the interaction between individual lake environmental and phytoplanktonic properties, involving numerous feedback mechanisms. From this, the general features of the spatial dynamics of phytoplankton within lakes are then concluded: their complexity and sensitivity; their scale and dimensionality; and the inter-relationship between temporal and spatial dimensions.

The final part of this chapter suggests future research that may follow from the outcome of this thesis. This research includes both, refinements to the techniques that have been used in this thesis, and suggestions for the further exploration of spatial dynamics within lakes.

9.2 Exploratory analysis: abilities and limitations

In the exploratory analysis, data on a relatively large number of lakes were required because it was necessary to examine the effects of a wide range of properties, such as phytoplankton structure, morphometry and wind regime. The alternative of

restricting the analysis to a small number of lakes would have made the inferences drawn far less generic. However, the analysis of such a large number of lakes required the use of archived images and supporting data that were obtained from different sources. These data had not been acquired specifically for modelling relationships and were of variable quality, causing potential for error. Both, estimates of spatial distributions of phytoplankton and estimates of lake environmental properties will have involved errors. As a result, there would be errors in establishing relationships between spatial distributions of phytoplankton and causative processes.

9.2.1 Estimating phytoplankton spatial distributions through remote sensing

The dominant method of estimating spatial distributions of phytoplankton was through remote sensing. The success with which spatial distributions could be estimated depended upon the *comprehensiveness, spatial and spectral resolution*, and *consistency* of the remotely sensed data.

i. Comprehensiveness

The comprehensiveness with which remote sensing was able to provide information on spatial distributions of phytoplanknton, with a near-complete coverage of most of the lake surfaces, was the main advantage of remote sensing. Intricate patterns were observed in some lakes at particular times, and the lack of well-defined structure in others gave an indication of the variation that occurs between lakes. Lake sampling through contact measurements would have been unable to successfully characterise the great range of spatial variation that existed. However, remote sensing was unable to provide any data on spatial distributions in the vertical dimension. In addition, with the remotely sensed data available, there was often very little information on the changes in spatial distributions within the temporal dimension, restricting the analysis to spatial *distributions* rather than spatial *dynamics*.

ii. Spatial and spectral resolution

The minimum spatial scale at which information on surface properties was available was the ground spatial resolution of the image. Because this study involved high spatial resolution imagery, interpretation of spatial distributions of chlorophyll was

possible at fine spatial resolutions (less than 10 m), and in some cases this enabled very detailed pattern to be resolved. For example, micro-scale surface chlorophyll distributions as a result of Langmuir circulation were apparent in the Esthwaite Water images (Section 5.3.1.3).

The spectral resolutions of the sensors were relatively high, but were not high enough to determine the specific types of phytoplankton present. This was a great limitation as often no *in vitro* studies of dominant phytoplankton types had been made.

iii. Consistency

Data consistency, in the sense that the relationship between the property being measured (phytoplankton) and the measurement (a chlorophyll index) remained constant, was required to enable comparison between different data, be it a comparison between different parts of one lake, or the same part of one lake at different times, or between different lakes.

Consistency for any given lake did not exist for several reasons. Firstly, chlorophyll index images were affected by the radiances of properties other than chlorophyll-*a*, including the lake bed, macrophytes, suspended sediments and DOC. Pozdnyakov *et al.* (1998) have criticised the use of such indices for this reason. Secondly, many of the images, particularly those acquired by the ATM in the 1980s, were affected by look-angle effects, creating spurious chlorophyll index gradients in some of the images of oligotrophic lakes that had no relationship to actual chlorophyll-*a* gradients. Calibration data were not available to minimise look-angle effects. Thirdly, all the images were affected by atmospheric effects, including cloud shadow and changes in transmissivity. These atmospheric effects could not be removed because of a lack of detailed meteorological data from the time at which the images were acquired.

Consistency between images of different lakes did not exist for the reasons mentioned previously, plus the fact that different sensors and different chlorophyll indices were used for different lakes. It was necessary to change chlorophyll indices between lakes to, firstly, optimise sensor wavebands, and secondly, reduce the proportion of radiance from water quality properties other than chlorophyll-*a* within

the wavelengths used by the chlorophyll indices. Use of a different sensor or different index would have produced a different value for the same chlorophyll-*a* concentration because the sensitivity to chlorophyll-*a* was sensor- or index-dependent. Only when specific wavebands for chlorophyll-*a* in inland water are used and standardised between different sensors, can fully robust analytical algorithms (such as those developed by Dekker *et al.*, 1992b) be used to facilitate a full comparison of actual chlorophyll concentrations between different lakes.

Despite the lack of data consistency, remote sensing was still a valid technique by which to determine spatial distributions of phytoplankton. Areas that were adversely affected by noise were removed from the study, which still left a comprehensive dataset. Additionally, the effect of using different sensors or indices was small in comparison to the effects of the lake environmental properties on spatial distributions, and it was considered valid to make some fairly approximate comparisons between lakes. Remote sensing was, therefore, the optimal technique for the estimation of the spatial distributions of phytoplankton within the lakes.

The variogram had little application because of the lack of consistency. However, when it was used (to aid in the comparison of images of different lakes acquired at the same time by the same sensor, or images of a specific lake acquired at different times by the same sensor) it was effective in summarising the general features of the spatial distributions. In fact, it proved very useful for analysing how the macro-scale spatial distribution in Esthwaite Water changed over time (Section 5.3.1.3). However, it was unable to characterise many patterns. For example, the Langmuir streaks and shearing fronts in the images of Esthwaite Water were not identifiable from the variogram because they occupied a relatively small proportion of the lake. Qualitative interpretation of pattern was therefore the dominant approach.

9.2.2 Establishing lake environmental properties

The two methods used for establishing lake environmental properties (qualitative interpretation of patterns in remotely sensed images and empirical modelling) both had potential for error. Qualitative interpretation of the remotely sensed images involved considerable user-subjectivity, and the empirical models involved questionable assumptions and were often based on data that were not appropriate for

the lakes concerned.

i. Estimation through remote sensing

Qualitative estimates of hydrometry through the analysis of spatial distributions of a thermal index or chlorophyll index were very subjective, because for any given pattern, there could be many causes. For example, a patch of lower chlorophyll index values could either be indicative of wind-induced upwelling or displacement away from an inflow: without direct measurement of the hydrometry, it was impossible to determine which. The interpretation was made more difficult because there was often no temporal aspect to the data.

However, some phenomena were clearly evident, particularly in the aerial photographs. For example, the presence of waves indicated that wind speeds were above a threshold value, and the orientation of wave fronts indicated the direction of surface currents.

ii. Estimation through empirical modelling

Data acquired *in situ* and concurrently with the remotely sensed images for establishing environmental properties were often unavailable, so it was necessary to estimate these properties from other sources. Some environmental properties were estimated from off-site measurements. For example, wind vectors often had to be obtained from weather stations at distances of tens of kilometres from the lakes. The recorded wind speeds were only indicative of the general wind environment and will have differed to the specific wind environment at the lake under consideration. Additionally, estimation of the effect of lake valleys on wind direction was highly subjective, and will have affected estimates of the depth of wave-induced mixing. Other environmental properties had to be estimated from measurements taken at different times. For example, it was often necessary to estimate thermal profiles from ones that had been measured for the same time of year in previous years.

The empirical models used to estimate processes (such as surface current speed or the depth of wave-induced mixing) from the environmental data involved error for two reasons. Firstly, the empirical models were established for lakes different to those used in this study, so their coefficients will not necessarily be suited to the environmental properties of the lakes of this study. Secondly, any measurement

errors made when the empirical models were established will have introduced errors into estimates in this study. Perhaps the greatest drawback to using empirical modelling, however, was the assumption of the achievement of a steady-state equilibrium between processes and causative factors. For example, a given surface current speed was estimated for a given wind speed. This will not be the case for a dynamic environment which would have involved a time lag between the forcing-function and the response. The implicit assumption of a steady-state scenario for the accurate estimation of lake processes has been strongly criticised by Imberger (1994). However, Imberger (1994) concluded that steady-state equations could be used to put the relative strengths of the forces involved into context. Within the exploratory analysis of this thesis, where the emphasis was on identifying relationships that could be investigated more robustly using process modelling, the use of equations that involved steady-state assumptions was justified.

There was no way of verifying the estimates from either remote sensing or empirical modelling singly. However, because the approaches were used concurrently, conclusions from one approach could be used to verify conclusions from the other approach, so there was more certainty that estimates of approximate environmental conditions were valid. For example, if weather station data indicated that the wind originated in the south, and thermal remotely sensed data indicated lower temperatures on the southern shore of a lake, it was possible to infer with reasonable certainty that there was upwelling at the southern shore of the lake.

9.2.3 Establishing causative relationships

The establishment of the causes of spatial distributions of phytoplankton was highly subjective. From the analysis of archived data, there were spatial distributions of phytoplankton at the surface of the lake and rough approximations of hydrometry, but provision of anything more than a cursory explanation of possible relationships between these two was not possible, particularly because there was no way of verifying relationships.

9.2.4 Conclusion

To conclude, there were limitations to what the exploratory analysis was able to identify on the spatial dynamics of phytoplankton within lakes. Although, information was of high spatial resolution and involved coverage of up to the entire lake surface, there was a considerable drawback to the approach in that the information provided lacked dimensionality. There was generally no information on the temporal aspect of the spatial distributions (with the images solely providing a series of snapshots) and there was generally no information on the vertical distribution (such as the change in currents with depth, or the change in phytoplankton concentration with depth). Lakes are highly dynamic and information on how, for example, a front or downwelling area develops provides much more information on what is actually happening in the lake than a single remotely sensed snapshot. Likewise, lakes are three-dimensional and the inability to look at spatial distributions within one of these dimensions (the vertical) is a significant disadvantage.

However, given that the exploratory analysis of the remotely sensed images was to gain insight into the relationships between the spatial distributions of phytoplankton and causative processes for focusing further research through process modelling, its objective was accomplished successfully. The main hydraulic processes affecting phytoplankton distributions that could be seen were wind-induced convection, wind-induced turbulence, Coriolis deflection at the surface, upwelling and downwelling. Additionally, the effects of morphometry (islands, promontories and shallow areas) in causing shearing of water flows and obstructions to mixing were clearly evident. These could later be explored more rigorously through process modelling.

9.3 Process modelling: abilities and limitations

A more rigorous investigation of the ability of process modelling to provide information on the spatial dynamics of phytoplankton is required because this was the central technique used in this thesis. Initially, process modelling is examined here on the basis of how the dimensional and scale characteristics of the processes and resultant spatial distributions that it can generate may aid the analysis of the

spatial dynamics of phytoplankton.

Information is only useful if potential errors of its estimates may be qualified or quantified. Therefore, attention will then focus upon possible errors and subjectivities that may have affected process model outputs. The information provided by the process model depended upon whether the model was used to simulate processes within real lakes or hypothetical basins, so its value specific to either of these is then discussed.

9.3.1 Dimensional and scale characteristics

i. Dimensionality

The information provided by SSIIM2.0 on the spatial dynamics of phytoplankton was highly dimensional. This included relationships on the dynamics in three spatial dimensions and a temporal dimension.

Because the model was spatially three-dimensional, it was possible to simulate velocity fields and spatial distributions of phytoplankton in the vertical dimension as well as the horizontal dimension. In all the real lakes modelled in this thesis, sub-surface return flows were identified. Additionally, in Esthwaite Water and Blelham Tarn, the existence of basin-wide convection cells in the vertical dimension was shown to be instrumental in determining the spatial dynamics of phytoplankton. Therefore, a vertical dimension was essential. Past CFD modelling has shown the necessity of using three dimensions to provide greater coherence between measured and simulated flows, and to provide a greater understanding of system dynamics (Falconer, 1991; Guting and Hutter, 1998). Empirical based work has substantiated the importance of the vertical dimension in affecting surface spatial distributions (Herman and Denman, 1977).

Because the model had a temporal dimension, it was possible to analyse the time-dependent development of phytoplankton spatial distributions: that is, analysis of spatial *dynamics* was possible because there was not the implicit assumption of steady-state conditions. Information provided on spatial dynamics included the temporal aspect of dynamic systems, such as the time lag between forcing function and system response.

ii. Scale

The minimum scale at which relationships could be analysed with SSIIM2.0 was determined by grid cell size. Not only did grid cell size limit the minimum dimension of any field properties that could be simulated, but many field characteristics such as return flows could be characterised only by considering changes in field properties between cells (with typically 4 to 7 cells being the minimum number required). Vertical cell resolution was less than 2 m, so many micro-scale vertical phenomena, such as the diurnal vertical movement of phytoplankton could be simulated. However, horizontal cell resolution was approximately 100 m, so micro-scale phenomena in the horizontal dimension could not be simulated. Imberger (1994) has criticised CFD models for being unable to resolve the full spectral range of the scales of motion in lakes, but this problem is not intrinsic to CFD modelling. For example, with SSIIM2.0, spatial resolution could have been increased to a comparative resolution of that of the remotely sensed images if more computational power had been available.

iii. Complexity and sensitivity

Through modelling it was possible to analyse the effects of a wide range of external boundary conditions (morphometric, atmospheric, hydrometric, phytoplanktonic) on the spatial dynamics of phytoplankton. SSIIM2.0 was more advanced than most available hydrodynamic water quality models. Most hydrodunamic models, for example, do not include the Kromkamp and Walsby (1990) cyanobacterial buoyancy feature.

Much of the sensitivity of the spatial dynamics of phytoplankton to environmental and phytoplanktonic properties was shown by the model. However, because the modelling process inevitably involved simplification, the full sensitivity of the dynamics could not be simulated. For example, in analysing the development of cyanobacterial blooms, Reynolds (1987) emphasised the great sensitivity to several environmental conditions, with small changes in these conditions determining whether blooms could occur. That is, thresholds were involved. When modelling with SSIIM2.0, responses to a change in external boundary conditions were continuous, suggesting that thresholds were not in operation.

9.3.2 Errors and subjectivities

Simulation validity, in terms of whether processes were being modelled correctly, was both lake-specific and time-specific because different processes occurred in different lakes at different times. For the simulations of the real lakes, discrepancies between simulated and measured spatial distributions of phytoplankton were small, but there was no way of verifying that the hydrometries had been modelled correctly. For the simulations of the hypothetical basins, the simulation validity could not be determined directly because there were, by definition, no real measurements with which to compare the model outputs. As a means by which the general model validity can be estimated it is necessary to examine the hydrodynamic and biological components of the model with regard to their propensity for causing error.

i. Hydrodynamic component

In the hydrodynamic component, errors would have been involved in estimates of turbulence, momentum transfer, mass transfer at small scales, and flow properties.

- ***Turbulence***

  Because an adaptive turbulence model was used in most simulations (the k-ε turbulence model), the effect of turbulent energy transport by the mean flow and diffusion, and the production and destruction of turbulence was possible, making it superior to those based on a constant eddy exchange coefficient (Versteeg and Malalasekera, 1995). However, the k-ε turbulence model does not accurately estimate the turbulence field, which results in inaccurate estimates of the convectional velocity field. This affects the spatial scale and magnitude of the phenomena being estimated. For example, when using this model, the length of re-circulation zones cannot be predicted with an accuracy of greater than 10 to 30 % (Olsen, 1997).

- ***Momentum transfer***

  Imberger (1994) has criticised hydrodynamic models for ignoring internal wave transport around the metalimnion. This transport is considered to be important because it causes the transfer of nutrients across the metalimnion which may sustain phytoplankton growth in the epilimnion.

- ***Mass transfer at small scales***

  The model was unable to simulate Langmuir cells, even when spatial resolution was set to a comparable scale. That is, the spatial resolution of the model was not preventing their appearance in the simulations but rather, the model itself was unable to simulate this type of circulation. This limitation of the model will have adversely affected results, as it has been shown that Langmuir circulation has a great effect on mixing within the epilimnion (Scott *et al.*, 1969). Moreover, the inability to simulate mass transfers of water or phytoplankton at the smallest scales meant that it was not possible to determine the effect of high frequency temporal variation in irradiant intensity on the spatial dynamics of phytoplankton. This was a strong drawback as short-term variation in irradiant intensity has a great effect on the daily integral (Schubert and Forster, 1997).

- ***Flow properties***

  Upwind difference schemes produce errors when flows are not aligned with the grid configuration. These errors are defined as false diffusion because they have a diffusion-like appearance. The amount of false diffusion depends upon the grid configuration: *grid aspect ratio* (the ratio of a grid cell's maximum length to its minimum length) and *grid expansion ratio* (the ratio of a grid cell's length to the length of a cell connected to it). The model involved a finite volume grid because this enabled grids to be fitted accurately to, in some cases, very complex morphometries, and enabled grid resolution to change according to morphometric complexity. However, this grid resulted in aspect ratios and expansion ratios that would have contributed greatly to false diffusion. This became evident when altering the grid resolution because the Navier-Stokes equations had more than one solution (Olsen *et al.*, 1998). The probability of this was increased if the geometry of the basin had high rates of expansion and contraction because these caused re-circulation zones where flows were not aligned with the grid. This was particularly evident with the simulation of Esthwaite Water (Section 7.4), but occurred to some extent in all the real lakes that were modelled. However, the disadvantages of false diffusion were probably outweighed by the advantages of a well-fitting grid.

ii. Biological component

In the biological component, errors would have been involved in the estimates of the rising velocities and the estimates of the specific growth rates.

- ***Rising velocity models***

  The model by Kromkamp and Walsby (1990) was used to estimate cyanobacterial buoyancy for inclusion in Stokes' law (Equation 3-12) because, firstly, it was generic enough to be applied to all species of cyanobacteria and, secondly, it required few data to run (a time-series of irradiance). This model has been the dominant one used to estimate cyanobacterial density throughout the last decade and has been successfully validated. It may therefore be inferred that errors were minimal.

  The dinoflagellate motility model was less well validated. However, it was possible to simulate vertical profiles for Esthwaite Water fairly successfully (Section 7.4.4) even with the very crude validation used in this thesis. Additionally, the dinoflagellate model was only used for one simulation so its total effect on the merit of the overall process model simulations was small.

- ***Growth models***

  Growth rates were estimated according to simple Michaelis-Menton kinetics. However, the system by which parameters of the kinetic relationships are estimated, such as incubation of phytoplankton in controlled environments before the *in situ* analysis of their growth within lakes, may be too simple to describe the response of phytoplankton to irradiance or nutrients. Harris (1980b) criticised the use of static bottle chains for estimating *in situ* growth rates, arguing that the lack of turbulent mixing within bottle chains prevents the periodic displacement of phytoplankton by turbulent mixing to depths of lesser irradiance. Capblanq and Catalan (1994) have found that when cells are being incubated at fixed irradiance levels before *in situ* experiments they exhibit adaptive responses, the time scales of which are of a similar magnitude to the time scales of the *in situ* experiments, suggesting that the results of such experiments have less application to lake conditions. Reynolds and Irish (1997)

have criticised the whole use of this system as a means of determining irradiance-dependent and nutrient-dependent growth rates, reasoning that certain species of phytoplankton have mechanisms to scale their demand for light or nutrients according to what is available within the environment.

Recent trends in biological modelling have included more complex responses of phytoplankton growth behaviour to environmental conditions. For example, stochiometric functions have been used in which growth rates depend upon the cell physiological state (Droop, 1974; Gotham and Rhee 1981). Cell stochiometry inevitably changes in phytoplankton because a cell respiring at night will not release nitrogen and phosphorus in proportion to the respired carbon. However, more complex models could not be employed because data were not available on cell stochiometry for the simulations in this thesis. More importantly, for most of the simulations in this thesis, it is doubtful whether a more advanced growth model would have caused much difference in the spatial dynamics of phytoplankton. For the real and hypothetical lakes that were simulated, spatial distributions were predominantly the result of interaction between phytoplankton structure and the velocity field (Section 9.4).

The functioning of the rising velocity and growth models depended upon irradiance levels. Irradiance was estimated approximately. Factors affecting irradiance that were not included in the model were the relative proportion of diffuse and direct irradiance, the effect of surface waves in altering the surface azimuth angle (and therefore the proportion or irradiance deflected at the surface), and the change in the spectral properties of irradiance with increasing depth.

Other possibly relevant factors that were not included in the biological model included grazing by zooplankton, phytoplankton senescence and photo-inhibition. Grazing by zooplankton was probably negligible over the time scales considered. Phytoplankton concentrations in the lakes modelled defined the lakes as being mesotrophic or eutrophic. In such lakes the impact of grazing on phytoplankton biomass diminishes (McQueen, 1990) and, by implication, so does the impact on the spatial dynamics of phytoplankton. Senescence was not included because in most cases nutrient concentrations were sufficiently high to prevent the collapse of the

population. Photo-inhibition was not included because irradiant intensities, averaged over the upper cell layer, were less than those required to inhibit photosynthesis (Reynolds, 1983).

9.3.3 Process modelling applied to real lakes

The application of process modelling to real lakes involved two potentials for error that were caused by data limitations. Firstly, lake environmental properties were not known with sufficient accuracy to establish accurately external boundary conditions. For example, wind vectors were estimated from off-site measurements and diurnal irradiance profiles were estimated from a measurement of the daily integral. In the modelling of hypothetical basins, the spatial dynamics of phytoplankton were shown to be sensitive to both wind and irradiance environments, so the discrepancies between the estimates of the model and the measured spatial distributions were expected (Hedger *et al.*, 1999a, 1999b; Olsen *et al.*, 1998, 1999). Secondly, the initial spatial distributions of phytoplankton were not known and it was necessary to estimate these. Again, discrepancies resulted. These problems are not intrinsic to process modelling and may be largely removed if the measurement of lake environmental and phytoplanktonic properties is made with the objective of the data being used for modelling (Section 9.7.1).

The application of process modelling to real lakes also involved user-subjectivity. In all cases, it was necessary to apply several grid configurations to produce one that provided a reasonable representation of the lake morphometry, and yet still prevented divergence. More importantly, because the objective of the modelling process was to simulate distributions that were already known, model parameters were fixed to simulate these distributions, and there was no method of verifying whether the model parameters had been chosen correctly. For example, with Loch Leven, the objective was to simulate a downwind accumulation of a negatively buoyant species so the zero-equation turbulence model was included because it created more turbulence in the deeper downwind areas (the standard k-ε model would have caused upwind accumulation). However, there was no way of verifying that the correct turbulence model had been chosen because there were no available measurements of the spatial distribution of turbulent intensity within the lake (Hedger *et al.*, 1998).

9.3.4 Process modelling applied to hypothetical basins

The simulations of hypothetical basins did not have the data problem that affected the simulations of the real lakes: external boundary conditions were not based on real measurements. As with the modelling of real lakes, the modelling of hypothetical basins also involved user-subjectivity. It was beyond the scope of this thesis to simulate all processes affecting the spatial dynamics of phytoplankton, so it was necessary to choose those that it was believed were most important, or could be most readily simulated. It is, therefore, possible that relevant properties were ignored.

There was the additional difficulty that the requirement for independence between model external boundary conditions conflicted with the dependence that exists in the real world. When testing one property, it was necessary to keep all other properties constant. That is, independence was assumed, but this independence is not always found in lakes. For example, basin area is often positively correlated with basin depth. This limited the relevance of the outcomes of the hypothetical basins' simulations to the real world.

The variogram was highly applicable, and was a useful statistic for summarising the system responses to changes in external boundary conditions. The variogram was adequately at describing system responses because they were relatively simple. For instance, there were changes in the scale-dependent magnitude of variation (either directional or omnidirectional) but there were not the fully complex patterns that were seen in the exploratory analysis (Chapter 5). The variogram would have been less able to describe the latter (Section 9.2.1).

9.3.5 Conclusion

To conclude, the main advantage of using process modelling for understanding the relationships between the spatial dynamics of phytoplankton and causative processes was that the information provided was highly dimensional, involving both vertical and temporal dimensions. Spatial resolution was poor in comparison to that which could be obtained with high resolution remote sensing, so micro-scale processes and spatial dynamics could not be simulated, but most processes over a horizontal scale of approximately 100 m and a vertical scale of 1 to 2 m could be analysed effectively

through modelling.

Errors were involved in process modelling. Some were intrinsic to the model, such as the inaccurate estimates of turbulence produced by the k-ε model. Some were extrinsic, such as errors in the establishment of the external boundary conditions for the real lakes. Despite these errors, however, it is believed that the main processes and spatial dynamics of phytoplankton within lakes were modelled effectively because they were consistent with past research (George and Edwards, 1976; George and Heaney, 1978; George, 1981a).

9.4 Summary of relationships

In the model simulations (Chapters 7 and 8), the spatial dynamics of phytoplankton were the result of either differential displacement or differential growth of phytoplankton (the same causes are inferred as the dominant cause of the spatial dynamics of phytoplankton in the lakes in the exploratory analysis in Chapter 5, although this was not proven in this thesis). Differential displacement involved interaction between hydrometry and the structural characteristics of the phytoplankton; differential growth involved interaction between the physiological characteristics of the phytoplankton and the irradiance and nutrient fields.

9.4.1 The spatial dynamics of phytoplankton and hydrometric properties

9.4.1.1 Forcing of hydrometry

Hydrometry was seen to be caused by two processes: wind stress, and inflows and outflows. The other cause of hydrometry (the overturn of a water column at the time of destratification) will have occurred within some of the lakes in this study but was not apparent in the remotely sensed images available, and was not simulated.

i. Wind stress

Wind stress was the primary force driving hydrometry in most situations considered in this thesis. Wind speed determined current speed, and wind direction determined current direction (although there was modification by Coriolis acceleration and morphometry). There were two components of the flow: a convectional component

and a turbulent component. Convection caused spatial dynamics at macro-scales; turbulence caused spatial dynamics at micro-scales. Within the exploratory analysis where wind-forcing was the dominant cause of hydrometry (Section 5.3), it was possible to divide the remotely sensed images of the lakes into two categories according to wind speed. Firstly, in lakes where wind speeds were generally less that 5 m s^{-1}, macro-scale gradients existed, and it was inferred that these were caused by convection cells. Convection cells caused the gradients because phytoplankton were partially able to resist vertical flows according to their buoyancies and there was displacement of phytoplankton away from upwind shores through the upwelling of relatively phytoplankton-free water. This occurred in most lakes, from those that were relatively large, such as Loch Ness and Loch Awe, to those that were relatively small, such as Esthwaite Water and Blelham Tarn. Secondly, in lakes where wind speeds were greater than 5 m s^{-1}, there was an absence of macro-scale gradients, and it was inferred that this was caused by turbulent mixing having homogenised the lakes. This absence was particularly evident in Bassenthwaite, Derwentwater and Wastwater, which exhibited no macro-scale heterogeneity. The process modelling of Eglwys Nynydd (Section 7.3) and the modelling of the effect of wind speed in a hypothetical basin (Section 8.3.2.1) both confirmed the importance of wind-speed in determining the spatial dynamics of phytoplankton.

ii. Inflows and outflows

Inflows and outflows had a much smaller effect on hydrometry in most of the lakes because the forces imparted by hydrometry will have been less than those imparted by wind stress. The effects of inflows and outflows on hydrometry were localised to meso- and micro-scales. However, in the smaller Loosdrecht lakes inflows clearly had effects, and where the inflowing water contained different concentrations to those within the lakes, caused increased meso-scale spatial variation.

9.4.1.2 Modification of hydrometric properties

Hydrometric properties were not only determined by the forces that initiated circulation but also by boundaries, which served to modify circulation. These boundaries were either impervious to flow (the bed and walls, as determined by the

morphometry) or partially impervious to flow (density gradients at the thermocline).

i. Morphometry

Hydrometry was modified by the areas, depths and shapes of the lakes. These affected hydrometry either through providing physical boundaries to flows or through affecting the wind environment.

Lake area determined the horizontal spatial scale of macro-scale convection cells by acting as a physical boundary, and determined the rate of displacement by affecting the amount of wind stress applied. The effect of area on the spatial dynamics of phytoplankton was difficult to determine in the exploratory analysis, because relationships were obscured to varying extents by other properties. Process modelling of hypothetical basins showed that, with other factors remaining constant, the magnitude of the variation increased with an increase in area. This was because greater amounts of wind stress were required to mix larger lakes.

Lake depth determined the propensity for return flows to occur at the surface, and determined the vertical spatial scale of macro-scale convection cells. The effect of depth on the spatial dynamics of phytoplankton was again difficult to determine in the exploratory analysis for the same reasons as that of area. In general, with a decrease in depth there was a decrease in the magnitude of variation. Lakes of the Loosdrecht lake system which were relatively unaffected by inflows exhibited relatively little spatial variation. Bassenthwaite and Derwentwater also exhibited relatively little variation. In the modelling of hypothetical basins, it was shown that this decrease in variation was caused by a weakening of the vertical dimension convection cell, an initiation of surface return flows, and a possible entrainment of near-surface phytoplankton in any existent sub-surface return flows. However, it was not inevitable that shallow lakes had homogeneous spatial distibutions. In the presence of inflows, a shallow depth actually increased the impact of the inflows because it decreased the residence time. Additionally, in shallow lakes where there were positively buoyant species, macros-scale gradients occurred, such as in Eglwys Nynydd (Section 7.3). Alternatively, if there was spatial variation in turbulent intensity, macro-scale spatial dynamics could occur, such as in Loch Leven (Section 7.2).

Lake shape (elongation and complexity) greatly affected the complexity of the hydrometry. In the process modelling of hypothetical basins, an increase in basin elongation caused an increased anisotropy of the variation (Section 8.3.3.3) and an increase in basin complexity caused a decrease in the magnitude of the spatial variation at horizontal scales approaching that of the basin (Section 8.3.3.4). A decrease in the magnitude of the variation was not, however, always associated with an increase in basin complexity. One of the reasons that Esthwaite Water had much meso-scale variation in phytoplankton concentration was because it had promontories that caused meso-scale variation in the amount of displacement of phytoplankton (Section 7.4).

The importance of basin morphometry in affecting the spatial dynamics of nutrients, and therefore the spatial dynamics of phytoplankton as a result of growth is discussed in Section 9.4.2.2.

ii. Density gradients caused by the thermal profile

Hydrometry was also modified by the thermal profile. If a thermocline was present, the vertical dimensions of convection cells were constrained, and return flows occurred nearer to the surface, within the epilimnion. This was particularly apparent in simulations of Esthwaite Water in which the lake was strongly stratified (Section 7.4). The effect of this on the spatial dynamics of phytoplankton was difficult to determine, although the upwind accumulation of dinoflagellates in Esthwaite Water (Section 7.4.4) would probably not have occurred if the lake was unstratified, and sub-surface return flows had occurred at greater depths.

9.4.2 The spatial dynamics of phytoplankton and phytoplanktonic properties

9.4.2.1 Structural properties

In all cases, it was the interaction between structural properties of phytoplankton and hydrometry that determined displacement-induced spatial dynamics. In most cases in the exploratory analysis, it was not possible to quantify the importance of structural properties because there were no data on these (with the exception of the Esthwaite Water and Blelham Tarn). It was merely possible to infer that

displacement away from upwelling areas was occurring in stratified water columns.

Process modelling of the effect of phytoplanktonic properties in the hypothetical basins (Section 8.4) showed that cell radius and form resistance were important in determining rising velocities. The greater the absolute rising velocity of the species, the greater the magnitude of both horizontal and vertical variation, so irradiance environments which contributed towards high cyanobacterial rising velocities increased the magnitude of the variation. Process modelling of real lakes suggested that density was important, with positively buoyant phytoplankton accumulating at downwind shores.

9.4.2.2 Physiological properties

In circumstances where there was a nutrient gradient, macro-scale gradients in phytoplankton concentrations followed. Phytoplankton gradients existed in Loch Lomond and Ullswater, and typically occurred over distances of tens of kilometres. Nutrient gradients were dependent upon input gradients and morphometry. In Loch Lomond and Ullswater, nutrient gradients existed because of land-use differences: the southern basin of Loch Lomond and the northern basin of Ullswater had greater phytoplankton concentrations because there was more agricultural land-use in the surrounding sub-catchment causing greater nutrient inputs. Morphometry affected gradients by affecting the amount of mixing that occurred. Phytoplankton gradients that could be attributed to differential growth were only exhibited in larger lakes, and it may be inferred that mixing within smaller lakes will have reduced nutrient gradients. Additionally, phytoplankton gradients arising from differential growth were only seen in lakes that had complex shapes, involving relatively narrow or shallow areas. These sections of lakes further reduced mixing. Loch Ness was of a scale comparable to that of Loch Lomond, but did not have a phytoplankton gradient that was caused by differential growth (the chlorophyll index gradient was in the opposite direction to what would be expected if this was the case) because there were no obstructions to mixing (Section 5.3.1.1).

Irradiance was also important in determining spatial dynamics through differential growth. With the Loch Leven simulation, increased phytoplankton growth at the

surface contributed to the macro-scale gradient in phytoplankton concentration (Section 7.4).

9.5 Interaction and feedback mechanisms

So far, the effects of lake environmental and phytoplanktonic properties have been considered on an individual basis. The spatial dynamics of phytoplankton, however, are the combined results of these properties acting together. For any given volume within a lake, the interaction between hydrometry (which is determined by morphometric, atmospheric and inflow and outflow properties) and phytoplankton structural characteristics determines phytoplankton concentration through fluxes into that volume (Figure 9-1). Likewise, for any given volume within a lake, the interaction between the lake environmental properties (irradiance, and nutrient concentration) and the phytoplankton physiological growth properties determines phytoplankton concentration through growth within that volume (Figure 9-1).

Two feedback mechanisms are associated with phytoplankton growth and an additional feedback mechanism is associated with cyanobacterial rising velocity (Figure 9-1). Firstly, the growth rate is dependent upon nutrient concentration, but growth decreases nutrient concentration, so a negative feedback mechanism is introduced that regulates phytoplankton concentration. Secondly, the growth rate is dependent upon irradiance levels, but an increase in population numbers causes an increase in attenuation and a decrease in irradiance levels. Another negative feedback mechanism is therefore introduced. With cyanobacteria, a feedback mechanism involving irradiance and cell density operates. The greater the irradiance, the greater the density so the lower the rising velocity. Whether this acts as a positive or a negative feedback mechanism depends upon the position of the phytoplankton within the water column. An increase in density may cause phytoplankton cells to sink, reducing concentrations near to the surface but increasing concentrations deeper within the water column. Near to the surface, this decrease in concentration results in less attenuation so a positive feedback mechanism is produced. At greater depths, however, the increase in concentration results in greater attenuation so a negative feedback mechanism may be introduced.

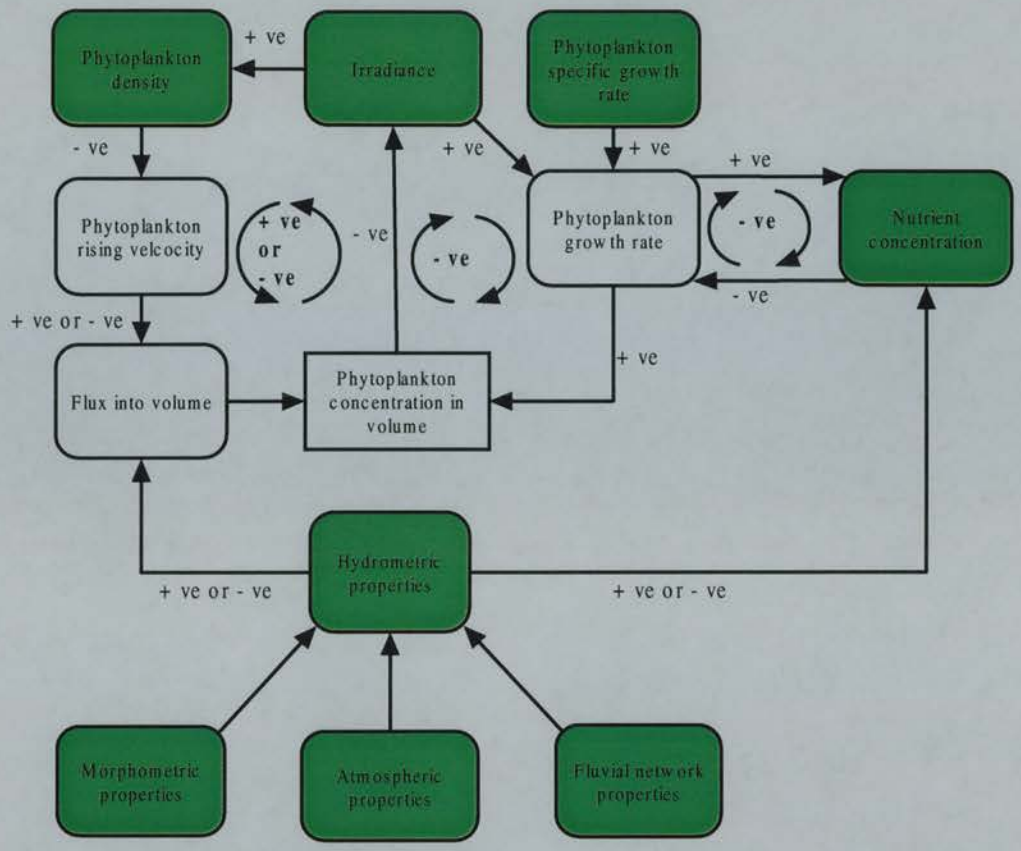

Figure 9-1. Inter-relationships and feedback mechanisms involved in the determination of phytoplankton concentration within a given volume. Lake environmental and phytoplanktonic properties are shown in green.

Because the interactions vary spatially, different concentrations are produced in different parts of the lakes. Figure 9-2 and 9-3 show how environmental and phytoplankton properties act to alter both the scale and the magnitude of variation. In both cases, variation depends upon displacement and growth.

The scale at which variation occurs may be related to wind forcing, the inflow and outflow configuration and lake morphometry (Figure 9-2). Wind drives the hydrometry of the lake: wind speeds of less than approximately 5 m s^{-1} may cause macro-scale gradients through convection; wind speeds greater than approximately 5 m s^{-1} may cause micro-scale variation through the disintegration of macro-scale spatial distributions through turbulent mixing. In the presence of inflows and outflows, their configuration may define the scale over which growth rates can change. Lake morphometry acts as a physical boundary defining the maximum scale over which variation can exist, determining the maximum size of macro-scale

convection cells.

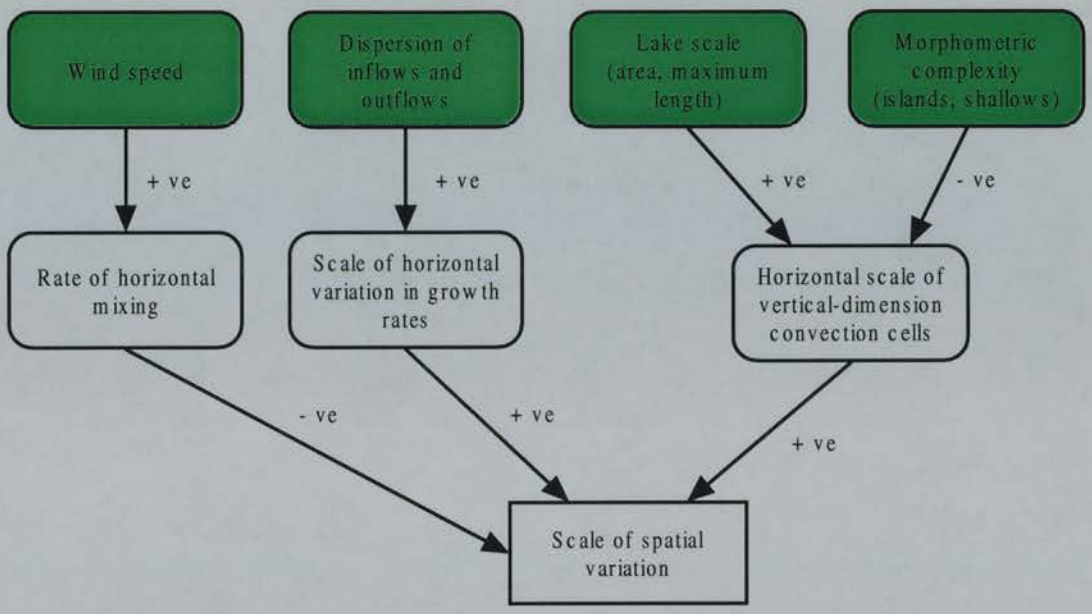

Figure 9-2. Main factors affecting the scale of phytoplankton spatial variation.

The factors affecting the magnitude of spatial variation in phytoplankton concentration show a similar complexity (Figure 9-3). The magnitude of variation in phytoplankton concentration is dependent upon the magnitude of variation in circulation rates and growth rates. These in turn depend upon morphometric, atmospheric and inflow and outflow properties.

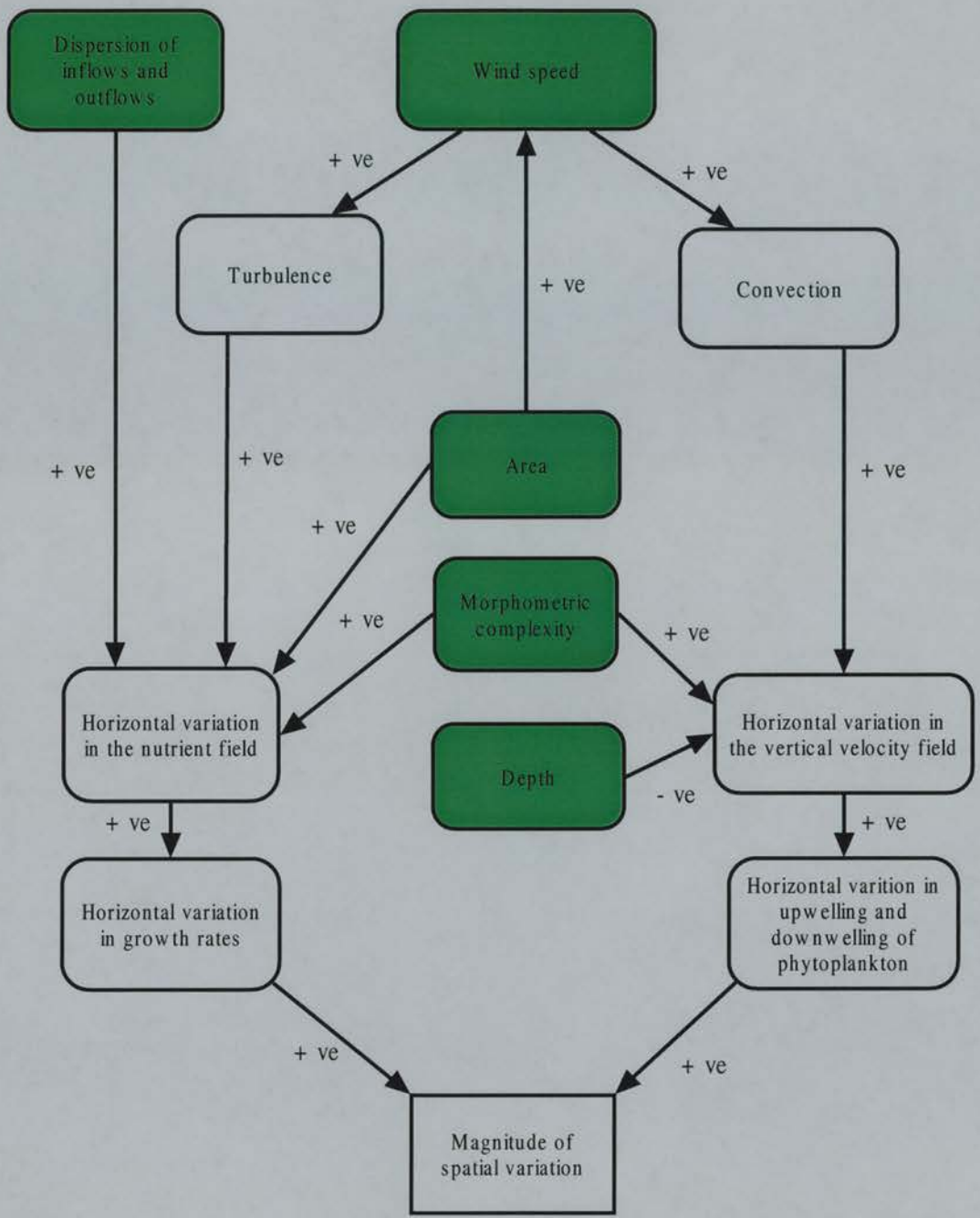

Figure 9-3. Main factors affecting the magnitude of phytoplankton spatial variation.

9.6 General conclusions on the characteristics of the spatial dynamics of phytoplankton

To conclude, three characteristics of the spatial dynamics of phytoplankton in lakes have been evident in this study. Firstly, the spatial dynamics of phytoplankton in lakes exist at specific spatial scales, in three dimensions with interdependence between the horizontal and vertical dimensions. Secondly, the spatial dynamics of phytoplankton in lakes are inextricably bound with temporal dynamics. Thirdly, the spatial dynamics of phytoplankton in lakes are highly complex, resulting from the interaction of a large number of lake environmental and phytoplanktonic properties.

9.6.1 Scale and dimensionality

The spatial dynamics of phytoplankton exist at a great range of scales, varying from macro- to micro-scales. Lake environmental and phytoplanktonic properties determine these scales.

The spatial dynamics of phytoplankton are highly dimensional. In the vertical dimension, sharp changes in irradiance, temperature and turbulent mixing causes sharp changes in phytoplankton concentration. In the horizontal dimension, phytoplankton concentrations exhibit more gradual changes, although phytoplankton fronts may occur in the horizontal dimension around obstructions such as islands.

Dynamics in the horizontal dimension are inextricably bound with dynamics in the vertical dimension, largely because of lake-wide convection cells operating in both dimensions. Horizontal distributions may be created by the interaction between the vertical distribution and hydrometry. For example, from an initial situation of horizontal homogeneity and vertical heterogeneity, a vertical dimension convection cell may cause horizontal heterogeneity at the surface. Lesser concentrations at greater depths in the vertically heterogeneous column may be upwelled to the surface reducing surface concentrations upwind, causing this surface heterogeneity. This situation occurs even if phytoplankton are acting as passive scalars of the velocity field (although the initial vertical heterogeneity still requires phytoplankton to have regulated their position within the water column).

9.6.2 Spatial and temporal dynamics

Lakes are truly dynamic environments. Spatial distributions are achieved in the temporal domain, and as a result there is a positive correlation between spatial and temporal scales. This is because the time required for a causative process, such as convection, to cause a micro-scale spatial change may be insufficient to cause a macro-scale spatial change.

Different processes may be responsible for different spatial dynamics of phytoplankton. For example, convection-induced trends may operate over short time scales and shorter distances while growth-induced trends may operate over greater time scales and greater distances. However, it is important not to over-simplify. Convection, for example, has an important role in producing macro-scale trends in large lakes such as Loch Ness.

9.6.3 Complexity and sensitivity

Spatial dynamics are complex. Interaction is the key element in determining the complexity of these dynamics, this interaction occurring between a large number of properties, many of which are affected by feedback mechanisms. These mechanisms generally served to regulate the system but may on occasion amplify change.

The sensitivity of spatial dynamics to causative processes was difficult to gauge in this thesis because all environmental and phytoplanktonic properties act concurrently. The analysis was made more complex because time lags of varying magnitude exist between forcing-functions and system responses depending upon the properties affecting the system. For example, the time lag between maximum solar elevation and maximum sub-surface irradiance is almost instantaneous, the time lag between maximum wind speed and maximum current speed may be greater than 30 minutes. Spatial distributions are, therefore, not just the result of forcing at the time at which they exist, but are dependent upon what has happened in the past. To interpret the effect of a property on spatial dynamics it is necessary to consider not just the property but also the response lag to this property.

This complexity and sensitivity makes analysis of lake systems more difficult because procedures used for one lake may not be entirely applicable for another lake.

For example, if the objective of the analysis is to characterise the hydrometry of a given lake, drogues that are solely influenced by surface flows should be used if the dominant return flow of the lake occurs at the surface, and more emphasis should be placed on drogues that are influenced by sub-surface flows if the dominant form of return flow of the lake occurs beneath the surface. Alternatively, if attempting to characterise the spatial variation of phytoplankton concentration using contact measurements, the sample size for a lake that is characterised by heterogeneity in phytoplankton concentration should be greater than that for a lake which is usually well-mixed (Appendix F).

9.7 Future Work

The approaches used in this thesis have partially achieved the objectives outlined in the introduction: that is, an understanding of how the interaction between lake environmental properties and phytoplanktonic properties cause the spatial dynamics of phytoplankton in lakes. However, the use of archived data (although necessary to enable the conclusions of this thesis to be generic) limited the quality of the analysis that could be performed. With data acquired specifically for the research intentions, the techniques used in this thesis may be further refined, and the techniques may then be applied to more robust investigation of the spatial dynamics of phytoplankton within lakes.

9.7.1 Refining the techniques

Specific techniques that need to be improved are the remote sensing, statistical modelling and process modelling of spatial dynamics.

i. Remote sensing of spatial dynamics

Most research on the remote sensing of lake water quality has focused on the detection of water quality properties (for example, how algorithms can be used with concurrent contact measurements to estimate absolute values for chlorophyll-*a* concentration within a given pixel). Very little research has focussed on how resolution affects the ability to look at spatial dynamics. Throughout this thesis, it has become apparent that, although remote sensing is an ideal technique for resolving

spatial distributions, analysis of spatial dynamics is made difficult because the temporal dimension is not fully covered at the spatial resolutions available.

Future research should explore this. In particular, research should focus upon the extent to which the positive correlation between spatial and temporal scales in lakes is matched by the relationships between spatial and temporal resolutions of remote sensing systems. There is often a trade-off between the spatial and temporal resolutions of remote sensing systems: many remote sensing systems with high repeat intervals have coarse spatial resolutions; other remote sensing systems with lower repeat intervals have higher spatial resolutions. For given dynamics, associated with scales ranging from Langmuir cells to basin-wide convection cells, optimal spatial and temporal resolutions, and therefore the appropriate sensors, need to be identified.

ii. Statistical modelling of spatial dynamics

Three main areas of statistical research should be conducted: firstly, a robust evaluation of the variogram and alternative techniques for summarising spatial distributions; secondly, the use of statistical modelling to establish relationships between spatial distributions and morphometry; and thirdly, the optimisation of sampling of lake water quality within spatial and temporal domains.

- ***Evaluation of the variogram for summarising spatial distributions***

  There has been little research applied to methods of quantifying spatial distributions within lakes. Variograms, as used in this thesis, provided a means of summarising scales of spatial variation through the use of several model coefficients. However, much of the information on variation within the remotely sensed images was lost through the representation of the variation by these coefficients. For example, in this study it was not possible to identify from a variogram the presence or absence of fronts, Langmuir cells or boat wakes. Future research is required to gauge the validity of the variogram as a means of summarising spatial distributions. This could be done by analysing the extent to which specific dynamic processes, such as dispersion from a stream entrance or shearing fronts, produce specific spatial distributions, and identifying whether the variogram can detect the differences between these distributions. A

comparison could be made with alternative methods for quantifying spatial variation, such as power spectral analysis and fractal analysis (Bradbury *et al.*, 1984; Bunimovich *et al.*, 1993).

- ***Statistical relationships for the Scottish lakes***

  Research is recommended to develop statistical techniques to establish relationships for a large number of Scottish lakes. These are of the scale where satellite imagery can be used to determine spatial distributions concurrently within all the lakes. Additionally, because these lakes often have persistent spatial distributions, remotely sensed snapshots will be more representative of longer-term spatial distributions. This work should also involve an exploration of morphometric parameters that may be more representative of the diverse morphometries involved, because the morphometric parameters used in this thesis had limited abilities for describing lake shape.

- ***Optimising sampling strategies***

  Optimising sampling is important because comprehensive coverage from remote sensing is often unavailable. Through the use of systematic sampling and geostatistics the intention is to produce sampling strategies where the regional mean and variance in water quality can be estimated with minimum effort and minimum error. In this study, emphasis has been on optimising in the spatial domain (Appendix F). However, considering the temporally dynamic nature of the environment, it may be possible to produce sampling strategies that not only minimise the number of observations on a single occasion, but also minimise the number of observations required over a period of time to enable monitoring of water quality to occur. This can be achieved by making the sampling strategy dependent upon the temporal scale of the variation in addition to the spatial scale.

iii. Process modelling of spatial dynamics

One of the difficulties involved in analysing relationships was that archived data were used throughout this thesis to determine lake environmental properties. Simulations, therefore, only approximated the spatial dynamics of phytoplankton, so

only a fairly simple analysis of the spatial dynamics of phytoplankton dynamics within lakes was possible. With more accurate and precise measurements it should be possible to explore more rigorously the system characteristics. This should involve on-site measurements of wind and irradiance properties. Phytoplankton spatial distributions with which to initiate the model should be determined through remote sensing, and through contact measurement. Buoys and drogues should be used in verification of the lake hydrometries.

9.7.2 Spatial dynamics

Specific areas of spatial dynamics that need to be analysed are the inter-relationship between spatial and temporal dimensions, and the spatial dynamics of large lakes.

i. Inter-relationship between temporal and spatial dimensions

There has been very little research in the last decade where remote sensing has been used to monitor lake water quality over a sustained time period. There is considerable scope for further remote sensing work because of the errors associated with surface sampling. This may be achieved at two scales. Firstly, using airborne imagery, spatial dynamics at relatively small scales may be analysed over a period of several days. Secondly, using satellite imagery, spatial dynamics at larger scales may be analysed over a period of several months to several years.

ii. Spatial dynamics of large lakes

Certain macro-scale processes are only evident in lakes larger than those that have been investigated in this thesis. These include persistent thermal bars, gyres, and persistent currents parallel to the shore. In this thesis, the scale of the data provided by the airborne imagery and the optimum scale at which the CFD model operated were incompatible with the analysis of the spatial dynamics of large lakes. Future research could investigate spatial dynamics in large lakes using coarser scale satellite data, which may be of a compatible scale to those of the spatial dynamics of large lakes.

9.8 Implications for water management

This thesis has direct implications for the management of phytoplankton populations

within lakes. Monitoring has a role in informing management strategies, and it is here where the conclusions of this thesis may contribute. Firstly, it has been shown that it is necessary to obtain the right type of data: that is, contiguous, comprehensive data in, both, spatial (in the vertical and horizontal) and temporal domains. Secondly, it has been shown that it is necessary to focus upon the right characteristics for management: that is, characteristics that are specific to the lake being managed, because different lakes have different dominant characteristics that determine the spatial dynamics of phytoplankton within them.

In regards to characterising the spatial dynamics of phytoplankton, this thesis has focussed on the spatial dimension, but the importance of the temporal dimension has also been shown in relation to growth rates in the exploratory analysis (Section 5) and in relation to short-term wind-forced gradients in the modelling of both real lakes (Section 7) and hypothetical situations (Section 8). For obtaining such data, the main sources may be via contact sampling or remote sensing. When conducting contact sampling, it is necessary to sample spatially, with the sampling regime dependent upon parameters of the lake under consideration. Spatial variation in both vertical and horizontal dimensions should be resolved. It is also necessary to configure sampling within the temporal dimension to the lake under consideration: for example, it may be necessary to vary the sampling regime according to changing wind conditions. Remote sensing may play an effective part in managing lakes because it may provide contiguous, spatially comprehensive data. If remote sensing is used, it is necessary to ensure a high repeat interval and favourable atmospheric conditions. With remote sensing, contact sampling is still necessary at present to quantify the dominant phytoplankton types and resolve velocity field properties.

For the optimal management of lakes, it is necessary to focus on the characteristics of the lakes under consideration. It has been shown throughout this thesis that a wide variety of different factors cause the spatial dynamics of phytoplankton. These have been seen to include wind environments, irradiance, phytoplanktonic characteristics and morphometry. It may, therefore, be possible to identify key parameters for given lakes (wind-induced mixing may be the dominant factor in certain lakes; in other lakes, phytoplankton types may be more important) and these should be the focus of lake management schemes.

Appendices:

Appendix A: Notation

To retain conventional usage of the notation, some duplication has occurred.

A_L	area of lake
a_1	maximum scale at which data are a spatially dependent
c_0	non-spatially dependent semivariance
c_1	spatially dependent semivariance
c_1	rate of constant density increase
c_2	rate of constant density decrease
c_3	minimal rate of density decrease
c_μ	constant of k-ε model
c	phytoplankton concentration
C_D	friction coefficient
C	Coriolis parameter
d	horizontal diffusivity
D_*	depth of frictional resistance
D_E	lake effective depth
D_L	lake depth
E_L	Elongation
F	flux
F	fetch
g	gravitational attraction
h	lag
i	space dimension
j	space dimension
I_0	sub-surface irradiance at depth of 0 m
I_{opt}	optimum irradiance
I_p	average irradiance experienced in previous day
I_{ran}	irradiance range parameter
I_z	irradiance at depth z

k turbulent kinetic energy

k net rate of increase of population

k' exponential specific growth rate

k_{max} maximum specific growth rate

k_{20} growth rate at 20°C

k_i irradiance specific growth rate

k_n nutrient specific growth rate

K damping coefficient

K_i half saturation growth coefficient given no nutrient limitation

K_h coefficient of eddy viscosity in the horizontal dimension

K_n half saturation growth coefficient given no irradiance limitation

K_v coefficient of eddy viscosity in the vertical dimension

L' characteristic length scale

m mass

$m(\mathbf{h})$ number of pairs of observations

n nutrient concentration

n_w refractive index of water

n_a refractive index of air.

P pressure

r colony radius

r_c critical patch size

r_p roughness coefficient

R reflection coefficient

R_e Reynolds Number

t time

T_s wave period

u fluctuating velocity caused by turbulence

u_* wind-induced friction velocity

U average velocity between surface and depth z

U_i Reynolds averaged velocity

U_s surface current velocity

U_z velocity at depth z

ν_k	kinematic viscosity
ν_T	turbulent eddy viscosity
w	phytoplankton rising velocity
w_{max}	maximum dinoflagellate swimming velocity
W	wind speed
z	depth
$z(\mathbf{x}_i)$	observed value at sampling point $\mathbf{x}_i$
Z_{eu}	depth of the euphotic zone
δ	Kroneker delta term
ε	rate of dissipation of turbulent kinetic energy
ε	vertical extinction coefficient
ε_{min}	minimum vertical extinction coefficient
ϕ	latitude
γ	semivariance
φ	form resistance
λ_s	length of surface waves
η	water viscosity
Γ	turbulent mixing coefficient
σ_{bed}	bed shear stress
$\sigma_{critical}$	critical bed shear stress
θ	temperature-dependent growth coefficient
θ_a	zenith angle of the incident light in the air
θ_w	zenith angle of the light in the water
ρ_a	air density
ρ_c	phytoplankton density
ρ_w	water density
τ_s	wind shear stress
Ω	angular velocity of Earth

Appendix B: Maps of lakes

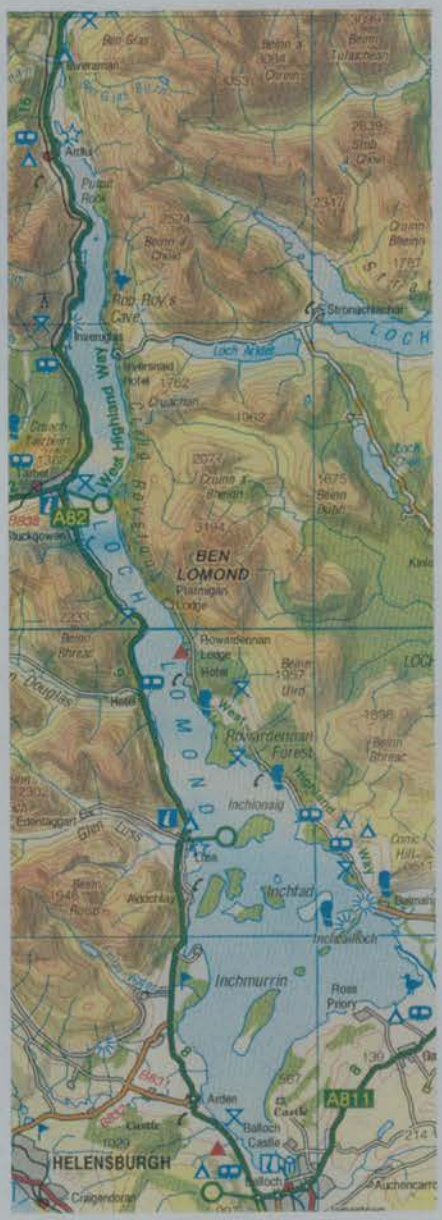

Figure B-1. Map of Loch Lomond (1:250,000).

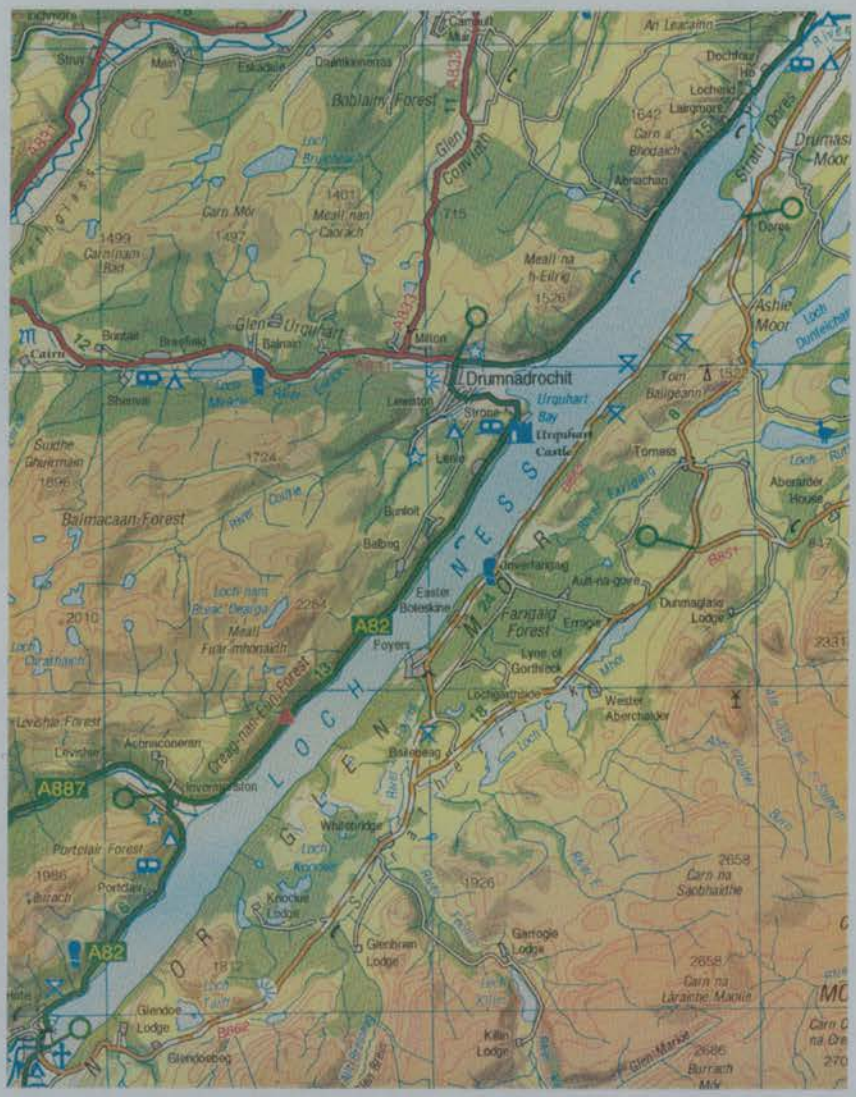

Figure B-2. Map of Loch Ness (1:250,000).

Figure B-3. Map of Loch Awe (1:250,000).

Figure B-4. Map of Loch Leven (1:250,000).

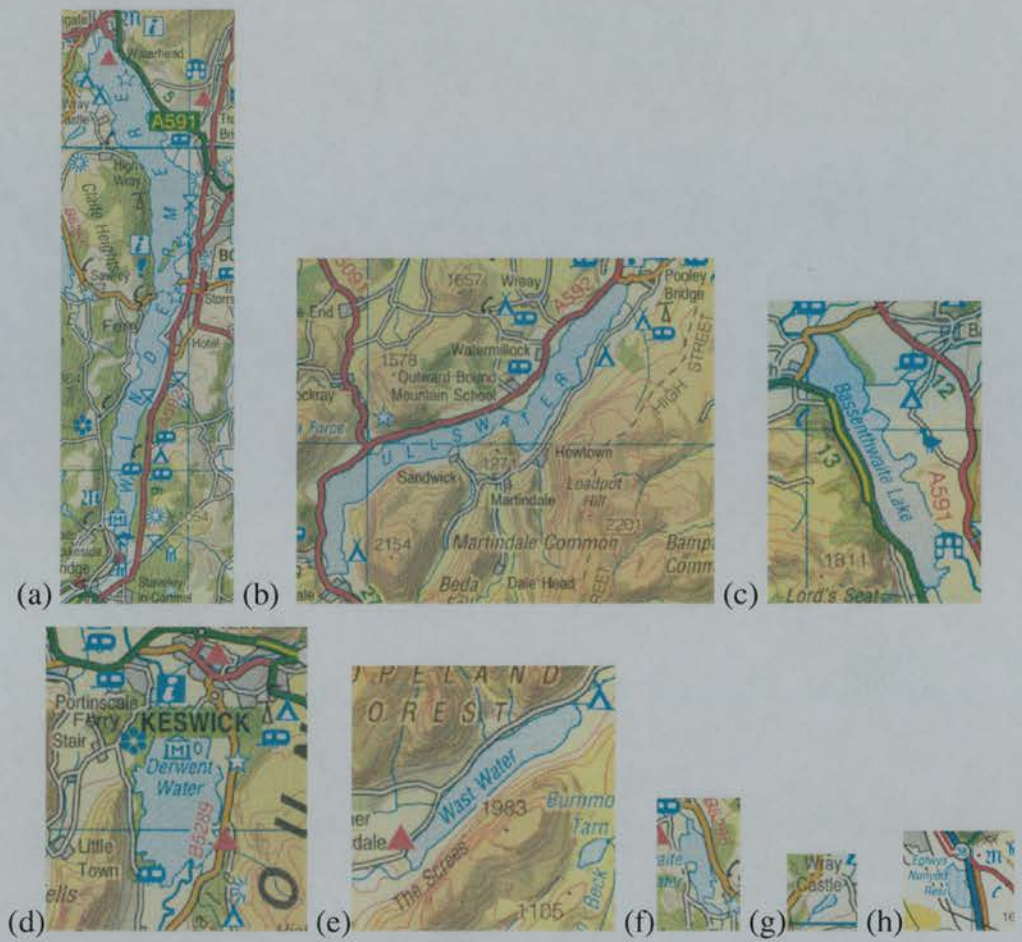

Figure B-5. Maps of the English lakes (1:250,000): (a) Lake Windermere; (b) Ullswater Lake; (c) Bassenthwaite Lake; (d) Derwent Water; (e) Wast Water; (f) Esthwaite Water; (g) Blelham Tarn; (h) Eglwys Nynydd.

Figure B-6. Map of Loosdrecht and Northern Vecht lakes (1:250,000).

Appendix C: Sensor characteristics

C1: NERC Daedalus AADS Airborne Thematic Mapper (ATM)

The ATM uses a rotating scan mirror to direct electromagnetic radiation onto a spectrometer. This uses a combination of filters and detectors to measure radiance in 11 wavebands at various wavelength ranges from 420 to 13,000 nm (Table C-1). Wavelength ranges of each waveband vary from approximately 30 nm to approximately 4500 nm.

Table C-1. ATM bandset.

Waveband	Shortest wavelength (nm)	Longest wavelength (nm)	Bandwidth (nm)
1	420	450	30
2	450	520	70
3	520	600	80
4	605	625	20
5	630	690	60
6	695	750	55
7	760	900	140
8	910	1050	140
9	1550	1750	200
10	2080	2350	270
11	8500	13000	4500

Source: Wilson (1986)

Images are 10-bit (1024 DN range). Distortion correction mechanisms within the ATM partially correct for pixel compression at the end of the swath, and for an aircraft roll distortion of +/- 15°. The Instantaneous Field of View (IFOV) is 2.5 mrad. Thus for an altitude of 1000 m there would be a nominal ground spatial resolution of 2.5 m (Malthus *et al.*, 1986).

C2: NERC Compact Airborne Spectrographic Imager (CASI)

The CASI uses a pushbroom spectrometer to measure electromagnetic radiation. The spectrometer has 512 spatial pixels and 288 spectral channels. The CASI can operate in one of three modes: spatial mode, spectral model and enhanced spectral mode. In the spatial mode, a spatially contiguous image can be acquire with a swath width of 512 pixel in up to 14 channels. Channels are determined by the user. The

bandset used in this thesis is shown in Table C-2 and Table C-3.

Table C-2. CASI bandset used in remote sensing of the English Lake District Lake (Default SeaWIFS / Ocean colour bandset)

Waveband	Shortest wavelength (nm)	Longest wavelength (nm)	Bandwidth (nm)
1	402	422	20
2	432	453	21
3	480	499	19
4	501	519	18
5	545	565	20
6	610	629	19
7	660	679	19
8	681	685	4
9	705	715	10
10	744	759	15
11	760	764	4
12	766	784	24
13	815	824	9
14	845	884	39

Source: Wilson (1986)

Table C-3. CASI bandset used in remote sensing of the Loosdrecht and Northern Vecht lakes.

Waveband	Shortest wavelength (nm)	Longest wavelength (nm)	Width (nm)
1	430	450	20
2	509	531	22
3	553	577	24
4	591	611	20
5	625	642	17
6	644	652	8
7	660	668	8
8	675	686	11
9	702	713	11
10	780	803	23

Source: Wilson (1986)

In the spectral mode, all 288 channels can be used, but only in a limited number of look directions or pixel positions (a maximum of 39). In the enhanced spatial mode, a three-dimensional data cube is produced of 101 adjacent pixel for all the 288 channels.

Images are 16-bit (65536 DN range). Distortion correction and spatial resolution are similar to the ATM.

Appendix D: Estimation of sub-surface irradiance

i. Above-surface irradiance

Above surface irradiance was estimated as follows:

- ***Irradiance after atmospheric effects***

  Irradiance at a zenith angle of zero was estimated as the product of the solar constant (6200 μE m^{-2}), the mean proportion of irradiance penetrating atmosphere (0.66) and the mean proportion of irradiance that is photosynthetically active, PAR (0.47). In the presence of cloud a further reduction was necessary.

- ***Irradiance as a function of time and latitude***

  Irradiance as a function of time was estimated as the product of the sine of the solar elevation (one minus the zenith angle) and the irradiance at a zenith angle of zero. Solar elevation was estimated from the time of year and the latitude (Spencer, 1971).

ii. Sub-surface irradiance

Sub-surface irradiance was estimated as the product of above surface irradiance and unity minus the reflectance coefficient. Reflectance (r) was estimated from Fresnel's Equation.

$$R = \frac{1}{2}\frac{\sin^2(\theta_a - \theta_w)}{\sin^2(\theta_a + \theta_w)} + \frac{1}{2}\frac{\tan^2(\theta_a - \theta_w)}{\tan^2(\theta_a + \theta_w)}$$

where θ_a is the zenith angle of the incident light in the air and θ_w is the zenith angle of the light in the water. The change in angle was determined by Snell's law.

$$\frac{\sin\theta_a}{\sin\theta_w} = \frac{n_w}{n_a}$$

where n_w is the refractive index of water and n_a is the refractive index of air.

Appendix E: Weather stations

E.1: Sources of ground station data

Table E-1. Weather stations.

Lake	Weather Station	O.S. BNG. Co-ordinates	Geographical co-ordinates	Data frequency
Loch Lomond	Blairlinnans	230,688 (NS 302882)		Hourly
Loch Ness	Dunstaffnage	188,734 (NM 881340)		Hourly
	Tain	278,882 (NM 881340)		Hourly
	Kinloss	306,862 (NJ 067627)		Hourly
Loch Awe	Dunstaffnage	188,734 (NM 881340)		Hourly
Loch Leven	Edinburgh Turnhouse	315,673 (NT159739)		Hourly
Ullswater	Newton Rigg	349,530 (NY 493308)		Daily
Bassenthwaite Rydal Esthwaite Water Blelham Tarn	Ambleside	337,504 (NY 372040)		Daily
Esthwaite Water	Haws Wood	338,490 (NY 385905)		Hourly
Loosdrecht and Northern Vecht lakes	Schiphol Airport		52°55' N 4° 90' E	Hourly

E.2: Wind speed and direction for lakes used in exploratory analysis

Table E-2. Wind data for Loch Lomond (29 May 1985).

Loch Lomond 29 May 1985		
Time (Hrs)	Blairlinnans	
	Direction	Wind speed
00:00	230	2.6
01:00	250	1.0
02:00	230	1.5
03:00	0	1.0
04:00	210	1.0
05:00	210	1.0
06:00	260	1.0
07:00	170	1.0
08:00	250	3.6
09:00	250	4.6
10:00	250	4.6
11:00	230	4.6
12:00	240	5.7

Table E-3. Wind data for Loch Ness (3 June 1985).

Loch Ness 3 June 1997						
Time (Hrs)	Weather Station					
	Kinloss		Tain		Dunstaffnage	
	Direction	Wind speed	Direction	Wind speed	Direction	Wind speed
00:00	70	4.1	10	4.1	20	1.03
01:00	70	3.6	20	4.1	300	1.03
02:00	60	3.6	350	3.1	210	1.03
03:00	60	3.1	350	3.6	210	1.03
04:00	70	2.1	340	2.6	200	1.03
05:00	70	2.6	330	3.1	200	1.03
06:00	60	2.6	330	3.1	310	1.03
07:00	60	2.1	350	2.6	310	1.03
08:00	60	2.1	50	2.1	300	1.03
09:00	70	3.1	90	3.1	300	1.03
10:00	80	3.1	110	3.1	320	2.575
11:00	80	4.1	110	3.1	10	3.09
12:00	60	4.6	120	3.6	330	2.575

Table E-4. Wind data for Loch Awe (23 May 1997).

Loch Awe (23 May 1997)				
Time (Hrs)	Weather station			
	Blairlinnans		Dunstaffnage	
	Direction	Wind speed	Direction	Wind speed
00:00	70	1.5	100	1.0
01:00	110	2.1	140	1.0
02:00	70	2.1	140	2.6
03:00	60	1.5	70	2.6
04:00	90	1.5	120	1.0
05:00	100	1.0	70	1.0
06:00	80	2.1	30	1.0
07:00	90	3.6	30	1.0
08:00	110	3.1	20	1.0
09:00	100	3.1	320	1.0
10:00	90	3.1	320	3.1
11:00	120	3.1	300	3.6
12:00	100	2.6	310	3.1

Table E-5. Wind data for Ullswater (24 May 1994 – 30 May 1994, 7 July 1994 – 13 July 1994, 29 June 1995 – 26 June 1995).

Ullswater		
Date	Newton Rigg	
	Direction	Wind speed
24-May-94	110	1.0
25-May-94	70	1.0
26-May-94	70	9.8
27-May-94	320	1.0
28-May-94	160	2.6
29-May-94	90	2.6
30-May-94	250	4.6
07-Jul-94	320	1.0
08-Jul-94	180	1.0
09-Jul-94	180	1.0
10-Jul-94	180	9.8
11-Jul-94	160	2.6
12-Jul-94	0	0.0
13-Jul-94	360	2.6
20-Jun-95	270	4.6
21-Jun-95	270	4.6
22-Jun-95	360	1.0
23-Jun-95	360	1.0
24-Jun-95	320	1.0
25-Jun-95	320	1.0
26-Jun-95	320	1.0

Table E-6. Wind data for Bassenthwaite, Derwent Water and Wast Water (9 June 1995 – 15 June 1995).

Bassenthwaite, Derwent Water, Wast Water		
Date	Ambleside	
	Direction	Wind speed
09-Jun-95	320	9.5
10-Jun-95	360	4.7
11-Jun-95	320	7.7
12-Jun-95	360	6.1
13-Jun-95	360	6.1
14-Jun-95	360	11.3
15-Jun-95	360	4.7

Table E-7. Wind data for the Loosdrecht and Northern Vecht Lakes (16 August 1992 to 18 August 1992).

Loosdrecht lakes						
Hrs	Schiphol Airport					
	Date					
	16-Aug		17-Aug		18-Aug	
	Direction	Wind speed	Direction	Wind speed	Direction	Wind speed
00:00	170	6.0	190	3.0	180	2.0
01:00	170	5.0	230	3.0	200	2.0
02:00	180	5.0	220	3.0	170	1.0
03:00	170	5.0		2.0		1.0
04:00	180	5.0	200	2.0	130	1.0
05:00	170	5.0	200	3.0	80	1.0
06:00	180	5.0	220	4.0		1.0
07:00	190	6.0	210	5.0	110	2.0
08:00	180	5.0	220	5.0	120	3.0
09:00	170	6.0	260	7.0	110	4.0
10:00	190	6.0	250	9.0	120	3.0
11:00	200	6.0	250	9.0	120	3.0
12:00	200	7.0	260	9.0	120	3.0
13:00	210	6.0	250	8.0		
14:00	230	5.0	250	9.0		
15:00	190	5.0	240	8.0		
16:00	220	5.0	230	8.0		
17:00	240	5.0	240	7.0		
18:00	180	5.0	230	6.0		
19:00	200	4.0	230	4.0		
20:00	210	4.0	210	4.0		
21:00	220	4.0	210	3.0		
22:00	200	4.0	210	3.0		
23:00	230	3.0	190	2.0		

E.3: Wind speed and direction for data used in process modelling.

Table E-8. Wind data for Loch Leven (9 May 1985 – 11 May 1985).

Loch Leven (9-11 May 1985)						
Hrs	Edinburgh Turnhouse					
	Date					
	09-May		10-May		11-May	
	Direction	Wind speed	Direction	Wind speed	Direction	Wind speed
00:00	60	1.5	120	1.0	90	2.6
01:00	100	1.0	290	1.0	100	2.1
02:00	210	1.0	280	1.0	90	2.6
03:00	160	1.0	300	1.0	90	1.5
04:00	50	1.0	300	1.0	80	1.0
05:00	30	1.0	340	1.0	90	2.1
06:00	40	1.0	360	1.5	90	2.6
07:00	360	1.0	350	1.0	90	3.6
08:00	40	1.0	350	2.1	70	4.1
09:00	60	1.0	30	2.6	70	4.1
10:00	250	1.0	60	2.1	80	3.6
11:00	230	1.0	80	4.1	60	3.6
12:00	240	2.1	80	4.1	40	3.6
13:00	230	2.6	80	3.6		
14:00	250	1.5	80	4.1		
15:00	50	1.0	100	4.1		
16:00	60	2.1	90	4.1		
17:00	50	1.0	90	4.6		
18:00	90	1.0	90	4.6		
19:00	60	1.0	90	5.7		
20:00	20	1.0	90	4.6		
21:00	40	1.0	90	4.6		
22:00	120	1.0	80	4.1		
23:00	140	1.0	80	3.6		

Table E-9. Wind data for Eglwys Nynydd.

Eglwys Nynydd				
Hrs	On-site			
	Date			
	Quiescent		Turbulent	
	Direction	Wind speed	Direction	Wind speed
01:00	170	0.1	300	0.5
02:00	170	0.1	310	0.4
03:00	160	0.1	310	0.5
04:00	180	0.1	310	0.4
05:00	180	0.1	310	0.1
06:00	180	0.2	305	0.1
07:00	180	0.1	330	0.3
08:00	180	0.2	320	0.4
09:00	180	0.2	330	0.5
10:00	170	0.3	340	0.5
11:00	180	0.4	360	0.5
12:00	190	0.3	10	0.5

Table E-10. Wind data for Esthwaite Water (2 August 1973 and 9 August 1973).

Esthwaite Water				
Hrs	Haws Wood			
	Date			
	2 August 1973		9 August 1973	
	Direction	Wind speed	Direction	Wind speed
00:00	Calm	0	210	3
01:00	Calm	0	200	4
02:00	Calm	0	190	2
03:00	Calm	0	200	2
04:00	170	1	180	3
05:00	190	2	180	2
06:00	210	3	180	1
07:00	190	3	180	4
08:00	190	2	180	6
09:00	200	2	180	7
10:00	200	2	190	7
11:00	210	3	190	8
12:00	200	2	190	6
13:00	190	3	190	4

Appendix F: Optimal sampling

INTRODUCTION

The simplest possible sampling strategy for estimating water quality properties of a specific lake, such as the mean chlorophyll-*a* concentration, involves a single observation within the lake. For example, Bondarenko *et al.* (1996) described how most studies of Lake Baikal were based around samples of a single observation. The drawback of using a single observation is that it is unlikely to be representative of the lake as a whole, and generally, lake sampling involves many observations in an attempt to characterise the variation that occurs (Hedger *et al.*, 1996). Thus, transect samples often have been implemented (George and Heaney, 1978; George, 1981b; Jones *et al.*, 1995). Some authors have been able to link sample size requirements to the characteristics of specific lakes. Patalas and Salki (1993), for example, showed that it was necessary to increase sample size with an increase in lake size to produce an estimate that was representative of the population. George (1981a) suggested that where it was possible to distinguish between persistent variation and transient variation, it may be possible to adjust sampling so as to minimise bias. Few authors, however, have quantified statistically the relationships between the sample size, the spatial distribution of the water quality property under investigation, and the error associated with estimation. Fewer still, have used the more advanced statistical techniques that are available, such as those of geostatistics (a notable exception being that of Simmard *et al.,* 1992).

With geostatistics, instead of basing the sampling strategy on the dispersion variance of the entire sample, the sampling strategy is based upon local variance as a function of distance and direction of separation. Key to this is the concept of spatial dependence, in which values at positions near to one another are more likely to be similar (and generally have less variance) than values at distances further apart from one another (Matheron, 1971).

This section explores the design of sampling strategies with reference to spatial distributions of chlorophyll in two Scottish Lakes (Loch Awe and Loch Ness). The

first objective is to show that it is necessary to sample lakes spatially with sampling intervals dependent upon the spatial variation in water quality. The second objective is to show that, because this spatial variation is specific to lake properties (such as morphometry or wind regime), different sampling regimes will be required for different lakes and for different times if the intention is to monitor lake water quality with acceptable accuracy. That is, it will be necessary to take into account the full dynamic nature of the environment. The third objective is to show that a geostatistical approach will lead to more accurate estimates than the classical approach that is commonly implemented.

STATISTICAL BACKGROUND

In the absence of remotely sensed data, the mean population value of a given water quality property for the whole lake, or the *regional mean,* is generally estimated from a small number of lake observations due to cost considerations. The sample mean tends to differ from the population mean as a consequence of spatial variation. In particular, the form of variation in lake water quality determines how representative individual observations are of the population mean. To determine how much confidence may be placed in the estimate of the population mean it is necessary to quantify the s*tandard error of the estimate* (the square root of the variance of the estimates around the true mean). Two main approaches may be used: a *classical* approach and a *geostatistical* approach.

In the classical approach, the regional mean is estimated as follows:

$$\hat{z}(\mathbf{B}) = \frac{\sum_{i=1}^{n} z(\mathbf{x}_i)}{n} \qquad \text{(F-1)}$$

where $z(\mathbf{B})$ is the estimated mean over area $|\mathbf{B}|$, and $z(\mathbf{x}_i)$ are the values of variable Z at each observation $\mathbf{x}_i$, for $i = 1$ to n. The standard error of the estimate is calculated as follows:

$$S_{\varepsilon} = \sqrt{\frac{\left(\sum_{i=1}^{n} z(\mathbf{x}_i)^2 - \hat{z}(\mathbf{B})\right)}{n}} \qquad \text{(F-2)}$$

where S_{ε} is the standard error of the estimate. From Equation F-2 it is clear that the standard error varies as the inverse of the sample size, the limit being where the total population is sampled and the standard error is zero.

The main disadvantage of a classical sampling approach is that it ignores spatial dependence. If spatial dependence exists, random sampling may lead to data redundancy. The geostatistical approach, in contrast, exploits the spatial dependence or spatial structure between observations. Estimation of the regional mean is performed using a technique referred to as Kriging, which involves a weighted average of the observations:

$$\hat{z}(\mathbf{B}) = \sum_{i=1}^{n} \lambda_i z(\mathbf{x}_i) \qquad \text{(F-3)}$$

where z($\mathbf{B}$) is the estimated value for area $|\mathbf{B}|$, and λ_i are the weights. The weights are chosen to ensure unbiasedness (the weights sum to one) and to minimise the standard error of the estimate, and are calculated as follows:

$$\sum_{i=1}^{n} \lambda_i \gamma(\mathbf{x}_i, \mathbf{x}_j) + \psi = \bar{\gamma}(\mathbf{x}_i, \mathbf{B}) \text{ for all } j \qquad \text{(F-4)}$$

where $\gamma(\mathbf{x}_i,\mathbf{x}_j)$ is the semivariance between the ith and jth observations, $\gamma(\mathbf{x}_i,\mathbf{B})$ is the integral semivariance between the ith observation and area $|\mathbf{B}|$, and ψ is the Lagrange multiplier. Sampling may occur on different grid configurations: a triangular grid is preferable in that there is an equal distance between observations, and redundancy is minimised, but a square grid is often used as it is more efficient computationally. The standard error of the estimate is estimated as follows:

$$\hat{\sigma} = \sum_{j=1}^{n} \lambda_i \bar{\gamma}(\mathbf{x}_i, \mathbf{B}) + \psi - \bar{\gamma}(\mathbf{B}, \mathbf{B}) \qquad \text{(F-5)}$$

where, $\gamma(\mathbf{x}_I, \mathbf{B})$ is the semivariance between point $\mathbf{x}_i$ and area $|\mathbf{B}|$ and $\gamma(\mathbf{B},\mathbf{B})$ is the

average semivariance within area $|\mathbf{B}|$, the within-block variance. The semivariances are obtained from the variogram (Equation 2-18).

The procedures commonly used to estimate the standard error by both classical and geostatistical means are shown in Figure F-1.

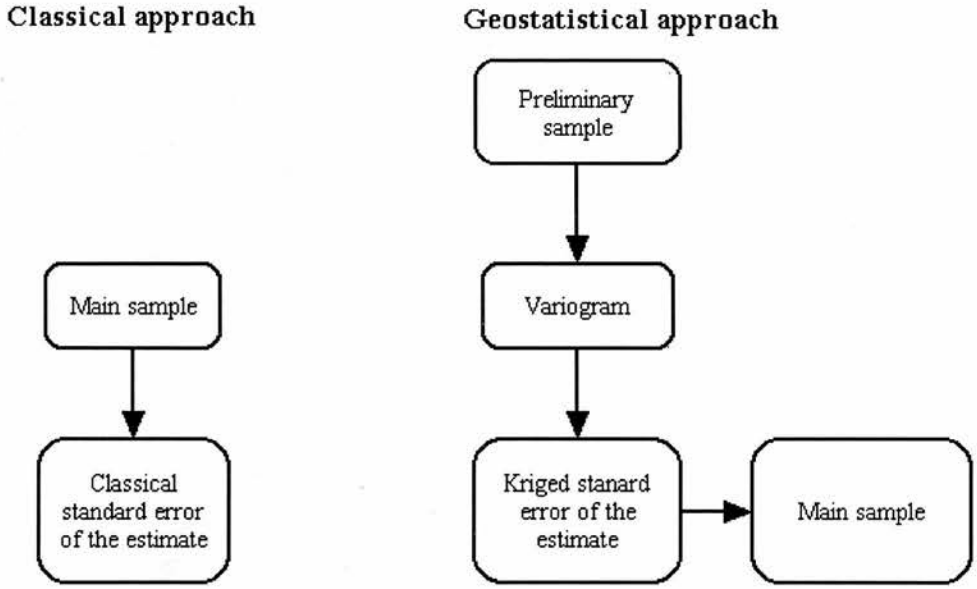

Figure F-1. Procedures used in classical sampling and geostatistical sampling.

DATA AND INITIAL PROCESSING

Two lakes in the United Kingdom were investigated in this study: Loch Ness (Section 5.3.1.1) and Loch Awe (Section 5.3.1.2). Spatial distributions of surface chlorophyll were determined from Airborne Thematic Mapper (ATM) images. Remote sensing was chosen as the ideal technique for determining spatial distributions because it enabled comprehensive coverage of the whole of each lake, which would not have been possible through surface sampling. The rôle of remote sensing was to provide the preliminary sample data, from which the sample variogram was estimated, to be used subsequently in Kriging (Equation F-3).

Loch Awe was imaged on 23 May 1997 and 29 May 1997, while Loch Ness was imaged on 24 May 1997 and 3 June 1997. Ground reference data were not available so a simple waveband ratio exploiting reflectance maxima (Channel 3) and minima (Channel 2) was used to produce a chlorophyll index. The index was multiplied by

one hundred to reduce floating-point errors when estimating variograms.

It is worth stating here that, even with remote sensing, lake contact measurements are required because the spatial distribution of a given chlorophyll index is likely to differ from the spatial distribution of chlorophyll-*a*. For example, variation in the vertical structure of near surface chlorophyll-*a* concentration may cause variation in the chlorophyll index that may not be correlated with variation in surface chlorophyll concentration. Remotely sensed spatial distributions are used here merely to aid in illustrating the points of this section: (i) that it is necessary to sample spatially; (ii) that the sample size must be chosen in relation to the variation in water quality (as caused by boundary conditions such as morphometry and wind environment); and (iii) that the sampling regime may be optimised through the use of geostatistics provided that the water quality property is spatially dependent.

ANALYSIS AND RESULTS

1. Variance and variograms

Loch Awe showed much greater variance than Loch Ness on all dates (Table F:1).

Table F-1: Mean and variance of the chlorophyll indices of Loch Awe (23 May 1997 and 29 May 1997) and Loch Ness (24 May 1994 and 3 June 1997).

Lake	Mean	Variance
Loch Awe (23 May 1997)	75.73	33.15
Loch Ness (29 May 1997)	84.59	35.37
Loch Ness (24 May 1997)	72.90	3.36
Loch Ness (3 June 1997)	75.41	9.39

The sample variograms for all the lakes (Figure F-2) were fitted well in a weighted least squares sense by a linear combination of the CNSD exponential and linear models together with a nugget component (McBratney and Webster, 1986):

$$\gamma(\mathbf{h}) = c_0 + c_1\left(1 - \exp\left(\frac{-\mathbf{h}}{a_1}\right)\right) + c_2\mathbf{h} \qquad \text{(F-7)}$$

where $\gamma(\mathbf{h})$ is the semivariance at lag $\mathbf{h}$, c_0 is the spatially independent variance, c_1 is

the spatially dependent variance of the exponential term, a_1 is the non-linear parameter, m is the gradient of the linear term (Oliver and Webster, 1991). Variograms of the two lakes were greatly different (Figure F-2 and Table F-2).

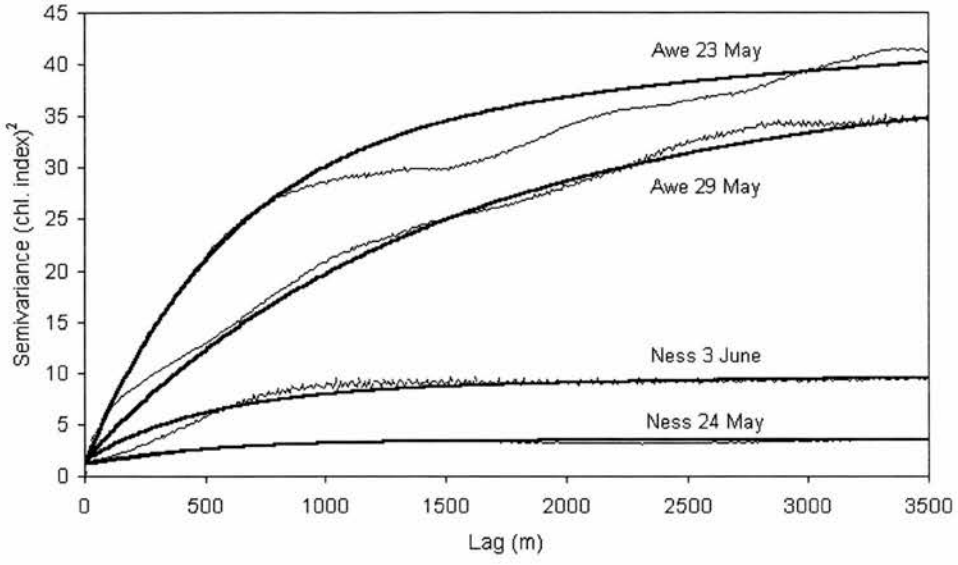

Figure F-2. Omnidirectional variogram of chlorophyll indices of Loch Awe (23 May 1997 and 29 May 1997) and Loch Ness (24 May 1994 and 3 June 1997). Thin lines are semivariograms, thick lines are variogram functions.

Table F-2: Coefficients of the variograms of chlorophyll indices of Loch Awe (23 May 1997 and 29 May 1997) and Loch Ness (24 May 1994 and 3 June 1997).

Lake	Model	c_0 (Chl. index)	c_1 Chl. index)	a_1(m)	m_2 (Chl index)
Loch Awe (23 May 1997)	Exponential	1	31	1200	
Loch Awe (29 May 1997)	Exponential + linear	1.5	32.5	1300	3.0 E-05
Loch Ness (24 May 1997)	Exponential	1.1	2.4	500	
Loch Ness (3 June 1997)	Exponential + linear	1.5	7.1	500	5.0 E-05

For Loch Awe, the a_1 coefficient of the exponential model ranged between 1200 and 1300 m; whereas for Loch Ness, the a_1 coefficient of the exponential model was much less (500 m). Likewise the sill variance of Loch Awe was much greater (approximately 30 chl. index^2) than Loch Ness (approximately 10 chl. index^2). The variograms for each lake also varied between each date, but to a lesser extent. The variogram for Loch Awe on 23 May 1997 had a slightly smaller sill than that on 29

May 1997, and did not have a linear model component. The variogram for Loch Ness on 24 May 1997 had a sill that was less than half that on 3 June 1997, and did not have a linear component.

2. Evaluating the effect of sampling strategy

In all cases, whether using a classical or geostatistical sampling scheme, an increase in sample size (through a decrease in the mean sample interval) resulted in a decrease in the standard error of the estimate (Figure F-3). Two additional features in Figure F-3 can be identified. Firstly, for a given sample interval, the greater the variance in the data, the greater the standard error of the estimate. For example, Loch Awe produced greater standard errors than Loch Ness. This suggests that for long-term monitoring, a sample of greater spatial density would be required in Loch Awe than Loch Ness to achieve the same accuracy (although, it would be preferable to have several additional images to verify this). Secondly, for a given sample size, the standard error in each lake varied between the dates. This shows the response of spatial distributions of chlorophyll to processes occurring within the temporal domain. When conducting long-term monitoring, it may be necessary to change sample regimes temporally in response to, for example, changes in wind regime.

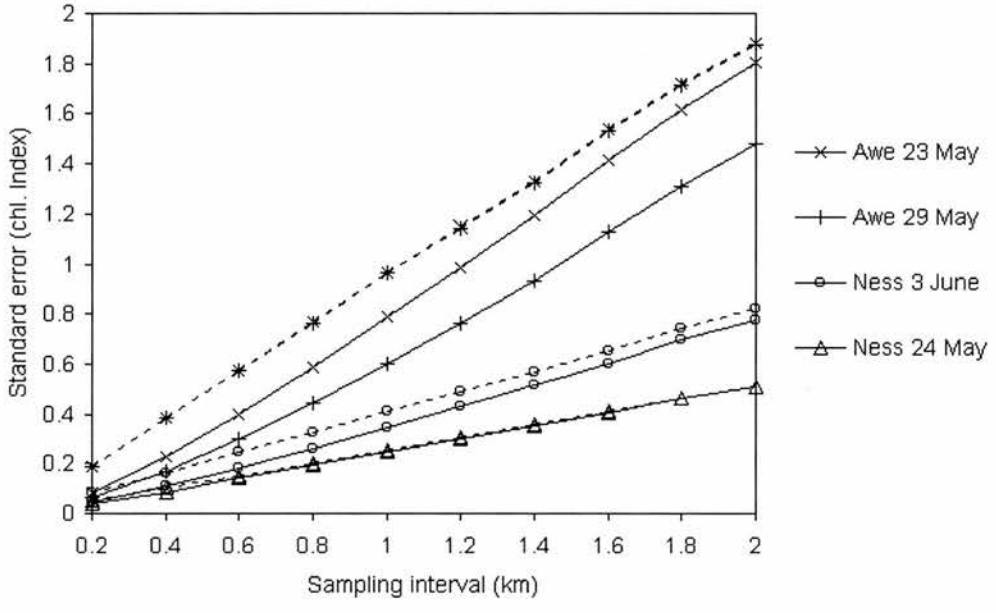

Figure F-3. Standard errors as a function of sample interval for Loch Awe (23 May 1997 and 29 May 1997) and Loch Ness (24 May 1997 and 3 June 1997). Dashed lines are classical standard errors, solid lines are geostatistical standard errors.

For every sample interval, the geostatistical standard error was less than the classical standard error (Figure F-3). These results were in agreement with past literature (e.g., Webster *et al.,* 1989, Atkinson, 1991). Use of geostatistics, therefore, always resulted in greater precision, but the relative merits of the geostatistical and classical approach depended on the sample interval and the relative proportion of spatially dependent variation in the data. This may be seen more clearly in Figure F-4, where the geostatistical standard errors are expressed as a percentage of the classical standard errors and plotted against sample interval. Firstly, the merit of the geostatistical approach increased with a increase in sampling interval. Secondly, the merit of the geostatistical approach increased with an increase in the proportion of the variance that was spatially dependent (c_1 / c_0). For a given sample interval, geostatistical standard errors of Loch Ness on 24 May 1997 were not that much less than classical standard errors because a relatively high proportion of the variance was spatially independent. In contrast, for a given sample interval, geostatisical standard errors of Loch Awe on 29 May 1997 were much less than classical standard errors because only a small proportion of the variance was spatially independent.

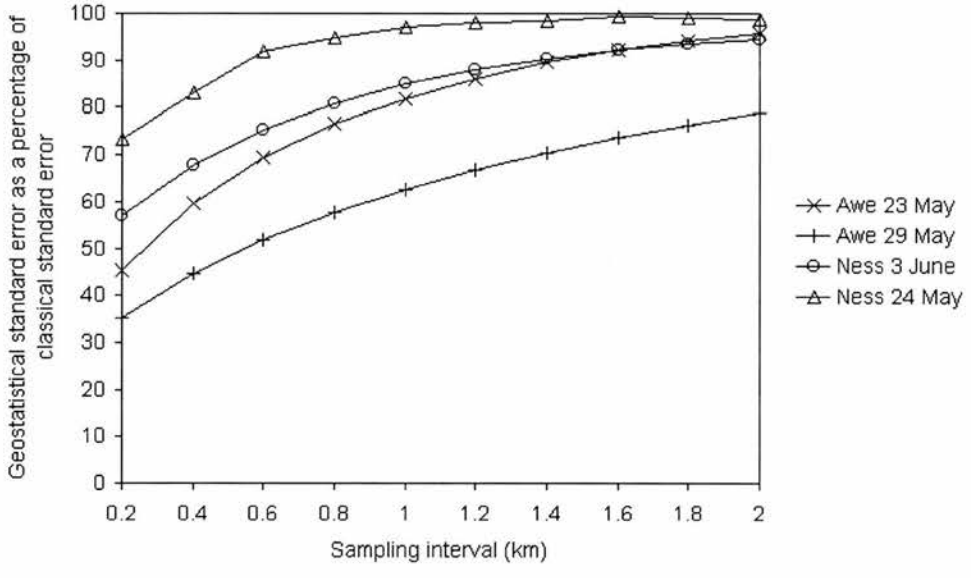

Figure F-4. Geostatistical standard errors as a percentage of the classical standard errors plotted as a function of sample interval for Loch Awe (23 May and 29 May 1997) and Loch Ness (24 May 1997 and 3 June 1997).

CONCLUSION

Three conclusions can be made in relation to optimising the sampling of lake water quality.

1. It is necessary to sample spatially

The number of observations required to achieve a given accuracy depends on the spatial variation in lake water quality. Because there is often much spatial variation in water quality in a given lake, the number of observations traditionally used by monitoring agencies will inevitably be too small.

2. Sample sizes should be determined in relation to the spatial distribution in water quality

Spatial variation in the water quality depends on many factors (including morphometry and wind regime). Therefore, when monitoring lake water quality it may be beneficial to vary the sample size from date to date. For example, if at one time of year it is known that a turbulent wind environment causes homogenisation then a smaller sample size will be necessary. Alternatively, if at another time of year it is known that a more quiescent wind environment allows the formation heterogenous spatial distibutions, then a larger sample size will be necessary.

3. Geostatistical sampling is generally preferable to classical sampling

Ignoring the cost involved in sampling, a geostatistical scheme is always more efficient than a classical scheme because for a given sample interval a smaller standard error of the estimate is obtained. The relative advantage of the geostatistical approach over the classical approach is lake-specific, and depends on, firstly, sample interval, and, secondly, the ratio of the spatially dependent component of the variation to the non-spatially dependent component of the variation in the data. If there a low proportion of spatially dependent variance within the data or the intention is to use a small number of observations, then use of the geostatistical approach may not necessarily be justified because it involves more effort.

References

Addison, P., 1997, *Fractals and chaos. An illustrated course*, (Bristol: Institute of Physics Publishing).

Angel, P.L., Hernandez R, R.J.A, Agudelo, R, J.J., 1999, Fuzzy expert system model for the operation of an urban water supply system, *Proceedings of the International Conference on Computing and Control for the Water Industry, CCWI'99*, Exeter, UK.

Armstrong, R.A., 1993, Remote-sensing of submerged vegetation canopies for biomass estimation, *International Journal of Remote Sensing*, 14, 3, 621-627.

Atkinson, P.M., 1991, Optimal ground-based sampling for remote sensing investigations: estimating the regional mean, *International Journal of Remote Sensing,* 12, 559-657.

Atkinson, P.M., Webster, R., Curran, P.J., 1992, Cokriging with ground-based radiometry, *Remote Sensing of the Environment*, 41, 45-60.

Atkinson, P.M., Webster, R., Curran, P.J., 1994, Cokriging with airborne MSS imagery, *Remote Sensing of the Environment*, 50, 335-345.

Ayles, G.B., Lark, J.G., Barica, J., Kling, H., 1976, Seasonal mortality of rainbow trout (*Salmo gairdneri*) planted in small eutrophic lakes of central Canada, *Journal of Fisheries Research Board of Canada*, 33, 647-655.

Bailey-Watts, A.E., 1976, Planktonic diatoms and some diaton-silica relations in a shallow eutrophic Scottish loch, *Freshwater Biology*, 6, 69-80.

Bailey-Watts, A.E., 1978, A nine-year study of the phytoplankton of the eutrophic and non-stratifying Loch Leven (Kinross, Scotland), *Journal of Ecology*, 66, 741-771.

Bailey-Watts, A.E., 1981, Studies on the control of the early spring diatom maximum in Loch Leven. In *Algae and the Aquatic Environment*, edited by F.E. Round (Bristol: Biopress).

Bailey-Watts, A.E., 1986, The abundance, size distribution and species composition of unicellular centrales assemblages at late winter-early spring maxima in Loch Leven (Kinross, Scotland) 1968-1985, *Proceedings of the 9th Diatom Symposium.*

Bailey-Watts, A.E., 1992, The algal plankton of Loch Leven, Kinross, *Proceedings of the Royal Society of Edinburgh*, (B), 74,9.

Bailey-Watts, A.,E., Duncan, P., 1981, The phytoplankton. In *The ecology of Scotland's largest lochs: Lomond, Awe, Ness, Morrar and Shiel*, edited by P.S. Maitland (The Hague: Junk), pp. 91-181.

Bailey-Watts, A.E., Smith, I.R., Kirika, A., 1989, The dynamics of silica in a shallow diatom-rich Scottish loch II: the influence of diatoms on an annual budget, *Diatom Research*, 4, 2, 191-205.

Bailey-Watts, A.E., Kirika, A., May, L., Jones, D.H., 1990, Changes in phytoplankton over various time scales in a shallow eutrophic lake: the Loch Leven experience, with special reference to the influence of flushing rate, *Freshwater Biology*, 23, 85-111.

Banks, R.B., 1975, Some features of wind action in shallow lakes, *Proceedings of the American Society of Civil Engineers*, 12, 1587-1603.

Belov, A.P., Giles, J.D., 1997, Dynamical model of buoyant cyanobacteria, *Hydrobiologia*, 349, 87-97.

Bennet, S., 1994, An assessment of the Use of the Daedalus 1268 AADS Airborne Thematic Mapper for the study of water quality parameters in inland waters, *Unpublished MSc Thesis,* University of Edinburgh.

Bengtsson, L., 1973, Wind stress on small lakes, *Teniska Hxgskolan*, Lund, Sweden.

Best, G.A., Traill, I., 1994, The physico-chemical limnology of Loch Lomond, *Hydrobiologia*, 29-38.

Bindloss, M., 1976, The light-climate of Loch Leven, a shallow Scottish lake, in relation to primary production by phytoplankton, *Freshwater Biology*, 6, 501-518.

Blais, J.M., Kaleff, J., 1995, The influence of lake morphometry on sediment focusing, *Limnology and Oceanography*, 40, 3, 582-588.

Bondarenko, N.A., Guselnikova, N.E., Logacheva, N.F., Pomazkina, G.V., 1991, Spatial distribution of phytoplankton in Lake Baikal, *Freshwater Biology*, 35, 517-523.

Bouchart, F.J.C., Hampartzoumian, E., 1999, Use of genetic algorithms with a reinforcement model for multiple reservoir operation, *Proceedings of the Fourth International Conference on Computing and Control in the Water Industry*, Exeter, UK.

Boyce, F.M., 1974, Some aspects of Great Lake physics of importance to biological and chemical processes, *Journal of Fisheries Research Board of Canada*, 31, 689-730.

Bowles, C., Dafferm C.D., Ashford-Frost, S., 1998, The independent validation of SSIIM – a 3D Numerical model, *Proceedings of the 4th Hydroinformatics Informatics Conference*, Copenhagen, Denmark.

Bradbury, R.H., Reichelt, R.E., Green, D.G., 1984, Fractals in ecology: methods and interpretation, *Marine Ecology - Progress Series*, 14, 295-296.

Bruno, E.J., McLaughlin, J.J.A., 1977, The nutrition of the freshwater dinoflagellate cearatium hirundinella, *Journal of Protozoology*, 24, 548-543.

Bunimovich, L.A., Ostrovskii, A.G., Umatani, S., 1993, Observations of the fractal properties of the Japan surface temperature patterns, *International Journal of Remote Sensing*, 14, 11, 2185-2201.

Bychkova, I.A., Victorov, S.V., Vinogradov, V.V., 1985, Using satellite data for studies of upwelling and frontogenesis in the Baltic Sea, *Earth Studies from Space*, 2, 12-19.

Capblancq, J., Catalan, J., 1994, Phytoplankton: which, and how much? In: *Limnology Now: A Paradigm of Planetary Problems*, edited by R. Margalef (Amsterdam: Elsevier Science), pp. 9-36.

Carpenter, D.J., Carpenter, S.M., 1983, Modeling inland water quality using Landsat data, *Remote Sensing of the Environment*, 13, 345-352.

Carmichael, W. W., 1994, The toxins of cyanobacteria, *Scientific American*, January,

78-86.

Carrick, H.J., Worth, D., Marshall, M.L., 1994, The influence of water circulation on chlorophyll-turbidity relationships in Lake Okeechobee as determined through remote sensing, *Journal of Marine Research,* 16, 9, 1117-1135.

Chacon-Torres, A., Ross, L.G., Beveridge, M.C.M., Watson, A.I., 1992, The application of SPOT multispectral imagery in the assessment of water quality in Lake Patzcuaro, Mexico, *International Journal of Remote Sensing*, 13, 4, 587-603.

Chapra, S.C., 1997, *Surface water quality modeling*, (Singapore: McGraw-Hill).

Clarke, G.L., Ewing, G.C., Lorenzen. C.J., 1970, Spectra of backscattered light from the sea obtained from aircraft as a measure of chlorophyll concentration, *Science*, 167, 119-21.

Curran, J.C., 1986, Effluent dispersal and the physical environment, *Proceedings of the Royal Society of Edinburgh*, (B), 90, 97-115.

Curran, J.C., Poodle, T., 1994, Aspects of the hydrology and hydrography of Loch Lomond, *Hydrobiologia*, 21-28.

Davey, M.C., Walsby, A.E., 1985, The form resistance of sinking algal chains, *British Phycological Journal*, 20, 3, 243-248.

Davis, J.C., 1986, *Statistics and data analysis in geology*, (Chichester: John Wiley and Sons).

Daviescolly, R.J., Pridmore., R.D., Hewitt, J.E., 1986, Optical properties of some fresh-water phytoplanktonic algae, *Hydrobiologia*, 133, 2, 167-178.

Daviescolly, R.J., Vant, W.N., Wilcock, R.J., 1988, *Water Resources Bulletin*, 23, 1, 11-19.

Dekker, A.G., 1993, *Detection of optimal water quality parameters for eutrophic waters by high resolution remote sensing,* (Amsterdam: Free University).

Dekker, A.G., Malthus, T.J., Wijnen, M.M., Seyhan, E., 1992a, Remote sensing as a tool for assessing water quality in Lake Loosdrecht lakes, *Hydrobiologia*, 233, 137-159.

Dekker, A.G., Malthus, T.J., Wijnen, M.M., Seyhan, E., 1992b, The effect of spectral

bandwidth and positioning on the spectral signature analysis of inland water, *Remote Sensing of the Environment*, 41, 221-225.

Denman, K.L., Platt, T., 1976, The variance spectrum of phytoplankton in a turbulent ocean, *Journal of Marine Research*, 34,4, 592–601.

Denman, K.L., Gargett, A.E., 1983, Time and space scales of vertical mixing and advection of phytoplankton in the upper ocean, *Limnology and Oceanography*, 28, 5, 801-815.

Deutsch, C.V., Journel, A.G., 1992, *GSLIB geostatistical software library and user's guide,* (Oxford: Oxford University Press).

Droop, 1973, Some thoughts on nutrient limitation in algae, *Journal of Phycology*, 9, 264-272.

Dugdale, 1967, Nutrient limitation in the sea: dynamics identification and significance, *Limnology and Oceanography*, 12, 685-695.

Ekman, V.W., 1905, On the influence of the earth's rotation on ocean currents, *Arkiv fur matematik, astronomi och Fysik*, 2, 52.

Engelsen, G.B., Kal, B.F.M., Buyse, J.J., Van Pruissen, F.G.M., 1992, The hydrology of the Lake Loosdrechts area, *Hydrobiologia*, 233, 11-21.

Eppley, R.W., 1972, Temperature and phytoplankton growth in the sea, *Fishery Bulletin*, 70, 4, 1063-1085.

Ester, L., Holloway, J., 1992, Estimators of bottom reflectance spectra, *International Journal of Remote Sensing*, 13, 2, 393-397.

Falconer, R.A., George, D.G., Hall, P., 1991, Three-dimensional numerical modelling of wind driven circulation in a shallow homogeneous lake, *Journal of Hydrology*, 124, 59-79.

Farmer, J.G., 1994, Environmental change and the chemical record in Loch Lomond sediments, *Hydrobiologia*, 290, 39-49.

Ferrandino, F.J., Aylon, D.E., 1985, Enhanced longitudinal mixing in a lake caused by inflow-induced circulation, *Water Resources Research*, 21, 2, 221-228.

Ferguson, A.J.D., 1997, The role of modelling in the control of toxic blue-green

algae, *Hydrobiologia*, 348, 1-4.

Ferziger, J.H., Peric, M., 1996, Computational methods for fluid dynamics (Berlin: Springer-Verlag).

Fisher, S.G., 1994, Pattern, process and scale in freshwater systems: some unifying thoughts. In *Aquatic ecology scale, pattern and process*, edited by P.S. Giller, A.G. Hildrew, D.G. Raffaelli (Oxford: Blackwell Science Ltd), pp. 575-591.

Foy, R.H., Gibson, C.E., Smith, R.V., 1976, The influence of daylength, light intensity and temperature on the growth rates of planktonic blue-green algae, *British Phycological Journal*, 11, 151-163.

Gao, S.B., Stefan, H.G., 1999, Multiple linear regression for lake ice and lake temperature characteristics, *Journal of Cold Regions Engineering*, 13, 2, 59-77.

George, D.G., 1981a, Wind-induced water movements in the South Basin of Windermere, *Freshwater Biology*, 11, 36-60.

George, D.G., 1981b, The spatial distribution of nutrients in the South Basin of Windermere, *Freshwater Biology*, 11, 405-424.

George, D.G., 1993, Physical and chemical scales of pattern in freshwater lakes and reservoirs, *The Science of the Total Environment*, 135, 1-15.

George, D.G., 1997, The airborne remote sensing of phytoplankton chlorophyll in the lakes and tarns of the English lake District, *International Journal of Remote Sensing*, 18, 9, 1971-1975.

George, D.G., Edwards, R.W., 1976, The effect of wind on the distribution of chlorophyll-a and crustacean plankton in a shallow eutrophic reservoir, *Journal of Applied Ecology*, 13, 667-690.

George, D.G., Heaney, S.I., 1978, Factors influencing the spatial distribution of phytoplankton in a small productive lake, *Journal of Ecology*, 66, 135-155.

George, D.G., Jones, D.H., 1987, Catchment effects on the horizontal distribution of phytoplankton in five of Scotland's largest freshwater lochs, *Journal of Ecology,* 75, 43-59.

George, D.G., Allen, C.M., Smith, D.G., 1988, The remote sensing of phytoplankton

chlorophyll in Esthwaite Water, Cumbria, *Proceedings of the NERC 1987 Airborne Campaign Workshop*, Swindon, UK, 59-74.

George, D.G., Charlton, F.L., 1996, Inland use of airborne remote sensing. Monitoring water quality in the English Lake District, *Natural Environment Research Council*, R&D Technical Report E5.

Gons, H.J., Burger-Wiersma, T., Otten, J.H., Rijkeboer, M., 1992, Coupling of phytoplankton and detritus in a shallow, eutrophic lakes (Lake Loosdrecht, the Netherlands), *Hydrobiologia*, 233, 51-60.

Goldman, J.C., McCarthy, J.J., Peavey, D.G., 1979, Growth rate influence on the chemical composition of phytoplankton in oceanic waters, *Nature*, 279, 210–215.

Gordon, H.R., Clark, D.K., Brown, J.W., Brown, O.B., Evans, R.H., Broenkow, W.W., 1983, Phytoplankton pigment concentrations in the Middle Atlantic Blight: comparison of ship determinations and CZCS estimates, *Applied Optics*, 22, 20-36.

Gordon, H.R., 1989, Dependence of the diffuse reflectance of natural waters on the sun angle, *Limnology and Oceanography*, 34, 1484-9.

Gotham, I.J., Rhee, G.Y., 1981, Comparative kinetic studies of phosphate limited growth and phosphate uptake in phytoplankton in continuous culture, *Journal of Phycology*, 17, 257-265.

Guting, P.S, Hutter, K., 1998, Modelling wind-induced circulation in the homogeneous Lake Constance using k-epsilon closure, *Aquatic Sciences*, 60, 3, 266-277.

Haines, D.A., Bryson, R.A., 1961, An empirical study of wind factor in Lake Mondota, *Limnology and Oceanography*, 6, 356-364.

Hallegraeff, M., 1993, A review of harmful algal blooms and their apparent global increase, *Phycologia*, 32, 2, 79-98.

Han, L., Rundquist, D.C., 1998, The impact of a wind-roughened water surface on remote sensing measurements of turbidity, *International Journal of Remote Sensing*, 195-202.

Hanna, M., Peters, R.H., 1991, Effects of sampling protocol on estimates of

phosphorus and chlorophyll concentrations in lakes of low to moderate trophic status, *Canadian Journal of Fisheries and Aquatic Science*, 48, 1979-1086.

Hamill, L., 1995, *Understanding hydraulics,* (London: McMillan Press).

Harper, D., 1992, *Eutrophication of freshwaters: principles, problems and restoration,* (London: Chapman and Hall).

Harris, G.P., 1980a, Spatial and temporal scales in phytoplankton ecology. Mechanisms, methods, models and management, *Canadian Journal of Fisheries and Aquatic Science*, 37, 877-900.

Harris, G.P., 1980b, The measurement of photosynthesis in natural populations of phytoplankton. In The *Physiological Ecology of Phytoplankton,* edited by I. Morris (Oxford: Blackwell).

Harris, G.P., 1983, Mixed layer physics and phytoplankton populations: studies in equilibrium and non-equilibrium ecology, *Progress in Phycological Research*, 2, 1-52.

Harris, G.P., 1986, *Phytoplankton Ecology: structure, function and fluctuation* (London: Chapman and Hall).

Harris, G.P., 1994, Pattern, process and prediction in aquatic ecology. A limnological view of some general ecological problems, *Freshwater Biology*, 32, 143-160.

Heaney, S.I., 1976, Temporal and spatial distribution of the dinoflagellate *Ceratium hirundinella* O.F. Muller within a productive lake, *Freshwater Biology*, 6, 531-542.

Heaney, S.I., Furnass, T.I., 1980, Laboratory models of diel vertical migration in the dinoflagellate *Ceratium hirundinella*, *Freshwater Biology*, 10, 163-170.

Heaney, S.I., Talling, J.F., 1980, Dynamic aspects of dinoflagellate distribution patterns in a small productive lake, *Journal of Ecology*, 68, 75-94.

Hedger, R.D., Atkinson, P.M., Malthus, T.J., George, D.G., 1996, Planning optimal sampling strategies for estimating the regional mean water quality in lakes, *Proceedings of the 22nd Annual Conference of the Remote Sensing Society*, Durham, UK.

Hedger, R.D., Olsen, N.R.B., Malthus, T.J., Atkinson, P.M., George, D.G., 1998, Dynamically modelling chlorophyll-*a* concentration in a remotely sensed image of Loch Leven, *Proceedings of the 24th Annual Conference of the Remote Sensing Society*, Greenwich, UK.

Hedger, R.D., Olsen, N.R.B., Malthus, T.J., Atkinson, P.M., 1999a, The analysis of water quality spatial distributions in lakes by the integration of computational fluid dynamics with remote sensing, *Proceedings of the 25th Annual Conference of the Remote Sensing Society*, Cardiff, UK.

Hedger, R.D., Olsen, N.R.B., George, D.G., Atkinson, P.M., Malthus, T.J., 1999b, Dynamic modelling of the spatio-temporal distribution of phytoplankton in a small productive lake, *Proceedings of the 4th International Conference on GeoComputation*, Fredericksberg, USA.

Herman, A.W., Denman, K.L., 1977, Rapid underwater profiling of chlorophyll with an in situ fluorometer mounted on a 'BATFISH' vehicle, *Deep Sea Research*, 24, 385-397.

Hilton, J., Rigg, E., 1984, A pascal program for the calculation of effective fetches as used in wave height and frequency predictions, *Computers and Geoscience*, 11, 4, 493-500.

Hofstra, J.J., Van Liere, L., 1992, The state of the environment of the Loosdrecht lakes, *Hydrobiologia*, 233, 11-21

Holden, A.V., Caines, L.A., 1972/73, Nutrient chemistry of Loch Leven, Kinross, *Proceedings of the Royal Society of Edinburgh*, (B), 74, 7, 101-121.

Houghton, J.T., 1986, *The physics of atmospheres,* (Cambridge: Cambridge University Press).

Howard, A., 1993a, Problem cyanobacterial blooms: explanation and simulation modelling, *Transactions of the Institute of British Geographers NS*, 19, 213-223.

Howard, A., 1993b, SCUM – simulation of cyanobacterial underwater movement, *CABIOS*, 9,4, 413–419.

Howard, 1997, Computer simulation modelling of buoyancy change in Microcystis,

Hydrobiologia, 349, 111-117.

Howard, A., Kirby, M.J., Kneale, P.E., McDonald, A.T., 1995, Modelling the growth of cyanobacteria (GrowScum), *Hydrological Processes*, 9, 809–821.

Huttula, T., Jopopnen, J., Lehtinin, K., Wahlgren, A., Niinioja, R., 1996, Water currents and spreading of river load in Lake Pyhaselka, Saimaa, Finland, *Hydrobiologia*, 322, 117-224.

Hutchinson, G.E., 1957, *A Treatise on Limnology, Volume 1*, (Chichester: John Wiley and Sons).

Imberger, J., 1985, The diurnal mixed layer, *Limnology and Oceanography*, 30, 4, 737-770.

Imberger, J., 1994, Transport processes in lakes: a review. In *Limnology now: a paradigm of planetary problems*, edited by R. Margalef (Amsterdam: Elsevier), pp. 99-193.

Imberger, J., Hamblin, P.F., 1982, Dynamics of lakes, reservoirs, and cooling ponds, *Annual Review of Fluid Mechanics*, 14, 153-187.

Iturriaga, R., Siegel, D.A., 1989, Microphotometric characterization of phytoplankton and detrital absorption properties in the Sargasso Sea, *Limnology and Oceanography*, 6, 129-48.

Jackson, G.A., 1980, Phytoplankton growth and zooplankton grazing in oligotrophic oceans, *Nature*, 284, 439-41.

Jakeman, A.J., Beck, M.B., McAleer, M.J., 1993, *Modelling changes in environmental systems*, (Chichester: John Wiley and Sons).

Jerlov, N.G., 1976, *Marine Optics,* (Amsterdam: Elsevier).

Jones, R.I., Fulcher, A.S., Jayakody, J.K.U., Laybourn-Parry, J., Shine, A.J., Wlaton, M.C., Yound, J.M., 1995, The horizontal distribution of plankton in a deep oligotophic lake - Loch Ness, Scotland, *Freshwater Biology*, 33, 161-170.

Jones, R.I., Young, J.M., Hartley, A.M., Bailey-Watts, A.E., 1996, Light limitation of phytoplankton development in an oligotrophic lake - Loch Ness, Scotland, *Freshwater Biology*, 35, 533-543.

Keller, W., Conlon, M., 1994, Crustacean zooplankton and lake morphometry in precambrian shield lakes, *Canadian Journal of Fisheries and Aquatic Sciences*, 51, 11, 2424-2434.

Kierstead, H., Slobodkin, L.B., 1953, The size of water masses containing plankton blooms, *Journal of Marine Research*, 12, 141-4.

Kirk, T.O., 1994, *Light and photosynthesis in aquatic ecosystems,* (Cambridge: Cambridge University Press).

Kirby, R.J., 1972/1973, The morphological history of Loch Leven, Kinross. *Proceedings of the Royal Society of Edinburgh* (B), 74,4.

Kneale, P.E., Howard, A., 1997, Statistical analysis of algal and water quality data, *Hydrobiologia*, 59-63.

Kolmogorov, A.N., 1941, The local structure of turbulence in incompressible viscous fluids for very large Reynolds numbers, *Dolk. Akad. Nauk.*, 30, 301.

Kondratyev, K., Ya., Pozdnayakov, S.V, 1994, Application of remote sensing in the visible spectrum for hydrodynamics studies in lakes, *Water Pollution Research Journal of Canada*, 29, 2/3, 385-402.

Kromkamp, J, Walsby, A.E., 1990, A computer model of buoyancy and vertical migration in cyanobacteria, *Journal of Plankton Research*, 12, 1,161-183.

Langmuir, 1938, Surface motion of water induced by the wind, *Science*, 87, 119-123.

Lam, D.C.L., Simons, T.J., 1976, Numerical computations of advective and diffusive transports of chloride in Lake Erie, *Journal of the Fisheries Board of Canada*, 33, 537-549.

Larsen, C.P.S., Macdonald, G.M., 1993, Lake morphometry, sediment mixing and the selection of sites for fine resolution paleoecological studies, *Quaternary Science Reviews*, 12, 9, 781-792.

Lee, A.C., Mysak, L.A., 1979, Transverse upwelling in a long narrow lake, with application to Babine Lake and Lake Michigan, *Atmosphere and Oceans*, 17, 3, 200-218.

Levasseur, M., Therriault, J.C., Legendre, L., 1983, Tidal currents, winds and the

morphology of phytoplankton structures, *Journal of Marine Research*, 41, 655-672.

Liegh-Abott, M.R., Coil, J.A., Powell, T.M., Richerson, P.J., 1978, Effects of a costal front on the distribution of chlorophyll in Lake Tahoe, California-Nevada, *Journal of Geophysical Research*, 83, 9, 4668-4672.

Livingstone, D.A., 1954, On the origin of lake basins, *American Journal of Science*, 252, 547-552.

Lorenz, E.N., 1963, Deterministic non-periodic flow, *Journal of Atmospheric Science*, 20, 130-141.

Macan, T.T., 1970, *Biological studies of the English lakes*, (London: Longman).

Margalef, R., 1990, Limnology: reconsidering ways and goals, *Memorie dell'Istuto di Idrobiologia*, 46, 57-76.

Mailtand, P.S., 1978, *Biology of freshwaters*, (Glasgow: Blackie).

Maitland, P.S., Smith, I.R., Bailey-Watts, A.E., Smith, B.D., Lyle, A., 1991, Comparison and synthesis. In: *The ecology of Scotland's largest lochs: Lomond, Awe, Ness, Morrar and Shiel*, edited by P.S. Maitland (The Hague: Junk), pp. 253-284.

Maitland, P.S., Boon, P.J., McLusky, D.S., 1994, *The freshwaters of Scotland. A natural resource of international significance,* (Chichester: John Wiley and Sons).

Malthus, T.J., 1996, An evaluation of the Airborne Thematic Mapper sensor for monitoring inland water quality, *Proceedings of the 22nd Annual Conference of the Remote Sensing Society*, Durham.

Mather, P., 1987, *Computer processing of remotely sensed images: an introduction*, (Chichester: John Wiley and Sons).

Matheron, 1971, The theory of regionalized variables and its applications. *Les cahiers du CMM*, facs. 5, Ecole Nationale Superieur des mines, Paris, Fontainebleau, 211.

McBratney, A.B., Webster, R., 1986, Choosing functions for semi-variograms of soil properties and fitting them to sampling estimates, *Journal of Soil Science*, 37, 617-639.

McCarthy, J.J., Goldman, J., 1979, Nitrogenous nutrition of marine phytoplankton in nutrient depleted waters, *Science*, 203, 670–672.

McNown, J.S., Malaika, J., 1950, Effect of particle shape on settling velocities al low Reynold number, *Transactions of the American Geophysical Union*, 31, 74-82.

McQueen, D.J., 1990, Manipulating lake community structure: where do we go from here? *Freshwater Biology*, 23, 613-620.

Middleman, S., 1988, *An introduction to fluid dynamics: principles of analysis and design* (New York: Wiley).

Mill, H.R., 1895, *Geographical Journal*, 6.

Moloney, C.L., Field, 1991, The size-based dynamics of plankton food webs. I. A simulation model of carbon and nitrogen flows, *Journal of Plankton Research*, 13, 5, 1003-1038.

Morel, A., Gordon, H.R., 1980, Report of the working group on water colour, *Boundary Layer Meteorology*, 18, 343-355.

Mosisch, T.D., Arthington, A.H., 1998, The impacts of power boating and water skiing on lakes and reservoirs, *Lakes and Reservoirs: Research and Management*, 3, 1-17.

Munchane, M.W., 1996, Comparison of the isotope record in micrite, Lake Turkana, with the historical record over the last century. In *The limnology, climatology and paleoclimatology of the East African Lakes*, edited by T.C. Johnson and E.O. Odada (Amsterdam: Overseas Publishers Association), pp. 431-441.

Murray, L., Pullar, L., 1910, *Bathymetric survey of the freshwater lochs of Scotland,* (Edinburgh: Challenger) Volumes 1–6.

Murthy, C.R., 1976, Horizontal diffusion characteristics in Lake Ontario, Journal of Physical Oceanography, 6, 76-84.

Murty, V.S.N., Subrahmanyam, B., Gangadhara Rao, L.V., Reddy, G.V., 1998, Seasonal variation of sea surface temperature in the Bay of Bengal during 1992 as derived from NOAA-AVHRR SST data, *International Journal of Remote Sensing*, 19, 12, 2361-2372.

Nicklisch, A., Kohl, J.G., 1983, Growth rates of *Microsystis aeruginosa* (Kutz) as a basis for modelling its population dynamics, *Internationale Revue des Gesamenten Hydrobiologie*, 68, 317-326.

OECD, 1982, *Eutrophication of Waters, Monitoring, Assessment and Control*, Organisation for Economic Co-operation and Development, Paris.

Oke, T.R., 1987, *Boundary layer climates,* (London: Methuen).

Okubo, A., 1971, Oceanic diffusion diagrams, *Deep Sea Research*, 18, 789-802.

Oliver, M.A., Webster, R., 1991, How geostatistics can help you, *Soil Use and Management*, 7, 4, 1991

Olsen, N.R.B., 1997, *Computational fluid dynamics in hydraulic and sedimentation engineering*, Division of Hydraulic and Environmental Engineering, The Norwegian University of Science and Technology.

Olsen, N.R.B., 1998, Two-dimensional numerical modelling of flushing processes in water reservoirs, *IAHR Journal of Hydraulic Research*, 3.

Olsen, N.R.B., Hedger, R.D., George, D.G. and Heslop, S., 1998, 3D CFD modelling of spatial distribution of algae in Loch Leven, Scotland, *Proceedings of the 3rd International Conference on Hydroscience and Engineering*, Cottbus, Germany.

Olsen, N.R.B., Hedger, R. D., Heslop, S., George, D. G., 1999, Computing spatial variation of algae in water supply reservoirs, *Proceedings of the International Conference on Computing and Control for the Water Industry, CCWI'99*, Exeter, UK.

Ollson, P., Edler, L., 1991, Dinoflaellate distribution in the southeastern Kattegut during an Autumn bloom, *Sarsia*, 75, 1-2, 23,28.

Overton, W.S., 1977, A strategy for model construction. In *Ecosystem modelling in theory and practice,* edited by A.S. Hale and J.W. Day (New York: John Wiley and Sons), pp. 49-74.

Paasche, E., 1980, Silicon. In *The physiological ecology of phytoplankton,* edited by I. Morris (Oxford: Blackwell).

Parsons, T., Takahashi, M, 1973, *Biological oceanographic processes,* (Oxford:

Pergammon Press).

Patalas, K., Salki, A., 1992, Spatial variation of crustacean plankton in lakes of different size, *Canadian Journal of Fisheries and Aquatic Sience*, 50, 2626-2639.

Pantankar, S.V., 1980, *Numerical Heat Transfer and Fluid Flow* (New York: McGraw-Hill Book Company).

Peters, R.H., 1986, The role of prediction in limnology, *Limnology and Oceanography*, 31, 5, 1143-1159.

Pierce, L., 1999, Loch Lomond: an example of Quaternary Megageomorphology, *Scottish Geographical Journal*, 115,1, 71-80.

Platt, T, Sathyendranath, S, 1994, Scale, pattern and process in marine ecosystems: concluding remarks. In *Aquatic ecology scale pattern and process*, edited by P.S.Giller, A.G. Hildrew, and D.G. Raffaelli (Oxford: Blackwell Sciences), pp. 601–606.

Pozdnyakov, D.V., Kondratyev, Ya, K., Bukata, R.P., Jerone, J.H., 1998, Numerical modeling of natural water colour: implications for remote sensing and limnological studies, *International Journal of Remote Sensing*, 19, 10, 1913-1932.

Recknagel, F., 1997, ANNA – Artificial neural network model for predicting species abundance and succession of blue algae, *Hydrobiologia*, 47-57.

Reynolds, 1972, Growth, has vacuolation and buoyancy in a natural population of planktonic blue-green alga, *Freshwater Biology*, 2, 87-106.

Reynolds, C.S., 1973a, The seasonal periodicity of planktonic diatoms in a shallow eutrophic lake, *Freshwater Biology*, 3, 89-110.

Reynolds, C.S., 1973b, Growth and buoyancy of Microcystis aeruginosa Kütz. Emend. Elenkin in a shallow eutrophic lake, *Proceedings of the Royal Society of London*, (B), 184, 29-50.

Reynolds, C.S., Jaworski, G.H.M., Cmeich, H.A., Leedale, G.F., 1981, On the annual cycle of the blue-green algae Microcystis aeruginosa Kütz. emend. Elenkin, *Philosophical transactions of the Royal Society of London*, (B), 293, 419-77.

Reynolds, C.S., 1983, A physiological interpretation of the dynamic responses of

populations of a planktonic diatom to physical variability of the environment, *New Phytologist*, 95, 41-53.

Reynolds, C.S., 1984, *The ecology of freshwater phytoplankton,* (Cambridge: Cambridge University Press).

Reynolds, C.S., 1987, Cyanobacterial water-blooms, *Advances in Botanical Research*, 13, 67-141.

Reynolds, C.S., 1990, Temporal scales of variability in pelagic environments and the response of phytoplankton, *Freshwater Biology*, 23, 25-53.

Reynolds, C.S., 1999, Modelling phytoplankton dynamics and its application to lake management, *Hydrobiologia*, 396, 123-131.

Reynolds, C.S., Jaworski, C.H.M., Cmiech, H.A., Leedale, G.F., 1981, On the annual cycle of the blue-green alga *Mycrocystis aeruginosa* Kutz. emend. Elenkin. *Philosophical Transactions of the Royal Society of London*, (B), 293, 419-77.

Reynolds, C.S., Thompson, J.M., Ferguson, A.J.D, Wiseman, S.W., 1982, Loss processes in the populations of phytoplankton maintained in closed systems, *Journal of Plankton Research*, 4, 561-600.

Reynolds, C.S., Irish, A.E., 1997, Modelling phytoplankton dynamics in lakes and reservoirs: the problem of in–situ growth rates, *Hydrobiologia*, 349, 5–17.

Richerson, P.J., Armstrong, R., Goldman, C.R., 1970, Contemporaneous disequilibrium: a new hypothesis to explain the ecology of phytoplankton, *Proceedings of the National Academy of Science*, 67, 1710-1714.

Rigler, F.H., 1982, Recognition of the possible: an advantage of empiricism in ecology, *Canadian Journal of Fisheries and Aquatic Science*, 1323-1331.

Rigler, F.H., Peters, R.H., 1995, *Science and Limnology,* (Oldendorf: Ecological Institute).

Sakshaug, E, 1980, Problems in the methodology of studying phytoplankton. In *The physiological ecology of phytoplankton,* edited by I. Morris (Oxford: Blackwell).

Schindler, D.W., 1978, Factors regulating phytoplankton production and standing crop in the world's freshwater, *Limnology and Oceanography*, 23, 478-486.

Scheffer, M., 1998, *Ecology of Shallow Lakes,* (London: Chapman and Hall).

Schubert, H., Forster, R.M., 1997, Sources of variability in the factors used for modelling primary productivity in surface waters, *Hydrobiologia,* 349, 75-85.

Scott, J.T., Myer, G.E., Stewart, R., Wlather, E.G., 1969, On the mechanisms of langmuir circulations and there role in epilimnion mixing, *Limnology and Oceanography,* 14, 493–503.

Seed, D., 1997, *River training and channel protection – validation of a 3D numerical model*, Report SR 480, HR Walingford, UK.

Siegel, H., Gerth, M., Neumann, T., Doerffer, R., 1999, Case studies on phytoplankton blooms in coastal and open waters of the Baltic Sea using Coastal Zone Color Scanner data, *International Journal of Remote Sensing*, 20, 7, 1249-1264.

Simmard, Y., Legendre, P., Lavoie, G., Marcotte, D., 1992, Mapping, estimating biomass, and optimizing sampling programs for spatially autocorrelated data: case study of the Northern Shrimp (*Pandalus borealis*), *Canadian Journal of Fisheries and Aquatic Science*, 49, 32-45.

Simons, T.J, 1974, Verification of numerical models of Lake Ontario: Part 1. Circulation in spring and early summer, *Journal of Physical Oceanography*, 4, 507-523.

Smayda, 1970, The suspension and sinking of phytoplankton in the sea, *Annual Review of Oceanography and Marine Biology*, 8, 353-414.

Smayda, 1974, Some experiments on the sinking rates of two freshwater diatoms, *Limnology and Oceanography*, 10, 499-500.

Smith, I.R., 1972/1973, The structure and physical environment of Loch Leven, Scotland. *Proceedings of the Royal Society of Edinburgh,* (B), 74,6.

Smith, I, R, 1979, Hydraulic conditions in isothermal lakes, *Freshwater Biology*, 8, 199-145.

Smith, I.R., 1992, *Hydroclimate: the influence of water movement on freshwater ecology,* (London: Elsevier Science Publishers).

Smith, I.R., Sinclair, I.J., 1972, Deep water waves in lakes, *Freshwater Biology*, 2, 387-399.

Smith, I.R., Lyle, A., Rosie, A., 1981, Comparative physical limnology. In *The ecology of Scotland's largest lochs: Lomond, Awe, Ness, Morrar and Shiel.* edited by P.S. Maitland (The Hague: Junk), pp. 29-66.

Spence, D.H.N., 1967, Factors controlling the distribution of freshwater macrophytes with particular reference to the lochs of Scotland, *Journal of Ecology*, 55, 147–170.

Spencer, J.W., 1971, Fourier series representation of the position of the sun. *Search*, 2, 172.

Spigel, R.H., Coulter, G.W., 1996, Comparison of hydrology and physical limnology of the East African Great Lakes: Tanganyika, Malawi, Victoria, Kivu and Turkana (with reference to some North American Greta Lakes). In *The limnology, climatology and palaeoclimatology of the East African Lakes*, edited by T.C. Johnson and E.O. Odada (Amsterdam: OPA), pp. .

Stoesser, T., 1998, Numerical modelling as a tool in hydraulics – in cases of reservoir sedimentation processes in mountainous regions, *MSc Thesis*, Institute of Hydraulic Engineering and Water Resources Management, University of Karlsruhe, Germany.

Stommel, 1963, The varieties of oceanographic experience, *Science*, 139, 572-576.

Stauffer, R.E., Armstrong, D.E., 1984, Lake mining and its relationship to epilimnetic phosphorus Shagawa Lake, Minnesota, *Canadian Journal of Fisheries and Aquatic Science*, 41, 5769.

Stumpf, R.P., Tyler, M.A., 1988, Satellite detection of bloom and pigment distributions in estuaries, *Remote Sensing of the Environment*, 24, 385-404.

Tivy, J., 1980, *The effect of recreation on freshwater lochs and reservoirs in Scotland*, Countryside Commission for Scotland.

Triton, D.J., 1998, *Physical fluid dynamics,* (Oxford: Oxford University Press).

Uncles, R.J., Morris, J.P., Stephens, J.A., Robinson, M.C., Murphy, R.J., 1999, Aircraft and sea-truth observations of salinity and temperature within the Tweed

Estuary and coastal-zone frontal system, *International Journal of Remote Sensing*, 20, 3, 609-626.

U.S. Army, 1962, Waves in inland reservoirs, *Technical Memo. Of the Beach Erosion Board*, U.S., 132.

Versteeg, H.K., Malalasekera, W., 1995, *An introduction to computational fluid dynamics: the finite volume method,* (London: Longman).

van Dorn, W., 1953, Wind stress on an artificial pond, *Journal of Marine Research*, 12, 249–276.

Van Liere, L., Parma, S., Gulati, R.D., 1992, Working group water quality research Loosdrecht lakes: its history, structure, research programme, and some results, *Hydrobiologia*, 233, 1-11.

Van Tongeren, O.F.R., Van Liere, L., Gulati, R.D., Postema, G., Boesewinkelde Bruyn, P.J., 1992, Multivariate analysis of the plankton communities in the Loosdrecht lakes: relationship with the chemical and physical environment, *Hydrobiologia*, 233, 105-118.

Victorov, S., 1996, *Regional Satellite Oceanography,* (London: Taylor and Francis).

Vincent, W.F., 1983, Phytoplankton production and winter mixing: contrasting effects in two oligotrophic lakes, *Journal of Ecology,* 71, 1-20.

Viscum Jørgensen, P., 1999, Standard CZCS Case 1 algorithms in Danish coastal waters, *International Journal of Remote Sensing*, 1289-1302.

Vollenweider, R.A., 1968, Scientific fundamentals of eutrophication of lake and flowing waters with special reference to phosphorus and nitrogen, *Organisation for Economic Co-operation and Development*, Paris.

Wasser, H. J., 1988, *Physical model research to wind-driven currents in Lake Loosdrecht lakes*, WQL-report 1986-6, Free University, Institute of Earth Sciences, Amsterdam.

Webster, R., Curran, P.J., Munden, J.W., 1989, Spatial correlation in reflected radiation from the ground and its implications for sampling and mapping by ground-based radiometry, *Remote Sensing of the Environment*, 29, 67-78.

Welch, P.S., 1948, *Limnological methods,* (New York: McGraw-Hill).

Whitehead, P.G., Howard, A., Arulmani, C., 1997, Modelling algal growth and transport in rivers: a comparison of time series analysis, dynamic mass balance and neural network techniques, *Hydrobiologia*, 39-46.

Whittow, J.B., 1984, *Dictionary of physical geography*, (London: Penguin Books).

Wilson, A.K., 1995, *NERC Scientific Services Airborne Remote Sensing Facility user guide handbook*, Natural Environment Research Council (Swindon: UK).

Wroblewski, J.S., O'Brien, J.J., 1976, A spatial model of phytoplankton patchiness, *Marine Biology*, 35, 161-175.

Wu, J., 1969, Wind shear stress and surface roughness at air–sea interface, *Journal of Geophysical Research*, 74, 444–445.

Zacharias, I, Ferentinos, G, 1997, A numerical model for the winter circulation in Lake Trichonis, Greece, *Environmental Modelling and Software*, 12, 4, 311-321.